MASTER'S RESEARCH THESIS

ANALYSIS OF FLUID STRUCTURE INTERACTION (FSI) DUE TO OIL HAMMERING IN A PIPING NETWORK OF A MOBILE CRANE

BY

IQBAL MUHAMMAD KHAN

2007-NUST-MS PhD-Mech-13

ADVISOR

Prof. Dr. MUHAMMAD AFZAAL MALIK

NATIONAL UNIVERSITY OF SCIENCES AND TECHNOLOGY,
COLLEGE OF ELECTRICAL AND MECHANICAL ENGINEERING

RAWALPINDI, PAKISTAN

December, 2010

National University of Sciences & Technology, Pakistan

FORM TH-4

MASTER'S THESIS WORK

We hereby recommend that the dissertation prepared under our supervision by

Iqbal Muhammad Khan 2007-NUST-MSc-Mech-13

Analysis of Fluid Structure Interaction (FSI) due to Oil Hammering in a Piping Network of a Mobile Crane

Be accepted in partial fulfillment of the requirements for the award of Master of Science Degree.

Guidance and Examination Committee

Name: Dr. Mehmood Anwar Khan Signature: _____

Dept: Mechanical Engineering

Name: Col. Dr. Syed Waheed ul Haq Signature: _____

Dept: Mechanical Engineering

Name: Dr. Ikhlaq Ahmad Chohan Signature: _____

Dept: Basic Sciences & Humanities

Advisor's Name: Dr. M. Afzaal Malik Signature: _____

Associate Dean College of E&ME Date: December 22, 2010

_____	Dec 22, 2010	_____	Dec 22, 2010
Head of Department	Dated	Dean/ Commandant	Dated

College of Electrical and Mechanical Engineering, Rawalpindi

Dedicated to my mother, wife, and beloved children.

ACKNOWLEDGEMENTS

I am thankful to Allah Almighty for providing me an opportunity to undergo this research work successfully and also enabling me to acquire some more knowledge.

I am highly indebted to my advisor, Professor Dr. M. Afzaal Malik, Associate Dean, NUST College of E&ME for his keen interest in my work and fruitful co-operation and discussion on oil hammering and Fluid structure interaction (FSI) and related affairs. I thank for his kind, valuable and precise guidance for improvement and the encouraging support during the entire project. I am particularly grateful for his elderly behavior and excellent coaching style, which instilled in me a spirit to complete this research work in-time.

I am indebted to all my teachers at the College of Electrical and Mechanical Engineering (E&ME). I am also thankful to Professor Dr. Mehmood Anwar Khan HOD Mechanical Engineering, Associate Prof. Colonel Dr. Syed Waheed Ul Haq and Assistant Professor Dr. Ikhlaq Ahmad Chohan Department of Basic Sciences and Humanities; members of the guidance and examination committee.

Equally I would like to thank Dr. A.S Tijsseling (Endhoven University of Technology) for qualifying my project up to the level of fluid structure interaction (FSI).

I am also very grateful to Col. (Retd) Farrukh Javed Beg Director (NDC) who has provided me necessary help and guidance during my experimentation work based upon his vast experience and given me the opportunity to take up this study.

I am also very grateful to Mr. Nabeel Akram Manager (NDC), Mr. Hashmat Ullah Manager (NDC) of QC Directorate and Mr. Himayat Ullah Manager (NDC) for providing me necessary help during my experimentation work.

My sincere gratitude to my friend Muhammad Jamil General Manager (NDC) for his technical ideas and physical support during my stay at the College of E&ME.

My Special thanks to my friends Mr. Tahir Qayym who has contributed in compiling the data and finalizing the thesis report.

Special thanks to my elder brother, Professor Dr. Taj Muharram Khan for providing his personal attention, motivation to finish the thesis work in time and his encouragement in this research studies, its experimentation and write up.

Thanks to my mother, wife, brothers and my children for their constant prayers, reminders, motivation and encouragements in completion of this MS studies.

Special thanks to my good friend Mr. Ashfaq Khan UK for his personal attention, investing his precious time and his encouragement in the experimentation and write-up stages of this research work.

Finally, my sincere thanks to Major General Muhammad Shahid, Commandant College of E&ME and all his staff for rendering me all possible assistance and help in experimentation and compilation of thesis work.

ABSTRACT

The objective of the present study is to model mathematically the combination of Fluid Structure Interaction (FSI) due to Oil hammering, write a computer code against a mathematical model and then experimentally verify this model for a hydraulic system. The hydraulic system under investigation is a mobile crane. Also the study involves the destructive testing of the hydraulic system to optimize the thickness of tubes used for the flow of Fluid (oil) and experimentation for optimizing the number of clamps for holding the fluid lines.

The mathematical model presented here is the modified form of A.S. Tijssiling model (A.S. Tijssiling, 2007). In which he assumes pressure head while in this research pressure generated by a hydraulic pump driven by an electric motor is assumed. The model developed is one-dimensional quasi-static based on oil hammering and beam theories. The three interaction mechanisms such as friction coupling, poisson coupling and junction coupling are taken into account. The friction coupling represents the mutual friction between liquid and pipe. While the poisson coupling relates the pressure in the liquid to the axial stresses in the pipe through the radial contraction and the expansion of the pipe wall. It is he named after Poisson in connection with the his contraction coefficient and is associated with the breathing or hope mode of the pipe. The poison leads to the precursor waves. Junction coupling act as a specific point in a pipe system such as unrestrained valves, bends and tees. The Mac Cormac's scheme is used as a discritization tool for the solution of the given model.

The experiment has been carried out by making a hydraulic circuit which consists of an electric motor hydraulic pump lines or tubes, directional control valve and hydraulic jack. This experiment is similar to the experiment by Body and Fan of University of Dundy, UK (A.S. Tijssiling, 2007) whose apparatus consist of an isolated parts of a pipe system closed at end and connected with a tank situated at a height H.

Also Optimization of thickness of the tubes used for fluid flow is optimized by conducting destructive bursting testing of the lines. At the moment, the pipes thickness installed on the existing system are suggested on the basis of experience. The experiments show that the thickness of the tubes used for the fluid flow is over

designed and weight and cost of the system can be reduced by using tubes of smaller thickness.

Optimization of the number of clamps used for securing the fluid lines to the system and controlling the axial and flexural vibrations is carried out. Currently the number of clamps used is suggested on the basis of experience. The experiments show that the number of clamps used on the current system under production is too high and their number can be halved while maintaining a reasonable level of safety.

In summary the research study has resulted in the development of mathematical model for investigating the FSI in a oil based hydraulic system, developed an efficient code for easy use of the mathematical model for future researchers. The knowledge gained by the development of the FSI model for the hydraulic system would be critical for designing of future higher capacity hydraulic systems. Experiments were conducted and the mathematical model was found to be within 10% error range. Also experiments were conducted on optimizing the number of clamps needed to mount a hydraulic system's lines. Moreover thickness of the tubes needed to handle the pressure flow has also been optimized.

Table of Content

CHAPTER # 1

1 INTRODUCTION

1.1 Introduction

Fluid power is the technology which deals with the generation, control, and transmission of power using the pressurized fluids (either liquids or gases) when this power is used to provide force and motion to mechanisms. This force and motion could be in the form of pushing, pulling, rotating, regulating, or driving. It can be said that Fluid power is the muscle that move industry. Fluid power includes hydraulics, which involves liquids, and pneumatics, which involves gases. Liquids and gases are similar in many respects. [Anthony Esposito 2003]

Fluid power systems are designed specially to perform work. The work is achieved by a pressurized fluid bearing directly on an operating fluid cylinder or fluid motor. [Majumdar2002]

Fluid Power system has been in use at least as long as paddle wheels have been used to turn the grindstone as mills. However if we consider the more modern era in which we live, we can see that current-day Fluid Power system had their beginnings before the end of the nineteenth century when the invention of efficient prime movers, such as watt's steam engine and the development of the factory system spurred the need to develop a method of transmitting power from one point to another. At that time, transmission of power could be handled in a mechanical manner with belts and drive trains, but this proved to be difficult to control and accuracy of effort often was sacrificed.

The solution to this problem was sought to transmit power using fluid under pressure rather than a traditional mechanical systems. During the industrial revolution, the development of fluid power was emphasized and industrial countries such as England developed large hydraulic circuits using high pressure oil pipes and steam engines-driven pumps conveyed power to mills.[Majumdar2002]

These advancements in fluid power were quiet impressive. Near the World War II, application of power transmission characterized by high effort and fast response was needed. These applications were made manifest in the wartime machinery that was

required on warship gun turrets and land-roving vehicles. In this case electrical power was limited due to the fact that ferromagnetic materials saturate at the low flux density and therefore the torque output per unit mass of iron in a motor armature is relatively low. This means that transmission of large amount of torque using electrical devices is sluggish and that fast response for high torque devices must be sought elsewhere. So hydraulic transmission was the obvious solution to the problem because it offered a tremendous torque-to-inertia ratio and interestingly enough it is still the highest in the market place.[www.tpub.com]

1.2 HYDRAULIC Power Pack

Hydraulic Power Pack is a basic need for the Fluid Power system.

1.2.1 Basic Function:

The following five components are integrated in the form of one unit called power pack.

I. A tank (reservoir) to hold the hydraulic oil.
II. A pump to force the oil through the system
III. An electric motor or other power source to drive the pump
IV. Valve to control oil direction, pressure, and flow rate
V. Piping which carries the oil from one location to another

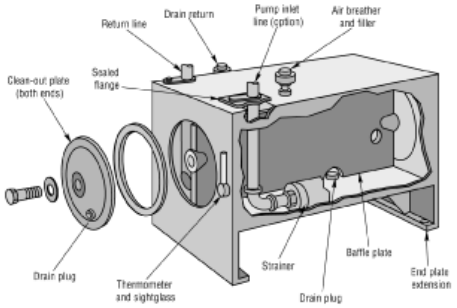

1.2.2 Description:

The hydraulic power pack is basically a complete package of hydraulic power source containing its own electric motor, pumps, shaft coupling, reservoir, piping pressure gauges, valves and other components as required for the proper and smooth functioning of hydraulic system.[Anthony Esposito 2003]

1.3 Hydraulic Oil:

1.3.1 Basic Function:

“Hydraulic Oil serves as a medium to transfer hydraulic oil pressure and flow to various part of hydraulic system” hydraulic oil has the following four primary functions:

- Transmit power
- Lubricate moving part
- Seal clearances between mating parts
- Dissipate heat [

1.3.2 Description:

An ideal fluid would have these characteristics: [Anthony Esposito 2003]

- Good lubricity
- Ideal viscosity
- Compatibility with system materials
- High degree of incompressibility
- Fire resistance
- Good heate transfer capability
- Low density
- Foam resistance
- Thermal stability (Nontoxicity)
- Hydrolytic stability(low volatility)
- Low chemical corrosiveness
- High anti-wear characteristics
- Low tendency to cavities
- Long life
- Total oil rejection
- Constant viscosity, regardless of temperature, and Low cost.

Typical Physical Characteristics

Shell Tellus Oil ISO Oil Type	T15 HV	T32	T46 HV	T100 HV
Kinematic Viscosity @ 0°C cSt 20°C cSt 40°C cSt 100°C cSt (IP 71)	 75 30 15 3.8	 32.4 6.4	 310 105 46 9.0	 960 268 100 15.5
Viscosity Index (IP 226)	150	155	150	150
Density @ 15°Ckg/l (IP 365)	0.872	0.868	0.874	0.877
Flash Point °C (Pensky-Martens Closed Cup) (IP 34)	150	160	180	190
Pour Point °C (IP 15)	-42	-45	-39	-30

1.4 HYDRAULIC Jack

Reliability of hydraulic system not only depends on the system design but also on factor such as component design and their correct choice. This is true while selecting the cylinder too. A good number of hydraulic system failures may be attributed to defect in

jack design. And in our system for the jack designing the contribution of FSI Analysis has an important role.[Anthony Esposito 2003]

1.4.1 Basic Function:

A device which converts Fluid Power into Linear mechanical force and motion. As the main source of transmission of power, a hydraulic jack should have optimum reliability.

1.4.2 Description:

A correct Hydraulic jack in a Fluid Power system contributes to:

- Optimize system maintainability
- Ensure minimum down time
- Ease the process of repairing and trouble shooting
- Maximize the rapidity of recommissioning of the machine and plant
- Ensure maximum work accuracy, and
- Maintain least economic liability and financial losses

1.5 HYDRAULIC Pipes, Hoses and Fittings

Pipes and tubes are very important parts in Fluid Power System and evolution of the hydraulic piping system is as interesting as other hydraulic components.

1.5.1 Basic Function:

A pipe can be defined as a functional connection for fluid flow in the Fluid Power systems and the fluid flow efficiency is greatly influenced by the physical characteristics of the piping system.

1.5.2 Description:

In hydraulic system iron pipes may be used for low to medium pressure range as they are widely available and economical. But the heavy wall thickness, lack of annealing characteristic and inability to absorbed high hydraulic pressure search are certain basic problems associated with iron pipes. Compare to iron pipes steel tubes are more commonly used because of their advantages. [Anthony Esposito 2003]

1.6 Crane

A mobile crane is a special machine which is used for lifting the loads. It is equipped with a telescopic boom with wire rope drum. The wire rope drum is actually used for

lifting/lowering the loads/ material and also move them horizontally. There is hydraulics jack(s) are installed below the telescopic boon to up and down the boom for loading purposes. One hydraulic jack is installed inside the telescopic section of boom in order to opening and closing the boom section.

A mobile crane is used as machine to produce a mechanical advantage and so a load can be move beyond the normal capability of a human.

In transport industry a crane can be used for the loading and unloading the weight, while in construction industry it can be used for the movement of construction material from one place to another place. [www.truckcranedirectory.com]

A design point view a mobile crane is very simple in construction but can perform Herculean tasks which would otherwise seem to be impossible. This machine is able to raise multi-tons bridge beams in construction of highways, heavy machines in factories and even lift beachfront houses onto pilings. [www.truckcranedirectory.com]

Figure 1-3 [Truck mounted crane Courtesy: www.truckcranedirectory.com]

Hydraulically operated cranes are commonly widely in the industry for lifting varying load capacities. In the fig 1-3 a hydraulic truck crane in action, it's hard to believe just how much weight it's moving because it deals with these multi-tons objects with relative ease.

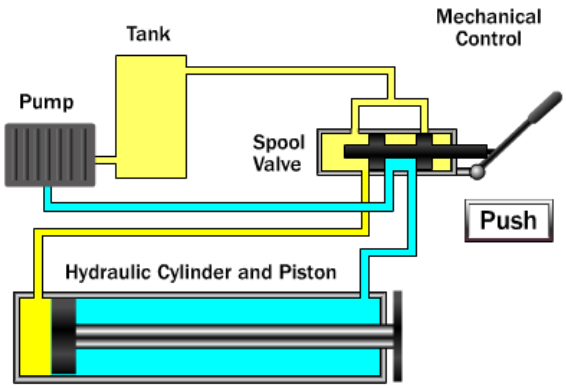

Mobile cranes are available in different power rating. It is very easy to understand that how much a particular crane can lift the load just by the name of i.e.: A 40-ton crane can lift 40 tons (80,000 lb or 40,000 kg). [www.truckcranedirectory.com]

Figure 1-4[Heavy duty hydraulic mobile crane Source: www.sciencehowstuffwork.com]

There is huge number of mobile cranes which have a boom with multi telescoping sections. In the fig 1.4 shown a 70-ton Link-Belt mobile crane that has a boom with three telescoping sections. This particular boom has a length of 127 feet (38.7 meters). Some booms are equipped with a jib, which is the lattice structure attached to the end of the boom. On the 70-ton hydraulic truck crane, the jib is 67 feet (20.4 m) long, giving the crane a total length of 194 feet (59.1 m). As the load is lifted, the sections telescope out to the desired height. [www. Sciencehowstuffwork.com]

Reinforced-steel cable lines run from a winch just behind the operator's cab, extending up and over the boom and jib. Each line is capable of holding a maximum load of 14,000 pounds (6,350 kg). So, a 70-ton hydraulic truck can use up to 10 cable lines for a total of 140,000 pounds (63,503 kg), or 70 tons. The lines run up the boom and jib and attach to a 285-pound (129 kg) metal ball that keeps the lines pulled taut when no load is attached to the hook. [www. Sciencehowstuffwork.com]

Mobile cranes provide brute strength to move objects, machines and even large animals that would otherwise be very difficult to budge. Using a very simple principle of hydraulics, these machines move thousands of pounds with relative ease, making them an essential component of most construction projects and a great example of the power of basic physics. [N. Steffen, 2001, Hydraulic in Mobile Equipment Bosch Rexroth AG]

1.7 Basic Concepts

In this section the author of this research will explain the important terminologies that will be used the preceding sections like, Oil hammering, cavitations, structural dynamics and fluid structure interaction FSI.

1.7.1 Oil Hammering

Oil hammering is basically hydraulic shock which is the cyclic increase in pressure, and normally occurs in a fluid power system when there is a sudden change of direction or velocity of the oil. When a rapidly closed valve suddenly stops oil flowing in a pipeline or tubes, pressure energy is transferred to the valve and pipe wall. Shock waves are set up within the system. Pressure waves travel backward until encountering the next solid obstacle, then forward, then back again. The pressure wave's velocity is equal to the speed of the sound; therefore it "bangs" as it travels back and forth, until dissipated by friction losses. Anyone who has lived in an older house is familiar with the "bang" that resounds through the pipes when a faucet is suddenly closed. This is an effect of oil hammer. A less severe form of hammer is called surge, a slow motion mass oscillation of oil caused by internal pressure fluctuations in the system. This can be pictured as a slower "wave" of pressure building within the system. Both oil hammer and surge are referred to as transient pressures. If not controlled, they both yield the same results: damage to pipes or tubes, fittings, and valves and accessories (Gauges etc.), causing leaks and shortening the life of the system. Neither the pipe nor the oil will compress to absorb the shock. [Skalak 1956]

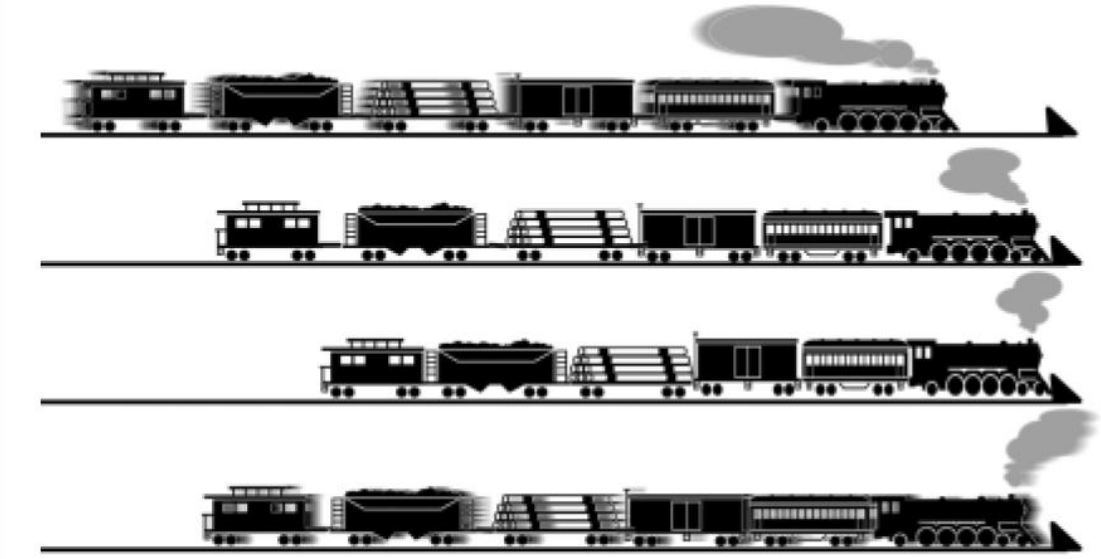

Figure 1-5 (Illustration of Oil Hammer phenomenon Source: Pickford, John1969)

A well know and self elaborated example of oil hammering is shown in a given Fig 1-5. In which a freight train is moving on a track with such speed and suddenly an obstacle is placed in the way of train. The train suddenly stopped by hitting that obstacle due to which some of the cabins move up from the track as shown in figure.

1.7.2 Causes of Oil Hammer:

In our mobile equipment of fluid power system in transportation of oil for load lifting the operating conditions are almost never at a steady state. Pressures and flows are commonly changes continually when pump starts and stop, a demand fluctuates, and tank levels almost changes. In addition to these normal events, unforeseen events, such as power outages and equipment malfunctions, can sharply change the operating conditions of a system. Any change in liquid flow rate, regardless of the rate or magnitude of change, requires that the liquid be accelerated or decelerated from its initial flow velocity. A rapid change in flow rate requires large forces that are seen as large pressures, which cause oil hammer. Entrained air or temperature changes of the oil also can cause excess pressure in the oil lines. Air trapped in the line will compress and will exert extra pressure on the oil. Temperature changes will actually cause the oil to expand or contract, also affecting pressure. The maximum pressures experienced in a piping system are frequently the result of vapor column separation, which is caused by the formation of void packets of vapor when pressure drops so low that the liquid boils or vaporizes. Damaging pressures can

occur when these cavities collapse. The causes of oil hammer are varied. There are, however, four common events that typically induce large changes in pressure:

Pump startup can induce the rapid collapse of a void space that exists downstream from a starting pump. This generates high pressures.

Pump power failure can create a rapid change in flow, which causes a pressure upsurge on the suction side and a pressure down surge on the discharge side. The down surge is usually the major problem. The pressure on the discharge side reaches vapor pressure, resulting in vapor column separation. [www.nesc.wvu.edu.com]

The opening and closing of a Directional Control Valve is fundamental to the operational activity of any oil base hydraulic system. Closing a valve at the downstream end of a pipeline creates a pressure wave that moves toward the hydraulic pump. Closing a valve in less time than it takes for the pressure surge to travel to the end of the pipeline and back is called "sudden valve closure." Sudden valve closure will change velocity quickly and can result in a pressure surge. The pressure surge resulting from a sudden valve opening is usually not as excessive. [A.S Tijsseling]

Improper operation or incorporation of surge protection devices can do more harm than good. An example is over sizing the surge relief valve or improperly selecting the vacuum breaker-air relief valve.

1.7.3 Cavitations

Oil hammering is not only lead to high pressure but it also develops due to low pressures. Low pressure can collapse the pipe, especially in case of underground buried pipelines. When the pressure comes below a certain level, cavitations are produce. There are two kind of cavitations gaseous and vaporous cavitations. Gaseous cavitations are developed when the pressure falls down below the saturations pressure of the gas, so that it comes out of its solution. This is relatively low process compared to vaporous cavitations. Vaporous cavitations are developed when the pressure drops down to the vapor pressure vapor cavitations are formed in liquid. When the vapor cavities appear as small tiny bubbles dispersed throughout the liquid along entire lengths of the pipe, it is also known as distributed cavitations. When the vapor cavities adhere and form one local bubble occupying a large part of pipe cross-section, it is known as a column separation. Column separations generally develop near the specific points in a pipe system like valves, pumps,

high points. Column separations are normally develop in pipe intermediate points when two low pressure waves are meet, the collapse of column separations is commonly attend with almost instantaneous pressure rises. These may be avoided by positioning air-inlet valves at critical points in piping system. An fluid power expert should try to prevent the cavitations.[Vardy, A.S.Tijssling]

1.7.4 Structural Dynamics:

By the Steady flow and oil hammering analyses we understand about the liquid behaviors under operational conditions. The Static pipe stress and structural dynamics analysis give us the corresponding behavior of the pipe system. Where, the structural analysis provides us the dynamic stresses, reaction forces and resonant frequencies. It is not unusual to perform an uncoupled calculation.[ ] Pressure and stresses histories which is shown in the preceding section, resulting from a oil hammer analysis, are used as the dynamic loadings in a structural dynamics analysis whose equation will derive in the coming section. The calculation is called uncoupled since the predicted structural response is not influence the liquid pressures. This procedure is doubtful since pipe motion can significantly affect dynamics pressures. [A.S.Tijssling & A.E.Vardy 2005]

1.7.5 Fluid Structure Interaction (FSI)

The Fluid-structure interaction in piping system consists of the transfer of momentum and forces between piping and the contained liquid during unsteady flow[A.S.Tijssling 2007]

1.8 Conclusion

The chapter reviews the basics of a hydraulic system. The components used in any hydraulics system are explained in details. The function use and principal of Hydraulic power pack, jacks, pipe (tubes) and fittings and their combination in a crane were discussed in detail. The phenomenon such as oil hammering and Cavitation which is FSI which is common in a hydraulic system are also explained. The knowledge reviewed in this section would be useful in the following sections. In the next chapter a brief introduction about the Fluid Structure Interaction, damaged from Fluid Structure Interaction, common sources of Fluid Structure Interaction are brief in detail.

CHAPTER # 2

2 INTRODUCTION TO FSI

2.1 Introduction

Fluid Structure Interaction is at the general term used for the physical phenomena where moving boundaries between fluid and solid play an important role. The moving boundaries cause a dynamic coupling which makes a simultaneous treatment of the fluid and structure necessary when modeling the phenomenon. In this chapter we introduce the basics of Fluid Structure Interaction, apparatus involved with Fluid Structure Interaction in the piping network of a hydraulic system, description of Fluid Structure Interaction, damages from Fluid Structure Interaction and common sources of Fluid Structure Interaction are explained.

2.2 Fluid Structure Interaction (FSI)

The term Fluid Structure Interaction (FSI) is a general term used to describe certain phenomena. Let us first define the meaning of the term, since it is sometimes misused. The important aspect is that there must be genuine interaction between a fluid and a solid component. This implies that, at interface a property of the fluid influences a property of the solid and, crucially, vice versa.

Fluid Structure Interaction (FSI) is normally occurs in liquid-carrying pipes when pressure waves in the liquid produce stresses and strains in the pipes (and vice versa) by [A.S. Tijsseling.]

This project is concerned with Fluid Structure Interaction (FSI), using the term in its most common sense that is interaction of forces and the corresponding moment of the interface (momentum interaction) rather than thermal interaction. The movement of the solid because of momentum exchange with fluid can occur in one of two ways Fig 2.1: by the local deformation of the solid body, or by rigid body motion. The FSI is commonly used in flow of liquid in pipes to describe the effect of pressure on rigid body motion on complete structure. Extensive reviews by A.S. Tijsseling (1996) and A.S. Tijsseling and Wiggert (2001) describe the work perfume in this area. However this project investigate

the interaction the local deformation of stainless steel tubes and liquid pressure, in particular its effect on the propagation of pressure waves.

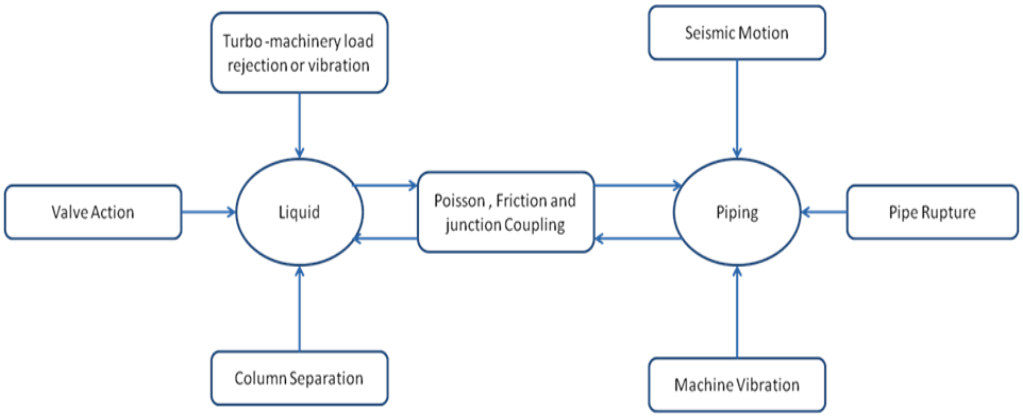

Figure 2- 1 [Source of Excitation and interaction between liquid and piping]

2.3 Description of FSI

Fluid-structure interaction in piping systems is basically the transfer of momentum and forces between piping and the contained liquid during unsteady flow. An Excitation mechanisms is also seems due to sudden changes in flow/velocity and pressure or due to the mechanical action of the piping. This interaction is manifested in pipe vibration and perturbations in velocity and pressure of the liquid. The resulting loads imparted on the piping are transferred to the support mechanisms such as clamps,& Structure , etc.[www.win.tue.nl.com]

Friction, Poisson and Junction Coupling are three types of liquid pipe coupling. Those coupling which are act along the entire pipe (distributed forces) are friction and Poisson coupling whereas that coupling which act at specific points (local forces) is called junction coupling or in other words junction coupling act at a junction or discontinuities in the piping systems).[Puddussis, A.S Tijsseling]

"Poisson coupling is associated with the circumferential Hoop stress perturbations produced by liquid pressure transients that translate to axial stress perturbations by virtue of the Poisson ratio coefficient. The axial stress and accompanying axial strain perturbations travel as waves in the pipe wall at approximately the speed of sound in solid beams. Typically the magnitude is three to five times greater than the acoustic velocity in the contained liquid in the pipe". [A.S Tijsseling]

The transient liquid shear stresses acting on the pipe wall forms friction coupling; normally it is insignificant when compared to the other two junctions and poisson coupling mechanisms. Along the axis of a pipe element there is both Poisson and friction coupling are distributed.

The Junction coupling, that is develope from the reactions set up by unbalanced pressure forces and by changes in liquid momentum at discrete locations in the piping such as bends, tees, valves, and orifices. Sources of excitation include not only those associated with liquid motion, but also from the structural side, see Fig. 2-1.[Vardy and Fan]

In stainless steel piping, oil hammer waves impacting at junctions may set up vibrations that in turn may translate to a variety of structural responses such as bending, torsion, shear, axial stresses at locations distant from the junction. In addition, the vibrating junction will induce fluid transients in the contained liquid column, with acoustic waves traveling away from the junction. The result will be complex interactive motions in both the piping and liquid, with subsequent waveforms highly dependent on the geometry of the piping structure.

To study the fluid structure interaction (FSI) in liquid carrying piping systems, I started the literature study by Wiggert (1986) and A.S.Tissling review paper which was very helpful. There was two aim: (i) to be starting-point for researcher who are new in the field of FSI and (ii) to be a state-of-the-art record of relevant contributions to the FSI.

FSI is presented as an extension of conventional oil hammer theory, as in Skalak's (1956) classical article. FSI, and some practical sources of excitation, are shown schematically in Figure 2-2.

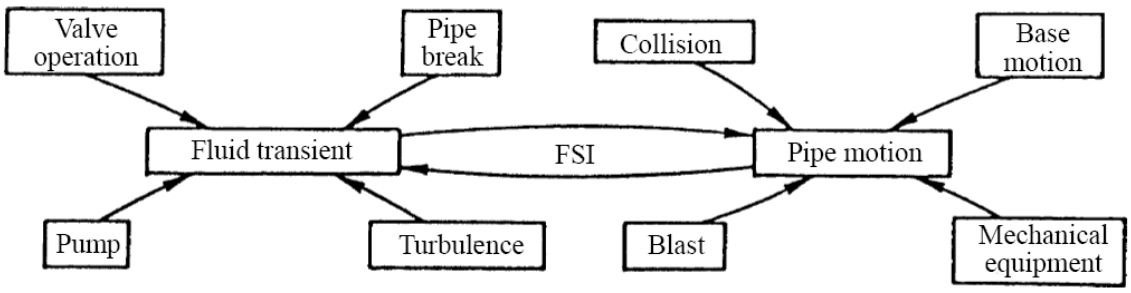

Figure 2- 2 [Sources of Fluid transients and Pipe motion]

Severe dynamic forces have been experience in piping system during an oil hammer event in case of mobile crane activity. Due to these forces the system move and so the FSI phenomenon occurs. So we will not treat separately the liquid and pipe systems in a theoretical analysis that is interaction mechanisms have to be taken into account. In the majority of the analyses reviewed, the pipes are slender, thin-walled, straight, prismatic and of circular cross-section. The liquid and the pipe-wall material are assumed linearly elastic and Cavitation is assumed not to occur .The theories developed are valid for long (compared to the pipe diameter) wavelength, acoustical (convective velocities neglected) phenomena. Important dimensionless parameters in FSI analyses are (i) the Poisson ratio, (ii) the ratio of pipe radius to pipe-wall thickness, (iii) the ratio of liquid mass density to pipe-wall mass density , and (iv) the ratio of liquid bulk modulus to pipe-wall Young's modulus. When the hydraulic and structural mass and elasticity, and hence the propagation speeds of pressure and stress waves , are of the same order of magnitude, FSI is likely to be of importance, provided that the transient excitation is sufficiently rapid . FSI is usually of no importance in gas-filled pipes because the mass density and elasticity (bulk) modulus of gases are negligible compared to those of solid pipes. A classification of one-dimensional FSI models according to their basic equations, written as a hyperbolic set of first-order partial differential equations, is often made, where the liquid pressure and velocity are the only two unknowns. The four-equation (two-mode) model allows for the axial motion of straight pipes, axial stress and axial pipe-wall velocity are the additional variables.

The objective of the present study is to model mathematically the combination of fluid structure interaction (FSI) due to Oil hammering and to write a computer code against a mathematical model. Validate the model with the experimental result.

The mathematical model presented her is the modified form of A.S. Tijsseling model. In which he assume pressure head while the author of this research will assume pressure. The model is one dimensional quasi static based on oil hammer and beam theories. The three interaction mechanism such as friction coupling, poison coupling and junction coupling are taken into account.

The friction coupling represents the mutual friction between liquid and pipe. While the poison coupling relates the pressure in the liquid to the axial stresses in the pipe through the radial contraction or the expansion of the pipe wall. It is the name after Poisson in

connection with his contraction coefficient ν , and is associated with the breathing or hope mode of the pipe wall. The poison leads to the precursor waves.

Junction coupling act as a specific point in a pipe system such as unrestrained valve, bends and tees. The numerical approach is on the discritization method and Mac Cormac's scheme has been used.

The experiment has been carry out by making a hydraulic circuit which consist of an electric motor hydraulic pump lines or tube directional control valve and hydraulic jack. This experiment is like the Body and Fan of University of Dundee UK who's apparatus consist of an isolated parts of a pipe system closed at end and connected with a tank situated at a height H.

2.4 Damage from FSI

Symptoms of FSI include vibrations, noise and fatigue damage to piping, supports and machinery. Other disruptions include leaking flanges, burst rupture disks, relief valve discharges and pipes jumping off their supports. FSI is not a widely recognized phenomenon and it is quite feasible that it is responsible for a significant number of unexplained piping failures and other unacceptable behavior.

Failures due to FSI are often attributed to other factors. For example, failure due to fatigue could in fact be FSI induced; failure due to corrosion could again be partially attributed to FSI, i.e. a weakened area together with an FSI event resulting in rupture.

2.5 Common Sources of FSI

The review of standards and other publications has enabled some key configurations to be identified. Some of these are especially important in the prediction of risk from transient failure; others are more significant indicators of potential vibrational disturbance. The generic issues are:

2.5.1 Long lengths of unsupported or poorly supported pipe network

When long lengths of pipe are poorly supported, there is a high probability of unacceptable response to external stimulus or to fluid-induced movement. More often than not, the response will be of a vibration nature giving rise to noise such as banging and rattling. It is also possible, however, for long lengths between supports to contribute to catastrophic responses to sudden events, including, for example, jumping off supports.

2.5.2 Unsupported/unrestrained elbows

Elbows are very commonly cited as potential sources of trouble from FSI. They are especially important in the response to fluid transients because sudden changes to rates of flow give rise to sudden changes in pressure and momentum forces on the pipe structure. Big accelerations can result, implying a need for very highly restraint forces to prevent significant pipe movement.

2.5.3 Unsupported/unrestrained valves

The action of valve closure or, less commonly, valve opening can give rise to extremely rapid transients, implying sudden changes in pressure forces. When these are imposed on valves that are not heavily restrained axially, significant axial pipe motion can occur. Such motion can damage the pipe adjacent to the valve itself. Alternatively, it can cause damage at more remote locations – for example, at an elbow at the other end of a straight length of pipe terminating at the valve.

2.5.4 T-junctions

T-junctions can occur in many forms. An obvious type is broadly similar to two mirror-image elbows acting together. In this case, a pressure or stress transient arriving along the central limb may be expected to induce sudden movements causing potentially significant axial stresses in the central limb.

Another important case is a T-junction where the lateral restraint of the central limb is much stronger than the axial restraint of the other two limbs. In this case, any induced axial movement of the latter pair will cause large shear and/or bending forces in the connection. This is an especially severe loading condition when the central limb is of smaller diameter than the main limbs. When assessing the degree of lateral restraint, it is important to allow for the lateral inertia of the central limb because this is a disadvantage in the situation under consideration. Special examples include bleed pipes with lumped masses such as valves.

2.5.5 Vibrating Machinery

Any vibrating object to which pipe network is connected will induce vibrations in the pipe network. These will be a potential stimulus of pipe vibration, the intensity of which will depend, in part, on the proximity of the frequency of vibration to a natural frequency of the pipe network.

2.6 Structural excitation

The most common cause of structural-induced FSI is vibrating machinery. Are our pipes connected directly to any pumps or other machines with rotating parts? If so, are it should be mounted in such a way that they can vibrate strongly? If the answer to these questions is "no", have another look to check that no source of vibration is likely to be transmitted to a pipe through its supports. This will always be possible in the case of earthquakes, but there might be less obvious causes - vibrations transmitted through the structure of the building, for example. You might also need to consider direct external impact from random causes. It is unlikely that these will be caused routinely, but they might result from such things as vehicle impact (from fork-lift trucks, for example).

2.7 Fluid excitation

The most common sources of fluid-induced FSI are pressure waves and slug flows. In addition to these, however, there is a small chance that flow instabilities might be a source of trouble.

Pressure waves are generated whenever a flow is caused to accelerate or decelerate. The most common cause of such behavior is a valve and problems are far more likely to arise from closing a valve than from opening it. So ask: "do you have any valves and are there any circumstances when they might be closed rapidly?" Interpret the word "valve" liberally. Include, for example, bursting diaphragms used for pressure relief.

Explosions are another good source of pressure waves. They cannot occur in most systems (e.g. oil-filled pipes) but they occasionally occur when chemically active fluids are transported. Indeed, this can be an intended outcome of certain processes. If so, it is likely that you will know where they might occur.

The above examples deal with inherently unsteady flows. Another possibility is the (nominally) steady flow of a strongly inhomogeneous fluid. Examples include liquid slugs in gas flows and gas slugs in liquid flows. When a slug reaches a pipe elbow, for instance, it can cause much bigger forces than those present when the gas phase exists locally.

Sometimes, instabilities can arise spontaneously. One example is valve flutter - where the fundamental frequency of vibration of a valve coincides closely with the fundamental

frequency of a fluid vibration. Float valves in domestic oil systems used to be a rich source of entertainment in this respect.

2.8 Conclusion

The chapter introduced the basics of FSI, a brief history of FSI, the damage caused by FSI and its common sources. Then the importance of the FSI for an oil based hydraulic system are explained and details are presented. The knowledge review in this chapter would be utilized in the subsequent sections to solve problems related to FSI in the pipes of an oil based hydraulic system. In the next chapter a review of literature is given in detail.

CHAPTER # 3

3 LITERATURE REVIEW ON FSI

3.1 Introduction

The chapter gives a detail literature review on FSI. Details of the phenomenon related to FSI such as Oil Hammering, Cavitation, Wave Propagation, junction and Poisson coupling are presented. The use of analysis software for structure and fluid coupling are also explained. The information reviewed in this chapter is to be utilized in the modeling and experimentation sections.

3.2 Review of Literature

In this section literature referring to the subject water Hammer, oil hammer, Cavitations, and fluid-structure interaction (FSI) is reviewed.

3.2.1 Water Hammer

The Water Hammer phenomenon first time introduced by Menabrea [1858, 1862]. After this several other publications were seen in the second half of the 19th century, the present oil hammer theory is based on the classic investigations of Joukowsky [1898] and Allievi [1903]. Joukowsky derived the following relation that he is experimentally validate in his experimentation conducted in the Moscow oil distribution system.

$$\Delta P = \rho f \, cf \Delta V$$

Frizell [1898] and early by Rankine [1870] derived the same relation. Where ΔP is the change in pressure, ΔV is the change in velocity, ρc is constant factor and ρf the mass density of fluid cf the velocity of sound in the fluid. In this experimentation Joukowsky used the sound velocity according to Kortewege [1878], which takes into account both the compressibility of the fluid and the elasticity of the pipe walls,

[Allievi 1913] has excellently explained mathematical treatment of the water hammer equations. [Allievi 1913] way of solution has been in use until the more practical graphical method was developed. This method is connected with the names of Schnyder [1929] and Bergeron [1935], although there were a few predecessors.

In the early sixties with the introduction of digital computers, water hammer calculations evolve to their present form. The method of characteristics (MOC) have becomes the standard numerical approach. Classic textbook of Streeter and Wylie [1967] can be found for all fundamentals. While paynter [1961], Wood [1970], Martin [1973], Anderson [1976] and Thorley [1976] can be seen for historical review.

3.2.2 Cavitation:

Cavitation is a a most important phenomenon in fluid power system and is a broad field of research. For information on the physical phenomena on a microscopic level, Simpson in [Simpson 1986] has given an excellent review on Cavitation due to water hammer which can be interpreted for the oil hammer also [A.S.Tissling]. Various models have been reviewed in De Almeida [1987] that are in use to stimulate transient Cavitation.

The first work on vapor cavities and column separation to Hogg & Trails [1926] and Langevin [1928] is attributed to Thorley [1976]. Angus [1935, 1937ab]. LeConte [1973], Knapp [1973ab, 1939] and Bergeron [1939] reviewed by in Simpson [1986] in which he completely surveyed the mid eighties work regarding the column separation and the work performed in Delft. The Occurrence of column separation at specific point in a pipe system; the danger of high pressures following cavity collapse is recognized in his early investigation.

By [Bergeron 1950; Streeter & Wylie 1967] column Separation can be adequately modeled in a simple manner. The models presented by [Baltzer 1967, Siemons 1967] was basically the **separated flow model** in which he assumes the cavities to coalesce at the upper part of a pipe, and forming one thin layer of vapor and/or gas and Regions of cavitating fluid are then treated as open-channels flows. A problem of appearances of gravity waves is encountered in this kind of modeling and the numerical treatment of the moving boundaries between cavitating and non-cavitating regions. Furthermore, the model is physically incorrect for vertical pipes.

[Kalkwijk & Kranenburg 1971] presented **the bubble flow model** which was more realistic in sense of distributed Cavitation. He treated the cavitating region as one- dimensional two phase flow and assumed that cavities dispersed throughout the region [Wallies 1969]. The numerical instabilities, the formation of shock waves and propagation of pressure-dependent wave are the difficulties of this way of modeling. That is why the Column

separations must be treated separately. According to the concentrated cavity models, that is also known as discrete or lumped cavity model, column separations and distributed cavitations regions are model mathematically in the same way. In this Cavities are allowed to form only at a fixed number of locations along the pipe. Pure liquid is assumed to exit between these locations. The occurrence of spurious oscillations and unrealistic pressure spikes are the great disadvantages of this method.

The concentrated cavity model have been used because of its simplicity, its general applicability and the fact that it fits in with the method of characteristic (MOC) approach employed in standard water hammer or oil Hammer calculations. It is validate from its predictions and the result of laboratory and field test. Provoost [1976] validates the model for laboratory experiments and fields measurements in his research with a 27.9 km long pipeline and a diameter of 1.8 m. Field measurements in a 12.3 km long, 0.25 m diameter, pipeline has been in Sharp [1977] research , in which he allows cavities to form at not more than six locations. Nevertheless he obtains reasonable result.

A clear explanation of the concentrated cavity model and use experiments in a 9.15 m long closed tube for validation is given by Kot & Youngdahl [1978ab]. A model has been applied to oil flow in a 250 m long, 0.09 m diameter, test rig by Aga et al. [1980]. A maximum pressure due to collapse of column separations in various pipe configurations investigatd by Gottlieb et al. [1980] and graze & Horlacher [1983]. They have use discrete cavities in their simulations. Evans & Sage [1983] have developed the model and use it for the oil hammer and oil hammer analysis of a practical situation. Carmona et al. [1987] have done an extensive measurements in a laboratory and set-up resembling that of [Provoost 1976] and showed numerical result as well.

An excellent agreement between computations and experimentation have been found by Golia & Greco [1990] with the data provided by Martin [1983]. Twenty three experiments have been performed in a nearly 5000 m long, 0.11 m diameter, and test circuit that are reported in Barbero & Ciaponi [1991]. They examine in their calculations the influence of initial free gas and gas release. Anderson et al. [199lab] has discuss many aspect of the concentrated cavity model and they show results of laboratory measurements for three levels of Cavitation severity. An excellent agreement between simulations and field data obtained in a 47 km long cross-country pipe line with a diameter of 0.84m by Wang & Locher [1991] which was very surprisingly.

The validation test quoted above it can be concluded that, despite its simplicity, the concentrated cavity model reproduces the essential features of transit cavitations. The versatility of the have been demonstrated by the variety of pipe systems used in the test. The appearance of non-physical oscillations in result is the major deficiency of the model which have highlighted by Wylie & Streeter [1978b]. The reduction and the generation of numerical oscillations and unrealistic pressure spikes have been studied by Provoost & Wylie [1985] in their papaers.

Streeter [1983] and Simpson [1986] have presented a physically better models. Streeter's consolidation method treats distributed Cavitation region in sloping pipes as areas of constant pressure moving under the influence of gravity and friction forces. Column separations are allowed to form at specific locations of the pipe system. The work performed by Simpson [Simpson 1986; Simpson & Wylie 1986, 1991; Bergant & Simpson 1992] is based on that of Streeter. However, his interface model allows column separation to form at any point in a pipe system when ever two low pressure waves meet. In [Simpson 1986] he compares predictions of both the interface model and the concentrated cavity model with experimental data obtained in a 36 m long upward sloping pipe of 0.02 m diameter. Although the interface model gives reliable result, it is too complicated for general use.

3.2.3 Fluid-Structure interaction (FSI)

3.2.3.1 Early developments

In the 19th century, the studies of standing waves in musical instruments and pulsatile flows in blood vessels asked for an accurate determination of the sound in fluid. The sound velocity in unconfined fluids was and is known to be

$$C_0 = \sqrt{\frac{K}{\rho_f}} \dots\dots\dots\dots\dots\dots\dots 3.2$$

Where K is the bulk modulus of the fluid. For liquids constrained in a tube the sound velocity was found to be much lower. Van Helmhotz [1848] correctly attributes his effect to the elasticity of the tube walls. Young [1808], Weber [1866], Resal [1876], and Moens [1878] have shown the formula for incompressible fluids in elastic tubes, like rubber hoses and blood vessels.

$$C_1 = \sqrt{\frac{Ee}{\rho_f D}} \ldots\ldots\ldots\ldots\ldots\ldots 3.3$$

Where E is Young's Modulus of the wall material, e is the wall thickness and D is the internal tube diameter. Korteweg [1878] derived the formula for compressibility fluids in elastic tubes:

$$\frac{1}{c_f^2} = \frac{1}{c_0^2} + \frac{1}{c_1^2} \ldots\ldots\ldots\ldots\ldots\ldots 3.4$$

Which is equivalent with

$$c_f = \sqrt{\frac{K}{\rho_f}\left(1 + \psi\frac{DK}{eE}\right)^{-1}} \ldots\ldots\ldots\ldots\ldots\ldots 3.5$$

Where the coefficient $\psi = 1$. The coefficient ψ is explained in subsection 3.2.4.

Formula (3.5) gives the pressure wave speed c_f used in standard oil hammer calculations. For compressible fluids in inelastic tubes, E>>K, c_f equals c_0, Where as for incompressible fluids in elastic tubes, K>>E, c_f equals c_1.

Kortewge [1878] considered the tube as a series of mass less rings expanding and contracting in accordance with the internal fluid pressure while deriving the formula (3.5),

P The hoop stress, σ_ϕ and the radial displacement, u_r of a ring are given respectively by

$$\sigma_\phi = \frac{R}{e}P \ldots\ldots\ldots\ldots\ldots\ldots 3.6$$

$$u_r = \frac{R^2}{eE}P \ldots\ldots\ldots\ldots\ldots\ldots 3.7$$

Where R is the inner radius of the tube. The tube walls follows the liquid, there is no question of fluid-structure interaction. Axial stress in the tube wall, σ_z and tube wall inertia are neglected:

$$\sigma_z = 0 \ldots\ldots\ldots\ldots\ldots\ldots 3.8$$

$$\rho_t = 0 \ldots\ldots\ldots\ldots\ldots\ldots 3.9$$

Where ρ_t the mass density of the tube wall material.

Kortwege in Kortewege [1878] has indicated that his theory is valid for long wave lengths. He has also highlighted that effects of Poisson's ratio occur when the axial stress in the wall of are not neglected. He has also explained that when, axial tube wall inertia is taken into account, axial stress waves will propagate along the tube. He has also investigated the influence of radial inertia. He has showed that for short wavelengths the radial inertia of both fluid and tube wall becomes of importance, there by leading to wave speeds varying with the wave length.

Jouksky [1898],has quoted the idea of Gormeka [1883] that taking pipe wall inertia into account when considering the incompressible fluid in elastic tube. He has given a bi-quadratic equation from which two wave speeds follows: one for the pressure waves in the fluid and one for the axial stress wave in the tube walls. Lamp's [1898] workr is very complete in the sense of treatment of the combined axial and radial vibrations of a fluid-filled tube. Poisson coupling is included in work performed by Lamp. Lamp has highlighted three kinds of vibrations, i.e.

I. The pressure waves in the fluid as modified by the yielding of the tube,
II. The axial vibrations of the tube wall as modified (very slightly) by the presence of the fluid, and
III. The radial vibrations of the system.

An equation which relates phase velocities to wavelengths has been derived by Lamp in which he said that for long wavelengths the pressure waves and the axial stress waves are predominant, with the propagation speeds close to cf and ct, respectively, where

$$c_t = \sqrt{\frac{E}{\rho_t}} \dots\dots\dots\dots\dots\dots 3.10$$

and c_t is given by (3.5). The radial vibrations are important only for short wave lengths. An extensive survey of the developments in the 19th century has been given Boulanger [1913] .

Wave propagation modes

Numerous researchers dealing with the problem of wave propagation in fluid-filled cylinders has extended the Lamb's [1898] work. Some researchers have used general approach i.e. to apply Fourier analysis to the basic equations and derived a dispersion equation is then derived, from which the natural modes of wave propagation achieved.

The under mentioned study is the basic idea presented by Richard Skalak [1956] presentation. He has extended the Lamb's [1898] work by including bending stiffness and rotatory inertia in his axially symmetric tube model. The equation in research he finds an infinite number of wave propagation modes. He observed that when the wave length approaches infinity and frequency approaches zero then only two lowest modes have a finite phase velocity. The first lowest mode corresponds to the pressure waves in the fluid, while the second lowest to the axial stress waves in the tube wall. The phenomenon of precursor waves is mentioned with the aid of clear pictures. Without dispersion effects simplified equations are given which permit precursor-type solutions.

A work has been presented by Lin & Morgan [1956ab] which was very similar to Skalak's work. They have considered transverse shear deformation in their tube model instead of bending stiffness and rotatory inertia. It is also noted that these matters are of importance only in the high frequency range.

Herrmann & Mirsky [1956] consider an empty tube and find basic equations that slightly differ from those of Lin & Morgan [1956a]. They survey the various models which are in use for axially symmetric motions of thin-walled cylinders. Equations governing the non-axially symmetric motion of cylinders are given in [Mirsky & Herrmann 1957], where as in [Mi & Herrmann 1958] thick-walled cylinders are considered.

In Spillers [1965] and Tang [1965] they have applied the method of characteristics to, respectively, Herrmann & Mirsky's and Lin & Morgan's equations.

King & Frederick [1968] have used Lin & Morgan's equations which was the extended theory of Skalak's work. They have applied a Hankel transformation to the two-dimensional fluid equations; they also find infinite system of one-dimensional wave equations for the fluid, and a finite set from this system along with three one-dimensional

wave equations for the tube have transformed into ordinary differential equations by means of the method of characteristics.

Skalak's approach have also been followed by Thorley [1969], but here he neglects transverse shear deformation, rotatory inertia and, partly, bending stiffness. He was the first who has observed the precursor waves. He has done the experiments with polythene pipes of 0.05 m diameter and 0.005 m wall thickness of steel and of aluminum alloy.

Lin & Morgan's has been extended by DeArmond & Rouleau [1972], in which they considered a viscous liquid in an elastic tube. In this research they have concentrated on the two lowest modes of wave propagation. The study for a viscous liquid in a visco-elastic tube for infinitely many mode has been discussed in study presented by Rubinow & Keller [1978]. In Kuiken [1984abcd], he has presented the comprehensive study on encompassing viscous liquids or gases, orthotropic visco-elastic tubes, pre-stressed and surrounded by other materials, and thermodynamic effects.

The advanced study of wave propagation in fluid-filled tubes is very important especially, in respect to pulsatile flows in mammalian arteries. For the description of pressure waves in piping systems one or two-mode of solutions are good enough. In which one-mode solutions can be found with classical water hammer theory, while two-mode solutions can calculated from the approach presented by A.S.Tijsseling [1999]. in which the tubes were assumed to be thin-walled.

3.2.4 Speed of Propagated Wave

With the classical water hammer theory, formulae for the pressure wave speed in both thin- and thick-walled pipes has been given in Halliwell [1963]. He has discussed the disparity in wave speed formulae available in the different textbooks. These disparities are due to the way pipe support conditions are considered. In Literature theoretically there are analyses three support conditions are given:

- "Pipe anchored with expansion joints throughout,
- Pipe anchored throughout against axial motion, and
- Pipe anchored at its upstream end only". A.S.Tijsseling [Review]

The correction factor ψ in the wave speed formula (3.5) accounts for the different support conditions. Support condition 1) corresponds to the situation described by Korteweg [1878], in which the axial stresses are neglected ($\psi = 1$). In condition 2) the axial

displacements are neglected, leading to $\psi = 1 - \nu^2$. In condition 3) the axial stress in the pipe wall is assumed to be proportional to the fluid pressure acting on a closed valve downstream, giving $\psi = 1 - \frac{\nu}{2}$. In deriving the values of ψ pipe wall inertia is neglected, so that quasi-static conditions prevail. The support condition 1) and 3) allow for axial pipe motion. For these cases it is assumed that the axial stress in the entire pipe is permanently equal to its value at the anchors or to its value at the valve. This approach is valid for a unique wave speed for a single pipe supported at its ends, which is physically correct since the wave speed should not depend on the end conditions: a disturbance generated at the middle of the pipe, and traveling at finite speed, does not know in advance which situation it will meet at the pipe ends. In this respect it is noted that ignoring axial pipe wall inertia leads to axial stress waves theoretically traveling at infinitely high velocity, so that the end conditions are permanently felt along the entire pipe.

3.2.5 Junction coupling

According to the classical Water hammer theory the fluid-structure interaction occur when the support conditions allow for pipe motion. Theoretically the most important interaction mechanism is junction coupling (As explain in section # 2). In fluid power system a pipe consists of straight sections of pipe, connected with elbows, tees and diameter changes, and terminated by reservoirs, pumps and valves. Here we consider the the connecting and terminal points as junctions. When a junction has the possibility to move in the axial pipe direction, which is the direction of the pressure waves, mutual forces between fluid and pipe system may cause a dynamic interaction, which is known as junction coupling.

A study regarding investigation pressure and velocity fluctuations in a straight pipe filled with rocket fuel has been presented in Regetz [1960]. In His experimental setup he has allow the pipe for axial pipe motion. He has tabulated the Pipe velocities at the unrestrained pipe end and these velocities have been incorporated in a standard water hammer analysis in the in frequency domain. He has observed that tha pipe motion has a definite effect on the fluid behavior.

Blade et al. [1962] followed the work presented by Regetz. He has experimented with a flexibly supported elbow included in the pipe system. He has modeled the Junction coupling by relating pressures and velocities in the fluid to stresses and velocities in the

pipe according to the local force equilibrium and continuity. Axial pipe motion is simulated by means of a spring-mass system.

In D'Souza & Oldenburger [1964], in the title of dynamic response in the fluid lines, they studied about the pressure waves in the fluid interact with stress waves in the pipe wall by way of junction coupling at an unrestrained pipe end. They have solved their basic equation by using the Laplace transformations in a frequency response. They have experimented for straight pipe filled with hydraulic oil and a very good and an excellent relation has been studied in between theory and experiments.

In the research presented by Davidson & Smith [1969] , they model curved pipes in a Timoshenko-beam-like manner with liquid-pipe interaction. The same model was validated against results of frequency response tests in an oil-filled single-elbow pipe system. In the work performed by Davidson & Samsury [1972] they have extended the work of Davidson & Smith to non-plane multi-elbow configurations.

A clear explanation of junction coupling in terms of moving hydraulic discontinuities has been presented by Wood [1968, 1969]. His research is basically a time-domain analysis in which the structure is represented by a spring-mass system while the fluid pressure is the driving force. In experimentation he use apparatus consists of a rigidly supported straight pipe terminated by a spring-mass device. The liquid is subjected to periodic disturbances in [Wood 1968], whereas in [Wood 1969] the system is excited by rapid valve-closure. In the latter it is shown that pressure rises may significantly exceed Joukowsky's value (3.1), when axial pipe motion occurs. A number of tests have been carried out on 30, 60, 90, 120 and 150 degrees meter bends and on a 90-90 degrees T-junction. No attempt has been made to model the structure; measured junction velocities have used as input to the analysis. It is concluded by his research that rigidly supported junctions have a negligible influence on pressure waves, whereas unrestrained junctions affect them significantly.

In Jones & Wood [1972] they have presented an analytically expression for the junction coupling induced pressure oscillations around Joukowsky's value in case of rapid valve-closure downstream in a single pipe. The experimental setup was the pipe consists of a spring-mass system. Results are compared with measurements in an unrestrained vertical pipe.

A junction coupling at a check-valve, a T-branch and 90 degrees are bend in an analysis of a practical system has been considered in the research of Ellis [1980]. He has modeled the pressure waves and axial stress waves. Flexural motion is accounted for by a spring-mass system. He has used the method of characteristics for the solution of the basic equations.

3.2.6 Junction and Poisson Coupling

In the research of D'Souza & Oldenburger [1964] and Ellis [1980] they have only modeled the axial stress waves in the pipe wall. However, they have not considered for Poisson coupling, which is the FSI-mechanism that relates internal fluid pressures to pipe wall axial stresses.

A rigorous mathematical treatment of axial wave propagation in liquid-filled co-axial cylinders, including Poisson coupling has been presented by Burmann [1974ab, 1975, 1980b]. He has solved the basic equation by the method of aracteristics (MOC). Non-axial effects are studied in [Burmann et al. 1979, 1983, 1 987c]. In Burmann [1980a, 1983] he compares the responses of three different tube models to oil hammer following by the rapid closure of a rigidly supported valve. In this study Burmann concluded that shell theory is very important for very short pipes and for achieving accurate solutions in the vicinity of very steep wave fronts. The classical oil hammer theory fails to predict pipe motion. The membrane theory is sufficient for most practical purposes in combination with extended oil hammer equations allows for precursor waves. In [Thielen & Burmann 1980; Burmann et al. 1980] they have presented a four-equation model to describe the coupled axial motion of pipe and liquid. In principle this was the simplified model of Skalak [1956]. A valuable and impressive series of field measurements in order to validate the theoretical work has been carried out by Burmann, and his group. In the research presented by [Burmann 1979; Burmann & Thielen 1988] they have tabulated the measurements on the filling pipe of a subterranean salt cavern. The pipe is shows motion in axial and lateral direction when it is excited by oil hammer due to pump stop. In [Bunnann et al. 1985, 1986b, 1987a] the pipe bridge of a oil main across the river Neckar is studied. Coupled motion of liquid and pipe is generated by rapid valve opening. At one end the pipe was lifted from its support to enhance axial motion.

A loading line, used for liquid transport between storage tanks and ships, has been studied in [Bunnann et al. 1986a, 1987b]. In this research they have used detailed description of the measurements and the corresponding simulations for all three cases. A very good relation seen that satisfactory agreement found between theory and field data, although measured data has been used as input in the simulations.

A theoretical study on the propagation of short duration pressure pulses in a straight elastic pipe, including Poisson and junction coupling has been studied by Walker & Phillips [1977]. They have derived a system of six-equation model in radial fluid and pipe inertia is taken into account.

An excellent experimental results has been achieved in steel, ABS and PVC pipes by Williams [1977].A tabulated data has been recorded in which the effect of pipe motion, brought about by axial stress waves, is clearly visible.

The propagation of axial stress and pressure pulses in oil- filled aluminum and acrylic plastic tubes has been studied by Krause et al. [1977]. A number of experimentation has been done by using a closed tube supported partly by strings and partly by blocks and very short duration pulses are generated by firing steel spheres onto the tube ends.

An extensive numerical study on coupled axial liquid and pipe motion in a single straight pipe has been done by Schwarz [1978]. He started with a six-equation model and solves it with the Method of Characteristic MOC. His approach was similar to that of Walker and Phillips [1977].

In Michigan State University the first research in respect of the fluid structure interaction in liquid filled pipe system has been with joint efforts of Wiggert (fluid mechanics) and Hatfield (structural mechanics). The same author has also worked with Otwell, Lesmez, Budny and Stuckenbruck, on the same subject for more than ten years. They have published many valuable research papers. They have worked for both the frequency and time domain. There are Two different method are followed, the component-synthesis method and the method of characteristic MOC method. These terms are basic name of the numerical treatment of the structure. The former method is associated with natura1 modes of vibration, whereas the latter corresponds to wave propagations. Experimental validation tests completed the investigations.

The present work under the titled of Fluid structure interaction due oil hammering is based on the findings of Wiggert, A.S Tijsseling and his team. The component-synthesis method is introduced in (Hatfield et al. 1982a] for application in the frequency domain in the structural motion is represented by a limited number of natural modes of vibration, and this is solved with a commercially available finite-element computer code.

The Fluid-structure interaction (FSI) is introduced by means of junction coupling. The method was validated against the experiment of Blade et at. [1962], and, in [Hatfield et al. 1982b or 1983], against the experiments of Davidson & Smith [1969] and Davidson & Samsury [1972]. Hatfield & Wiggert [1983] came to that conclusion that in general the time-domain solutions can be obtained from frequency-domain solutions by means of inverse Fourier transformations. While in actual this approach may lead to serious difficulties. Especially when the transient response to impact loads is studied, the approach is very impractical. As a result they developed a time-domain implementation of the component-synthesis method, in which the standard water hammer / oil hammer procedure is coupled to a modal representation of the structura1 motion [Wiggert & Hatfield 1983]. In this work the Poisson coupling is not considerd, which is actually an extension of [Otwell 1982].

In [Wiggert et at. 1983} he summarized the previous investigations and laboratory tests are presented in which the pressures, exceed Joukowsky's prediction (2.1). In [Otwell 1984; Wiggert et at. 1985a] they have carried of a number of tests, with copper pipes of 0.025 m diameter, and it simulated successfully. A four-equation model, including Poisson coupling, has been presented for axial motion and lumped stiffness considered for flexural motion. They have use the method of characteristic MOC for the numerical solutions. The paper presented by [Wiggert et al. 1985b, 1986, 1987a], they have presented a model of fourteen-equation with the axial, flexural and torsional motions of a liquid-filled pipe system. They have solved the same equation system by means of the MOC method. The same approach has been adopted by the famous researcher A.S Tijsseling and their team. This approach will also be used in this research which will be worked out in chapter 5and 6. In Wiggert et at. [1987b] in a way similar to that of Wilkinson [1978] has solved the fourteen-equation model is treated in the frequency domain with that Poisson coupling is taken into account. He validated the numerical results against the experimental data presented by Davidson & Smith [1969]. He also validated the numerical result against new experimental data on a U-bend [Lesmez 1989;

Lesmez et aI. 1990]. A brief review of literature is also given in [Wiggert 1986]. In the study presented by Hatfield & Wiggert [1987, 1990] they have examined frequency response of a straight pipe to seismic ground motion. The study regarding the axial motion of highly flexible tubes is presented by Stuckenbruck & Wiggert [1987]. He assumed Poisson's ratios nearly equal to 0.5.

In [Budny 1988; Budny etal. 1989, 1990, 1991]. They have investigated theoretically and experimentally the Structural damping, which is of less importance for the early-time solutions calculated in the study of Stuckenbruck & Wiggert.

The study of Jelev [1989]. Kojima et al. [1986] are regarding the structural damping and associated energy losses in straight pipe. They have used a four-equation model with Poisson coupling from fluid to pipe. They have also provided the Experimental data on an oil-filled pipe.

In Bettinali et al. [1991], presented a computer code for fluid structure interaction which is based on a solution technique similar to the method of characteristic and finite element method procedure of Lavooij & Tijsseling [1989], although the Poisson coupling is modeled in a different way. He has tabulated some some numerical results with respect to a simple single pipe system subjected to seismic excitation are shown.

De Almeida & Koelle [1992, pp. 60-61] show work of Vasconcelos [1991] on a reservoir- (pipe-valve system, in which classical oil hammer predictions are compared with results calculated with Poisson and friction coupling.

Tijsseling and Lavooij (2007; 2008) and Heinsbroek (2008) has worked on fluid structure interaction FSI in liquid-filled pipeline system by the method of characteristics and finite element method. In the study presented by Lee and Kim (1999) they have described a fully coupled pipe system in which dynamic theory is taking into account, the effect of circumferential strains occurring due to internal fluid pressure. Finite element formulation for the pipe dynamic theory is also introduced by the Lee and Kim.

3.3 Conclusion

An in depth review on the work done in the field of FSI, with special concentration to FSI of pipes has been presented in this chapter. A detailed explanation of water hammering, oil hammering, Cavitation, wave propagation, junction and Poisson coupling has been presented in this chapter. The detail of FSI phenomenon discussed in this chapter would

be utilized in the forth coming chapters for modeling of actual problems related to FSI and experimentation purposes. In the coming chapter the basic problem is formulated.

CHAPTER # 4

4 PROBLEM FORMULATION

4.1 Introduction:

The chapter formulates the problem to be solved in this research project. First the problem is presented and then a strategy to solve it is presented in detail. Explanation of the different type of hydraulic circuits which uses different shapes and sizes of tubes have been presented. The hydraulic circuit utilizes straight, L shaped and U shaped tubes with the straight tube being the most common one. The information of problem formulation gained in this chapter would be utilized in the preceding sections for mathematical modeling and experimentation.

4.2 Problem Formulation

Consider a tube while carrying oil from one reservoir to another as shown in fig 1(Prof. Dr. Richard Skalak, 1953). A sudden closure of the valve at B will generate a pressure wave which travel up the tube towards A. As the wave proceeds, it brings the fluid to rest and stretch the tube. On the other hand, if the valve at B is opened, but there is no flow due to the valve at A being closed, then sudden opening of the valve at A will result in a pressure wave from A toward B. This wave sets the fluid in motion and distends the tube as it proceeds. Such wave and their accompanying effect are generally known as oil hammer.

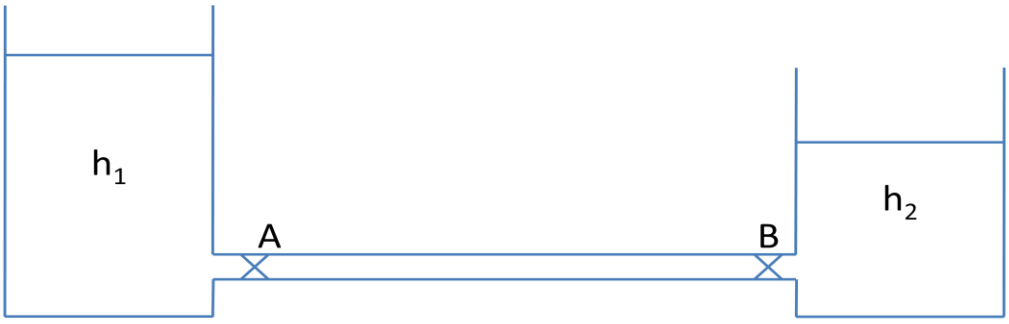

(An extension of the theory of water hammer, Prof. Dr.Richard Skalak, 1923-1997, Columbia University, USA)

Figure 4- 1

Phenomenon is of practical importance particularly in the case of a sudden stoppage of flow since the resulting pressure is likely to be the maximum experienced during the life of the conduit.

The existence of the oil hammer effect was apparently known for some time before research concerning theories and experiments began to appear in the technical literature in the 1880's.

In paper dealing to oil hammer directly, paper concerning the propagation of sound waves in the liquid filled tubes also contributed to the understanding of oil hammer.

In my research we will study the pressure fluctuation in hydraulic jack with different shapes of hydraulic pipes (e.g. Straight, L-Shaped and U-Shaped) due to oil hammering phenomena and experimentally the result will compare with the result obtained from mathematical model and finally calculate the percent errors between the results obtained from the model and experimentation.

Digitalized data has been taken for the same pipe at the steady state condition with different applied pressure. And the result is compared with the result obtained from the model of thick wall and thin wall and finally the percent is tabulated.

Also the experimentation for the bursting of the same tubes will be study in this research and the percent errors will also be calculated.

In the third phase an experiment will be carried out for the optimization of a number of tube clamps used for the clamping the pipes in order to avoid the vibratory motion.

A Hydraulic Power Pack is used to deliver pressurized fluid to the system. The power pack consists of Hydraulic pump which is coupled with electric motor/engine. As the motor rotates, the pump coupled with it also starts to rotate. The rotation of the pump results in oil flow to the system. The valve used here is closed, so the pressure is developed. This pressure is equal to the setting of the hydraulic relief valve. Pressure relief valve is used to release pressure in the fluid above its setting. This oil is directed to the tank till the valve remains close. Hydraulic actuator is connected to the valve. The valve used in our system/experiment is float center directional control valve. In float center direction control valve, the jack ports A and B are connected to the tank in normal center position. When the valve is actuated, the pump pressure is directed to the ports of

the actuator depending upon the sequence of the valve (as shown in the above figure). In our experiment the actuator is equipped with load. This load is acting vertically on the jack. This shows that only pressurized fluid from the pump can be used to lift the load acting on the actuator.

In hydraulic system we used hydraulic oil which is transform through tubes from pump to actuators. The oil used here is Shell Tellus T 46. This oil is ISO VG46 grade mineral oil.

The problem discussed in my thesis is based on the phenomenon that when the valve is actuated, the pressurized fluid hits the jack piston area, thereby producing jerk. This jerk is referred by many researchers to as Oil Hammer. In research the author will study the fluid structure interaction FSI, here the fluid is hydraulic oil which is viscous in nature and structure is the hydraulic lines and Jacks internal body.

In this research the author will use the strategy to built hydraulic circuit for a crane of 10 ton capacity. The circuit designing will include the proper selection of hydraulic components for the operation of sequences the crane will perform. This circuit design will include pump design, valve design, actuator design, tank design and tubing design. The simulation of circuit is validated using Automation Studio.

The circuit design phase will be followed by selection of hydraulic components. These components will be selected based on the requirements given in the circuit diagram. The author has used Parker components to obtain the desired features of the crane. The selection of components include pump selection , valve selection, hydraulic actuator selection, oil selection, tank design, tubes selection and gauges selection.

With the help of hydraulic component selection, the author has installed the components on the crane super structure as specified in the circuit diagram.

In this thesis work only a small portion of the hydraulic circuit is selected for research. This portion of the circuit includes a directional control valve which is connected to hydraulic actuator through hydraulic tubes. The pressure is fed to the directional control valve through tubes from hydraulic tank with the help of hydraulic pump. This pressurized fluid hits the piston of the actuator when the valve is actuated instantly.

Consider a hydraulic jack of a fluid power system (hydraulic crane) as shown in fig.

When pump makes pressure then this pressure stay on a point A at the directional control valve when that directional control valve actuate then the pressurized fluid runs to the jack and apply force on the piston and lift the load when the valve comes on the neutral position then the load movement stops but when suddenly activate the valve then again a jerk is feels on the structure this phenomenon is by the different researchers as oil hammering(in case of oil flow) or declared oil hammering(in case of oil flow). In present research the author will study the fluid structure interaction in case oil hammering, here the fluid is hydraulic oil which is viscous in nature and structure is the hydraulic lines and Jacks internal body.

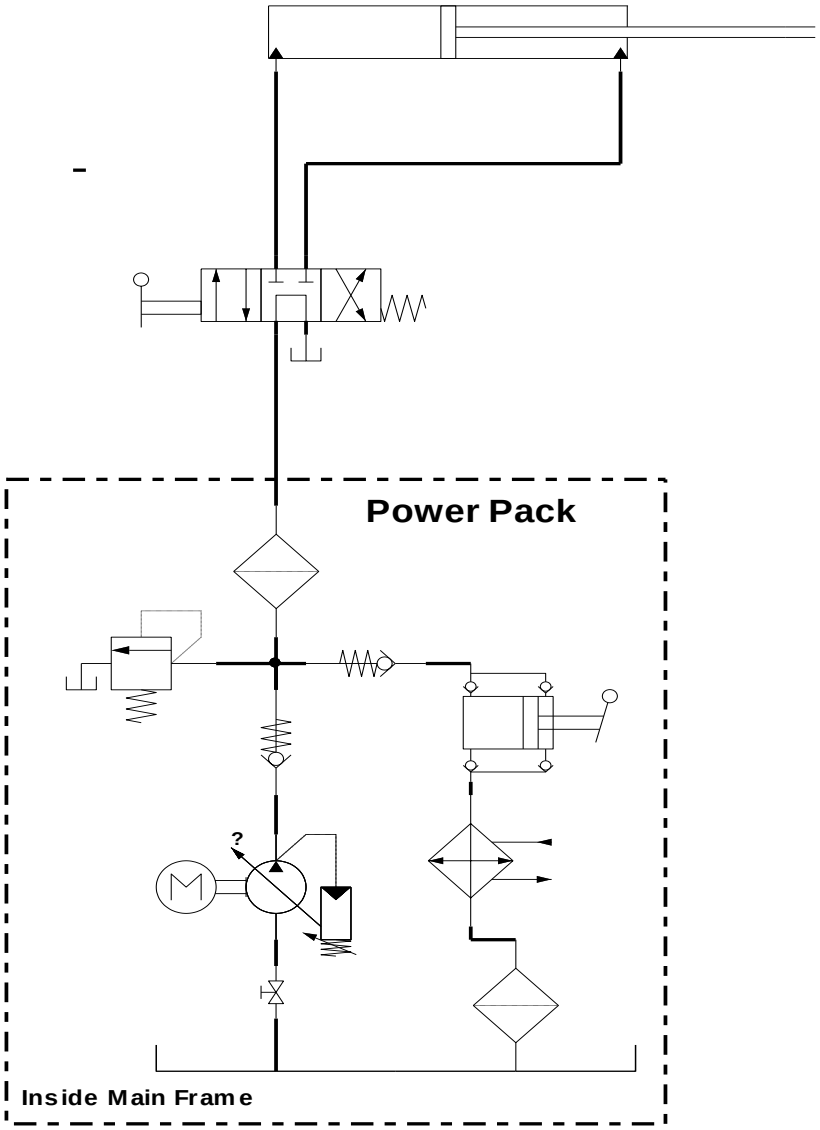

Figure 4-2 [Hydraulic Circuit with Straight Pipe]

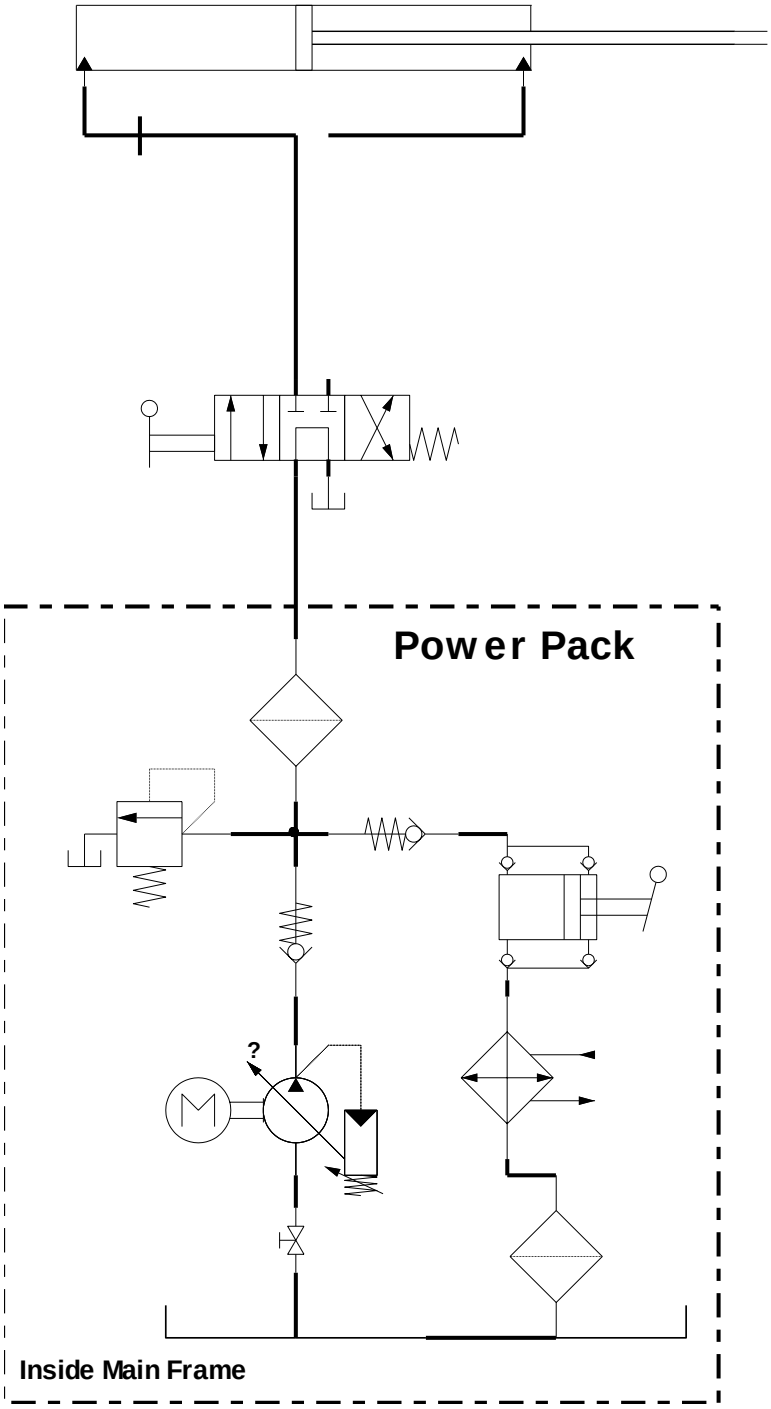

Figure 4-3 [Hydraulic Circuit with L-Shaped Pipe]

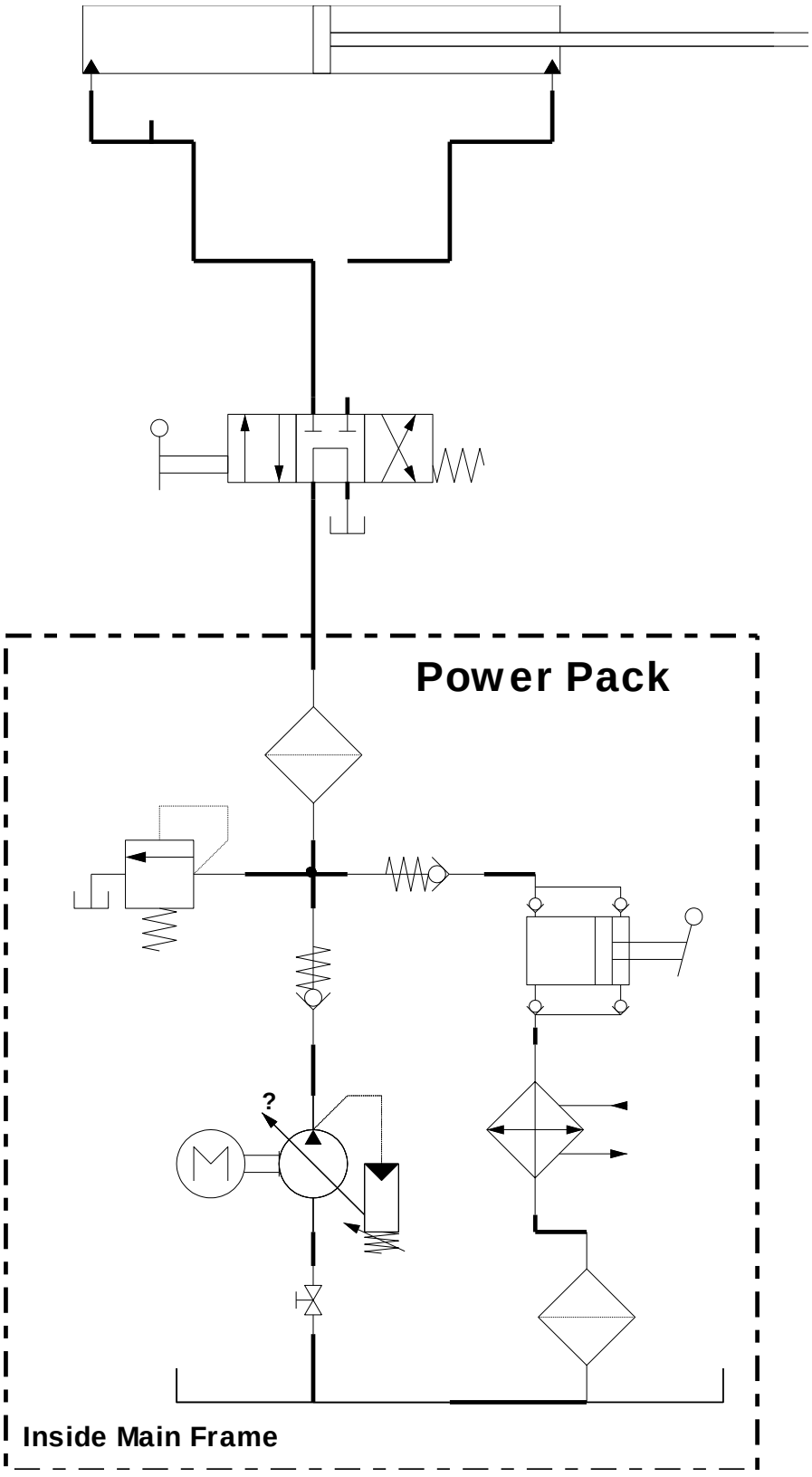

Figure 4-4 [Hydraulic Circuit with U-Shaped Pipe]

4.3 Conclusion

A detailed explanation of the problem and then a strategy to solve it is presented. Different types of tubes (Straight, L Shaped and U shaped) are presented which are utilized in a hydraulic circuit. An explanation of the strategy developed by other researcher has also been presented. The information of problem formulation gained in this chapter is to be utilized in the following sections for mathematical modeling and experimentation for solving the problem.

CHAPTER # 5

5 MATHEMATICAL MODEL

5.1 Introduction

In this chapter a one-dimensional mathematical model is developed with the combination of fluid structure interaction due to oil hammering. This mathematical model is basically the simplified form of model develop by A.S. Tijsseling which is derived on the bases of conventional water hammer and beam theories. First we will calculate equation for fluid and then for structure. Then we couple the equations at the boundary surface. The equations are simplified to matrix form and then discretization is carried in next section.

5.2 Mathematical Model

The following has been assumed for the derivation of equations. [A.S Tijsseling]

- The tube fill of oil is assumed to be straight, slender, thick walled and prismatic of circular cross section.
- A Viscous fluid of constant pressure is flowing inside the pipe.
- The pipe wall material is homogenous, isotropic, linearly elastic and subject to small deformation.
- The resistance to radial motion by inertia, bending stiffness and shear deformation in ignored.
- The contain liquid is Newtonian with homogeneous, isotropic and linearly elastic properties.
- Iso-thermal conditions prevail.
- Structural and liquid damping mechanism are designed, except for the friction between the liquid and pipe wall, which is modeled quasi-stationery.
- For torsional motion liquid and pipe are allowed to sip.

The model is one-dimensional; there is one spatial co-ordinate along the central axis of the pipe. This approach is valid for long wave length or low frequencies. i.e: $\lambda >>> D$.

The Liquid and pipe velocity are considered to be much less than the wave velocities, so that connection term may be neglected.

Lamb's H [1898] research in connection of the velocity of sound in a tube that affected by the elasticity of the wall is a good break through which is concern with the wave propagation in fluid filled pipe/tube. Lamb [1898] has applied the Fourier analysis to the basic equations and in this result he derived a depression equation from the discussed only axial or longitudinal motion of axially symmetric. Pressure liquid tube and in this case he attained a four equation solution model which gives two models solution.

Our strategy will be to first find the equation for liquid then for pipe/tube and finally will compare these two at the junction.

5.2.1 Liquid:

The approach of D'Souza & Oldenburger [1964], Kuiken [1986] and Budny [1988] will be used in order to derive the basic equation for the liquid.

Now start the discussion by the two dimensional continuity and Navier-Stokes equation in the cylindrical co-ordinate (r,θ,z) in which "*r*" is in radial co-ordinate and "z" is in axial co-ordinate. [According to {Birdetal. 1960}, {Mase. 1970}]

Due to the axial symmetry the circumferential co-ordinate Ø is omitted.

5.2.2 Continuity Equation:

The continuity equation is:

$$\frac{\partial \rho_{oil}}{\partial t} + V_1 \frac{\partial \rho_{oil}}{\partial z} + V_2 \frac{\partial \rho_{oil}}{\partial r} + \rho_{oil} \frac{\partial V_1}{\partial z} + \frac{\rho_{oil}}{r} \frac{\partial (rV_2)}{\partial r} \cdots\cdots\cdots\cdots\cdots 1$$

Where:

ρ_{oil} = Mass density of oil

V_1 = Axial component of velocity

V_2 = Radial component of velocity

5.2.3 Navier-Stokes Equation:

As we know that the Navier-stokes equation is basically the Linear movement balance equation of motion in axial, radial and Ø direction and have assume here that Ø direction is ignore So,

Axial Component of Navier-Stokes Equation:

This equation derived by the D'Souza & Oldenburger [1964], Kuiken [1986] and Budny [1988] we have.

$$\rho_{oil}\frac{\partial V_1}{\partial t}+\rho_{oil}V_1\frac{\partial V_1}{\partial z}+\rho_{oil}V_2\frac{\partial V_1}{\partial r}+\frac{\partial P}{\partial z}$$

$$F1+\left(\beta+\frac{1}{3}\mu\right)\frac{\partial}{\partial r}\left\{\frac{\partial V_1}{\partial z}+\frac{1}{r}\frac{\partial(rV_2)}{\partial r}\right\}+\mu\left\{\frac{1}{\mathrm{r}}\frac{\partial}{\partial \mathrm{r}}\left(\mathrm{r}\frac{\partial \mathrm{V}_2}{\partial \mathrm{r}}\right)+\frac{\partial^2 \mathrm{V}_2}{\partial \mathrm{z}^2}\right\}$$

Radial Component of Navier-Stokes Equation:

This equation for the Radial Component derived by D'Souza & Oldenburger [1964], Kuiken [1986] and Budny [1988] is:

$$\rho_{oil}\frac{\partial V_2}{\partial z}+\rho_{oil}V_1\frac{\partial V_2}{\partial z}+\rho_{oil}V_2\frac{\partial V_2}{\partial r}+\frac{\partial P}{\partial r}$$

$$=F_2+\left(\beta+\frac{1}{3}\mu\right)\frac{\partial}{\partial r}\left\{\frac{\partial V_1}{\partial z}+\frac{1}{r}\frac{\partial(rV_2)}{\partial r}\right\}+\mu\left\{\frac{1}{2}\frac{\partial}{\partial r}\left(r\frac{\partial V_2}{\partial r}\right)-\frac{V_2}{r^2}+\frac{\partial V_2}{\partial z^2}\right\}$$

Where:

V_1	:	Axial component of velocity
V_2	:	Radial component of velocity
ρ_{oil}	:	Mass density of oil
$F_1 = F_z$	:	Pressure
$F_2 = F_r$	:	Radial body force
β	:	Bulk velocity of oil
μ	:	Dynamic viscosity of oil

As we know from Annex A1

$$d\rho_{oil}=\rho_{oil}\frac{dp}{\beta}\ldots\ldots\ldots\ldots\ldots\ldots\ldots\ldots A1$$

Putting the equation "A1" into equation "1"

We get

$$\frac{\rho_{oil}}{\beta}\frac{\partial P}{\partial t} + v_1\frac{\partial \rho_{oil}}{\partial z} + v_2\frac{\partial \rho_{oil}}{\partial r} + \rho_{oil}\frac{\partial V_1}{\partial z} + \frac{\rho_{oil}}{r}\frac{\partial (rV_2)}{\partial r} = 0$$

The convective term i.e. the second and third term of above equation assume to be zero [As by D' Souza & Olden burger, 1964 appendix 2 []

$$\frac{\rho_{oil}}{\beta}\frac{\partial P}{\partial t} + \rho_{oil}\frac{\partial v_1}{\partial z} + \frac{\rho_{oil}}{r}\frac{\partial (rV_2)}{\partial r} = 0$$

As ρ =Constant for incompressible fluid.

So the above equation becomes

$$\frac{1}{\beta}\frac{\partial P}{\partial t} + \frac{\partial V_1}{\partial z} + \frac{1}{r}\frac{\partial (rV_2)}{\partial r} = 0 \ldots\ldots\ldots\ldots 6$$

It is a more simplified form of continuity equation.

5.2.4 Navier-Stokes Equation in axial Direction:

The equation # 2 =>

$$\rho_{oil}\frac{\partial V_1}{\partial t} + \rho_{oil}V_1\frac{\partial V_1}{\partial z} + \rho_{oil}V_2\frac{\partial V_1}{\partial r} + \frac{\partial P}{\partial z} + F_1 + \left(\gamma + \frac{1}{3}\mu\right)\frac{\partial}{\partial z}\left\{\frac{\partial V_1}{\partial_z} + \frac{1}{r}\frac{\partial (rV_2)}{\partial r}\right\} + \mu\left\{\frac{1}{r}\frac{\partial}{\partial r}\left(\frac{r\partial V_1}{\partial r}\right) + \frac{\partial^2 {V_1}^2}{\partial z^2}\right\}$$

As the second and 3rd term are the convective term so we ignore it {see D' Souza & Older Burger, 1964 appendix z []}

And as

$$F_{1=}\rho_{oil}.g.Sin \propto$$

In which ∝ denote the angle of inclination of the pipe with the horizontal line.

So the equation becomes

$$\rho_{oil}\frac{\partial V_1}{\partial t} + \frac{\partial P}{\partial z} = \rho_{oil}gSin \propto + \frac{\mu}{r}\frac{\partial}{\partial r}\left(r\frac{\partial V_1}{\partial r}\right) \ldots\ldots\ldots 7$$

5.2.5 Navier-Stokes Equation in Radial Direction:

Equation.3

$$\rho_{oil}\frac{\partial V_2}{\partial t}+\rho_{oil}v_1\frac{\partial V_2}{\partial z}+\rho_{oil}v_2\frac{\partial V_2}{\partial r}+\frac{\partial P}{\partial z}$$
$$=F_2+\left(\gamma+\frac{1}{3}\mu\right)\frac{\partial}{\partial r}\left\{\frac{\partial V_1}{\partial_z}+\frac{1}{r}\frac{\partial(rV_2)}{\partial r}\right\}+\mu\left\{\frac{1}{r}\frac{\partial}{\partial r}\left(\frac{r\partial V_1}{\partial r}\right)-\frac{V_2}{r^2}+\frac{\partial^2 V_2}{\partial z^2}\right\}$$

As the second and the third term are the convective term we ignore it. [see D' Souza & olden burger 1964, appendix 2]

The Radial body forces due to gravity $F_2 = F_r = 0$

$$F_2=\rho g Cos \propto = 0$$

The above equation becomes.

$$\rho_{oil}\frac{\partial v_2}{\partial t}+\frac{\partial P}{\partial r}=0 \dots\dots\dots 8$$

From equation '7' and '8' it is clear that the density in the above equation is constant, so liquid compressibility still exist.

To convert the above equation in one dimensional form we multiply equation '6' by $2\pi r$ and integrate w.r.t. r from 0 to R and divided by πR^2.

Where 'R' is the outer radius of the tube while 'r' is the inner radius of the tube.

Equation 6 =>

$$\frac{1}{\beta}\frac{\partial P}{\partial t}+\frac{\partial V_1}{\partial z}+\frac{1}{r}\frac{\partial(rV_2)}{\partial_r}=0$$

Multiply by $2\pi r$ and divided by πR^2

$$\frac{2\pi r}{\pi R^2}\frac{1}{\beta}\frac{\partial P}{\partial t}+\frac{2\pi r}{\pi R^2}\frac{\partial V_1}{\partial z}+\frac{2\pi r}{\pi R^2}\frac{1}{r}\frac{\partial(rV_2)}{\partial r}=0$$

Integrate both sides from 0 to R

$$\frac{1}{\beta}\frac{1}{\pi R^2}\int_0^R \frac{\partial P}{\partial t}2\pi r\, dr + \frac{\partial}{\partial z}\frac{1}{\pi R^2}\int_0^R 2\pi r\, V_1 dr + \frac{2\pi r}{\pi R^2}\frac{1}{r}\int_0^R \frac{\partial}{\partial r}(rV_2)dr = 0$$

Or The above equation becomes

$$\frac{1}{\beta}\frac{1}{\pi R^2}\int_0^R 2\pi r P\ dr + \frac{\partial}{\partial z}\frac{1}{\pi R^2}\int_0^R 2\pi r\, V_1 dr + \frac{2v_2}{R^2}\int_0^R dr = 0$$

or

$$\frac{1}{\beta}\frac{\partial}{\partial t}\frac{1}{\pi R^2}\int_0^R 2\pi r P\ dr + \frac{\partial}{\partial z}\frac{1}{\pi R^2}\int_0^R 2\pi r\, V_1 dr + \frac{2v_2}{R^2}\int_0^R dr = 0$$

Now Let

$$\bar{V} = \frac{1}{\pi R^2}\int_0^R 2\pi r V_1 dr = 0 \ldots\ldots\ldots\ldots\ldots 9$$

$$\bar{P} = \frac{1}{\pi R^2}\int_0^R 2\pi r P dr = 0 \ldots\ldots\ldots\ldots\ldots 10$$

Where $\bar{V}$ and $\bar{P}$ are the cross-sectional averaged axial velocity and pressure

Then the above equation becomes

$$\frac{1}{\beta}\frac{\partial \bar{P}}{\partial t} + \frac{\partial \bar{V}}{\partial z} + \frac{2V_2}{R^2}\int_0^R dr = 0$$

$$\frac{1}{\beta}\frac{\partial \bar{P}}{\partial t} + \frac{\partial \bar{V}}{\partial z} + \frac{2V_2}{R^2} r\Big|_0^R = 0$$

$$\frac{1}{\beta}\frac{\partial \bar{P}}{\partial t} + \frac{\partial \bar{V}}{\partial z} + \frac{2V_2}{R^2} R = 0$$

$$\frac{1}{\beta}\frac{\partial \bar{P}}{\partial t} + \frac{\partial \bar{V}}{\partial z} + \frac{2V_2}{R} = 0 \ldots\ldots\ldots\ldots\ldots 11$$

It is the one dimensional term of the continuity equation in which $\bar{P}$ is the cross-sectional averaged axial pressure of the fluid and $\bar{V}$ is the cross-sectional axial velocity of the fluid

while V_2 is the radial velocity component of the fluid and R is the outer radius of the fluid β is the Bulk Modulus of elasticity of fluid.

Similarly the convert the equation into one dimensional form we multiply equation (7) by $2\pi r$ and integrate w.r.t. r from 0 to R and divided by πR^2. Where R is the outer radius of the tube. While 'r' is the inner radius of the tube.

Equation 7 =>

$$\rho_{oil}\frac{\partial V_1}{\partial t}+\frac{\partial P}{\partial z}=\rho_{oil}g\sin\propto+\frac{\mu}{r}\frac{\partial}{\partial r}\left(r\frac{\partial V_1}{\partial r}\right)$$

$$\rho_{oil}\frac{\partial}{\partial t}\int_0^R\frac{1}{\pi R^2}2\pi r v_1 dr+\frac{\partial}{\partial z}\frac{1}{\pi R^2}\int_0^R 2\pi r P dr$$
$$=\rho_{oil}g\sin\propto+\frac{2\pi}{\pi R^2}\int_0^R r dr+\frac{\mu}{r}\frac{2\pi r}{\pi R^2}\frac{\partial V_1}{\partial r}\int_0^R\frac{\partial}{\partial r}(r)dr$$

$$\rho_{oil}\frac{\partial \bar{V}}{\partial t}+\frac{\partial \bar{P}}{\partial z}=\rho_{oil}g\sin\propto+\frac{2\pi}{\pi R^2}\frac{R^2}{2}+\frac{\mu}{r}\frac{2\pi}{\pi R^2}\frac{\partial V_1}{\partial r}R^2$$

$$\rho_{oil}\frac{\partial \bar{V}}{\partial t}+\frac{\partial \bar{P}}{\partial z}=\rho_{oil}g\sin\propto+\mu\frac{2}{r}\frac{\partial V_1}{\partial r}\ldots\ldots 12$$

Where $\bar{V}=\frac{1}{\pi R^2}\int_0^R 2\pi r V_1 dr$

And $\bar{P}=\frac{1}{\pi R^2}\int_0^R 2\pi r P dr$

are the cross-sectional averaged axial velocity and pressure.

As we know that the shear stress between liquid and pipe wall can be calculated as.

$$\tau=-\mu\frac{\partial V_1}{\partial r}\ldots\ldots 13$$

Put this value in Equation '12' we get.

$$\rho_{oil}\frac{\partial \bar{V}}{\partial t}+\frac{\partial \bar{P}}{\partial z}=\rho_{oil}g\sin\propto-\frac{2}{R}\tau\ldots.14$$

It is the one dimensional axial component of Navier-Stokes equation.

Now for Radial component of Navier-Stokes equation. We multiply Equation '8' by $\frac{2\pi r}{\pi R^2}$ and integrate w.r.t 'r' from 0 to R.

Equation '8'=>

$$\rho_{oil}\frac{\partial v_2}{\partial t}+\frac{\partial P}{\partial r}=0$$

$$\rho_{oil}\frac{1}{\pi R^2}\frac{\partial v_2}{\partial t}\int_0^R 2\pi r dr+\frac{\partial}{\partial r}\frac{1}{\pi R^2}=0$$

Or

$$\rho_{oil}\frac{\partial \bar{V}}{\partial t}+\frac{\partial P}{\partial z}=0$$

$$\frac{1}{2}\rho_{oil}R\frac{\partial v_2}{\partial t}+p-P=0\ldots\ldots\ldots..14-A$$

where

$$\bar{P}=\frac{1}{\pi R^2}\int_0^R 2\pi r dr$$

5.2.6 Equation of Pipe:

The approach of [line & Morgan 1956a] and Hermin & mirsky 1956 are followed. The two dimensional equation in cylindrical co-ordinates z(axial) and r(radial) [e.g. Kosky 1953, Mars 1970]. While the circumferential co-ordinate θ in ignored due to axial symmetry.

5.2.7 Liner Momentum equation in axial direction:

The liner momentum equation in axial direction is

$$\rho_t\frac{\partial \dot{u}_1}{\partial t}+\rho_t\dot{u}_1\frac{\partial \dot{u}_1}{\partial z}+\rho_t\dot{u}_2\frac{\partial \dot{u}_1}{\partial r}=\frac{\partial \sigma_1}{\partial z}+\frac{1}{r}\frac{\partial(r\tau_{12})}{\partial r}+F_1$$

Where $\dot{u}_1$ and $\dot{u}_2$ are the axial and radial velocities:-

ρ_t = The mass density of tube material

$\dot{u}_1$ & $\dot{u}_2$ = The axial radial stress

τ_{12} = Shear stresses between the axial and radial

F_1 = Body force density in axial direction

= $\rho_t g \sin\theta$

The 2nd and 3rd term of the above equation are the convective term and these are neglected because of small deformation assumption.

The above equation reduced to

$$\rho_t \frac{\partial \dot{u}_1}{\partial t} = \frac{\partial \sigma_1}{\partial z} + \frac{1}{r}\frac{\partial (r\tau_{12})}{\partial r} + \rho_t g \sin\theta$$

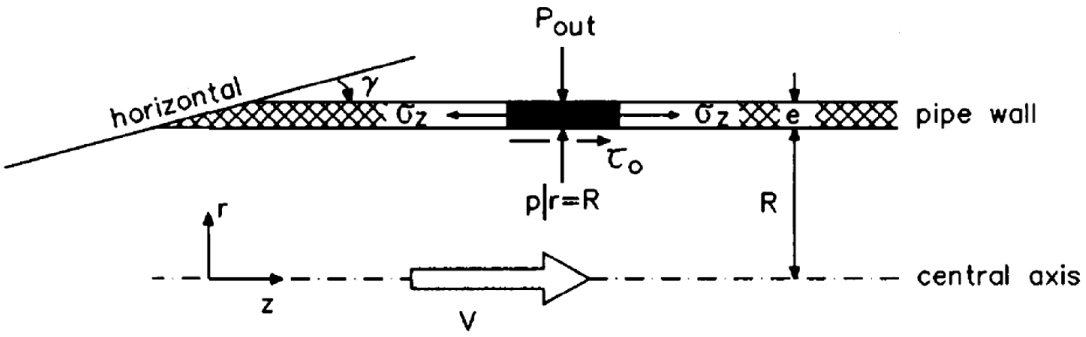

Fig 5-1. [Definition sketch, side view (z-r plane) stress acting on pipe wall] [Arris Tijssling].

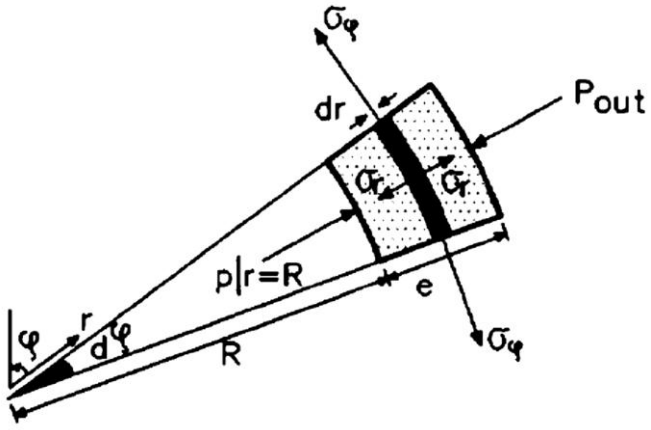

Fig 5-2. [Definition sketch, cross-sectional view (r- Ø)plane , normal stress acting on element of pipe wall.]

To convert the above equation into one dimensional form, we multiply the above equation by $2\pi r$ and integrate it w.r.t. r from R to (R+t) and divide by $2\pi\left(R+\frac{1}{2}t\right)t$, where r is the inner radius of the pipe and t is the wall thickness

$$\frac{2\pi r}{2\pi\left(R+\frac{1}{2}t\right)t}\left[\int_R^{R+t}\rho_t\frac{\partial\dot{u}_1}{\partial t}dr\right]$$

$$=\frac{2\pi r}{2\pi\left(R+\frac{1}{2}t\right)t}\left[\int_R^{R+t}\frac{\partial\sigma_1}{\partial z}dr+\int_R^{R+t}\frac{1}{r}\frac{\partial(r\tau_2)}{\partial r}dr+\int_R^{R+t}\rho_t g\sin\theta\,dr\right]$$

So, the remaining equation will be

$$\rho_t\frac{\partial\dot{u}_1}{\partial t}\frac{1}{2\pi\left(R+\frac{1}{2}t\right)t}\int_R^{R+t}2\pi\dot{u}_1dr$$

$$=\frac{\partial}{\partial z}\frac{1}{2\pi\left(R+\frac{1}{2}t\right)t}\int_R^{R+t}2\pi\dot{u}_2dr+\frac{1}{2\pi\left(R+\frac{1}{2}t\right)t}\int_R^{R+t}\frac{2\pi rt}{r}\frac{\partial(r\tau_2)}{\partial r}dr$$

$$+\frac{\rho_t g\sin\theta}{2\pi\left(R+\frac{1}{2}t\right)t}\int_R^{R+t}2\pi r dr$$

Now Let

$$\overline{\dot{u}_1}=\frac{1}{2\pi\left(R+\frac{1}{2}t\right)t}\int_R^{R+t}2\pi\dot{u}_1dr$$

And

$$\overline{\dot{u}_2}=\frac{1}{2\pi\left(R+\frac{1}{2}t\right)t}\int_R^{R+t}2\pi\dot{u}_2dr$$

$$\bar{\sigma}=\frac{1}{2\pi\left(R+\frac{1}{2}t\right)t}\int_R^{R+t}2\pi\sigma_1dr$$

Then the above equation reduced to

$$\rho_t\frac{\partial\overline{\dot{u}_1}}{\partial t}=\frac{\partial\bar{\sigma}}{\partial z}+\frac{\tau_{12}}{\left(R+\frac{1}{2}t\right)t}\int_R^{R+t}dr+\frac{\rho_t g\sin\theta}{\left(R+\frac{1}{2}t\right)t}\int_R^{R+t}rdr$$

Further simplify the above we get

$$\rho_t \frac{\partial \overline{\dot{u}_1}}{\partial t} = \frac{\partial \bar{\sigma}}{\partial z} + \frac{\tau_{12}}{\left(R + \frac{1}{2}t\right)t} r \Big|_R^{R+t} + \frac{\rho_t g \sin\theta}{\left(R + \frac{1}{2}t\right)t} \int_R^{R+t} \frac{r^2}{2}$$

$$\rho_t \frac{\partial \overline{\dot{u}_1}}{\partial t} = \frac{\partial \bar{\sigma}}{\partial z} + \frac{\tau_{12}}{\left(R + \frac{1}{2}t\right)t} [(R+t)R] \frac{\rho_t g \sin\theta}{\left(R + \frac{1}{2}t\right)t} \left[\frac{(R+t)^2}{2} \frac{R^2}{2}\right]$$

$$\rho_t \frac{\partial \overline{\dot{u}_1}}{\partial t} = \frac{\partial \bar{\sigma}}{\partial z} + \frac{R+t}{\left(R + \frac{1}{2}t\right)t} \tau_{12} - \frac{R}{\left(R + \frac{1}{2}t\right)t} \tau_{12} + \frac{\rho_t g \sin\theta}{\left(R + \frac{1}{2}t\right)t} \left[\frac{R^2 + t^2 + 2R + R^2}{2}\right]$$

$$\rho_t \frac{\partial \overline{\dot{u}_1}}{\partial t} = \frac{\partial \bar{\sigma}}{\partial z} + \frac{(R+t)\tau_{12}}{\left(R + \frac{1}{2}t\right)t} - \frac{R.\tau_{12}}{\left(R + \frac{1}{2}t\right)t} + \frac{\rho_t g \sin\theta}{\left(R + \frac{1}{2}t\right)t} \frac{t^2 + 2R}{2}$$

$$\rho_t \frac{\partial \overline{\dot{u}_1}}{\partial t} = \frac{\partial \bar{\sigma}}{\partial z} + \frac{(R+t)\tau_{12}}{\left(R + \frac{1}{2}t\right)t} - \frac{R.\tau_{12}}{\left(R + \frac{1}{2}t\right)t} + \rho_t g \sin\theta \ldots\ldots\ldots..15$$

Where $\overline{\dot{u}_1}$, $\overline{\dot{u}_2}$and $\bar{\sigma}$ are the average values of the pipe velocity and normal stress component.

The above equation '15' is the equation of motion relates the axial velocity to axial stresses.

5.2.8 Stress–Strain Relation:

The longitudinal strain components in x, y and z direction are:

$$\epsilon_x = \frac{\partial u}{\partial x}$$

$$\epsilon_y = \frac{\partial v}{\partial y}$$

$$\epsilon_z = \frac{\partial w}{\partial z}$$

While the shearing strain are:

$$\gamma_{xy} = \frac{\partial u}{\partial y} + \frac{\partial v}{\partial x}$$

$$\gamma_{yz} = \frac{\partial v}{\partial z} + \frac{\partial w}{\partial y}$$

$$\gamma_{zx} = \frac{\partial w}{\partial x} + \frac{\partial u}{\partial z}$$

These equations can be written in matrix form as:

$$\begin{bmatrix} \epsilon_x \\ \epsilon_y \\ \epsilon_z \\ \gamma_{xy} \\ \gamma_{yz} \\ \gamma_{zx} \end{bmatrix} = \begin{bmatrix} \frac{\partial}{\partial x} & 0 & 0 \\ 0 & \frac{\partial}{\partial y} & 0 \\ 0 & 0 & \frac{\partial}{\partial z} \\ \frac{\partial}{\partial y} & \frac{\partial}{\partial x} & 0 \\ 0 & \frac{\partial}{\partial z} & \frac{\partial}{\partial y} \\ \frac{\partial}{\partial z} & 0 & \frac{\partial}{\partial x} \end{bmatrix} \begin{Bmatrix} u \\ v \\ w \end{Bmatrix}$$

The equation which relates stress and strain (often referred to as the constitutive equation) are also developed in the literature, again we will summarize for equation for particular condition of continuum stress and strain for linearly elastic, homogenous and isotropic material.

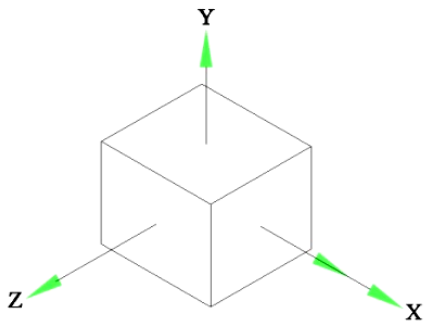

Fig 5-3

5.2.9 Uniaxial Stress:

The Simplest stress – strain relationship is for the case of uniaxial stress (as shown in fig 5.3)$\sigma_x = E\epsilon_x$

Where E is the modulus of elasticity

Note that in this case strain in the y and z direction is not zero but rather

$$\epsilon_x = \epsilon_x = -\nu\epsilon_x$$

Where ν is Poisson's ratio.

5.2.10 Plane Stress:

Refer to fig 5.2, For this case the normal and stress strain components acts in two coordinate's direction only.

Note that in general the longitudinal (stress is non zero in all coordinate directions and

$$\sigma_z = 0 = \tau_{zx} = \tau_{zy}$$

The relations between stress and strain are:

$$\sigma_x = \frac{E}{1-\nu^2}(\epsilon_x + \nu\epsilon_y)$$

$$\sigma_y = \frac{E}{1-\nu^2}(\epsilon_y + \nu\epsilon_x)$$

$$\tau_{xy} = G\nu_{xy}$$

Where: $G = \frac{E}{2C}$

The constitutive equations written in matrix form are:

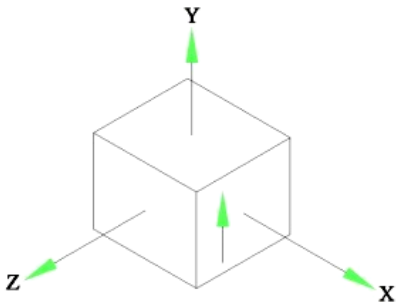

Fig 5-4 **[**Normal and sheer stresses on the x and y faces of differential series]

$$\begin{Bmatrix}\sigma_x\\ \sigma_y\\ \tau_{xy}\end{Bmatrix} = \frac{E}{(1-\nu^2)}\begin{bmatrix}1 & \nu & 0\\ \nu & 1 & 0\\ 0 & 0 & \frac{1-\nu}{2}\end{bmatrix}\begin{Bmatrix}\epsilon_x\\ \epsilon_y\\ \gamma_{xy}\end{Bmatrix}$$

Or

$$\{\sigma\} = [C]_\sigma\{\epsilon\}$$

Where $\{\sigma\}$ and $\{\epsilon\}$ are the stress and strain vector and $[C]_\sigma$ is the constitutive material for plane stress.

5.2.11 Plane Strain:

Referring to "fig5.2," we note that the stress in the z direction is not zero but is the value necessary to establish the linear strain in the z direction to be zero , Also

$$\gamma_{zx} = \gamma_{zy} = 0 = \epsilon_z$$

The stress – strain equation are

$$\sigma_x = \frac{E}{(1+\nu)(1-2\nu)}\left[(1-\nu)\epsilon_x + \nu\epsilon_y\right]$$

$$\sigma_y = \frac{E}{(1+\nu)(1-2\nu)}\left[\nu\epsilon_x + (1-\nu)\epsilon_y\right]$$

$$\sigma_z = \frac{E}{(1+\nu)(1-2\nu)}\left[\epsilon_x + \epsilon_y\right] = \nu(\sigma_x - \sigma_y)$$

$$\tau_{xy} = G\gamma_{xy}$$

Writing the x , y plane relationship in matrix form, we have

$$\begin{Bmatrix}\sigma_x\\ \sigma_y\\ \tau_{xy}\end{Bmatrix} = \frac{E}{(1+\nu)(1-2\nu)}\begin{bmatrix}1-\nu & \nu & 0\\ \nu & 1 & 0\\ 0 & 0 & \frac{1-2\nu}{2}\end{bmatrix}\begin{Bmatrix}\epsilon_x\\ \epsilon_y\\ \gamma\epsilon_x\end{Bmatrix}$$

Or

$$\{\sigma\} = [C]_\epsilon\{\epsilon\}$$

Where $[C]_\epsilon$ is the constitutive matrix for plane strain.

5.2.12 The Elasticity Equation:

With the points in continuum having displacement u, v and w in the x , y and z directions, respectively,

Then the linear strain – displacement relationship in the matrix form is

$$\begin{bmatrix} \epsilon_x \\ \epsilon_y \\ \epsilon_z \\ \gamma_{xy} \\ \gamma_{yz} \\ \gamma_{zx} \end{bmatrix} = \begin{bmatrix} \frac{\partial}{\partial x} & 0 & 0 \\ 0 & \frac{\partial}{\partial y} & 0 \\ 0 & 0 & \frac{\partial}{\partial z} \\ \frac{\partial}{\partial y} & \frac{\partial}{\partial x} & 0 \\ 0 & \frac{\partial}{\partial z} & \frac{\partial}{\partial y} \\ \frac{\partial}{\partial z} & 0 & \frac{\partial}{\partial x} \end{bmatrix} \begin{Bmatrix} u \\ v \\ w \end{Bmatrix}$$

Or

$$\{\epsilon\} = [£] \begin{Bmatrix} u \\ v \\ w \end{Bmatrix}$$

The Constitutive matrix for an isotropic material is

$$\{C\} = \frac{E}{(1+v)(1-2v)} \begin{bmatrix} 1-v & v & v & 0 & 0 & 0 \\ v & 1-v & v & 0 & 0 & 0 \\ v & v & 1-v & 0 & 0 & 0 \\ 0 & 0 & 0 & \frac{1-2v}{2} & 0 & 0 \\ 0 & 0 & 0 & 0 & \frac{1-2v}{2} & 0 \\ 0 & 0 & 0 & 0 & 0 & \frac{1-2v}{2} \end{bmatrix}$$

The stress is defined in the term of constitutive matrix $\{C\}$ and total strain vector $\{\epsilon\}$ is

$$\{\sigma\} = \{C\}\{\epsilon\}$$

5.2.13 Axisymmetric Elastisaly Equation:

A class of problem exists that in reality involve three dimensional continua and forces, but which reduce mathematically to two dimensions. These problems are called ax symmetric problem.

The stress components at a point in the continuum for the axisymmetric case in term of the cylindrical reference system are shown in fig below

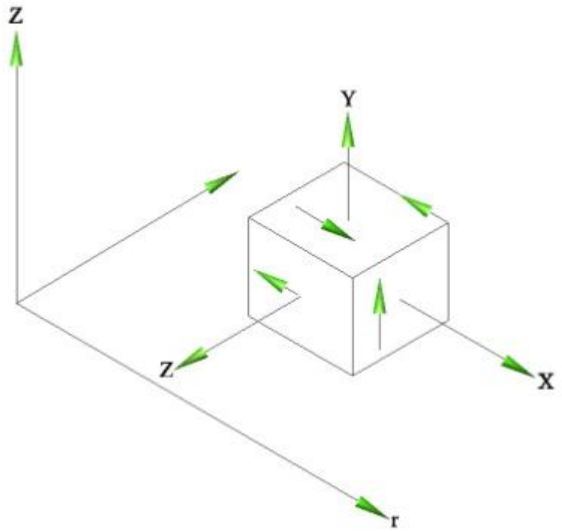

Fig 5-5. [Cylindrical coordinate stress components for axisymmetric case].

5.2.14 Axisymmetric Elasticity Equation:

For axisymmetric , all equation must be independent of θ and all displacement must be in the $r-z$ plane.

The strain displacement relationship in cylindrical coordinate is:

$$\epsilon_r = \frac{\partial u}{\partial r}$$

$$\epsilon_z = \frac{\partial w}{\partial z}$$

$$\epsilon_\theta = \frac{u}{r}$$

$$\gamma_{rz} = \frac{\partial w}{\partial r} + \frac{\partial u}{\partial z}$$

Note that although the strain is independent of θ co ordinate, there is a strain ϵ_θ in the circumferential direction .putting this relationship in matrix form, we have

$$\{\epsilon\} = \begin{Bmatrix} u \\ v \\ w \end{Bmatrix} = \begin{bmatrix} \frac{\partial}{\partial r} & 0 \\ 0 & \frac{\partial}{\partial z} \\ \frac{1}{r} & 0 \\ \frac{\partial}{\partial z} & \frac{\partial}{\partial r} \end{bmatrix} \begin{Bmatrix} u \\ w \end{Bmatrix}$$

Also for this case of symmetry, we have the following stress-strain relationship for isotopic material.

$$\{C\} = \frac{E}{(1+v)(1-2v)} \begin{bmatrix} 1-v & v & v & 0 \\ v & 1-v & v & 0 \\ v & v & 1-v & \frac{1-2v}{2} \end{bmatrix} \begin{Bmatrix} \epsilon_r \\ \epsilon_z \\ \epsilon_\theta \\ \gamma_{rz} \end{Bmatrix}$$

For above we can write as

$$\sigma_r = \frac{E}{(1+v)(1-2v)} \{(1-v)\epsilon_r + v(\epsilon_z) + v\epsilon_\theta\}$$

Or

$$\sigma_r = \frac{E}{(1+v)(1-2v)} \{(1-v)\epsilon_r + v(\epsilon_z + \epsilon_\theta)\}$$

and

$$\sigma_z = \frac{E}{(1+v)(1-2v)} \{v\epsilon_r + (1-v)\epsilon_z + v\epsilon_\theta\}$$

Or

$$\sigma_z = \frac{E}{(1+v)(1-2v)} \{(1-v)\epsilon_z + v(\epsilon_\theta + \epsilon_r)\}$$

And

$$\sigma_\theta = \frac{E}{(1+v)(1-2v)} \{v\epsilon_r + v\epsilon_z(1-v)\epsilon_\theta\}$$

or

$$\sigma_\theta = \frac{E}{(1+v)(1-2v)}\{(1-v)\epsilon_\theta + v(\epsilon_r + \epsilon_\theta)\}$$

Now here

$$\sigma_z = \sigma_1 = \frac{E}{(1+v)(1-2v)}\{(1-v)\epsilon_z + v(\epsilon_x - \epsilon_\theta)\}$$

But as we know that

$$\epsilon_z = \epsilon_1 = \frac{\partial u_1}{\partial z}$$

$$\epsilon_r = \epsilon_2 = \frac{\partial u_2}{\partial r}$$

$$\epsilon_\theta = \frac{u_2}{r}$$

So put in above

$$\sigma_1 = \frac{E}{(1+v)(1-2v)}\left\{(1-v)\frac{\partial u_1}{\partial z} + v(\frac{\partial u_2}{\partial r} - \frac{u_2}{r})\right\}$$

$$\sigma_1 = \frac{E}{(1+v)(1-2v)}\left\{(1-v)\frac{\partial u_1}{\partial z} + v\frac{1}{r}(\frac{\partial u_2}{\partial r})\right\}$$

Now differentiating the above,w.r.t."t" we have:,

$$\frac{\partial \sigma_1}{\partial t} = \frac{E}{(1+v)(1-2v)}\left\{(1-v)\frac{\partial}{\partial t}\frac{\partial u_1}{\partial z} + v\frac{1}{r}\frac{\partial}{\partial t}(\frac{\partial u_2}{\partial r})\right\}$$

Now multiply by 2πr, integrate w.r.t. r from R to R+t and divide by $2\pi\left(R+\frac{1}{2}t\right)t$ we get an equation for axial stress velocity relation,

$$\frac{\partial \overline{\sigma_1}}{\partial t} = \frac{E}{(1+v)(1-2v)}\left\{(1-v)\frac{\partial}{\partial t}\frac{\partial \overline{u_1}}{\partial z} + v\frac{R+t}{\left(R+\frac{1}{2}t\right)t}\dot{u_2} - v\frac{R+t}{\left(R+\frac{1}{2}t\right)t}\dot{u_2}\right\} \ldots 16$$

Unfortunately this equation is not appropriate for the present investigation

The more suitable equation is found by

$$\epsilon_z = \frac{1}{E}[\sigma z - v(\sigma\theta + \sigma x)]$$

As we know that

$$\epsilon_z = \epsilon_1, \qquad \sigma_z = \sigma_1, \ \ \sigma_r = \sigma_2$$

So

$$\epsilon_1 = \frac{1}{E}[\sigma_1 - v(\sigma_\theta + \sigma_2)]$$

But also we know that

$$\epsilon_z = \epsilon_1 = \frac{\partial u_z}{\partial z} = \frac{\partial u_1}{\partial z}$$

So, put in above

$$\frac{\partial u_1}{\partial z} = \frac{1}{E}[\sigma_1 - v(\sigma_\theta + \sigma_2)]$$

Or

$$\sigma_1 = E\frac{\partial u_1}{\partial z} + v\sigma_\theta + v\sigma_2$$

It is the equation for axial stress- displacement equation. So for convert it to axial velocity.

We differential it w.r.t 't' multiply by $2\pi r$ and integrate w.r.t r from R to (R+t) and divide by $2\pi\left(R + \frac{1}{2}t\right)t$ then we will an equation for axial stresses velocity i.e

$$\frac{\partial \sigma_1}{\partial t} = E\frac{\partial}{\partial t}\frac{\partial u_1}{\partial z} + v\frac{\partial}{\partial t}\sigma_\theta + v\frac{\partial}{\partial t}\sigma_2$$

$$\frac{2\pi r}{2\pi\left(R + \frac{1}{2}t\right)t}\int_R^{R+t}\frac{\partial \sigma_1}{\partial t}dr$$

$$= E\frac{2\pi r}{2\pi\left(R + \frac{1}{2}t\right)t}\int_R^{R+t}\frac{\partial}{\partial t}\frac{\partial u_1}{\partial z} + \frac{2\pi r v}{2\pi\left(R + \frac{1}{2}t\right)t}\int_R^{R+t}\frac{\partial}{\partial t}\sigma_\theta$$

$$+ \frac{2\pi r v}{2\pi\left(R + \frac{1}{2}t\right)t}\int_R^{R+t}\frac{\partial}{\partial t}\sigma_2$$

After Simplification we get the axial- stress velocity equation is

$$\frac{\partial \overline{\sigma_1}}{\partial t} = E\frac{\partial}{\partial t}\frac{\partial \overline{\dot{u}_1}}{\partial z} + v\frac{\partial \overline{\overline{\sigma_\theta}}}{\partial t} + v\frac{\partial \overline{\sigma_2}}{\partial t} \ldots\ldots 17$$

Where

$$\overline{\overline{\sigma\theta}} = \frac{1}{2\pi\left(R + \frac{1}{2}t\right)t}\int_R^{R+t} 2\pi r\dot{u}_z$$

And

$$\overline{\dot{u}_1} = \frac{1}{2\pi\left(R + \frac{1}{2}t\right)t}\int_R^{R+t} 2\pi r\dot{u}_z dr$$

$$\overline{\sigma_1} = \frac{1}{2\pi\left(R + \frac{1}{2}t\right)t}\int_R^{R+t} 2\pi r\sigma_2 dr$$

And

5.3 Linear Momentum Equation In Radial Direction or Equation Of Motion In Radial Direction

The linear momentums equation or equation of motion in radial direction in two-dimensional form is lin & Morgan [1956a] kolsky 1953, Mass [1970]

$$\rho_t\frac{\partial \dot{u}_2}{\partial t} + \rho_t\dot{u}_2\frac{\partial \dot{u}_2}{\partial z} + \rho_t\dot{u}_2\frac{\partial \dot{u}_2}{\partial r} = \frac{1}{r}\frac{\partial(r\sigma_2)}{\partial r} + \frac{\partial \tau_{21}}{\partial z} - \frac{\sigma_\theta}{r} + F_r$$

Where

$\dot{u}_1,\ \dot{u}_2$	=	Axial and radial velocities
ρ_t	=	The mass density of tube material
σ_2	=	Radial stresses
$\sigma_\theta = \sigma_3$	=	Hoop stress
τ_{21}	=	Shear stresses
$F_r = F_2$	=	Radial body force density for the pipe
t	=	Time

As the second and the third term of above equation are the connective term and as the deformation is small so these term may be ignored and F_r =o

So the above equation reduced to

$$\rho_t \frac{\partial \dot{u}_2}{\partial t} = \frac{1}{r}\frac{\partial (r\sigma_2)}{\partial r} + \frac{\partial \tau_{21}}{\partial z} - \frac{\sigma_\theta}{r}$$

To arrive at one-dimensional formulation the above equation are multiplied by 2πr, integrative with r from R to $R + t$ and divided by $2\pi\left(R + \frac{1}{2}t\right)t$, we get,

$$\frac{2\pi r}{2\pi\left(R + \frac{1}{2}t\right)t}\int_R^{R+t} \rho_t \frac{\partial \dot{u}_2}{\partial t} dr$$

$$= \frac{2\pi r}{2\pi\left(R + \frac{1}{2}t\right)t}\int_R^{R+t} \frac{1}{r}\frac{\partial (r\sigma_2)}{\partial r} dr + \frac{2\pi r}{2\pi\left(R + \frac{1}{2}t\right)t}\int_R^{R+t} \frac{\partial \tau_{21}}{\partial z} dr$$

$$- \frac{2\pi r}{2\pi\left(R + \frac{1}{2}t\right)t}\int_R^{R+t} \frac{\sigma_\theta}{r} dr$$

$$\frac{\partial}{\partial t}\rho_t \frac{1}{2\pi\left(R + \frac{1}{2}t\right)t}\int_R^{R+t} 2\pi r \dot{u}_2 dr$$

$$= \int_R^{R+t} \frac{2\pi r}{2\pi\left(R + \frac{1}{2}t\right)t}\frac{1}{r}\frac{\partial (r\sigma_2)}{\partial r} dr + \frac{\partial}{\partial z}\frac{1}{2\pi\left(R + \frac{1}{2}t\right)t}\int_R^{R+t} 2\pi r \tau_{21} dr$$

$$- \frac{1}{2\pi\left(R + \frac{1}{2}t\right)t}\int_R^{R+t} 2\pi r \frac{\sigma_\theta}{r} dr$$

Further simplifies the above equation

$$\rho_t \frac{\partial}{\partial t}\frac{1}{2\pi\left(R + \frac{1}{2}t\right)t}\int_R^{R+t} 2\pi r \dot{u}_2 dr$$

$$= \frac{\sigma_2}{2\pi\left(R + \frac{1}{2}t\right)t}\int_R^{R+t} 2\pi r dr + \frac{\partial}{\partial z}\frac{1}{2\pi\left(R + \frac{1}{2}t\right)t}\int_R^{R+t} 2\pi r \tau_{21} dr$$

$$- \frac{1}{2\pi\left(R + \frac{1}{2}t\right)t}\int_R^{R+t} \sigma_\theta dr$$

As we have approximated the long wave length i.e $\lambda \gg\gg D$ so, the axially symmetric shear force i.e $\int_R^{R+t} 2\pi r\tau_{21} dr$ is ignored so the above equation becomes

$$\rho_t \frac{\partial \overline{\ddot{u}_2}}{\partial t} = \frac{R+t}{\left(R+\frac{1}{2}t\right)t}\sigma_2 - \frac{R}{\left(R+\frac{1}{2}t\right)t}\sigma_2 + \frac{1}{\left(R+\frac{1}{2}t\right)t}\overline{\sigma_\theta} \ldots\ldots 18$$

Where

$$\overline{\ddot{u}_2} = \frac{1}{2\pi\left(R+\frac{1}{2}t\right)t}\int_R^{R+t} 2\pi r u_2 dr$$

And

$$\overline{\sigma_\theta} = \int_R^{R+t} \sigma_\theta dr$$

Where $\overline{\ddot{u}_2}$ and $\overline{\sigma_\theta}$ are the average values.

It is the required one dimensional equation is radial direction

5.3.2 Oil and Tube Coupling:

The oil and tube equation are coupled by means of boundary condition, which representing the contact between oil and tube wall interface at $r = R$, outside the pipe a constant pressure is assume to exist.

The interface conditions are:

Condition 1

$$\tau_{12} \quad at \quad r = R = -\tau_0$$

And ……19

$$\tau_{12} \quad at \quad r = R + t = 0$$

Condition 2

$$\sigma_2 \quad at \quad r = R = -p \quad \ldots\ldots 20$$

$$\sigma_2 \quad at \quad r = R + t = -P_{out}$$

Condition 1 and 2 is basically the dynamic condition

Condition 3

It is basically kinematic condition

$$(\dot{u}_r = \dot{u}_2) \quad at \quad r = R = (V_r = V_2) \quad at \quad r = R \quad .....21$$

$$(\dot{u}_r = \dot{u}_2) \quad at \quad r = \ R + t \ = (V_r = V_2)_{out}$$

Where $(V_2)_{out}$,the radial velocity of the external fluid, mostly air but in some cases fluid [A.S. Tissling]. Buried pipe are not considered.

The condition 1 & 2 above i.e. eq. 19 and 20 give the shear stress and fluid pressure acting on the pipe wall.

The condition 3 i.e. 21 (the kinematic condition) shows the adherence of solid and fluid. The fluid outside the tube is not modeled so we do not know the value of $(V_2)_{out}$.

As we have not modeled the fluid inside the pipe two-dimensional so we said previously by (i.e. in equ. 16) that is not suitable for our appropriate for one-dimensional approach.

Equation 10 =>

Axial motion of fluid i.e. Axial Component of Navier-Stroke equation.

$$\rho_{oil}\frac{\partial \bar{V}}{\partial t} + \frac{\partial \bar{P}}{\partial z} = \rho_{oil} gSin \propto + \frac{-2}{R}\tau$$

Divided throughout by ρ_{oil}

$$\frac{\partial \bar{V}}{\partial t} + \frac{1}{\rho_{oil}}\frac{\partial \bar{P}}{\partial z} = gSin \propto - \frac{2}{\rho_{oil} R}\tau \ldots\ldots\ldots 22$$

Where $\bar{V}$ = Cross-sectional averaged axial velocity.

$\bar{P}$ = Cross-sectional averaged pressure.

The continuity eq. 11 = >

$$\frac{1}{\beta}\frac{\partial \bar{P}}{\partial t}+\frac{\partial \bar{V}}{\partial z}+\frac{2V_2}{R}=0$$

The condition 3 i.e. equation 21 at r = R in above.

$$\frac{1}{\beta}\frac{\partial \bar{P}}{\partial t}+\frac{\partial \bar{V}}{\partial z}+\frac{2}{R}\dot{u}_2=0 \ldots\ldots 23$$

As we know that

$$\dot{u}_2=\frac{r}{E}\{\sigma_\theta-\nu(\sigma_z+\sigma_2)\}$$

$$\dot{u}_2=\frac{r}{E}\frac{\partial}{\partial t}\{\sigma_\theta-\nu(\sigma_z+\sigma_2)\}$$

Put in above.

5.4 Radial Motion of Fluid i.e. Radial Component of Navier-Stokes equation.

The equation for the radial flow is equation 14-A

$$\frac{1}{2}\rho_{oil}R\frac{\partial v_2}{\partial t}+p-\bar{P}=0 \ldots\ldots\ldots 14A$$

Or

$$p=\bar{P}-\frac{1}{2}\rho_{oil}R\frac{\partial v_2}{\partial t}$$

Put the condition 3 i.e. equation 21 in above.

$$p=\bar{P}-\frac{1}{2}\rho_{oil}R\frac{\partial \dot{u}_2}{\partial t} \ldots\ldots\ldots\ldots 24$$

5.4.1 For Pipe:

5.4.1.1 Equation of motion Pipe axial:

The equation of motion of pipe in axial direction is equation 15 =>

$$\rho_t \frac{\partial \dot{u}_1}{\partial t} = \frac{\partial \sigma_1}{\partial z} + \frac{(R+t)\tau_{12}}{\left(R+\frac{1}{2}t\right)t} - \frac{R\tau_{12}}{\left(R+\frac{1}{2}t\right)t} + \rho_t g \sin \propto$$

$$\frac{\partial \dot{u}_1}{\partial t} - \frac{1}{\rho_t}\frac{\partial \sigma_1}{\partial z} = \frac{1}{\rho_t}\left[\frac{(R+t)\tau_{12}}{\left(R+\frac{1}{2}t\right)t} - \frac{R\tau_{12}}{\left(R+\frac{1}{2}t\right)t} + g \sin \propto\right]$$

Put the condition 1 i.e. equation 19 in above.

$$\frac{\partial \dot{u}_1}{\partial t} - \frac{1}{\rho_t}\frac{\partial \sigma_1}{\partial z} = \frac{(R+t)\,0}{\rho_t\left(R+\frac{1}{2}t\right)t} - \frac{R\tau_0}{\rho_t\left(R+\frac{1}{2}t\right)t} + g \sin \propto$$

We get

$$\frac{\partial \dot{u}_1}{\partial t} - \frac{1}{\rho_t}\frac{\partial \overline{\sigma_1}}{\partial z} = \frac{R}{\rho_t\left(R+\frac{1}{2}t\right)t}\tau_0 + g \sin \propto \qquad \ldots.25$$

In addition, we know that from equation 17

$$\frac{\partial \overline{\sigma_1}}{\partial t} = E\frac{\partial \overline{\dot{u}_1}}{\partial z} + \nu\left[\frac{\partial}{\partial t}\left(\overline{\overline{\sigma\theta}} + \overline{\sigma 2}\right)\right]$$

Rearranging the term

$$\frac{\partial \dot{u}_1}{\partial z} - \frac{1}{E}\frac{\partial \overline{\sigma_1}}{\partial t} + \frac{\nu}{E}\frac{\partial}{\partial t}\left(\overline{\overline{\sigma\theta}} + \overline{\sigma 2}\right) \ldots\ldots 26$$

5.4.1.2 ***Equation*** *of motion of Pipe Radial*

As we know that equation 18 =>

$$\rho_t \frac{\partial \overline{\dot{u}_2}}{\partial t} = \frac{R+t}{\rho_t\left(R+\frac{1}{2}t\right)t}(\sigma_2) - \frac{R}{\rho_t\left(R+\frac{1}{2}t\right)t}(\sigma_2) - \frac{1}{\rho_t\left(R+\frac{1}{2}t\right)t}\overline{\sigma_\theta}$$

Put the condition 2 i.e. equation 20 in above

$$\rho_t \frac{\partial \overline{\dot{u}_2}}{\partial t} = \frac{R+t}{\rho_t\left(R+\frac{1}{2}t\right)t}(-P_{out}) - \frac{R}{\rho_t\left(R+\frac{1}{2}t\right)t}(-p) - \frac{1}{\rho_t\left(R+\frac{1}{2}t\right)t}\overline{\sigma_\theta}$$

Rearranging the term, we have.

$$\rho_t \frac{\partial \overline{\dot{u}_2}}{\partial t} = -\frac{R+t}{\rho_t\left(R+\frac{1}{2}t\right)t}P_{out} + \frac{R}{\rho_t\left(R+\frac{1}{2}t\right)t}p - \frac{1}{\rho_t\left(R+\frac{1}{2}t\right)t}\overline{\sigma_\theta}$$

Put the value of p from equation 24 into above

$$\rho_t \frac{\partial \overline{\dot{u}_2}}{\partial t} = -\frac{R+t}{\rho_t\left(R+\frac{1}{2}t\right)t}P_{out} + \frac{R}{\rho_t\left(R+\frac{1}{2}t\right)t}\left(\bar{P} - \frac{1}{2}\rho_{oil}R\frac{\partial \dot{u}_2}{\partial t}\right) - \frac{1}{\rho_t\left(R+\frac{1}{2}t\right)t}\overline{\sigma_\theta}$$

$$\rho_t \frac{\partial \overline{\dot{u}_2}}{\partial t} = -\frac{(R+t)}{\rho_t\left(R+\frac{1}{2}t\right)t}P_{out} + \frac{R}{\rho_t\left(R+\frac{1}{2}t\right)t}\bar{P} - \frac{R^2}{2\left(R+\frac{1}{2}t\right)t}\rho_{oil}\frac{\partial \dot{u}_2}{\partial t} - \frac{1}{\left(R+\frac{1}{2}t\right)t}\overline{\sigma_\theta}$$

$$\rho_t \frac{\partial \overline{\dot{u}_2}}{\partial t} + \frac{1}{2}\frac{R^2}{\left(R+\frac{1}{2}t\right)t}\rho_{oil}\frac{\partial \dot{u}_2}{\partial t} = \frac{R\bar{P}}{\left(R+\frac{1}{2}t\right)t} - \frac{(R+t)}{\rho_t\left(R+\frac{1}{2}t\right)t}P_{out} - \frac{1}{\left(R+\frac{1}{2}t\right)t}\overline{\sigma_\theta}$$

$$\rho_t\left(R+\frac{1}{2}t\right)t\frac{\partial \overline{\dot{u}_2}}{\partial t} + \frac{1}{2}R^2\rho_{oil}\frac{\partial \dot{u}_2}{\partial t} = R\bar{P} - (R+t)P_{out} - \overline{\sigma_\theta} \ldots\ldots\ldots 27$$

5.5 Quasic Static:

A system having highest order derivative as a liner i.e. There are no product or exponential of the highest order derivative they appears by themselves, multiplied by co-efficient which are function of dependent variable themselves, such a system in called Quasi static.

5.5.1 Four Equation Model :

As we have consider the long wavelength $\gg\gg D$ earlier, So according to [Skalak, 1956, Lin & Morgan 1956b, Schwarz, 1978] The acceleration in the above equation. i.e. we will

A quasi-Static relation which derived by the [Tissjling] between hoop stress and internal pressure is:

$$\overline{\sigma_\theta} = \frac{R}{t}p - \frac{R+t}{t}\rho_{Out}$$

And also [Tissjling] concluded that

$$\frac{\partial}{\partial t}[\overline{\overline{\sigma_\theta}} + \overline{\sigma_2}] = \frac{R}{t}\frac{1}{1+\frac{1}{2}\frac{t}{R}}\frac{\partial P}{\partial t}$$

Which 'P' is the Oil Pressure.

And also

$$\frac{\partial}{\partial t}[\sigma_\theta] = \left(\frac{R}{t}\frac{1+\frac{t}{R}}{2+\frac{t}{R}}\right)\frac{\partial P}{\partial t}$$

Putting in the equation

5.5.2 Final Equation of Couple System:

The final model for the liquid and Pipe in the axial direction are:

For Liquid, Axial

$$\frac{\partial V}{\partial t} + \frac{1}{\rho_{oil}}\frac{\partial P}{\partial z} = -\frac{2}{\rho_{oil}R}\tau_0 + g\sin\alpha \qquad \dots\dots A1$$

$$\frac{\partial V}{\partial t} + \left[\frac{1}{\beta} + \frac{2}{E}\left(\frac{R}{t} + \frac{1+\frac{t}{R}}{2+\frac{t}{R}} + v\right)\right]\frac{\partial P}{\partial t} - \frac{2v}{E}\frac{\partial \overline{\sigma_1}}{\partial t} = 0 \qquad \dots..A2$$

For Pipe, Axial

$$\frac{\partial \overline{\ddot{u}_1}}{\partial t} + \frac{1}{\rho_t}\frac{\partial \overline{\sigma_1}}{\partial z} = \frac{1}{\rho_t\left(1+\frac{1}{2}\frac{t}{R}\right)e}\tau_0 + g\sin\gamma \dots\dots A3$$

$$\frac{\partial \overline{\ddot{u}_1}}{\partial t} + \frac{1}{\rho_t}\frac{\partial \overline{\sigma_1}}{\partial z} = \frac{vR}{Et}\frac{1}{(1+\frac{1}{2}\frac{t}{R})}\frac{\partial P}{\partial t} = 0 \dots\dots A4$$

It is the equation (Model) for thick walled tube.

5.6 Solution of Four-Equation Model:

In this chapter we have solve the four equation derived previously by using the initial values.

As in, our case the tube pipe is thin walled i.e. $\left(\frac{D}{t} \gg 25\right)$

As we assumed that-previously the equation for AI-A4 are the equation because these wake Now we assume that the wall are their wall i.e. t << R in this case we can say that the related stress are the small compare to hoop and related stress i.e. from equation previously.

$$\bar{\sigma}_\theta = \frac{R}{t}P - \frac{R+t}{t}P_{out}$$

$$\bar{\sigma}_\theta = \frac{R}{t}P$$

And

$$\bar{\sigma}_2 = -\frac{3}{4}P$$

To by Darcy Wesbech equation we have

$$\triangle P = f\rho_{oil}\left(\frac{L}{D}\right)\left(\frac{V^2}{2}\right)$$

$$\triangle P\left(\frac{\pi D^2}{4L}\right) = \tau_o \pi DL$$

Putting the Value of $\triangle P$

$$\tau_o = \frac{\triangle PD}{4L} = \frac{f\rho_{oil}\left(\frac{L}{D}\right)\left(\frac{V^2}{2}\right)}{4L}D = \frac{f\rho_{oil}V^2}{8}$$

$$\tau_o = \frac{f\rho_{oil}Q^2}{8d4\pi^2} :=> Q = AxV = V = \frac{4Q}{\pi d^2}$$

Equation A1 =>

$$\frac{\partial v}{\partial t} + \frac{1}{\rho_{oil}}\frac{\partial P}{\partial z} = -\frac{2}{\rho_{oil}R}\frac{f\rho_{oil}Q^2}{8d4\pi^2} + g\sin\gamma$$

$$\frac{\partial v}{\partial t} + \frac{1}{\rho_{oil}}\frac{\partial P}{\partial z} = \frac{-2fQ^2}{R \times (2d)^4\pi^2} + g\sin\gamma$$

$$\frac{\partial v}{\partial t}+\frac{1}{\rho_{oil}}\frac{\partial P}{\partial z}=\frac{-2fQ^2}{R\times\left(2\frac{2R}{2}\right)^4\pi^2}+g\sin\gamma$$

$$\frac{\partial v}{\partial t}+\frac{1}{\rho_{oil}}\frac{\partial P}{\partial z}=\frac{-252fQ^2}{R^5\times\pi^2}+g\sin\gamma\ldots.A6$$

Now Equation A2

$$\frac{\partial v}{\partial z}+\frac{\partial P}{\partial t}\left[\frac{1}{\beta}+\frac{2}{E}\left(\frac{R}{t}+\frac{1+\frac{t}{R}}{2+\frac{t}{R}}+v\right)\right]-\frac{2\gamma}{E}\frac{\partial\overline{\sigma_1}}{\partial t}=0$$

By Putting as $\frac{t}{R}\ll 1$ So the above equation becomes

$$\frac{\partial v}{\partial z}+\frac{\partial P}{\partial t}\left[\frac{1}{\beta}+\frac{2R}{Et}\right]-\frac{2\gamma}{E}\frac{\partial\overline{\sigma_1}}{\partial t}=0$$

As the variation with r negligible in the wall tube, So the average value of the external in true

$$\frac{\partial v}{\partial z}+\left[\frac{1}{\beta}+\frac{2R}{Et}\right]\frac{\partial P}{\partial t}-\frac{2\gamma}{E}\frac{\partial\overline{\sigma_1}}{\partial t}=0$$

Now A3 =>

$$\frac{\partial\overline{\dot{u}_1}}{\partial t}+\frac{1}{\rho_t}\frac{\partial\overline{\sigma_1}}{\partial z}=\frac{1}{\rho_t\left(1+\frac{1}{2}\frac{t}{R}\right)e}\tau_0+g\sin\gamma$$

As this wall $\frac{t}{R}\ll 1$ and $\tau_0=0.202\,f\rho_{Oil}\frac{Q^2}{d^4}$

Put in above.

$$\frac{\partial\overline{\dot{u}_1}}{\partial t}+\frac{1}{\rho_t}\frac{\partial\overline{\sigma_1}}{\partial z}=\frac{1}{\rho_t(1+0)e}\tau_0+g\sin\gamma$$

As the variation in γ are negligible in thin wall tubes So, the average values of the tube variation are omitted. So the above equation becomes.

$$\frac{\partial\overline{\dot{u}_1}}{\partial t}+\frac{1}{\rho_t}\frac{\partial\overline{\sigma_1}}{\partial z}=g\sin\gamma\ldots\ldots\ldots\ldots.A8$$

Equation A4=>

$$\frac{\partial \overline{\dot{u}_1}}{\partial t} + \frac{1}{\rho_t}\frac{\partial \overline{\sigma_1}}{\partial z} = \frac{\gamma R}{Et}\frac{1}{\left(1+\frac{1}{2}\frac{t}{R}\right)}\frac{\partial P}{\partial t} = 0$$

As thin wall, So $\frac{t}{R} \ll 1$

$$\frac{\partial \overline{\dot{u}_1}}{\partial t} + \frac{1}{\rho_t}\frac{\partial \overline{\sigma_1}}{\partial z} = \frac{\gamma R}{Et}\frac{1}{(1+0)}\frac{\partial P}{\partial t} = 0$$

As the variation in γ are negligible in thin wall tube so, the average values of the tube variable are omitted So, the above equation become.

$$\frac{\partial \overline{\dot{u}_1}}{\partial t} + \frac{1}{\rho_t}\frac{\partial \overline{\sigma_1}}{\partial z} = \frac{\gamma R}{Et}\frac{\partial P}{\partial t} = 0 \ldots\ldots\ldots A9$$

5.7 Summary of Four-Equation Model are:

Liquid:-

$$\frac{\partial V}{\partial t} + \frac{1}{\rho_{Oil}}\frac{\partial P}{\partial z} = -\frac{0.808 f Q^2}{d^5} + g\sin\gamma \ldots\ldots\ldots\ldots A10$$

$$\left(\frac{1}{\beta}+\frac{2R}{Et}\right)\frac{\partial P}{\partial t} + \frac{\partial V}{\partial z} = \frac{2\gamma}{E}\frac{\partial \sigma_1}{\partial_t} \ldots\ldots\ldots\ldots\ldots\ldots\ldots A11$$

$$\frac{\partial \overline{\dot{u}_1}}{\partial t} + \frac{1}{\rho_t}\frac{\partial \overline{\sigma_1}}{\partial z} = 0.202 f \frac{\rho_{Oil}}{\rho_t}\frac{Q}{d^4}^2 + g\sin\gamma \ldots\ldots A12$$

$$-\frac{1}{E}\frac{\partial \dot{\sigma}_1}{\partial_t} + \frac{\partial \dot{u}_1}{\partial z} = -\frac{\gamma R}{Et}\frac{\partial P}{\partial t} \ldots\ldots\ldots\ldots\ldots\ldots\ldots\ldots A13$$

The above equation in matrix form can be written as.

$$M\frac{\partial y}{\partial_t} + N\frac{\partial y}{\partial z} = R$$

Where y is the vector of unknown and M & N are the matrix co-efficient and R is the right have side vector.

ρ is the Constant invariant

$$y = \begin{bmatrix} V \\ P \\ \dot{u}_1 \\ \sigma_1 \end{bmatrix}$$

$$M = \begin{bmatrix} 1 & 0 & 0 & 0 \\ 0 & \left(\frac{1}{\beta} + \frac{2R}{Et}\right) & 0 & 0 \\ 0 & 0 & 1 & 0 \\ 0 & \frac{-\gamma R}{Et} & 0 & -\frac{1}{E} \end{bmatrix}$$

$$N = \begin{bmatrix} 0 & \frac{1}{\rho_{Oil}} & 0 & 0 \\ 1 & 0 & 0 & 0 \\ 0 & 0 & 0 & -\frac{1}{\rho t} \\ 0 & 0 & 1 & 0 \end{bmatrix}$$

$$R = \begin{bmatrix} \frac{0.808 f Q^2}{d^5} + g \sin\gamma \\ 0.202 f \frac{\rho_{Oil}}{\rho_t} \frac{Q}{d^4}^2 + g \sin\gamma \\ 0 \end{bmatrix}$$

Here we have the following Parameters

ρ_{Oil} = 0.8976 kg/Liter

ρ_t = 6897 kg/m^3

E = 200 GPa = 200 x 10^3 N/mm^2

t = 1.5 mm

R = 4.5 mm

Q = 40 Liter/min

f = 0.005 (1+1/12d) = 0.005(1+1/12x9) =

β = 250000 Psi x = 17236.89 bar. =1724.138 N/mm^2

γ = 0.27----0.3

$$R = \begin{bmatrix} \dfrac{0.808 f Q^2}{d^5} + g \sin\gamma \\ 0.202 f \dfrac{\rho_{Oil}}{\rho_t} \dfrac{Q}{d^4}^2 + g \sin\gamma \\ 0 \end{bmatrix}$$

$$\frac{\partial V}{\partial t} + \frac{1}{\rho_{Oil}} \frac{\partial P}{\partial z} = -\frac{0.808 f Q^2}{d^5} + g \sin\gamma$$

$$\left(\frac{1}{\beta} + \frac{2R}{Et}\right) \frac{\partial P}{\partial t} + \frac{\partial V}{\partial z} = \frac{2\gamma}{E} \frac{\partial \sigma_1}{\partial_t}$$

$$\frac{\partial \overline{\dot{u}_1}}{\partial t} + \frac{1}{\rho_t} \frac{\partial \overline{\sigma_1}}{\partial z} = 0.202 f \frac{\rho_{Oil}}{\rho_t} \frac{Q}{d^4}^2 + g \sin\gamma$$

$$-\frac{1}{E} \frac{\partial \dot{\sigma_1}}{\partial_t} + \frac{\partial \dot{u_1}}{\partial z} = -\frac{\gamma R}{Et} \frac{\partial P}{\partial t}$$

CHAPTER # 6

6 MATHEMATICAL BEHAVIOR OF PARTIAL DIFFERENTIAL EQUATION

6.1 Introduction

As we see that the partial differential equation derived previously are the linear in order (highest order derivative occurs linearly i.e. there are no product or exponential of the highest order derivative they appears by themselves, multiplied by coefficient which are function of the dependent variable themselves.) Such system is called quasi linear system.

6.2 Basics of Discritization

Let us examine some mathematical properties of system of quasi linear partial differential equation .In the road map below we establish a classification of three type of partial differential equation all of three which are encountered in fluid dynamics [Anderson J.D 1995].

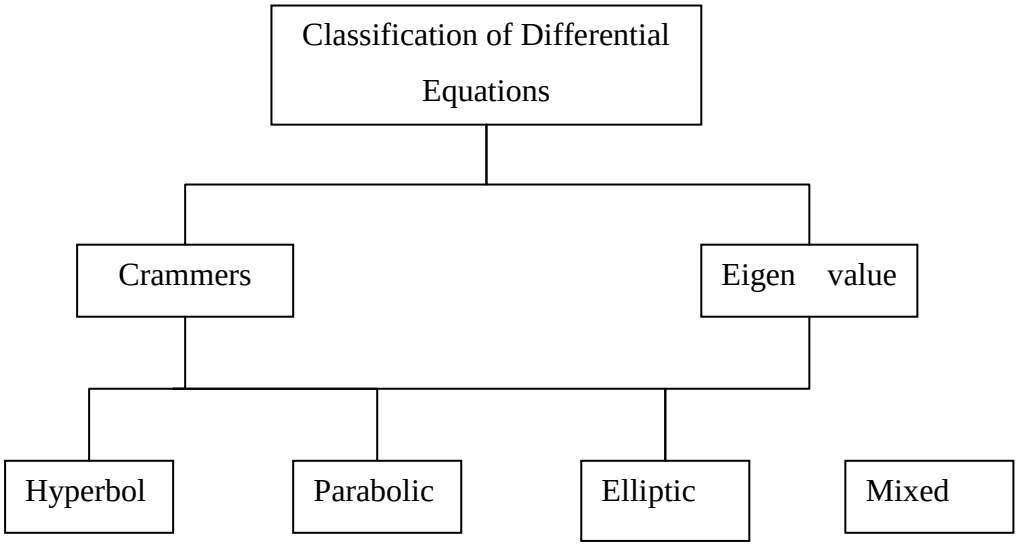

There are two different techniques for determining the classification of differential equation.

- Cramer's rules
- Eigen value method

A General Method of Determining the Classification of Partial differential equation The Eigen value method

I will use the Eigenvalue method because of more general and more sophisticated method then Cramer's rule for assessing the classification of quasi linear partial differential equation based on the Eigenvalue of the system. The Eigenvalue method is based on a display of the system of partial differential equation written in a column vector form such as

$$M\frac{\partial y}{\partial_t} + N\frac{\partial y}{\partial z} = R$$

Where y is the vector of unknown and M & N are the matrix co-efficient and R is the right hand side vector.

ρ is the Constant invariant, Here

$$y = \begin{bmatrix} V \\ P \\ \dot{u_1} \\ \sigma_1 \end{bmatrix}$$

$$M = \begin{bmatrix} 1 & 0 & 0 & 0 \\ 0 & \left(\frac{1}{\beta} + \frac{2R}{Et}\right) & 0 & 0 \\ 0 & 0 & 1 & 0 \\ 0 & \frac{-\gamma R}{Et} & 0 & -\frac{1}{E} \end{bmatrix}$$

$$N = \begin{bmatrix} 0 & \frac{1}{\rho_{Oil}} & 0 & 0 \\ 1 & 0 & 0 & 0 \\ 0 & 0 & 0 & -\frac{1}{\rho t} \\ 0 & 0 & 1 & 0 \end{bmatrix}$$

$$R = \begin{bmatrix} \frac{0.808 f Q^2}{d^5} + g\sin\gamma \\ 0.202 f \frac{\rho_{Oil}}{\rho_t}\frac{Q}{d^4}^2 + g\sin\gamma \\ 0 \end{bmatrix}$$

Here we have the following Parameters

ρ_{Oil} = 0.8976 kg/Liter

ρ_t = 6897 kg/m^3

E = 200 GPa = 200 x 10^3 N/mm^2

t = 1.5 mm

R = 4.5 mm

Q = 40 Liter/min

f = 0.005 (1+1/12d) = 0.005(1+1/12x9) =

β = 250000 Psi x = 17236.89 bar. =1724.138 N/mm^2

γ = 0.27----0.3

The above equation can be written as

$$M\frac{\partial y}{\partial_t} + N\frac{\partial y}{\partial z} = R$$

6.3 Discritization

The word “discritization” is required to be explained first. It comes from word “discrete,” which is defined in The American Heritage Dictionary of the English Language as “constituting a separate thing; individual; distinct; consisting of unconnected distinct parts.” Indeed, it seems to be unique to the literature of numerical analysis, first being introduced in the German literature by Wasow W.R. [1955], carried on by Ames W.F. [1965] and recently embraced by the CFD community as found in Anderson, Dale A.et al [1984], Fletcher, C.A. [1988] and Hirsch, Charles [1988].

In general discritization is the process by which a closed-form mathematical expression, such as a function or a differential or integral equation involving functions, all of which are viewed as having an infinite continuum of values throughout some domain, is approximated by analogous (but different) expressions which prescribe values at only a finite number of discrete points or volumes in the domain. Also, we will single out partial differential equations for purposes of discussion. Therefore, the remainder of this introductory section dwells on the meaning of “discritization.”

Analytical solutions of partial differential equations involve closed-form expressions which give the variation of the dependent variables continuously throughout the domain. In contrast, numerical solutions can give answers at only discrete points in the domain, called grid points. For example, consider Fig. 6.1, which shows a section of a discrete grid in the "tz" plane. For convenience, let us assume that the spacing of the grid points in the "z" direction is uniform and given by (Δ z) and that the spacing of the points in the "t" direction is also uniform and given by (Δ t) as shown in Fig. 6.1.

In general, (Δ z) and (Δ t) are different. Indeed, it is not absolutely necessary that (Δ z) or (Δ t) be uniform; we could deal with totally unequal spacing in both directions, where (Δ t) is a different value between each successive pairs of grid points, and similarly for (Δ t). However, the majority of CFD applications involve numerical solutions on a grid which contains uniform spacing in each direction, because this greatly simplifies the programming of the solution, saves storage space, and usually results in greater accuracy.

In any event, in this chapter we will assume uniform spacing in each coordinate direction but not necessarily equal spacing for both directions; i.e., we will assume Δz and Δt to be constants, but Δz does not have to equal Δt. (We should note that recent research in CFD has focused on unstructured grids, where the grid points are placed in the flow field in a very irregular fashion; this is in Cantrast to a structured grid which reflects some type of consistent geometrical regularity. Figure 6.1 is an example of a structured grid. Some aspects of unstructured grids will not be discussed in here.)

Returning to Fig. 6.1, the grid points are identified by an index "i" which runs in the "z" direction and an index "n" which runs in the "t" direction. Hence, if (i, j) is the index for point P in Fig. 6.1, then the point immediately to the right of P is labeled as (i + 1, j), the point immediately to the left is (i — 1, j), the point directly above is (i, j + 1), and the point directly below is (i, j — 1). Anderson, John D.[1995]

We are now in a position to elaborate on the word "discritization" Imagine that we have one-dimensional flow equations which has been derived by the Navier-Stokes equations and Continuity equation and coupled with structure equation (Pipe or tubes) as shown in chapter 4. These are partial differential equations.

An analytical solution of these equations would provides in principle, closed-form expressions for u, v, p, σ. etc., as functions of "z" and "t", which could be used to give

values of the flow-field variables at any point we wish to choose in the flow, i.e., at any of the infinite number of (t, z) points in the domain. On the other hand, if the partial derivatives in the governing equations are replaced by approximate algebraic difference quotients (to be derived in the next section), where the algebraic difference quotients are expressed strictly in terms of the flow-field variables at two or more of the discrete grid points shown in Fig. 6.1, then the partial differential equations are totally replaced by a system of algebraic equations which can be solved for the values of the flow-field variables at the discrete grid points only. In this sense, the original partial differential equations have been discretized. Moreover, this method of discretization is called the method of finite differences. Finite-difference solutions are widely employed in CFD, and hence much of this chapter will be devoted to matters concerning finite differences. Anderson, John D. [1995]

So this is what discritization means. All methods in CFD utilize some form of discritization the purpose of this chapter is to derive and discuss the more common forms of discritization in use today for finite-difference applications. This constitutes one of the three main headings in Fig. 6.2, which is the road map for this

6.4 Numerical solution method

In this chapter we have solved the four equation derived previously by using the initial values.

As in our case the tubes are thin walled (D/t > 25)

As we assumed that the equation form A1 to A4 are the equation based on thick walled. Now we assume that the wall are thin, i.e. t << R. In this sense we can say that the radial stress are the small compared to the hoop and radial stresses i.e. form equation previously

$$\sigma_\theta = \frac{R}{t} P - \frac{R+t}{t} P_{out}$$

Different techniques can be applied for the discretization of the governing mathematical equations. There are three main discretization methods:

- Finite Differencing Method (FD)
- Finite Volume Method (FV)
- Finite Element Method (FE),

6.5 Discretization Procedure

An engineering problem can be described by a set of partial differential equations

(PDEs). In order to solve the problem, the PDEs are discretised and expressed as a set of equivalent algebraic equations in a matrix form. The equations are solved computationally to obtain the solution of a certain variable at discrete points in space and time. The discritization involves two parts: the discritization of the computational domain and the equation discritization. The FD method discretises the differential form of the PDEs.

The discritization of the computational domain involves the time discritization and the space discritization. For time discritization, the time domain is broken down into a finite number of time steps. The size of the time step is specified and can be either constant or variable.

6.6 Mac Cormack's Technique

McCormack's technique is much simpler in its application. The Mac Cormack's method is an explicit finite-difference technique which is second-order-accurate in both space and time. First introduced in Mac Cormack, R.W, [1969] it became the most popular explicit finite-difference method for solving fluid equation for the next 15 years (Anderson). Today, Mac Cormack's method has been mostly supplanted by more sophisticated approaches. However, the Mac Cormack's method is very "student friendly;" it is among the easiest to understand and program. Moreover, the results obtained by using Mac Cormack's method are perfectly satisfactory for many fluid flow applications. For these reasons, Mac Cormack's method is highlighted here.

Consider two-dimensional grid shown in Fig. 6.3. For purposes of illustration, let us address again the solution of the equations derived in chapter. Here, we will address a time-marching solution using Mac Cormack's technique. We assume that the flow field at each point in Fig. 6.3 is known at time t, and we proceed to calculate the flow-field variables at the same grid points at time t + Δt, as illustrated in Fig. 6.2. First, consider the density at grid point (i, j) at time t + Δt. In Mac Cormack's method, this is obtained from:

$$M\frac{\partial y}{\partial t} + N\frac{\partial y}{\partial z} = R \ldots\ldots\ldots 6.1$$

Where M & N are defined earlier, the equation 6.1 simplified as

$$\frac{\partial y}{\partial t} = M^{-1}R - M^{-1}N\frac{\partial y}{\partial z} \dots\dots\dots 6.2$$

Where

$$y = \begin{Bmatrix} v \\ p \\ u \\ \sigma \end{Bmatrix} \dots\dots\dots 6.3$$

We assume that the flow field at grid points in Figure 6.1 is known as time t, and we proceed to calculate the flow field variable at the same grid points at time $t + \Delta t$, as shown in figure 6.2. First, consider the value of $y = \begin{Bmatrix} v \\ p \\ u \\ \sigma \end{Bmatrix}$ at grid point

(i, j) at time $t + \Delta t$.

In Mac Cormack, R.W, [1969] Method this is obtained from

$$y_i^{t+\Delta t} = y_i^t + \left(\frac{\partial y}{\partial t}\right)_{av} \Delta t \dots\dots\dots 6.4$$

Where $\left(\frac{\partial y}{\partial t}\right)_{av}$ is a representative mean value of $\left(\frac{\partial y}{\partial t}\right)$ between time $t + \Delta t$.

The average time derivative $\left(\frac{\partial y}{\partial t}\right)_{av}$ is obtained from predictor corrector philosophy as follow.

6.6.1 Predictor Step:

We can write equation 6.2 as

By replacing the spatial derivative on the R.H.S with forward differences

$$\left(\frac{\partial y}{\partial t}\right)_i^t = M^{-1}R - M^{-1}N\left[\frac{y_{i+1}^t - y_i^t}{\Delta z}\right] \dots\dots\dots 6.5$$

In equation 6.5 all flow veriable at time t are known values i.e, the R.H.S is known.

Know obtained a predicted value of $\bar{y}_i^{t+\Delta t}$ from the first two terms of the tailor series as follows:

$$\bar{y}_i^{t+\Delta t} = y_i^t + \left(\frac{\partial y}{\partial t}\right)_i^t \Delta t \ldots\ldots\ldots 6.6$$

In equation 6.6 y_i^t is known, and $\left(\frac{\partial y}{\partial t}\right)_i^t$ is a known number from equation 6.5

Hence $\bar{y}_i^{t+\Delta t}$ is readily obtained. The value of $\bar{y}_i^{t+\Delta t}$is only a predicted value of y; it is only first order accurate since equation 6.6 contains only the first orders terms in tailor series.

6.6.2 Corrector Step:

In the corrector step we first obtained a predicted value of time derivative at $t + \Delta t$, $\left(\overline{\frac{\partial y}{\partial t}}\right)_i^{t+\Delta t}$, By substituting the predictive value of Y by replacing the spatial derivative with backward differences.

$$\left(\overline{\frac{\partial y}{\partial t}}\right)_i^{t+\Delta t} = M^{-1}R - M^{-1}N\left[\frac{\bar{y}_{i+1}^{t+\Delta t} - \bar{y}_i^{t+\Delta t}}{\Delta z}\right] \ldots\ldots\ldots 6.7$$

The average value of time derivative of y which appears in 6.1 is obtained from the arithmetic mean of $\left(\frac{\partial y}{\partial t}\right)_i^t$, obtained from equation 6.5 and $\left(\overline{\frac{\partial y}{\partial t}}\right)_i^{t+\Delta t}$ is obtained from 6.7, we have

$$\left(\frac{\partial y}{\partial t}\right)_{av} = \frac{1}{2}\left[\left(\frac{\partial y}{\partial t}\right)_i^t + \left(\overline{\frac{\partial y}{\partial t}}\right)_i^{t+\Delta t}\right]$$

This allow us to obtained the final, corrected value of $Y^{t+\Delta t}$ at time $t + \Delta t$ from equation 6.1 as again repeated here.

$$y_i^{t+\Delta t} = y_i^t + \left(\frac{\partial y}{\partial t}\right)_{av} \Delta t$$

"The Predictor-corrector sequence described above yields the value of y at grid point (I, j) at time $t + \Delta t$, as illustrated in Fig. 6.2. This sequence is repeated at all grid point to obtain the y throughout the flow field at time $t + \Delta t$.

Mac Cormack's technique as described above, because a two-step predictor-Correcor Sequence is used with forward differences on the predictor and with backward difference on the corrector, is a second-order-accurate method". Anderson J.D [1995]

6.7 Space Marching

To illustrate the space-marching idea, let us apply Mac Cormack's technique to the same one-dimensional flow shown in Fig. 6.3. The general flow direction is from left to right in the "tz" plane. In the generic, conservation form, this system of equations is given by equation 6.1 and 6.2 as:

$$M\frac{\partial y}{\partial t} + N\frac{\partial y}{\partial z} = R \ldots\ldots\ldots 6.1$$

Where M & N are defined earlier, the equation 6.1 simplified as

$$\frac{\partial y}{\partial t} = M^{-1}R - M^{-1}N\frac{\partial y}{\partial z} \ldots\ldots\ldots 6.2$$

Since Eq. (6.1) is hyperbolic in this case, space marching is appropriate, and Mac Cormack's technique applicable. With this in mind, notice that Eq. (6.1) is written with the "t" derivative isolated on the left-hand side and the source term and "z" derivative on the right hand side. Return to Fig. 6.2. Assume that the flow-field variables are known along the vertical line in the "tz" plane; this line is the initial data line. Also assume that the flow is locally subsonic everywhere. Then a solution can be obtained, starting with the initial data line and marching downstream in the "z" direction. We will illustrate the process for a single spatial step using Mac Cormack's technique. The ideas are the same as discussed in Sec. 6.3 (Time Marching), except that here the spatial variable "z" performs te same role as the time variable "t" in Sec. 6.3 (Time Marching). For example, in Fig. 6.3 assume the flow variables are known along a vertical line at a given "z" location. (The calculation was started using the initial data along the vertical line t =t^o Let this vertical line run through the grid points (n,i+1), (n,i) and (n,i-1) in Fig. 6.3. That is, the flow variables at these three grid points are considered known. Mac Cormack's technique allows the calculation of the flow variables at grid point (n + 1, j) from the known values at (n, i+1), (n, i) and (n, i-1), as follows. The value of the solution vector y in Eq. (6.2) at grid point (n + 1,i) can be found from

$$y_i^{n+1} = y_i^n + \left(\frac{\partial y}{\partial z}\right)_{av}\Delta z \ldots\ldots\ldots 6.7$$

In equation $\left(\frac{\partial y}{\partial z}\right)_{av}$ is a representative average representative value of the "z" derivative of "y" evaluated between z and $z + \Delta z$ it is found from the equation 6.2 By mean of a predictor-character approach.

6.7.1 Predictor step:

In Eq. (6.2), replace the "z" derivative with a forward differences as

$$\frac{\partial y}{\partial t} = M^{-1}R - M^{-1}N\left[\frac{y_{i+1}^{n} - y_{i}^{n}}{\Delta z}\right] \ldots\ldots\ldots 6.8$$

In Eq. (6.8), all terms on the right side are known numbers, because the flow is

known along the vertical line through point (n, i). Calculate a predicted value for "y" at point (n + 1, i) from a Taylor series:

$$\bar{y}_{i}^{n+1} = y_{i}^{n} + \left(\frac{\partial y}{\partial z}\right)_{i}^{n} \Delta z \ldots..6.9$$

That is, $\bar{y}_{i}^{n+1}$ represents the predicted values of its individual elements, given for the present one-dimensional case:

$$\left(\frac{\partial \bar{y}}{\partial t}\right)_{i}^{n+1} = M^{-1}R - M^{-1}N\left(\frac{\partial \bar{y}}{\partial z}\right)_{i}^{n+1} \ldots\ldots\ldots 6.10$$

Before progressing further, the calculated values on the right side of Eq. (6.10) must be decoded to obtain predicted values of the primitive variables,

6.7.2 Corrector Step:

Calculate a predicted value of $\left(\frac{\partial \bar{y}}{\partial z}\right)_{i+1}^{n}$ at location z+Δz denoted by $\left(\frac{\partial \bar{y}}{\partial z}\right)_{i+1}^{n}$ by inserting the predicted values for y into Eq. (6.1), using backward differences. That is

$$\left(\frac{\partial \bar{y}}{\partial z}\right)_{i+1}^{n} = M^{-1}R - M^{-1}N\left(\frac{\bar{y}}{z}\right)_{i+1}^{n} - \left(\frac{\bar{y}}{z}\right)_{i+1}^{n} \ldots\ldots\ldots 6.10$$

In Eq. (6.29), the values of ‘ and are constructed from the predicted primitive variables which had been decoded earlier in the predictor step. The average value, (ÔF/ is now formed as an arithmetic mean IIOFY f

From Eq. (6.29)

In turn, the final, corrected value of F is obtained from Eq. (6.25), repeated below:

FJ 1 ((6.25)

Clearly, this spatial, downstream marching solution using Mac Cormack's [1969] technique is a direct analog of the time-marching solution discussed in Sec. 6.3, with the marching variable x playing the role of the earlier marching variable t.

There are two noteworthy differences associated with the downstream marching approach compared to the time-marching approach. The first has already been mentioned; it is associated with the need to decode the primitive variables from the flux variables. This decoding is simple when a time-marching solution of the conservation form of the equations is employed, as reflected in Eqs. (2.100) to (2.104), but it is more elaborate when a spatial-marching solution of the con-

6.8 Stability Analysis

In General two types of errors are introduced in the solution of finite difference equation. These errors may be caused by round off error, which is a property of a computer, or by the application of a particular numerical method, i.e., discretization errors. If the errors introduced into the finite difference equation are not controlled, the growth of the errors with the solution of finite difference equation will result in an unstable solution. Understanding and controlling these errors by stability analysis is essential for a successful solution of an finite difference equation. Here the stability analysis of mathematical derived earlier are introduced.

6.9 Von Neumann Stability Analyses

A number of methods exist to investigate the stability limits of a finite difference Scheme. One such a method is the Fourier or Von Neumann analysis (Mattheijet al., 2005; Hirsch, 1988; Anderson et al., 1984; Abbott and Basco, 1989). In this method a solution of the finite difference equation is expended in a Fourier series. The decay or growth of amplification factor in indicates whether or not the numerical algorithm is stable, recall that for a linear equation, various solution may be added. Therefore, when the finite difference equation under investigation is linear, it is sufficient to investigate only one component of the Fourier series. In fact, the linearity of the equation is general requirement for the amplification of the Von Neumann stability analysis. Furthermore, the effect of the boundary condition on the stability of the solution is not included with

this procedure. To overcome these limitations, one may locally linearize the non linear equation and subsequently apply the Von Neumann stability analysis. However, note that resulting stability requirement is satisfied locally. Therefore the actual stability requirement may be more restrictive then the one obtained from the Von Neumann stability analysis. Nevertheless, the results will provide very useful information on stability requirements.

According to Von Neumann stability criterion

$$y_j^n = Bounded\ Solution + Perturbation$$

Or

$$y_j^n = \left(y_j^n\right)_{Bounded\ Solution} + (g_k)^n e^{ikx}$$

Where for stability

$$|g_k| < 1$$

Put $(g_k)^n e^{ikx}$ In the above equation

This Method will be described here and will be used to investigate the stability of the numerical method for the solution of displacement equations used in the standard stress analysis and the velocity equation developed and used in this project.

6.10 Conclusion

The mathematical behavior of partial differential equation has been explained in the light of Eighon Value Method. An overview of discretization and discretization procedure are given Mec Cormacks's Technique has been applied in order to solve the equation and the stability analysis also discussed.

CHAPTER # 7

7 EXPERIMENTATION AND RESULT DISCUSSION

7.1 Introduction

In this chapter experimentation is conducted to verify the mathematical model developed earlier. The mathematical model developed earlier predicts the displacement and axial stress by the use of FSI calculations with pressure and velocity of the fluid as input. In this chapter we would carry out experimental analysis to validate the results of the FSI Mathematical model developed.

Also an optimization study is conducted to minimize the thickness of fluid carrying pipes and the number of clamps used in the currently available hydraulic system.

7.2 Brief review to previous work/Experimental setup

The Delft Hydraulic bench mark problem A, B, C concern a simple reservoir-pipe valve system in a reservoir is situated in a height due to which a head 'H" is achieved. The solution for this problem Wiggest [1987] has developed a code. On the basis of this code result [Lavoaj and Tisseling 1988] has solved the above problem with MOC-FEM and the obtained result is compared with FLUSTRIN code.

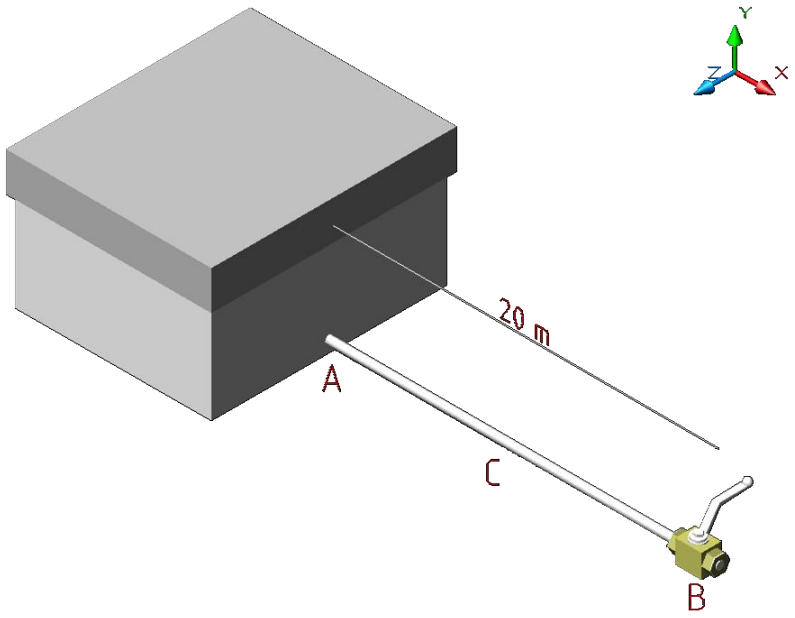

Figure 7.1

The above experimental approach consists of:

The Pipe and valve are allowed to move freely in axial (z) direction.

Length of the Pipe	(L)	=	20 m
Inner Diameter	(ID)	=	0.7970 m
Wall Thickness	(t)	=	0.008 m
Young's Modulus	(E)	=	210 Gpa.
Poison's Ratio	(v)	=	0.3
Shear Co-efficient	( )	=	0.53
Mass density of Pipe	( )	=	7900 Kg/m3
Wall Material		=	
Mass Density of Liquid()		=	1000 Kg/m3
Bulk Modus	()	=	2.1 GPa.
Darcy-Weisback friction of co-efficient		=	0.02
Inhaul Liquid velocity		=	1 m/sec
Pressure behind valve		=	0 Pa.
Valve closer time		=	0 Sec.

A second experimental perfumed in Delft Hydraulic in which a elbow pipe of 310m and 20m are connected with the reservoir and that reservoir is filled on the level of 'H' due to which head is achieved as show in the fig. below.

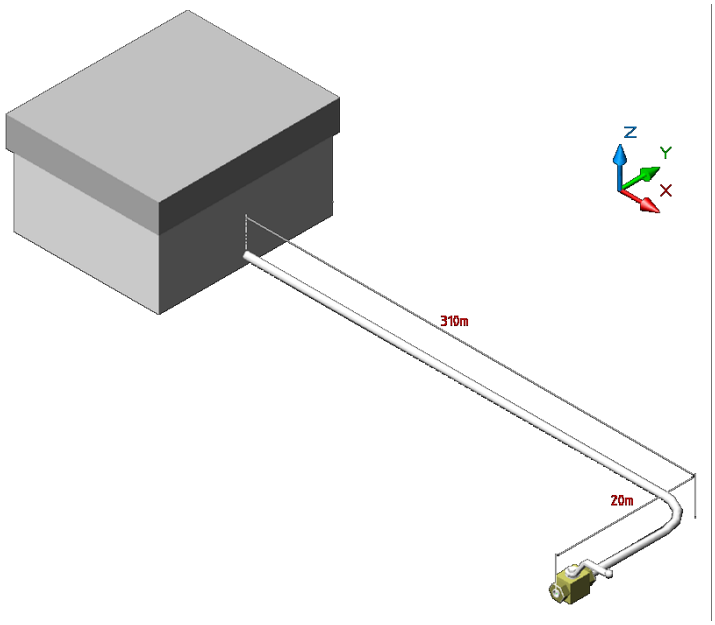

Figure 7.2 [view of experimentation apparatus performed in Delft]

The schematic representation of reservoir pipe-valve system with one elbow. The pipe and elbow are allowed to move freely in the horizontal y-z plane. The value is rigidly fixed to the grooved.

Length of the Pipe	(L)	=	310 m
Length of Short Pipe	(l)	=	20 m
Inner Diameter	(ID)	=	0.2064 m
Wall Thickness	(t)	=	0.00635m
Young's Modulus	(E)	=	210Gpa.
Poison's Ratio	(v)	=	0.3
Shear Co-efficient	( )	=	0.53
Mass density of Pipe	( )	=	7900Kg/m3
Wall Material		=	
Mass Density of Liquid	()	=	880 Kg/m3
Bulk Modulus	()	=	1.55 GPa.
Darcy-Weisback friction of co-efficient (f)		=	0.0
Inhaul Liquid velocity		=	4 m/sec
Pressure behind valve		=	0 Pa.
Valve closer time		=	0.5 Sec.

7.3 Basic Definitions

7.3.1 Strain

Stress is generates in the body when the external force applied to an elastic material which actually generates deformation of the material. Supposing the cross sectional area of the material to be A and the applied force to be P, stress σ will be P/A, since a stress is a force working on a definite cross sectional area.

On the other hand when an external force is applied on an elastic material At this time, the length L of the material change and it extends to L+ΔL if applied force is a tensile force. The ratio of ΔL to L, that is ΔL/L, is called strain. (Precisely, this is called normal strain or longitudinal strain.) On the other hand, if compressive force is applied, the length L is reduced to L- ΔL. Strain at this time is (- ΔL)/L. Strain is usually represented as ε. strain ε is proportional to stress σ, thus an equation $\sigma = E \times \varepsilon$ is satisfied, provided that the stress σ does not exceed the elastic limit of the material. "E" in the equation is the elastic modulus (Young's modulus) of the material.In a simple uni- axial stress field as illustrated below,

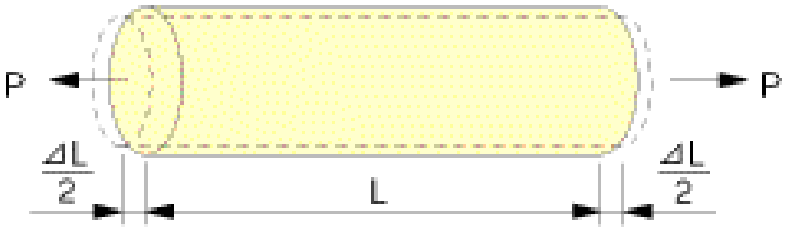

Figure 7.3 [Demonstration of Stress and Strain, www.tul.jp]

$$\varepsilon = \frac{\Delta L}{L}$$

E = ΔL/L

ε : Strain

L : Original length

ΔL : Change due to force P

Because a strain is a ratio between lengths of two parts, it is a quantity having no dimension. Usually it is represented in a unit of 1x10-6, since the ratio of deformation is often very small. For example, supposing L to be 100mm and ΔL to be 0.1mm, strain ε is indicated as 1000x10-6strain, because "0.1mm/100mm=0.001=1x10-3=1000x10-6". To indicate comparatively large strain, "% strain" is also used. In this case, 1% strain equals to 10000x10-6strain.

7.3.2 Strain and resistance change

When a metal (resistor) is expanded or contracted by external force, it experiences a change of electrical resistance. By bonding a metal (resistor) on the surface of a specimen with an electrical insulator between them, the metal changes its dimension according to

the expansion or contraction of the specimen, thus resulting a change of its resistance. Strain gauge (electrical resistance strain gauge) is a sensor to detect the strain of a specimen by this resistance change.

7.3.3 Strain gauge:

Strain gauge is constructed by bonding a fine electric resistance wire or photographically etched metallic resistance foil to an electrical insulation base(backing), and attaching gauge leads. Strain gauge is used for strain measurement by bonding it on the surface of the specimen with specified adhesive.

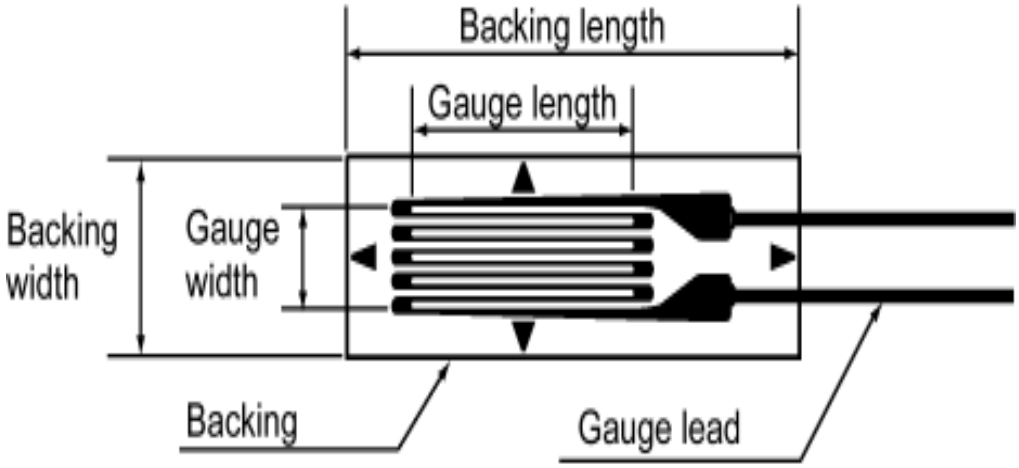

Figure 7.4 [An over view of Strain Gauge, Source: www.tml.jp]

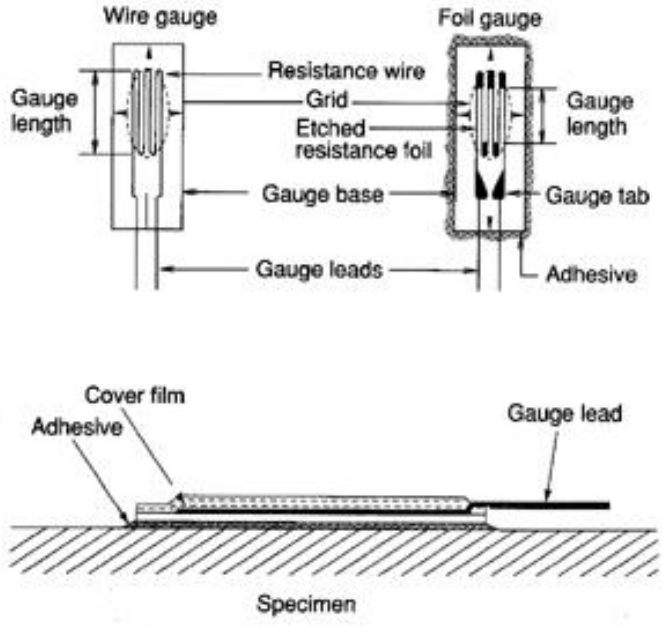

Figure 7-5 [An over view of Strain Gauge, Source: www.tml.jp]

The strain generated in the specimen is transmitted to the resistor(foil or wire) through the gauge base (backing), where expansion or contraction occurs. As a result, the resistor experiences a variation in resistance. This variation is proportional to the strain as indicated in the following equation.

$$\varepsilon = \frac{\Delta L}{L} = \frac{\Delta R / R}{K}$$

E : Strain

R : Gauge resistance

ΔR : Resistance change due to strain

K : Gauge factor as shown on the package

7.3.4 Features of a strain gauge

Strain gauges are provided with many convenient features as follows.

- Simple construction with a small mass and volume so as not to interfere with the stresses on the specimen.
- Small gauge length for evaluation of localized stress.
- Good frequency response for tracking rapid fluctuations in stress.
- Simultaneous measurement of multiple points and remote points.

Electrical output for easy data processing However, each strain gauge has its limitations in terms of temperature, the amount of strain, fatigue and the measurement environment. These limitations must be examined before using a strain gauge.

Strain measurement using a Wheatstone bridge circuit.

Resistance of a strain gauge changes proportionally to the received strain. To measure strain is to measure this resistance change. Since this resistance change is very small in usual case, it requires a Wheatstone bridge circuit to convert the resistance change into voltage output.

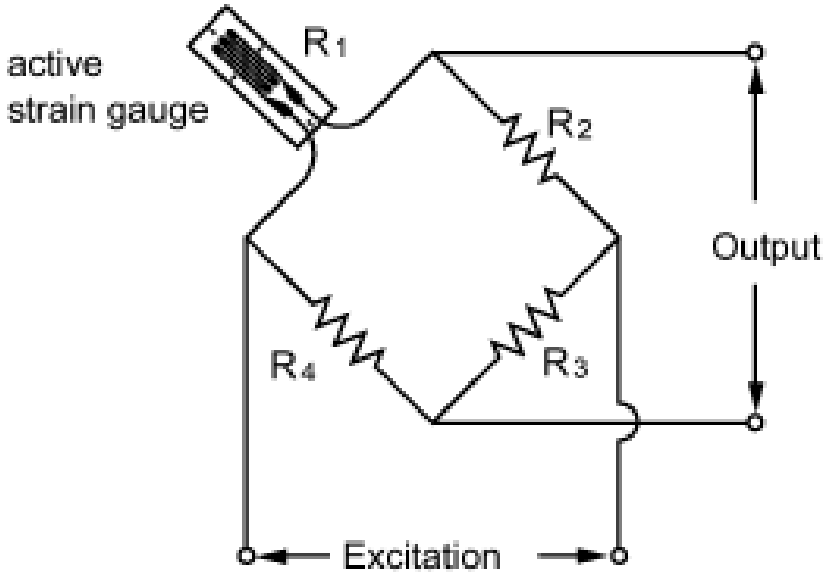

Figure 7.6 [Strain Gauge circuitry in form of whetstones bridge Source: www.tml.jp]

The output voltage of a bridge circuit is given as follows.

$$e = \frac{R_1R_3 - R_2R_4}{(R_1 + R_2)(R_3 + R_4)}E$$

e	:	Voltage output
E	:	Exciting voltage
R1	:	Gauge resistance
R2~R4	:	Resistance of fixed resistors

Assuming the value R as R=R1=R2=R3=R4, and the strain gauge resistance varies to R+ΔR due to strain, the output voltage Δe(variation) due to the strain is given as follows.

$$\Delta e = \frac{\Delta R}{4R + 2\Delta R}E$$

When ΔR<<R this is approximated to

$$\Delta e = \frac{\Delta R}{4R}E = \frac{E}{4}K\varepsilon$$

The strain gauge is connected to a strain meter, which provides Wheatstone bridge circuit and exciting input voltage. The strain (ε) is measured on a digital or analog display of the strain meter.

7.4 Percent Difference – Percent Error

Sometimes scientists will want to compare their results with those of others, or with a

theoretically derived prediction. Each of these types of comparisons call for a different type of analysis, percent difference and percent error respectively.

7.4.1 Percent Difference:

Applied when comparing two experimental quantities, E1 and E2, neither of which can be considered the "correct" value. The percent difference is the absolute value of the difference over the mean times 100.

$$\%\ Difference = \frac{|E_1 - E_2|}{\frac{1}{2}(E_1 + E_2)} \bullet 100$$

7.4.2 Percent Error:

Applied when comparing an experimental quantity, E, with a theoretical

quantity, T, which is considered the "correct" value. The percent error is the absolute value of the difference divided by the "correct" value times 100.

$$\%\ Error = \left|\frac{T - E}{T}\right| \bullet 100$$

7.5 Experimental Procedure

In this experimentation we analyze the FSI effects the following shaped pipes:

- In a straight,
- L shaped
- U shaped pipes.

Three different (diameters x wall thickness) are considered for each of the above mentioned shapes

- 10mm x 1mm
- 9mm x 1.5 mm
- 8mm x 2 mm

Also the same pipes are bursted and digitalize data has been taken.

7.6 Apparatus:

Before we discuss the experiments and results a brief review of the apparatus used for the experimentation is presented

7.6.1 Data Logger

The data logger with the following specification is used in order to achieve the digitalize data from the experimentation

Specification

a. **Data Loggers:** **TDS 303**
b. **Switching Boxes:** **ASW 50C**
c. **Data Acquisition Software:** **TDS 7150-Static Measurement Software**
d. **Host Computer:** **P-IV, 2.8 GHz**
e. **DC Power Supplies:** **Built In**

Figure 7.7 [Data Logger use in the experiment]

7.7 Tubes

The tube of the following specification are used for the experimentation

- 10mm x 1mm
- 9mm x 1.5 mm
- 8mm x 2 mm

Figure 7.8 [Tube use in the fluid power system source: www.parker.com]

7.8 Clamps

The clamps which have been optimized in the experimentation are shown in the figure 7-10.

Parker Fluid connectors “Metric Tube Clamps” the catalog needs to be moved to appendix

Figure 7.9 [Tube Clamps Used in the fluid power system source: www.parker.com]

7.9 Experimentation

7.9.1 Setup 1 – straight pipe

The author of this research has used the same idea for the experimental setup for the FSI study. The author used the hydraulic Power Pack which generates a maximum pressure of 210 bars.

In the previous experiment the respective author used the same pipe with water flowing inside the pipe while we will use the pressurized hydraulic oil Tellus T-46 inside the power pack. The author uses different pressure levels and observes the changes on the pipe at afferent pressure level of 0, 20 bar 40 bar 60 bar and 200bar.

The schematic diagram of this apparatus is:

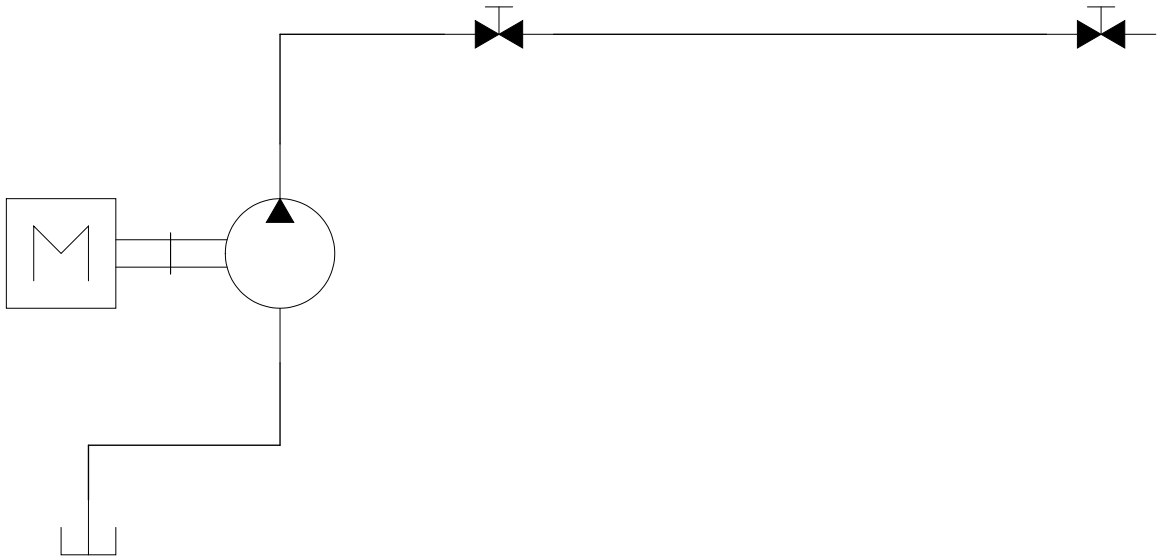

Figure 7.10 [schematic diagram for straight pipe]

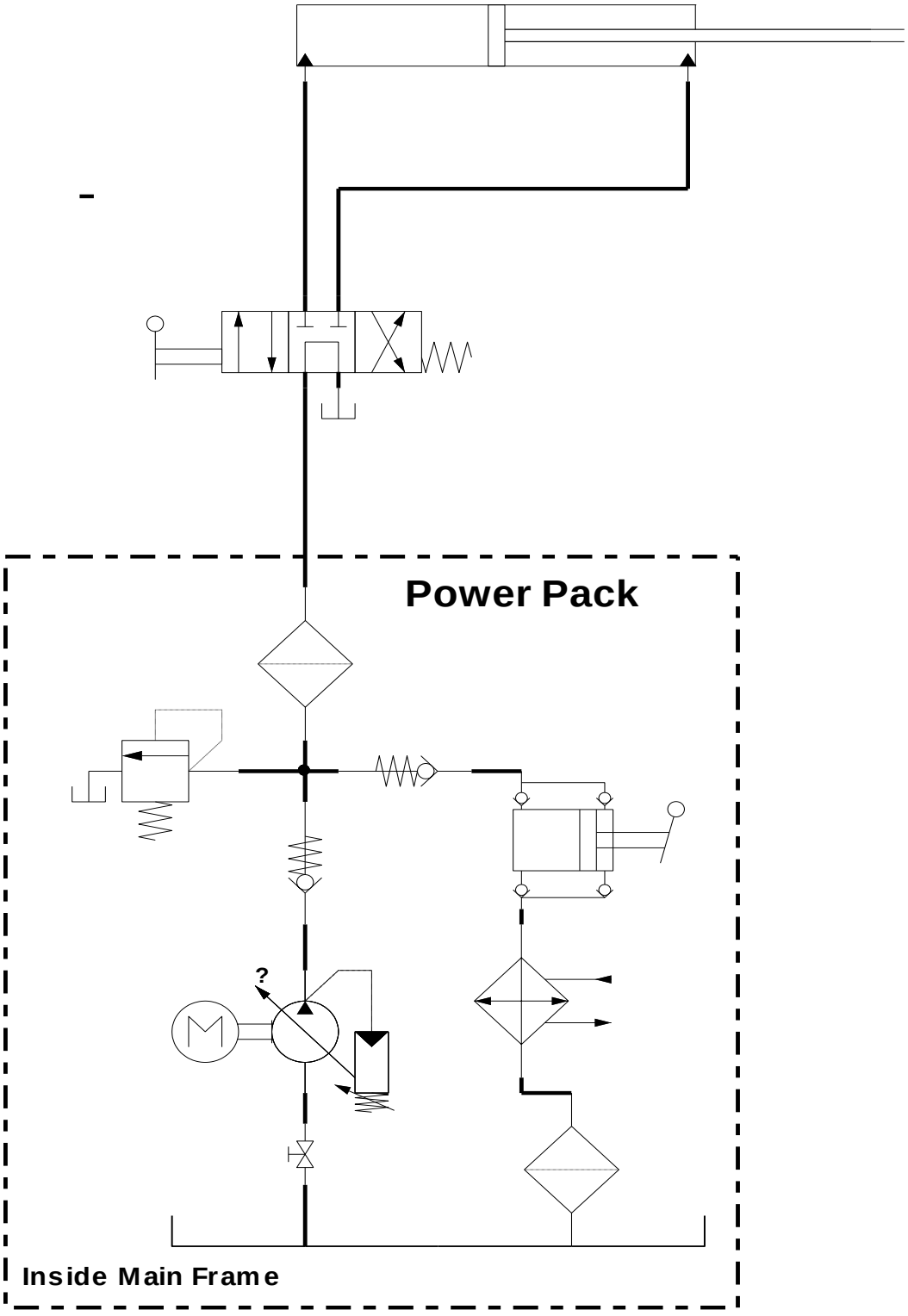

Figure 7.11 [Circuit diagram for Straight Pipe]

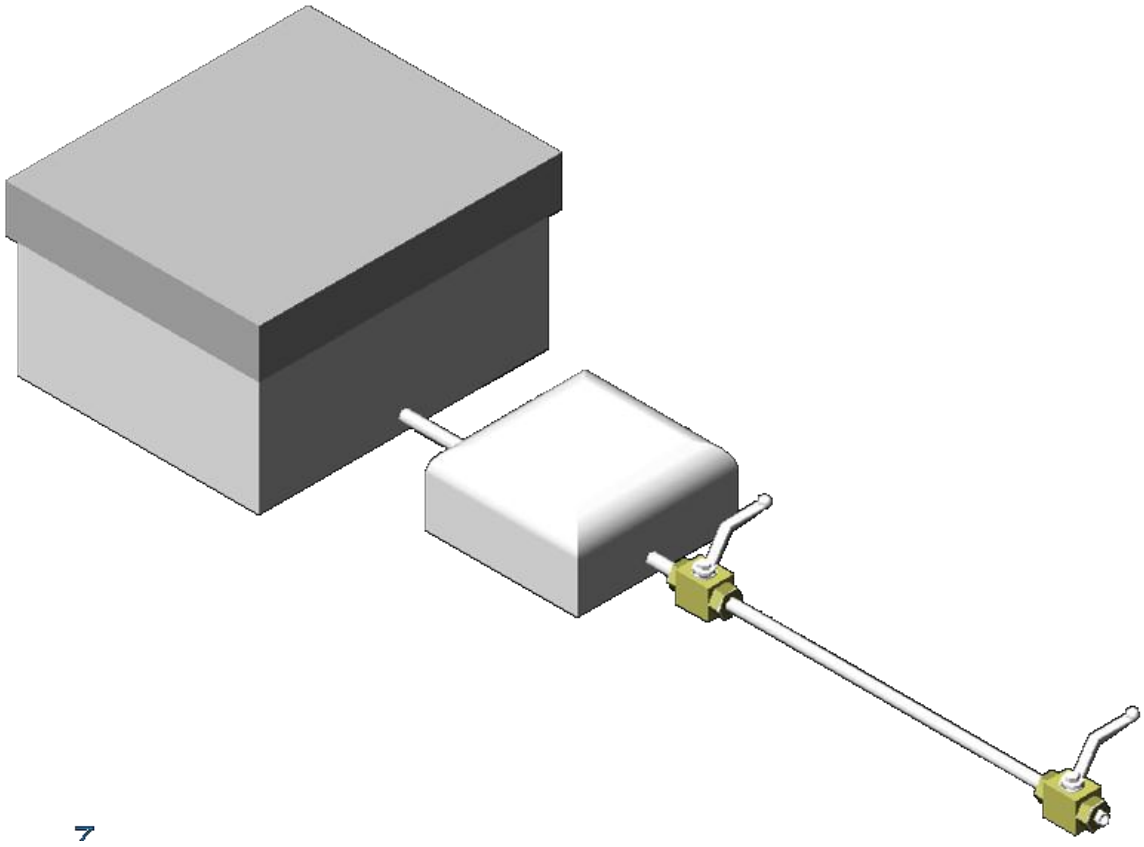

Figure 7.12 [Straight pipe]

The Pipe and valve are allowed to move freely in the z-direction.

Length of the Pipe	(L)	=	2m
Inner Diameter	(ID)	=	10mm
Wall Thickness	(t)	=	1mm
Young's Modulus	(E)	=	210Gpa.
Poison's Ratio	(ν)	=	0.3
Shear Co-efficient	( )	=	0.53
Mass density of Pipe	( )	=	7800Kg/m3
Wall Material		=	
Mass Density of Liquid()		=	874Kg/m3

Bulk Modus () = 1.6GPa.

Darcy-Weisback friction of co-efficient (f) $= 0.005\left(1+\frac{1}{12d}\right)$

Inside Liquid velocity = 8m/sec

Pressure behind valve = 200Bar

Valve closer time = 25MS.

To measure the axial strain in a pipe induced by the FSI, The circuit is assembled as per given in the above fig:

Figure 7.13[Photograph of experimental setup, a displacement sensor is seen]

Figure 7.14[A photograph of experimental setup, Strain Guages are seen on Jack]

In first case the circuit consists of a Power Pack (that is a complete model of hydraulic pump, electric motor, fittings, filter, directional control valve, hydraulic oil.). A pressure gauge of Parker rating 0-400 bar and pressure Transducer of Keller (o/p: 0-5 volts, i/p: 24 volts Dc, Measuring range: 0-400 bar) is attached with a pipe system. In this first case the straight pipe of 1000mm length is attached with a hydraulic jack. There is a shut off valve at the inlet passage of hydraulic jack i.e B-Port. At the stainless steel pipe there is a strain gauge (Omega strain gauge) attach in a form of ROSSETE as shown in a fig below.

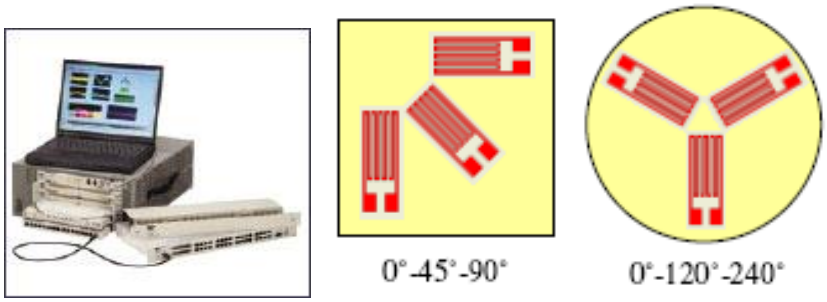

Figure 7.15[Strain gauges in Rosette form]

The result is obtained by the dada logger TDS-303 which has a 1000channels and frequency 50/60Hz. And measuring speed is 0.06 sec per channel.

There is a displacement sensor (Type: LVDT Spring Return, measuring range: 0-50 mm of Honeywell is installed on a Stainless Steel pipe which will give us the displacement gained by the oil hammering.

Physically dimensioned and material properties of pipe and oil in power pack used in the experiment are given in the table 7.1 together with the measuring position of the pressure gauge (transducer, strain gauge etc.)

The experiment is same as the experiment performed by the Arriss Tissjling in University of Delft. Prior to test, the pipe is filled with hydraulic oil Tellus T-46. The Circuit is bleeded in order to remove all the air entrapped in the tube. Un-screwing the fitting and bleeding the pipe many times to ensure the oil is free of air in the pipe. In this experiment the pipe is in the horizontal position, in such a way α=0.

Now start the power pack. The position of Directional control valve is such that he pressure line is blocked and the tank port is connected the A and B ports of cylinder. Actuate the directional control valve by using a DC power supply.

Signal from the strain gauge are received to data logger and from data logger to PC where they are plotted on the screen.

It must be decided before experiment that which part of the recorded signal is stored in the HDD. For most test 20 to 30 mille second after hammering the data is stored.

For experimentation setup the circuit is assembled according to the figure 7.15. We have seen that when hammering started, the pressure is fluctuated and is balanced after time ‘t’. Similarly the strain also fluctuates and balances as the pressure changes. We have take the reading at the peak. i.e at pressure p=200 bar (20.2MPa, 20.4MPa, 20.6MPa 20.8MPa and 21.0MPa)

The axial strain σ are noted at the data logger and converted to stress by software. The axial strain and the hoop stress are related to the pressure and the axial strain by While the axial pipe velocity was measured by the displacement sensors fixed with the Stainless Steel pipe.

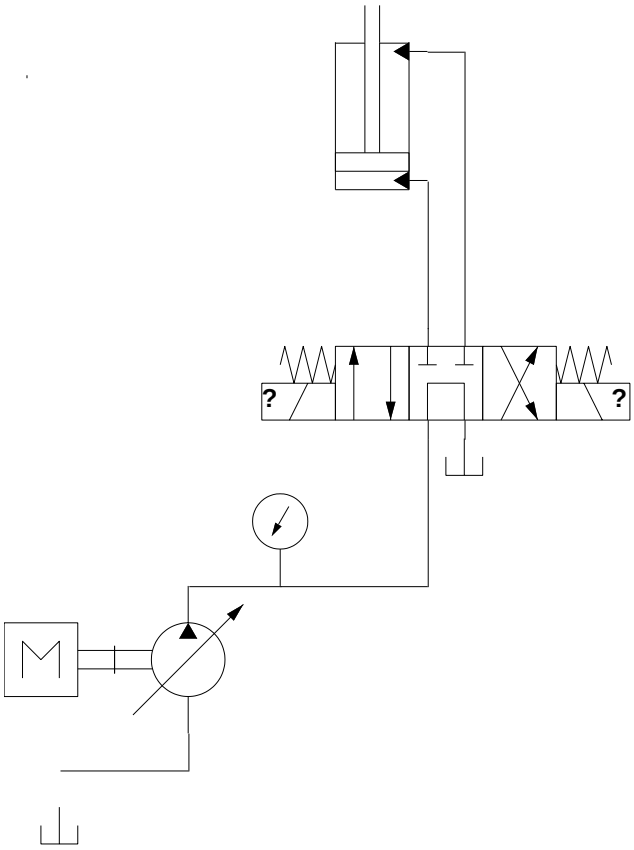

Figure 7.16

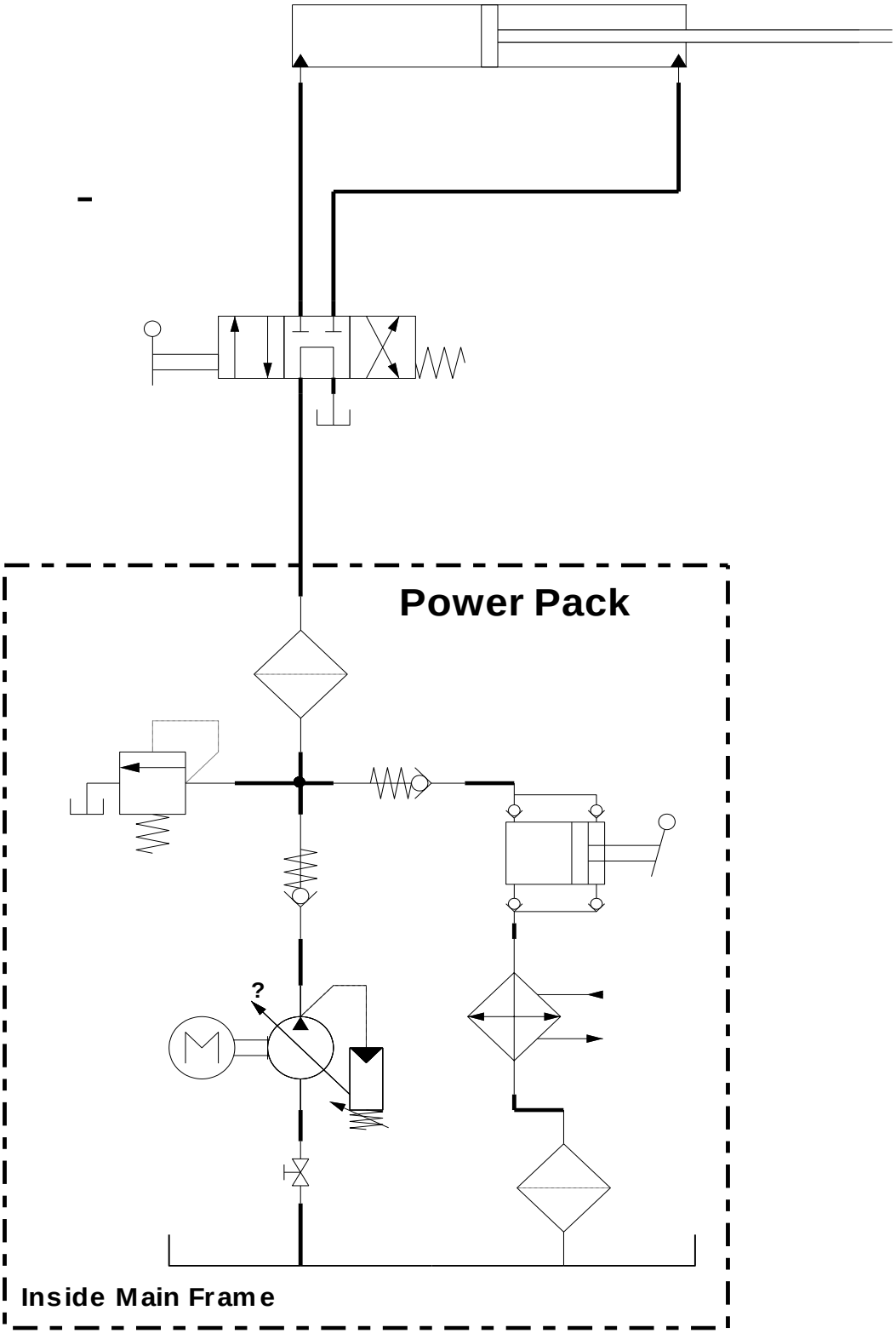

Figure 7.17 [Circuit diagram in the case of straight pipe]

7.9.2 CASE-2: One-Elbow Pipe System:

For the elbow system same pipe and same length is bended at one end shown in fig 7.17 below.

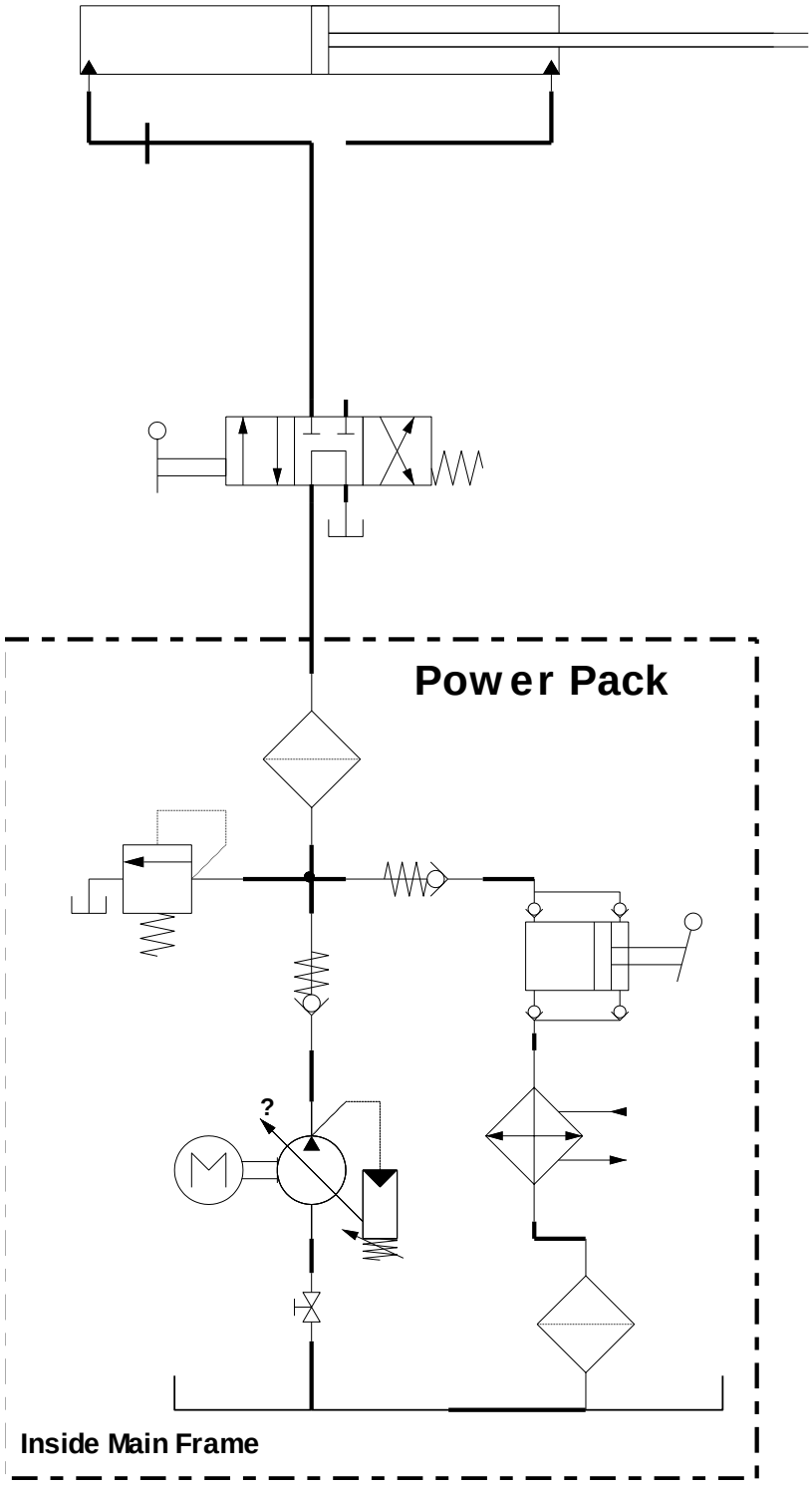

Figure 7.18 [Circuit diagram in the case of elbow]

7.10 RESULTS AND DISCUSSIONS

7.10.1 Data at the Impact End of Hydraulic Jack

When the experiment is started by the application of pressure produced by the hydraulic pump, some digitalized data is obtained from which a graph is received as shown in the Figure 7.20a, 7.20b, 7.20c, 7.20d, 7.20e and 7.20f. As it is seen by the graph 7.20a, when the pump pressure is 20MPa and actuate the directional control valve and by starting the first hammering the stresses fluctuate inside the hydraulic jack which is achieved by the strain gauges fixed on the outer surface of the hydraulic jack at the impact end. As clearly from this graph spikes of stress are obtained with maximum amplitude of 22MPa and are settled down in a millisecond of time period.

Similarly when by increasing the gauge pump pressure to 20.2MPa and similarly the hammering started then the graph shows that the maximum spikes of stress is 22.25MPa. A digitalize data is obtained on different pressure pulse like 20.4MPa, 20.6MPa, 20.8MPa and 21.0MPa and maximum amplitude of stresses have seen like Figure 7.20c, d, e and f.

The stresses produced by the application of pressure in case of oil hammering are obtained and tabulated against the pressure.

The σ_1 hoop stresses and σ_2 longitudinal stresses have been calculated, and von misses σ_{von}. the graph against each experiment is also plotted. They are straight line which shows that the stresses developed by the application of pressure pulse.

The result of FSI mathematical model is also calculated from the computer code and tabulated in the table under the heading of theoretical result.

The percent difference between the experimental and theoretical result is finally calculated and tabulated.

The percent error graph shows that there is less than 10% error in the experimental theoretical data.

The results for the three different pipe diameters are presented below:

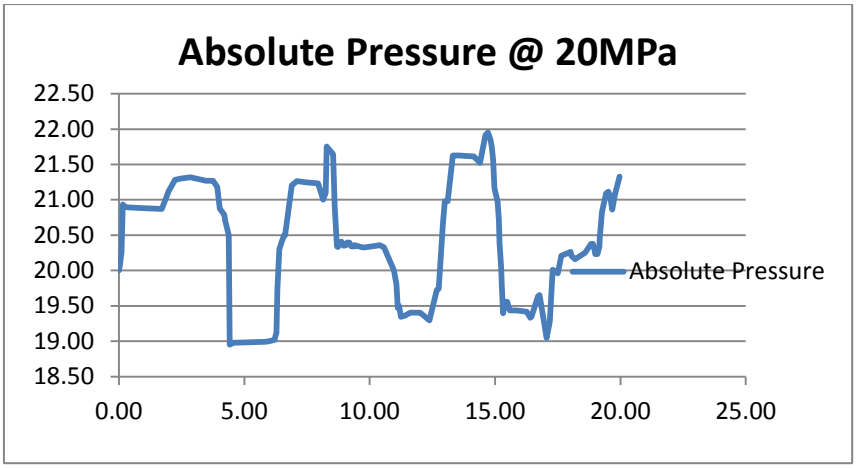

Figure 7.19a [Measure Stresses near the impact on a hydraulic jack at 20 bar]

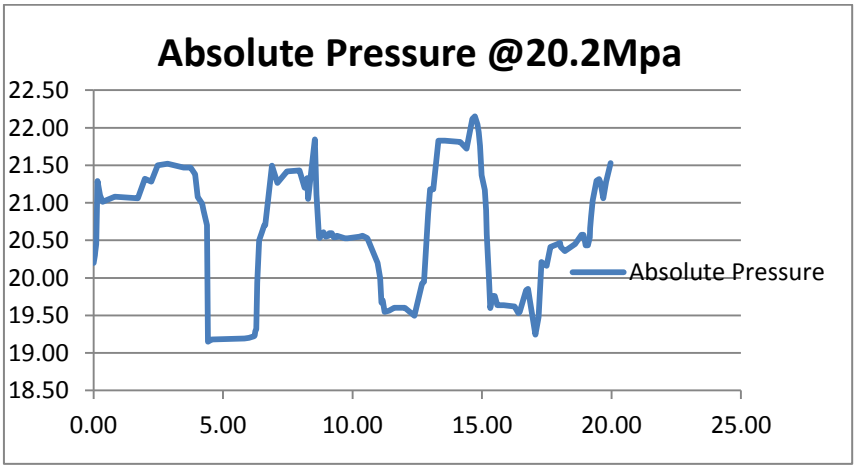

Figure 7.19b [Measure Stresses near the impact on a hydraulic jack at 202 bar]

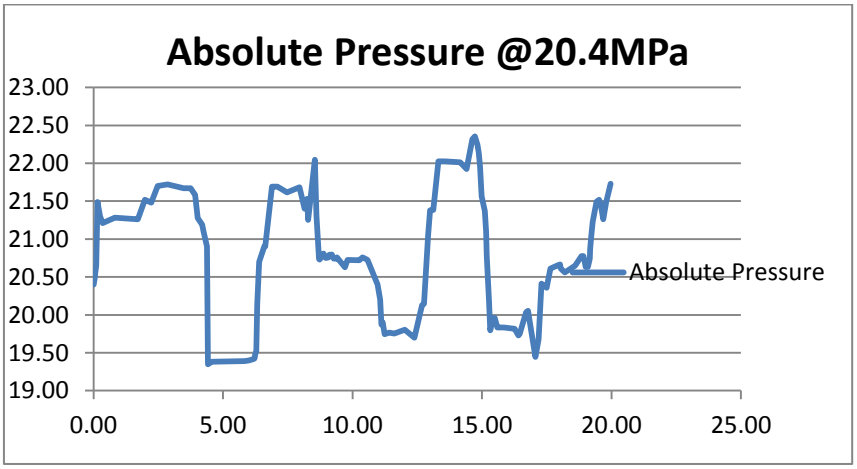

Figure 7.19c [Measure Stresses near the impact on a hydraulic jack at 204 bar]

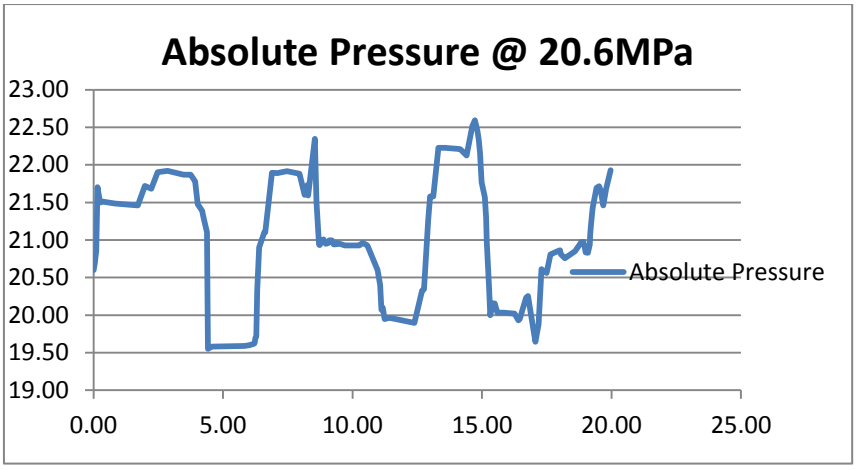

Figure 7.19d [Measure Stresses near the impact on a hydraulic jack at 206 bars]

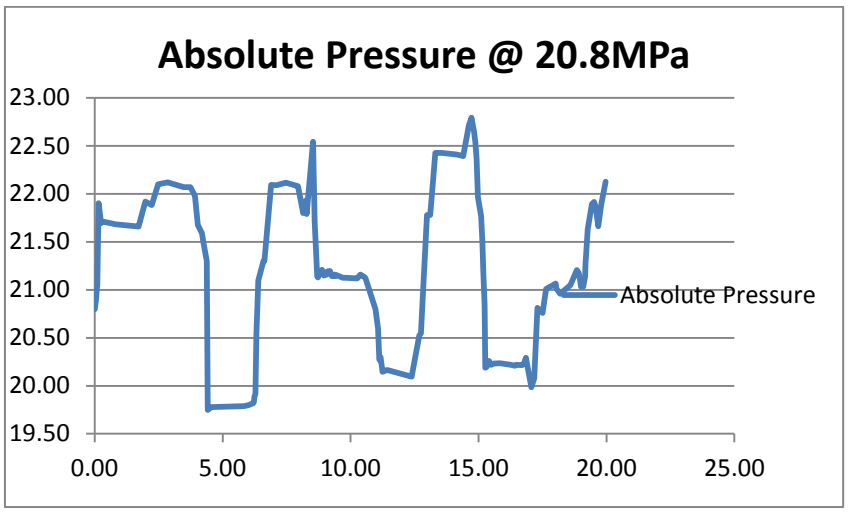

Figure 7.19e [Measure Stresses near the impact on a hydraulic jack at 208 bar]

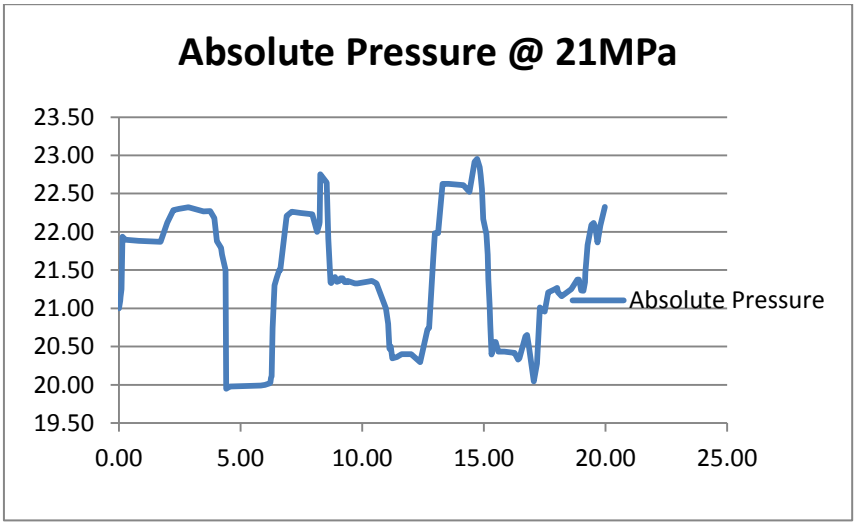

Figure 7.19f [Measure Stresses near the impact on a hydraulic jack at 210 bar]

7.11 Straight Pipe (1mm wall thickness)

In the second experiment the author obtained a digitalize data in case of oil hammering (Steady State Form). The data is tabulated in Table 7.2 with different pump pressures. The σ_1 hoop stresses, σ_2 longitudinal stresses achieved with respect to the different pressure readings and strain by the strain gauges while the von misses σ_{von} have been calculated by the conventional method.

A theoretical data also have been calculated by the conventional formula of the thick wall and thin wall. A percent error has also been calculated as shown in table 7.2.

As clearly from the figure 7.20 (Pressure vs Axial Stress) by increasing the pump pressure the axial stress also increased subsequently.

In Figure 7.21 (Pressure vs Axial Stress) a graph is drawn for the comparison of experimental axial and theoretical axial stresses.

In Figure 7.22 (Hoop vs Axial Stresses) a graph is drawn for the comparison of experimental Hoop stresses and experimental axial stresses. Which has shown that the axial stress is always half of the hoop stresses.

In Figure 7.23 Percent errors are plotted on a graph with respect to the pressure which shows that the percent error between the theoretical data and experimental data.

It is clear all the readings are within the range of 8% error which is acceptable in design criteria.

Table 7.2 [Experimental and Theoretical data and Percent error in case of 1.0 mm straight pipe]

Stress Analysis Results – 1mm straight pipe										
Ref. Test Report No.: RD(029)/HPTD/09					**Inner Dia**		**Thickness**	**Test Component ID: SP-04 (Straight Pipe)**		
					10.00		**1.00**			
P	Point		1	**P**	Point		2	**Percent Error**		
	Experimental Value (E)				**Theoretical Value (T)**					
	Principle Stress		Von Mises Stress		Principle Stress		Von Mises Stress	Principle Stress		Von Mises Stress
(BAR)	**σ1 (Mpa)**	**σ2 (Mpa)**	**σ (Mpa)**	**(MPa)**	***σ1 (Mpa)**	***σ2 (Mpa)**	***σ (Mpa)**	****σ1 (Mpa)**	****σ2 (Mpa)**	****σ (Mpa)**
0	0.00	0.00	0.00	0	0.00	0.00	0.00	0.00	0.00	0.00
20	9.00	5.00	7.81	2	10.00	5.00	8.66	10.00	0.00	9.82
40	18.00	9.00	15.59	4	20.00	10.00	17.32	10.00	10.00	10.00
60	27.00	14.00	23.39	6	30.00	15.00	25.98	10.00	6.67	9.98
80	36.00	19.00	31.19	8	40.00	20.00	34.64	10.00	5.00	9.95
100	45.00	23.00	38.97	10	50.00	25.00	43.30	10.00	8.00	9.99
120	54.00	28.00	46.78	12	60.00	30.00	51.96	10.00	6.67	9.98
140	67.25	33.00	58.24	14	70.00	35.00	60.62	3.93	5.71	3.92
160	76.00	37.00	65.83	16	80.00	40.00	69.28	5.00	7.50	4.99
180	87.00	42.00	75.36	18	90.00	45.00	77.94	3.33	6.67	3.31
200	99.25	47.00	85.99	20	100.00	50.00	86.60	0.75	6.00	0.70

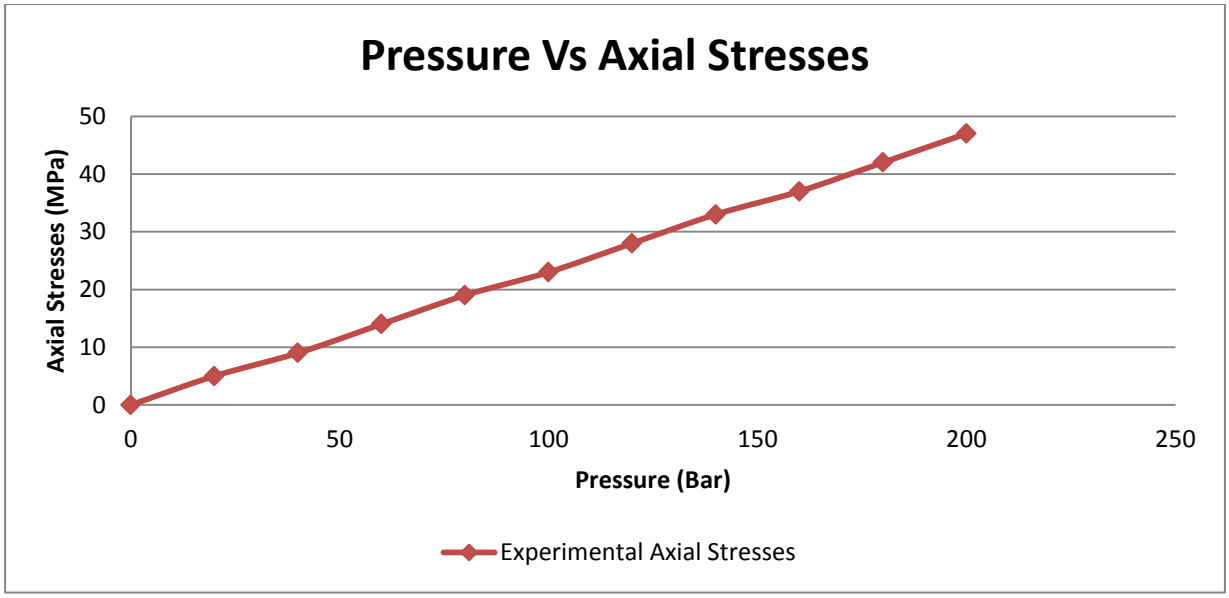

Figure 7.20 [Experimental Result of Axial Stresses]

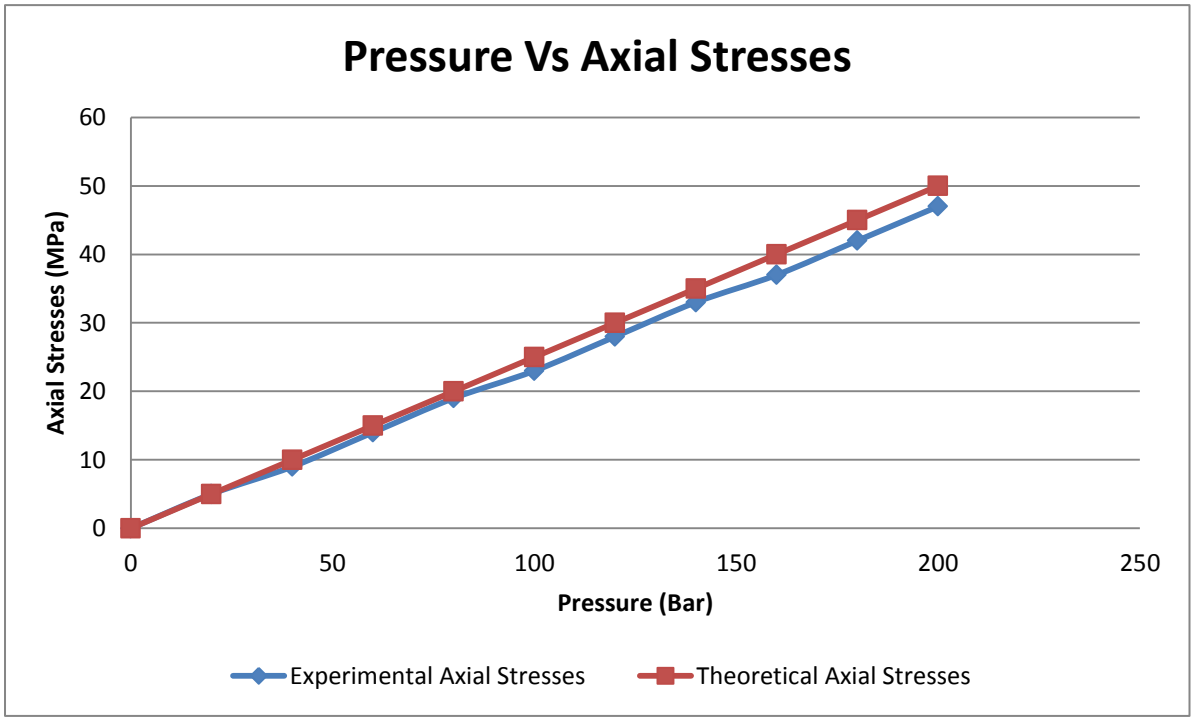

Figure 7.21 [Graph between experimental axial stresses and Theoretical axial stresses]

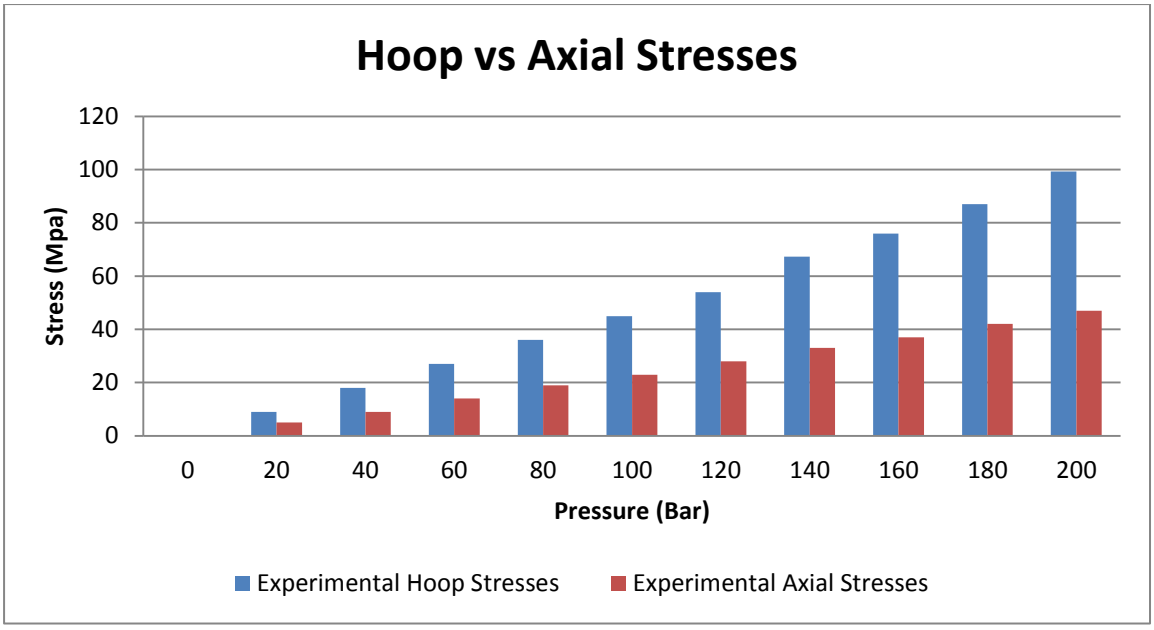

Figure 7.22 [Relation between axial stresses and Hoop stresses]

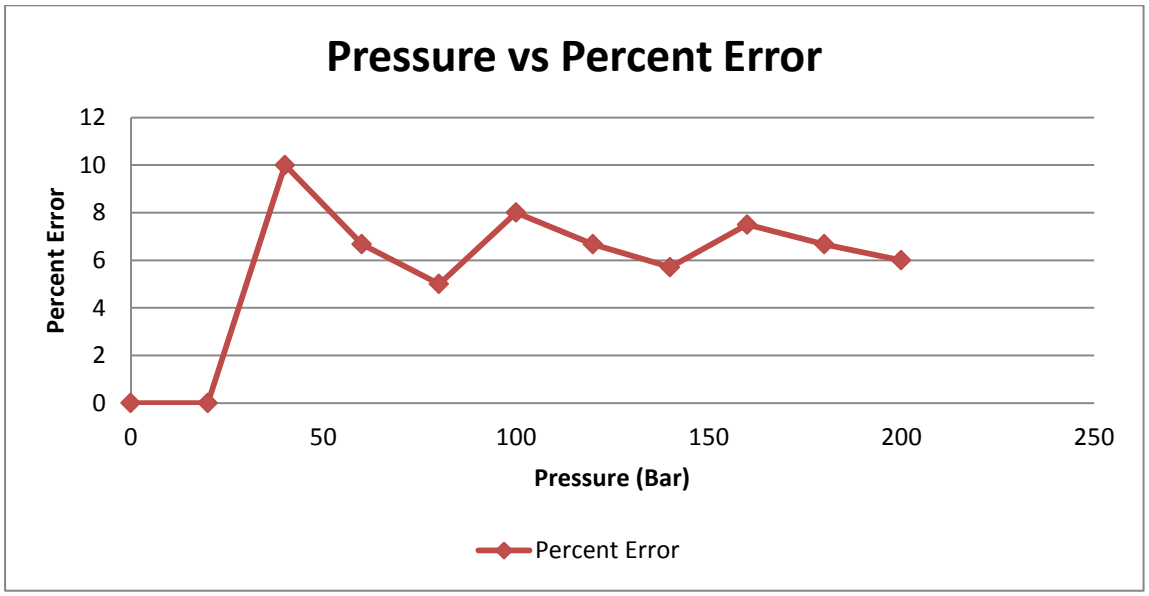

Figure 7.23 [Graph for the percent error achieved in between experimental & Theoretical]

7.12 L-Shaped Pipe (1mm wall thickness)

In this experiment the above straight pipe is changed with L-Shaped Pipe and a digitalize data is obtained in case of oil hammering (Steady State Form). The data is tabulated in Table 7.3 with different pump pressures. The σ_1 hoop stresses, σ_2 longitudinal stresses achieved with respect to the different pressure readings and strain by the strain gauges while the von misses σ_{von} have been calculated by the conventional method.

A theoretical data also have been calculated by the conventional formula of the thick wall and thin wall. A percent error has also been calculated as shown in table 7.3.

As clearly from the figure 7.24 (Pressure vs Axial Stress) by increasing the pump pressure the axial stress also increased subsequently.

In Figure 7.25 (Pressure vs Axial Stress) a graph is drawn for the comparison of experimental axial and theoretical axial stresses.

In Figure 7.26 (Hoop vs Axial Stresses) a graph is drawn for the comparison of experimental Hoop stresses and experimental axial stresses. Which has shown that the axial stress is always half of the hoop stresses.

In Figure 7.27 Percent errors are plotted on a graph with respect to the pressure which shows that the percent error between the theoretical data and experimental data.

It is clear all the readings are within the range of 8% error which is acceptable in design criteria.

Table 7.3[Experimental and Theoretical data and Percent error in case of 1.0 mm L- pipe]

Ref. Test Report No.: RD(029)/HPTD/09					**Inner Dia**		Thickness	**Test Component ID: SP-04 (L-Shaped Pipe)**		
					10.00		**1.00**			
P	Point		1	**P**	Point		2	**Percent Error**		
	Experimental Value (E)				**Theoratical Value (T)**					
	Principle Stress		Von Mises Stress		Principle Stress		Von Mises Stress	Principle Stress		Von Mises Stress
(BAR)	**σ1 (Mpa)**	**σ2 (Mpa)**	**σ (Mpa)**	**(MPa)**	***σ1 (Mpa)**	***σ2 (Mpa)**	***σ (Mpa)**	****σ1 (Mpa)**	****σ2 (Mpa)**	****σ (Mpa)**
0	0.00	0.00	0.00	0	0.00	0.00	0.00	0.00	0.00	0.00
20	9.10	4.65	7.88	2	10.00	5.00	8.66	9.00	7.00	8.99
40	18.25	9.50	15.81	4	20.00	10.00	17.32	8.75	5.00	8.72
60	27.50	14.13	23.82	6	30.00	15.00	25.98	8.33	5.80	8.32
80	36.52	19.00	31.64	8	40.00	20.00	34.64	8.70	5.00	8.68
100	45.56	23.86	39.47	10	50.00	25.00	43.30	8.88	4.56	8.85
120	55.10	28.00	47.72	12	60.00	30.00	51.96	8.17	6.67	8.16
140	63.02	32.12	54.58	14	70.00	35.00	60.62	9.97	8.23	9.97
160	73.00	38.00	63.24	16	80.00	40.00	69.28	8.75	5.00	8.72
180	82.00	42.68	71.03	18	90.00	45.00	77.94	8.89	5.16	8.86
200	92.00	49.00	79.73	20	100.00	50.00	86.60	8.00	2.00	7.93

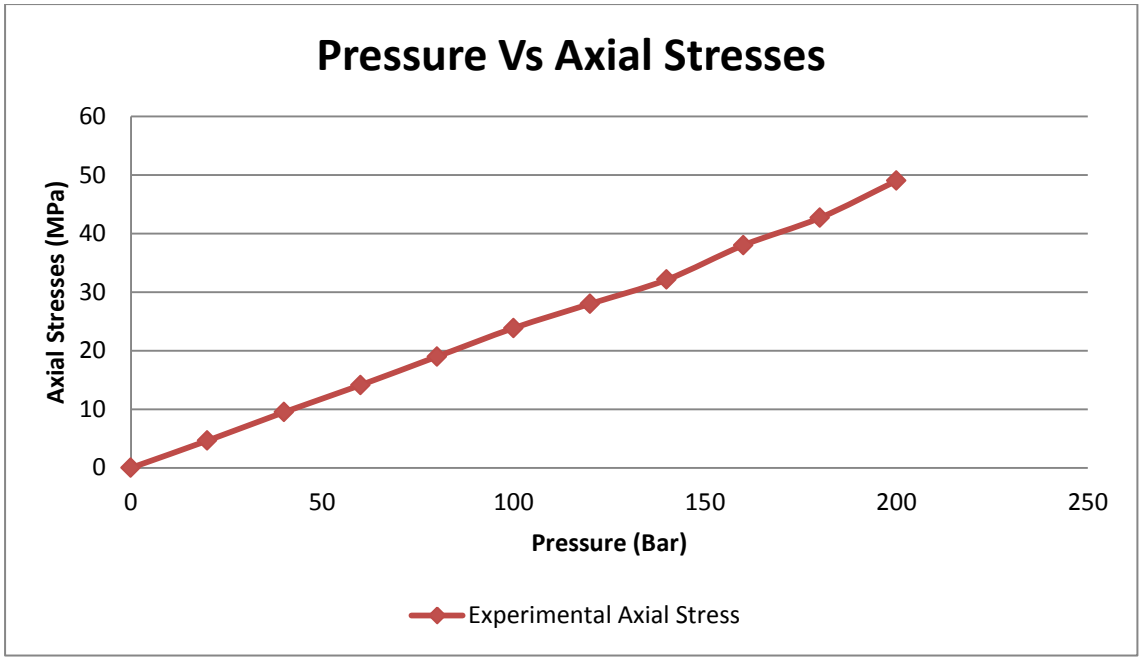

Figure 7.24 [Graph for the experimental axial stresses]

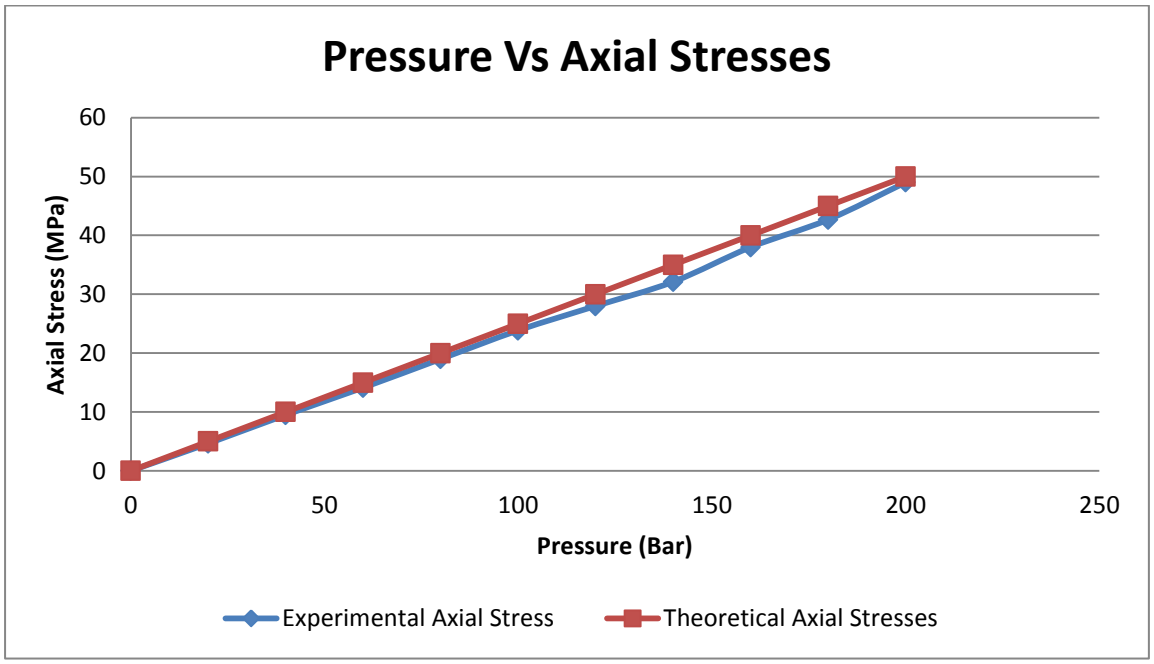

Figure 7.25 [Difference between experimental axial stresses &Theoretical axial stresses]

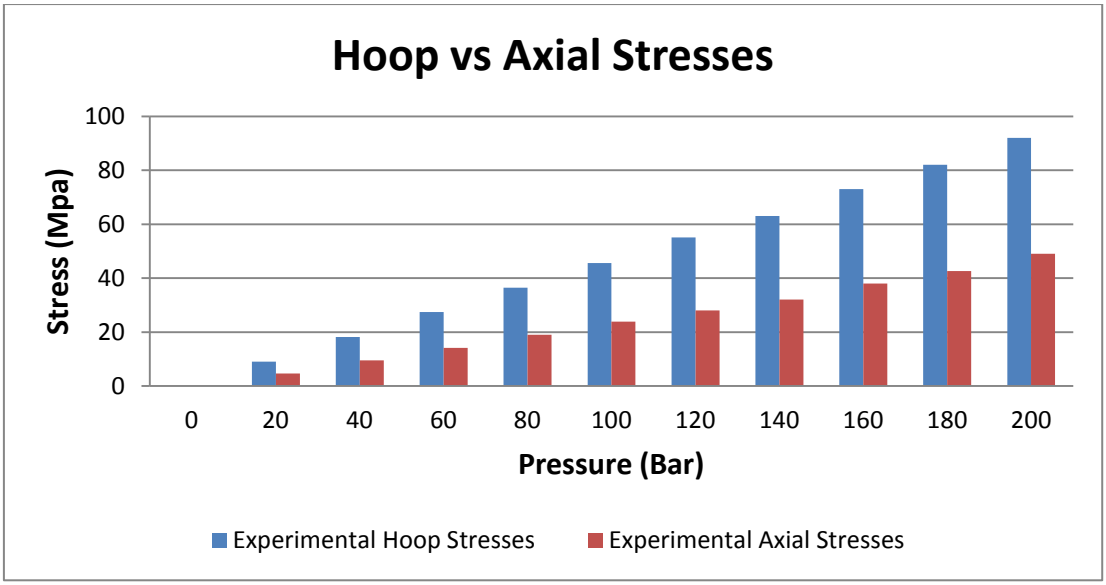

Figure 7.26 [Relation between experimental hoop stresses & experimental axial stresses]

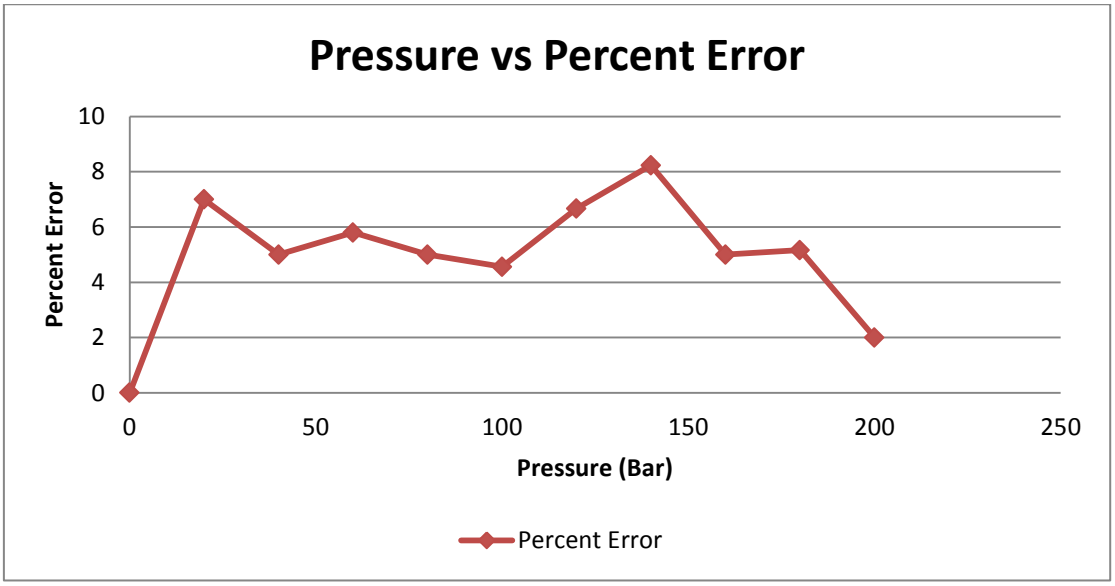

Figure 7.27 [Percent error calculated between experimental theoretical results]

7.13 U-Shaped Pipe (1mm wall thickness)

In this experiment the above straight pipe is changed with L-Shaped Pipe and a digitalize data is obtained in case of oil hammering (Steady State Form). The data is tabulated in Table 7.4 with different pump pressures. The σ_1 hoop stresses, σ_2 longitudinal stresses achieved with respect to the different pressure readings and strain by the strain gauges while the von misses σ_{von} have been calculated by the conventional method.

A theoretical data also have been calculated by the conventional formula of the thick wall and thin wall. A percent error has also been calculated as shown in table 7.4.

As clearly from the figure 7.28 (Pressure vs Axial Stress) by increasing the pump pressure the axial stress also increased subsequently.

In Figure 7.29 (Pressure vs Axial Stress) a graph is drawn for the comparison of experimental axial and theoretical axial stresses.

In Figure 7.30 (Hoop vs Axial Stresses) a graph is drawn for the comparison of experimental Hoop stresses and experimental axial stresses. Which has shown that the axial stress is always half of the hoop stresses.

In Figure 7.31 Percent errors are plotted on a graph with respect to the pressure which shows that the percent error between the theoretical data and experimental data.

It is clear all the readings are within the range of 8% error which is acceptable in design criteria.

Table 7.4[Experimental and Theoretical data and Percent error in case of 1.0 mm U pipe]

Ref. Test Report No.: RD(029)/HPTD/09					**Inner Dia**		**Thickness**	**Test Component ID: SP-04 (U-Shaped Pipe)**		
					10.00		**1.00**			
P	Point		1	**P**	Point		2	**Percent Error**		
	Experimental Value (E)				**Theoratical Value (T)**					
	Principle Stress		Von Mises Stress		Principle Stress		Von Mises Stress	Principle Stress		Von Mises Stress
(BAR)	**σ1 (Mpa)**	**σ2 (Mpa)**	**σ (Mpa)**	**(MPa)**	***σ1 (Mpa)**	***σ2 (Mpa)**	***σ (Mpa)**	****σ1 (Mpa)**	****σ2 (Mpa)**	****σ (Mpa)**
0	0.00	0.00	0.00	0	0.00	0.00	0.00	0.00	0.00	0.00
20	9.20	4.50	7.97	2	10.00	5.00	8.66	8.00	10.00	7.99
40	18.30	9.00	15.85	4	20.00	10.00	17.32	8.50	10.00	8.50
60	27.15	14.00	23.52	6	30.00	15.00	25.98	9.50	6.67	9.49
80	37.00	19.00	32.05	8	40.00	20.00	34.64	7.50	5.00	7.49
100	46.00	23.00	39.84	10	50.00	25.00	43.30	8.00	8.00	8.00
120	55.00	28.00	47.63	12	60.00	30.00	51.96	8.33	6.67	8.33
140	64.00	33.00	55.43	14	70.00	35.00	60.62	8.57	5.71	8.56
160	72.70	37.00	62.96	16	80.00	40.00	69.28	9.13	7.50	9.12
180	82.00	42.00	71.02	18	90.00	45.00	77.94	8.89	6.67	8.88
200	91.00	47.00	78.82	20	100.00	50.00	86.60	9.00	6.00	8.98

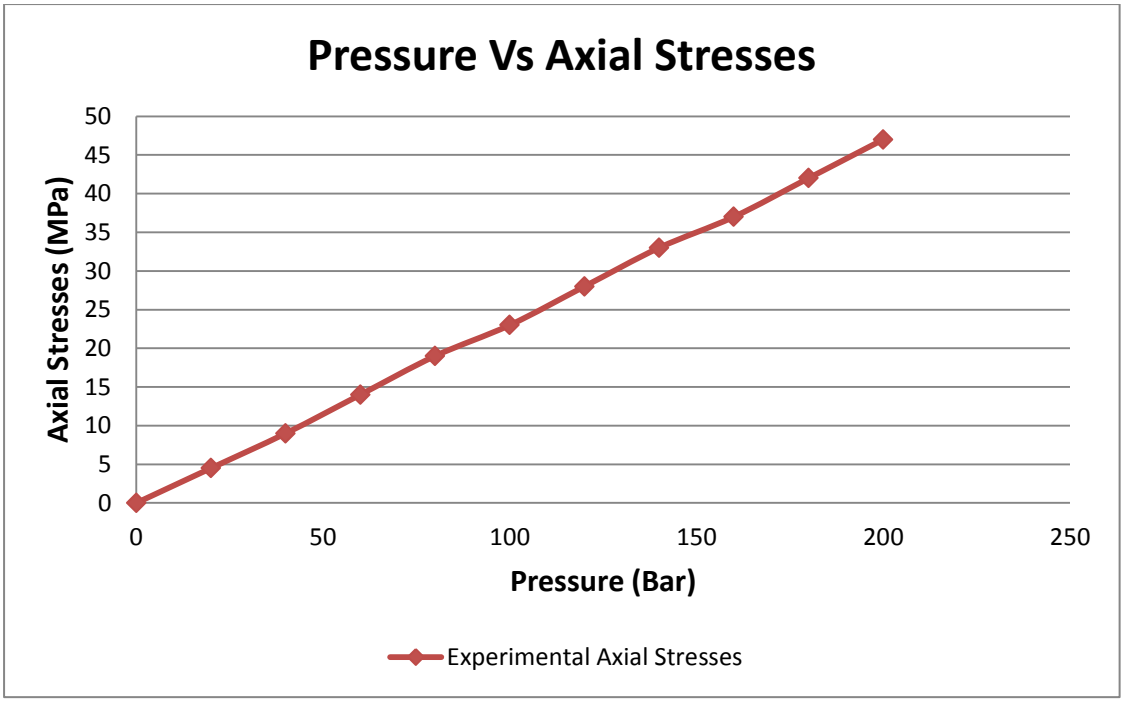

Figure 7.28 [Graph for the experimental axial stresses in case of U Shaped pipe]

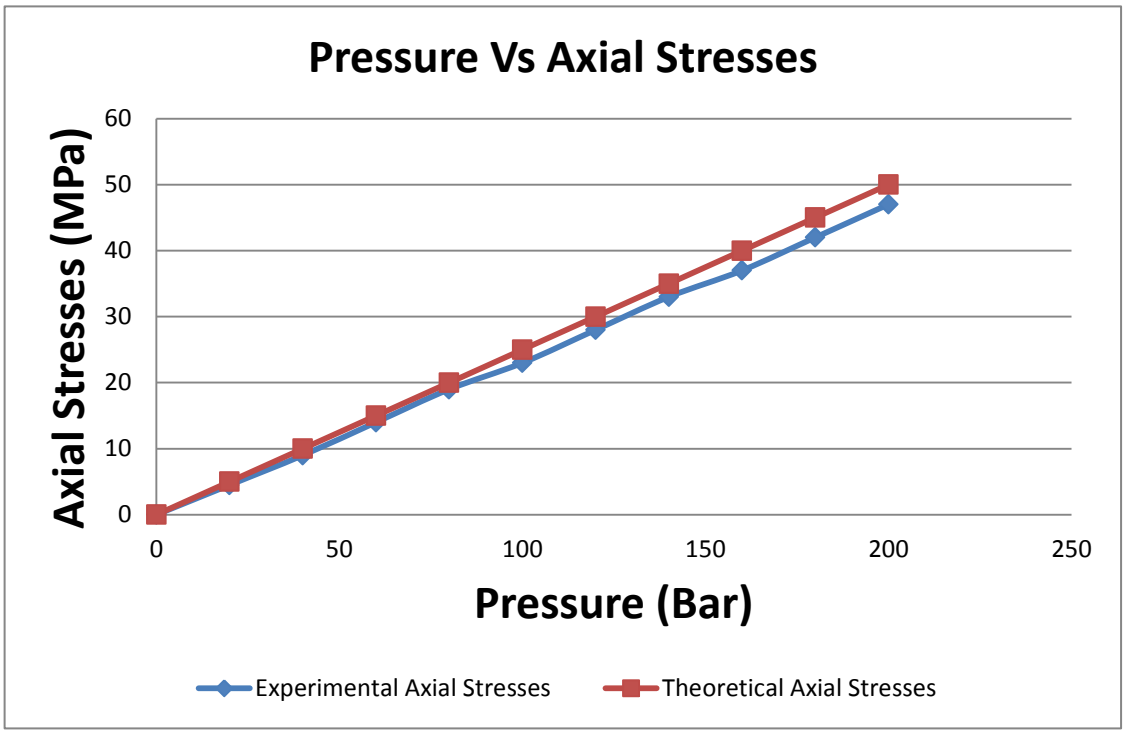

Figure 7.29 [Difference between experimental axial stresses & theoretical axial stresses]

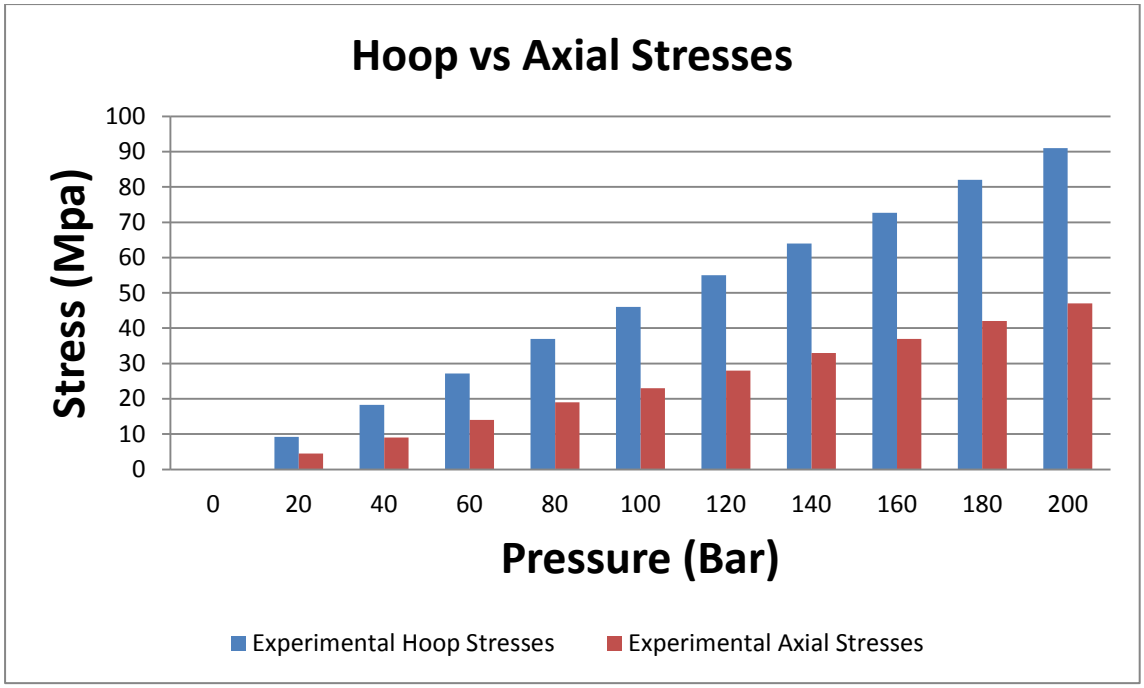

Figure 7.30 [Relation between experimental hoop stresses & theoretical axial stresses]

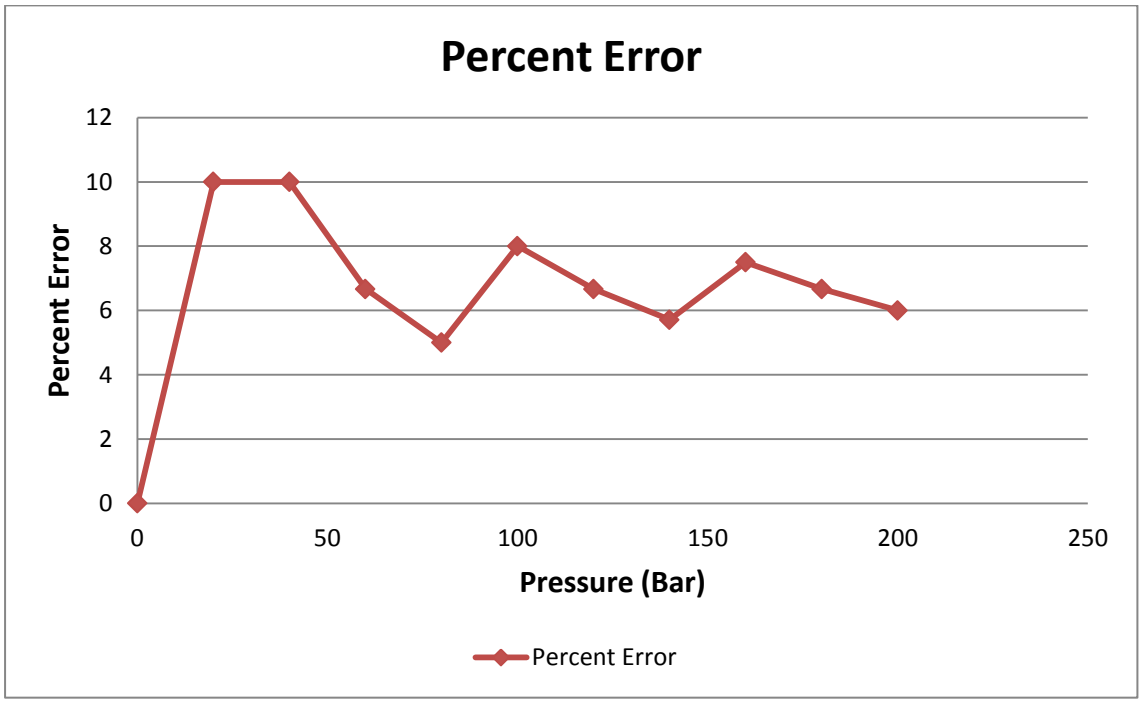

Figure 7.31 [Percent error calculated between experimental & theoretical results]

7.14 Straight Pipe (1.5mm wall thickness)

In the next phase the pipe of wall thickness of 1.5mm is taken with inner diameter of 9mm. In this experimentation a straight pipe is taken and the circuit is assembled as seen before. A digitalize data in case of oil hammering (Steady State Form) is obtained. The same data is tabulated in Table 7.5 with different pump pressure readings. The σ_1 hoop stresses, σ_2 longitudinal stresses achieved with respect to the different pressure readings and strain by the strain gauges while the von misses σ_{von} have been calculated by the conventional method.

A theoretical data also have been calculated by the conventional formula of the thick wall and thin wall. A percent error has also been calculated as shown in table 7.5.

As clearly from the figure 7.32 (Pressure vs Axial Stress) by increasing the pump pressure the axial stress also increased subsequently.

In Figure 7.33 (Pressure vs Axial Stress) a graph is drawn for the comparison of experimental axial and theoretical axial stresses.

In Figure 7.34 (Hoop vs Axial Stresses) a graph is drawn for the comparison of experimental Hoop stresses and experimental axial stresses. Which has shown that the axial stress is always half of the hoop stresses.

In Figure 7.35 Percent errors are plotted on a graph with respect to the pressure which shows that the percent error between the theoretical data and experimental data.

It is clear all the readings are within the range of 8% error which is acceptable in design criteria.

Table 7.5 [Experimental and Theoretical data and Percent error in case of 1.5 mm straight pipe]

Stress Analysis Results											
Ref. Test Report No.: RD(029)/HPTD/09					**Inner Dia**			Thickness	**Test Component ID: SP-04 (Straight Pipe)**		
					9.00			**1.50**			
P	Point		1	**P**	Point			2	**Percent Error**		
	Experimental Value (E)				**Theoratical Value (T)**						
	Principle Stress		Von Mises Stress		Principle Stress		Von Mises Stress	Principle Stress		Von Mises Stress	
(BAR)	**σ1 (Mpa)**	**σ2 (Mpa)**	**σ (Mpa)**	**(MPa)**	***σ1 (Mpa)**	***σ2 (Mpa)**	***σ (Mpa)**	****σ1 (Mpa)**	****σ2 (Mpa)**	****σ (Mpa)**	
0	0.00	0.00	0.00	0	0.00	0.00	0.00	0.00	0.00	0.00	
20	12.20	6.00	10.57	2	13.50	6.75	11.69	9.63	11.11	9.63	
40	25.00	12.75	21.65	4	27.00	13.50	23.38	7.41	5.56	7.40	
60	38.50	18.00	33.37	6	40.50	20.25	35.07	4.94	11.11	4.87	
80	50.00	25.00	43.30	8	54.00	27.00	46.77	7.41	7.41	7.41	
100	64.00	31.00	55.43	10	67.50	33.75	58.46	5.19	8.15	5.17	
120	78.00	37.00	67.58	12	81.00	40.50	70.15	3.70	8.64	3.66	
140	91.00	44.00	78.82	14	94.50	47.25	81.84	3.70	6.88	3.69	
160	105.00	51.00	90.95	16	108.00	54.00	93.53	2.78	5.56	2.76	
180	118.00	59.00	102.19	18	121.50	60.75	105.22	2.88	2.88	2.88	
200	130.00	64.00	112.59	20	135.00	67.50	116.91	3.70	5.19	3.70	

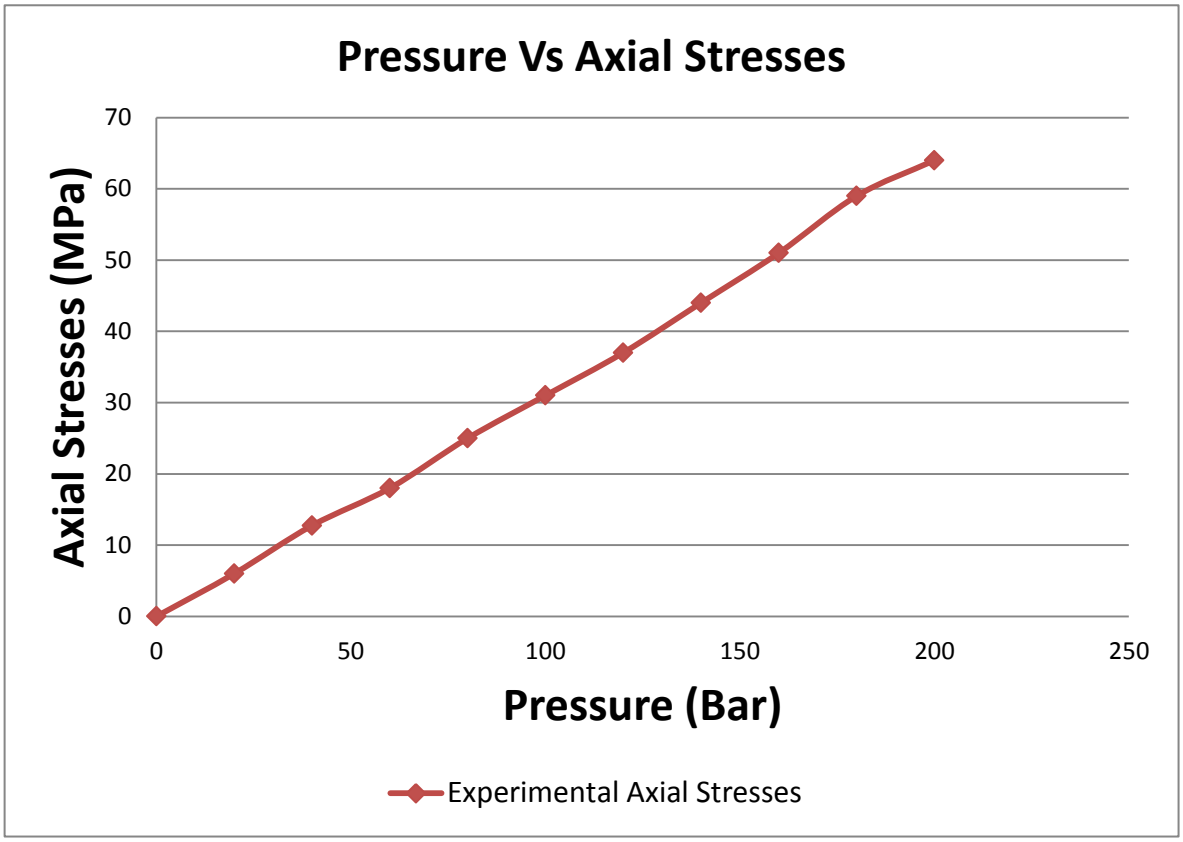

Figure 7.32 [Graph for the experimental axial stresses in case of 1.5 mm Straight pipe]

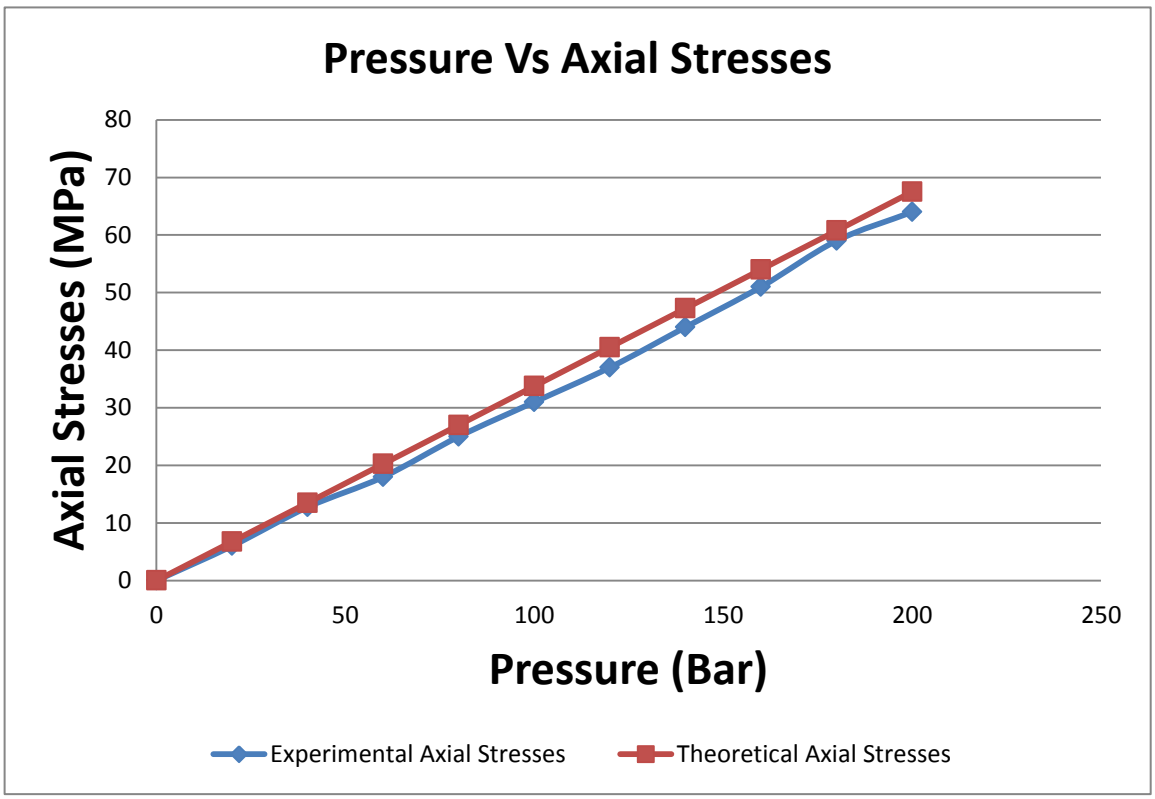

Figure 7.33 [Difference between axial stresses & theoretical axial stresses]

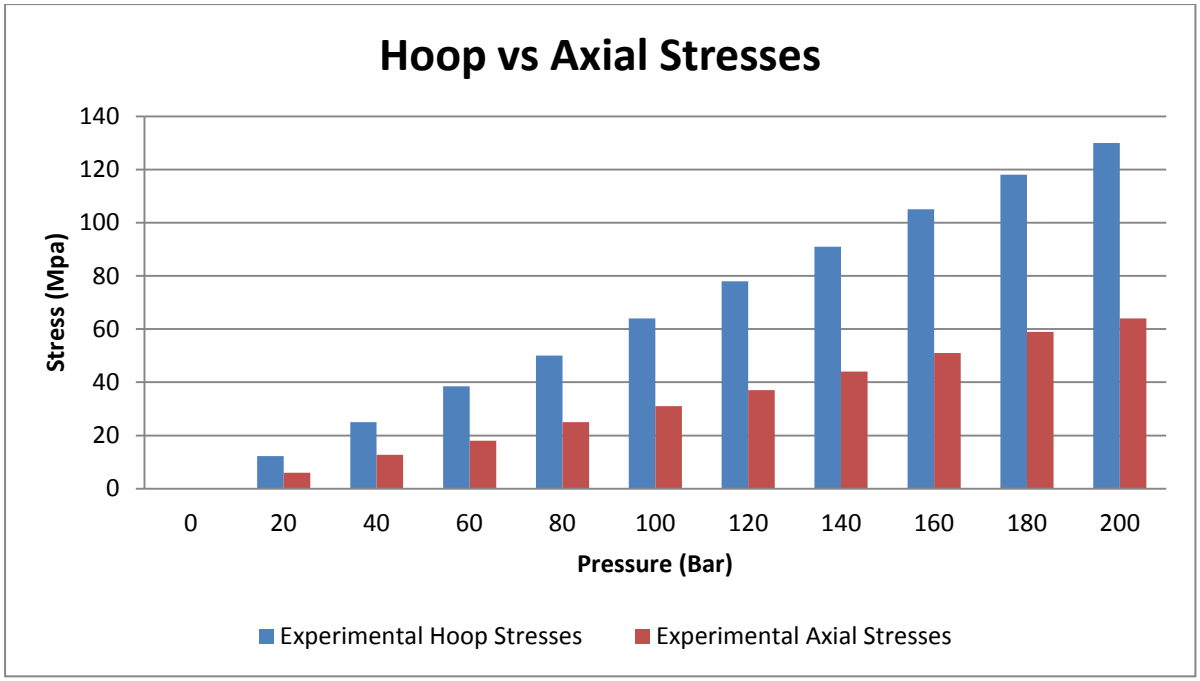

Figure 7.34 [Relation between experimental hoop stresses & experimental axial stresses]

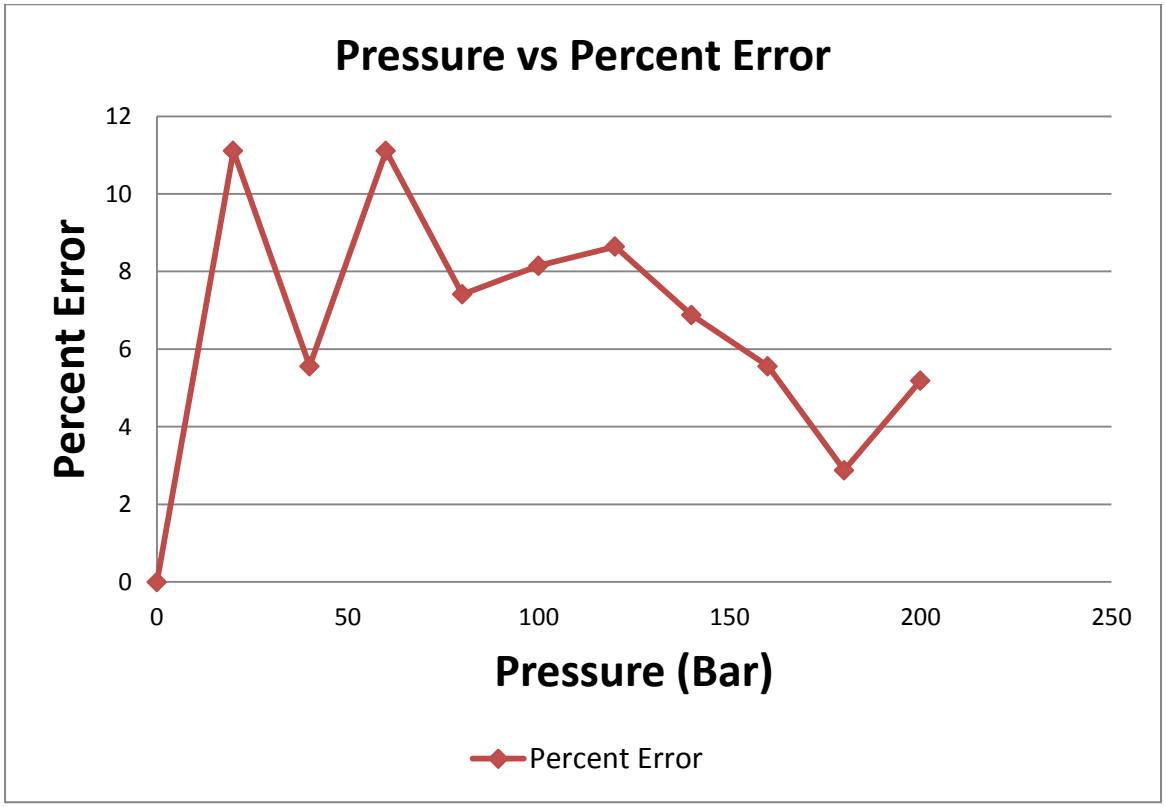

Figure 7.35 [Percent error calculated between experimental theoretical results]

7.15 L-Shaped Pipe (1.5mm wall thickness)

In the next phase the pipe of wall thickness of 1.5mm is taken with inner diameter of 9mm. In this experimentation an L-shaped pipe is taken and the circuit is assembled as seen before. A digitalize data in case of oil hammering (Steady State Form) is obtained. The same data is tabulated in Table 7.6 with different pump pressure readings. The σ_1 hoop stresses, σ_2 longitudinal stresses achieved with respect to the different pressure readings and strain by the strain gauges while the von misses σ_{von} have been calculated by the conventional method.

A theoretical data also have been calculated by the conventional formula of the thick wall and thin wall. A percent error has also been calculated as shown in table 7.6.

As clearly from the figure 7.36 (Pressure vs Axial Stress) by increasing the pump pressure the axial stress also increased subsequently.

In Figure 7.37 (Pressure vs Axial Stress) a graph is drawn for the comparison of experimental axial and theoretical axial stresses.

In Figure 7.38 (Hoop vs Axial Stresses) a graph is drawn for the comparison of experimental Hoop stresses and experimental axial stresses. Which has shown that the axial stress is always half of the hoop stresses.

In Figure 7.39 Percent errors are plotted on a graph with respect to the pressure which shows that the percent error between the theoretical data and experimental data.

It is clear all the readings are within the range of 8% 12 % error.

Table 7.6 [Experimental and Theoretical data and Percent error in case of 1.5 mm L pipe]

Stress Analysis Results										
Ref. Test Report No.: RD(029)/HPTD/09					**Inner Dia**		**Thickness**	**Test Component ID: SP-04 (L-Shaped Pipe)**		
					9.00		**1.50**			
P	Point		1	**P**	Point		2	**Percent Error**		
	Experimental Value (E)				**Theoretical Value (T)**					
	Principle Stress		Von Mises Stress		Principle Stress		Von Mises Stress	Principle Stress		Von Mises Stress
(BAR)	**σ1 (Mpa)**	**σ2 (Mpa)**	**σ (Mpa)**	**(MPa)**	***σ1 (Mpa)**	***σ2 (Mpa)**	***σ (Mpa)**	****σ1 (Mpa)**	****σ2 (Mpa)**	****σ (Mpa)**
0	0.00	0.00	0.00	0	0.00	0.00	0.00	0.00	0.00	0.00
20	12.20	6.00	10.57	2	13.50	6.75	11.69	9.63	11.11	9.63
40	25.00	12.75	21.65	4	27.00	13.50	23.38	7.41	5.56	7.40
60	38.50	18.00	33.37	6	40.50	20.25	35.07	4.94	11.11	4.87
80	50.00	25.00	43.30	8	54.00	27.00	46.77	7.41	7.41	7.41
100	64.00	31.00	55.43	10	67.50	33.75	58.46	5.19	8.15	5.17
120	78.00	37.00	67.58	12	81.00	40.50	70.15	3.70	8.64	3.66
140	91.00	44.00	78.82	14	94.50	47.25	81.84	3.70	6.88	3.69
160	105.00	51.00	90.95	16	108.00	54.00	93.53	2.78	5.56	2.76
180	118.00	59.00	102.19	18	121.50	60.75	105.22	2.88	2.88	2.88
200	133.25	64.00	115.43	20	135.00	67.50	116.91	1.30	5.19	1.27

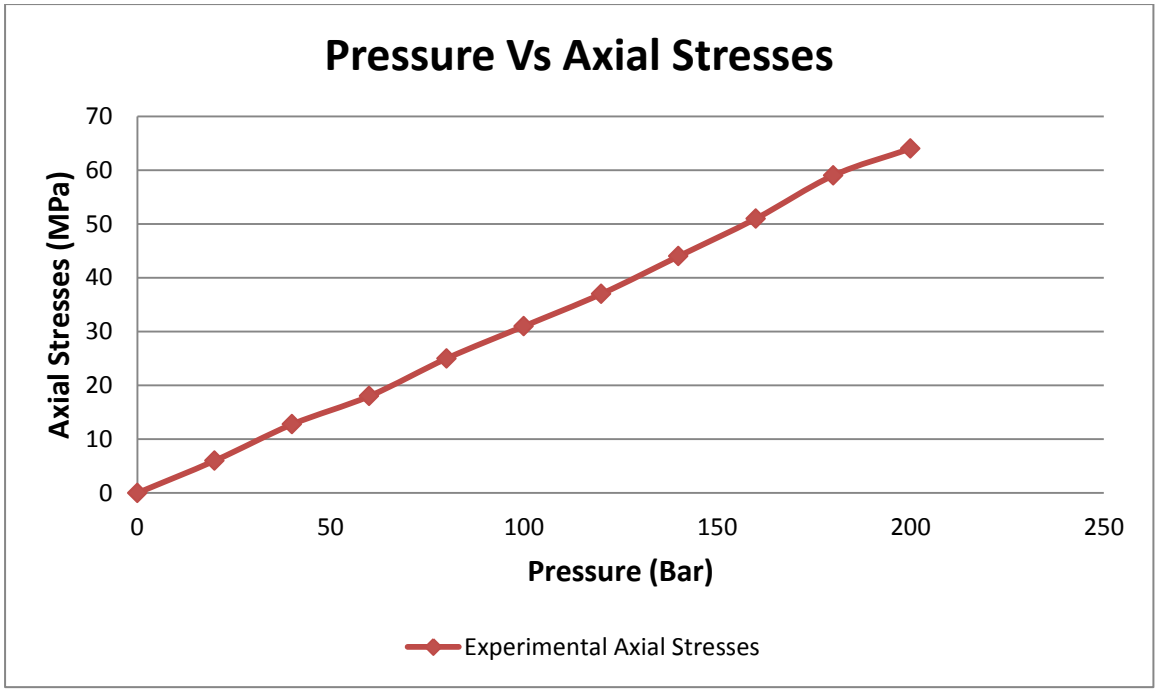

Figure 7.36 [Graph for the experimental axial stresses in case of 1.5mm shaped pipe]

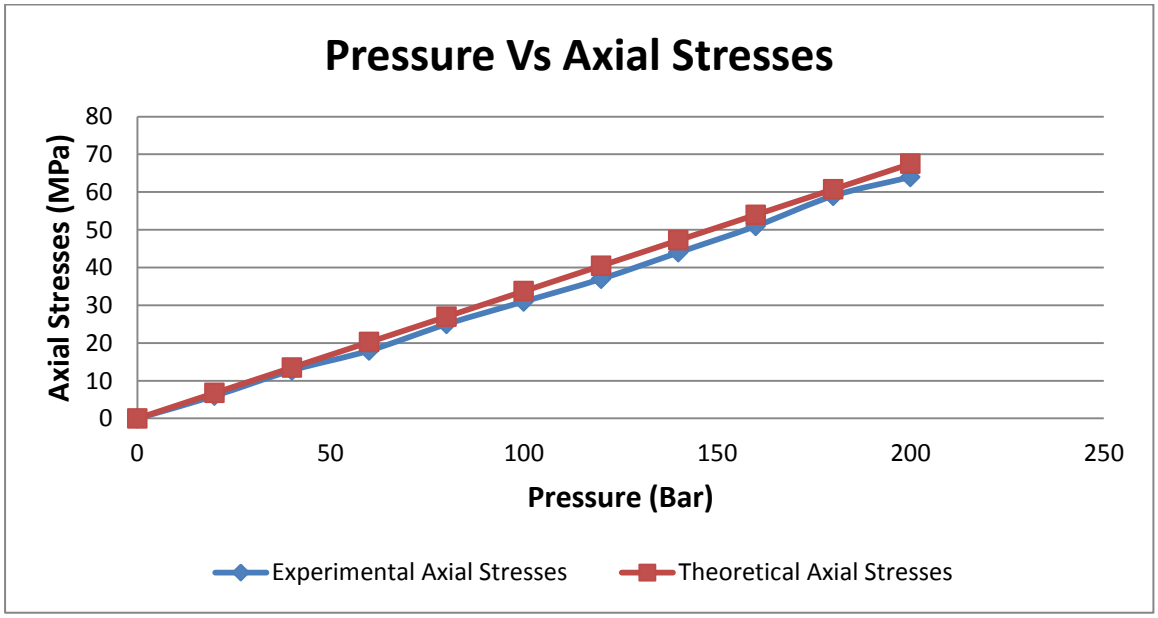

Figure 7.37 [Difference between experimental axial stresses & theoretical axial stresses]

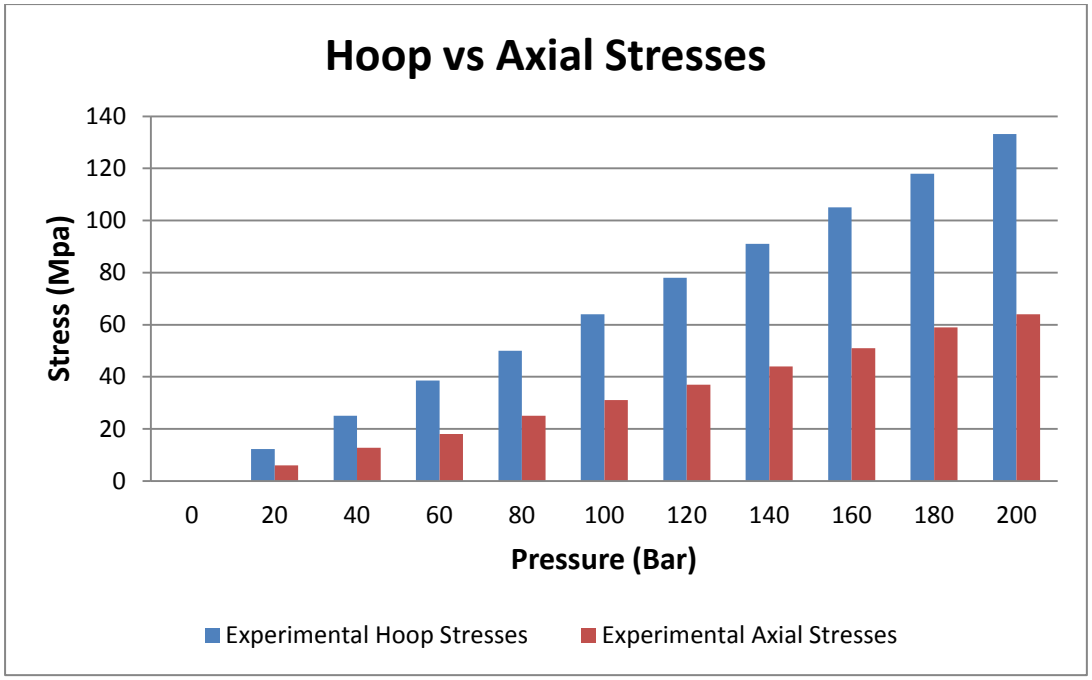

Figure 7.38 [Relation between hoop stresses & experimental axial stresses]

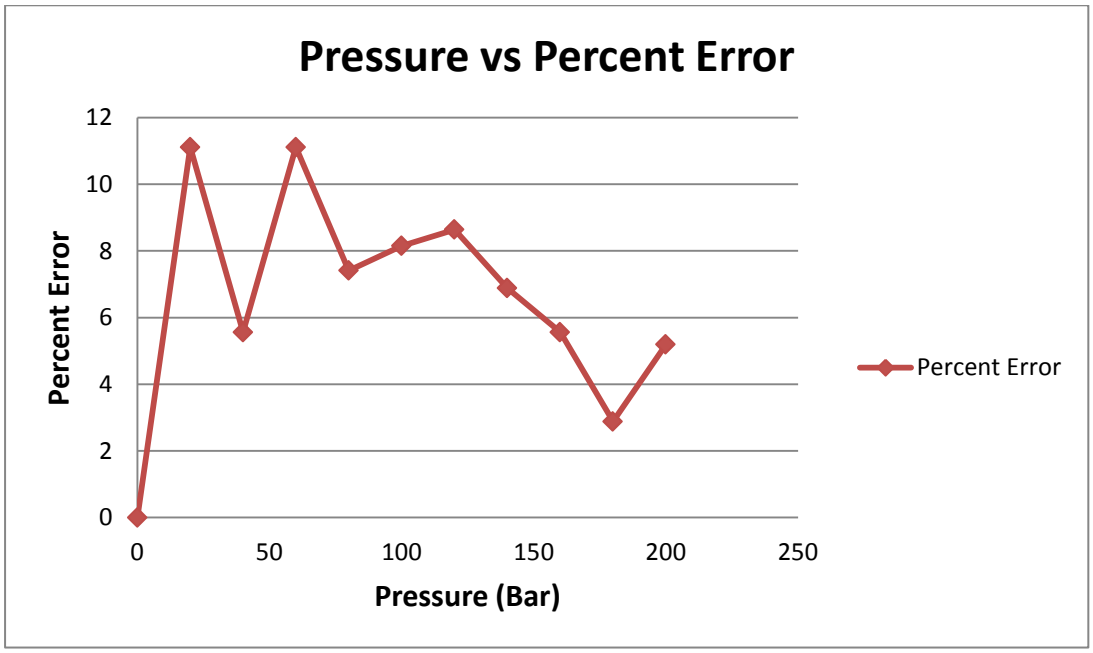

Figure 7.39 [Percent error calculated between experimental & theoretical results]

7.16 U-Shaped Pipe (1.5mm wall thickness)

In the next phase the pipe of wall thickness of 1.5mm is taken with inner diameter of 9mm. In this experimentation a U-shaped pipe is taken and the circuit is assembled as seen before. A digitalize data in case of oil hammering (Steady State Form) is obtained. The same data is tabulated in Table 7.7 with different pump pressure readings. The σ_1 hoop stresses, σ_2 longitudinal stresses achieved with respect to the different pressure readings and strain by the strain gauges while the von misses σ_{von} have been calculated by the conventional method.

A theoretical data also have been calculated by the conventional formula of the thick wall and thin wall. A percent error has also been calculated as shown in table 7.7.

As clearly from the figure 7.40 (Pressure vs Axial Stress) by increasing the pump pressure the axial stress also increased subsequently.

In Figure 7.41 (Pressure vs Axial Stress) a graph is drawn for the comparison of experimental axial and theoretical axial stresses.

In Figure 7.42 (Hoop vs Axial Stresses) a graph is drawn for the comparison of experimental Hoop stresses and experimental axial stresses. Which has shown that the axial stress is always half of the hoop stresses.

In Figure 7.43 Percent errors are plotted on a graph with respect to the pressure which shows that the percent error between the theoretical data and experimental data.

It is clear all the readings are within the range of 8% to 12% error.

Table 7.7 [Experimental and Theoretical data and Percent error in case of 1.5 mm U pipe]

Stress Analysis Results											
Ref. Test Report No.: RD(029)/HPTD/09					**Inner Dia**		**Thickness**	**Test Component ID: SP-04 (U-Shaped Pipe)**			
					9.00		**1.50**				
P	Point		1	**P**	Point		2	**Percent Error**			
	Experimental Value (E)				**Theoratical Value (T)**						
	Principle Stress		Von Mises Stress		Principle Stress		Von Mises Stress	Principle Stress		Von Mises Stress	
(BAR)	**σ1 (Mpa)**	**σ2 (Mpa)**	**σ (Mpa)**	**(MPa)**	***σ1 (Mpa)**	***σ2 (Mpa)**	***σ (Mpa)**	****σ1 (Mpa)**	****σ2 (Mpa)**	****σ (Mpa)**	
0	0.00	0.00	0.00	0	0.00	0.00	0.00	0.00	0.00	0.00	
20	12.20	6.00	10.57	2	13.50	6.75	11.69	9.63	11.11	9.63	
40	25.00	12.75	21.65	4	27.00	13.50	23.38	7.41	5.56	7.40	
60	38.50	18.00	33.37	6	40.50	20.25	35.07	4.94	11.11	4.87	
80	50.00	25.00	43.30	8	54.00	27.00	46.77	7.41	7.41	7.41	
100	64.00	31.00	55.43	10	67.50	33.75	58.46	5.19	8.15	5.17	
120	78.00	37.00	67.58	12	81.00	40.50	70.15	3.70	8.64	3.66	
140	91.00	44.00	78.82	14	94.50	47.25	81.84	3.70	6.88	3.69	
160	105.00	51.00	90.95	16	108.00	54.00	93.53	2.78	5.56	2.76	
180	118.00	59.00	102.19	18	121.50	60.75	105.22	2.88	2.88	2.88	
200	130.00	64.00	112.59	20	135.00	67.50	116.91	3.70	5.19	3.70	

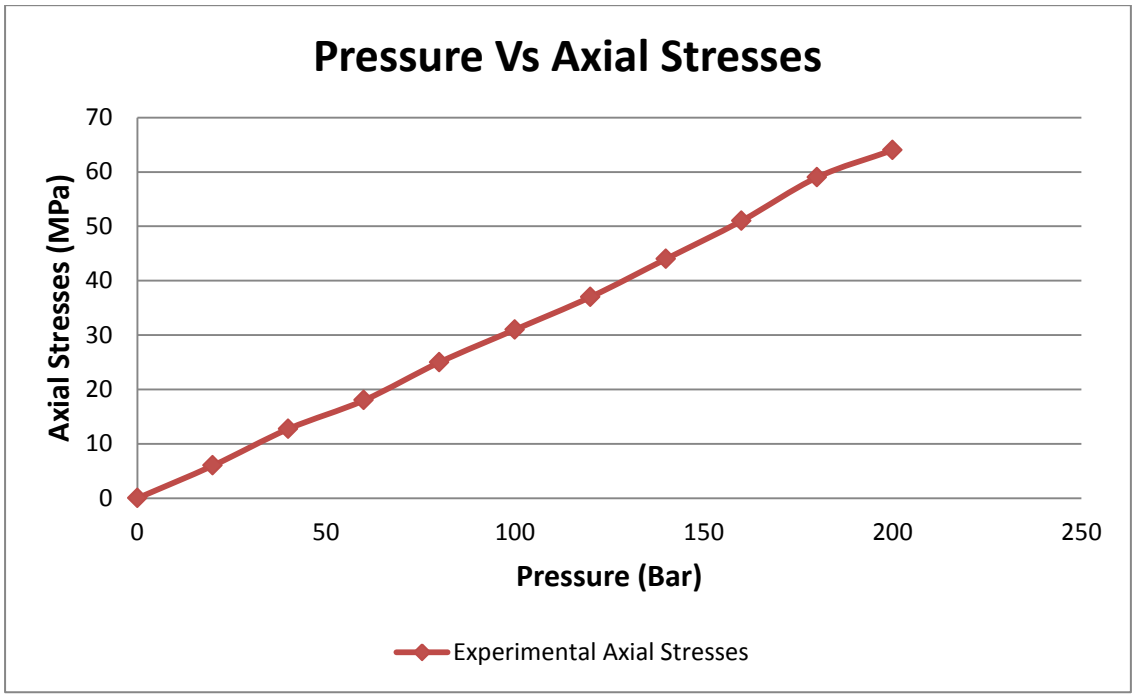

Figure 7.40 [Graph for the experimental axial stresses in case of 1.5mm U shaped pipe]

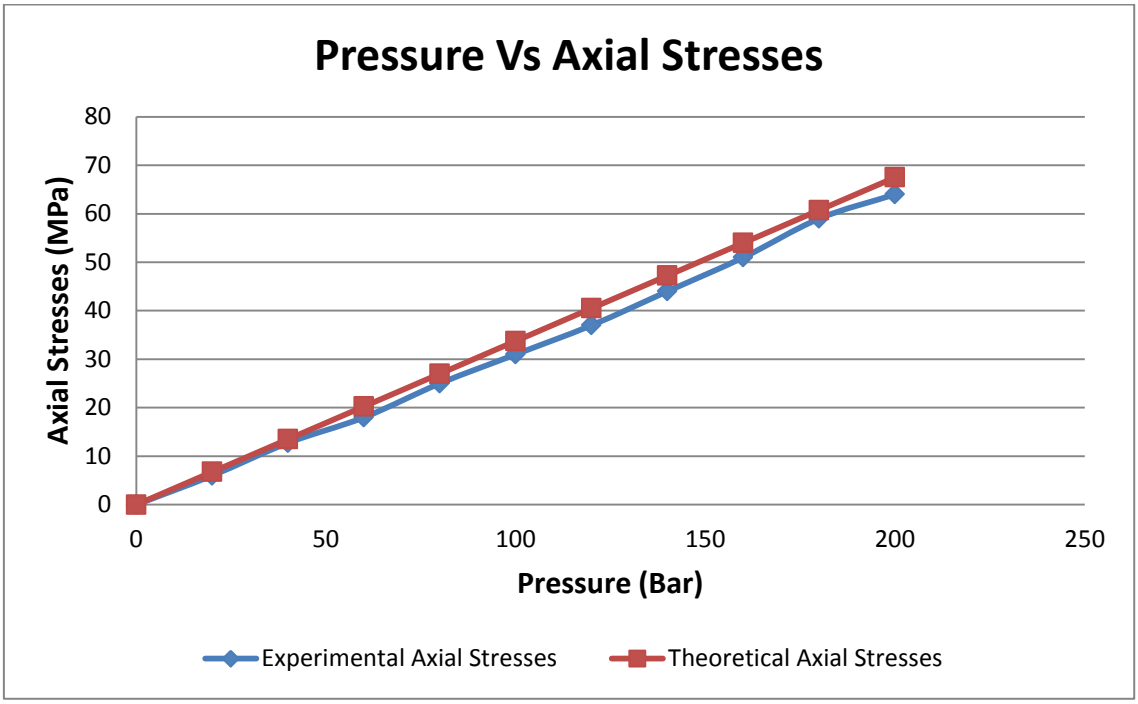

Figure 7.41 [Difference between experimental axial stresses & theoretical axial stresses]

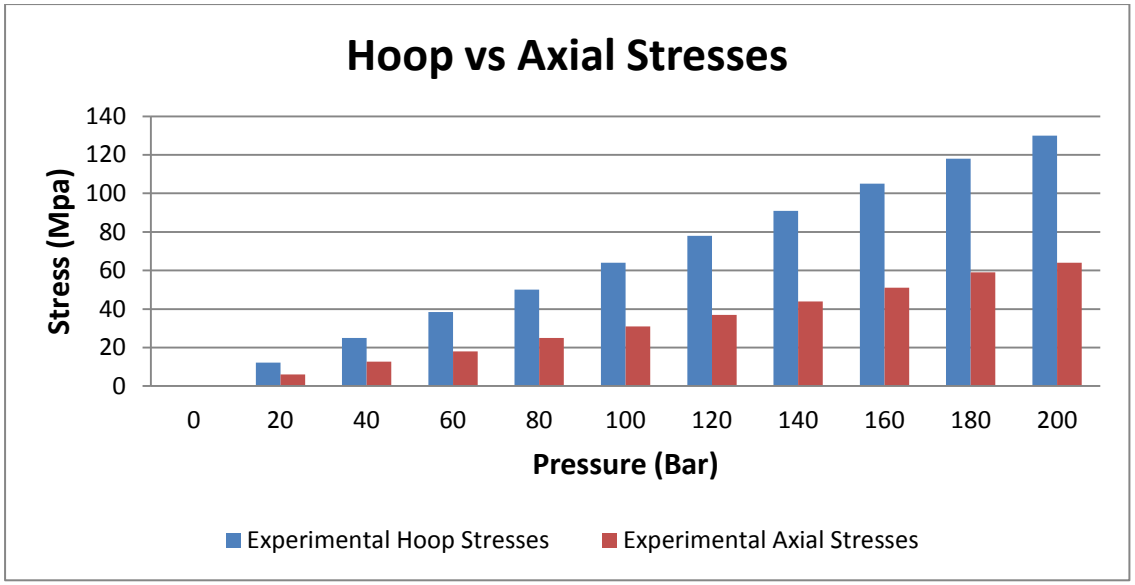

Figure 7.42 [Relation between experimental hoop stresses & experimental axial stresses]

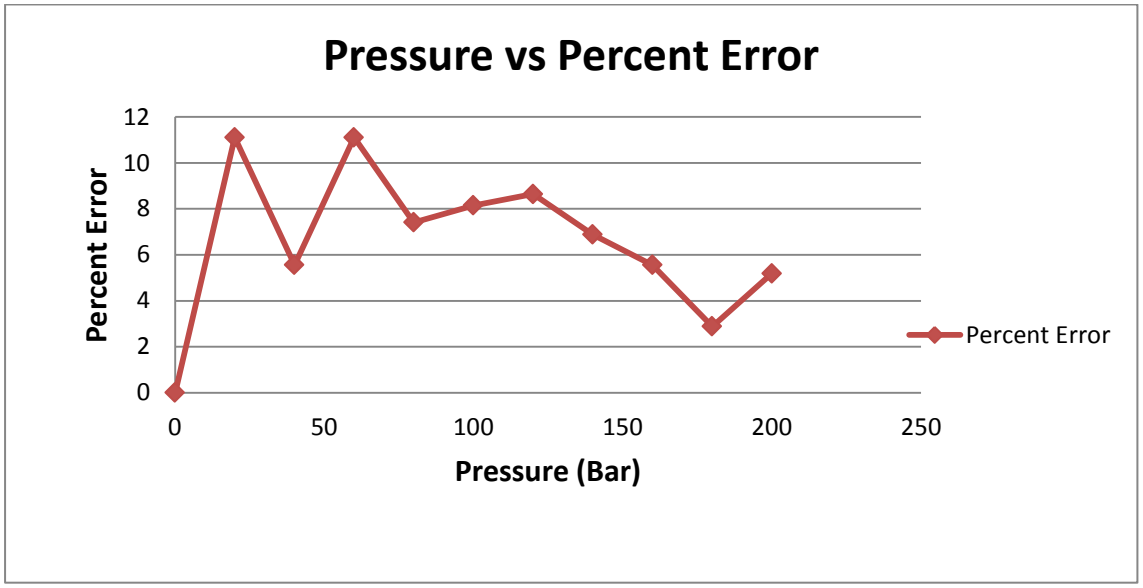

Figure 7.43 [Percent error calculated between the experimental and theoretical results]

7.17 Straight Pipe (2mm wall thickness)

In the next phase the pipe of wall thickness of 2mm is taken with inner diameter of 8mm. In this experimentation a straight pipe is taken and the circuit is assembled as seen before. A digitalize data in case of oil hammering (Steady State Form) is obtained. The same data is tabulated in Table 7.8 with different pump pressure readings. The σ_1 hoop stresses, σ_2 longitudinal stresses achieved with respect to the different pressure readings and strain by the strain gauges while the von misses σ_{von} have been calculated by the conventional method.

A theoretical data also have been calculated by the conventional formula of the thick wall and thin wall. A percent error has also been calculated as shown in table 7.8.

As clearly from the figure 7.44 (Pressure vs Axial Stress) by increasing the pump pressure the axial stress also increased subsequently.

In Figure 7.45 (Pressure vs Axial Stress) a graph is drawn for the comparison of experimental axial and theoretical axial stresses.

In Figure 7.46 (Hoop vs Axial Stresses) a graph is drawn for the comparison of experimental Hoop stresses and experimental axial stresses. Which has shown that the axial stress is always half of the hoop stresses.

In Figure 7.47 Percent errors are plotted on a graph with respect to the pressure which shows that the percent error between the theoretical data and experimental data.

It is clear all the readings are within the range of 8% error which is acceptable in design criteria.

Table 7.8 [Experimental and Theoretical data and Percent error in case of 2.0 mm straight pipe]

Stress Analysis Results											
Ref. Test Report No.: RD(029)/HPTD/09					**Inner Dia**		Thickness	**Test Component ID: SP-04 (Straight Pipe)**			
					8.00		**2.00**				
P	Point		1	**P**	Point		2	**Percent Error**			
	Experimental Value (E)				**Theoratical Value (T)**						
	Principle Stress		Von Mises Stress		Principle Stress		Von Mises Stress	Principle Stress		Von Mises Stress	
(BAR)	**σ1 (Mpa)**	**σ2 (Mpa)**	**σ (Mpa)**	**(MPa)**	***σ1 (Mpa)**	***σ2 (Mpa)**	***σ (Mpa)**	****σ1 (Mpa)**	****σ2 (Mpa)**	****σ (Mpa)**
0	0.00	0.00	0.00	0	0.00	0.00	0.00	0.00	0.00	0.00
20	14.50	6.50	12.58	2	16.00	8.00	13.86	9.38	18.75	9.21
40	29.00	14.00	25.12	4	32.00	16.00	27.71	9.38	12.50	9.36
60	43.50	22.00	37.67	6	48.00	24.00	41.57	9.38	8.33	9.37
80	57.80	30.00	50.07	8	64.00	32.00	55.43	9.69	6.25	9.67
100	73.00	38.00	63.24	10	80.00	40.00	69.28	8.75	5.00	8.72
120	88.00	45.00	76.22	12	96.00	48.00	83.14	8.33	6.25	8.33
140	101.70	54.50	88.15	14	112.00	56.00	96.99	9.20	2.68	9.12
160	116.80	60.00	101.16	16	128.00	64.00	110.85	8.75	6.25	8.74
180	132.10	70.00	114.47	18	144.00	72.00	124.71	8.26	2.78	8.21
200	146.50	76.00	126.90	20	160.00	80.00	138.56	8.44	5.00	8.42

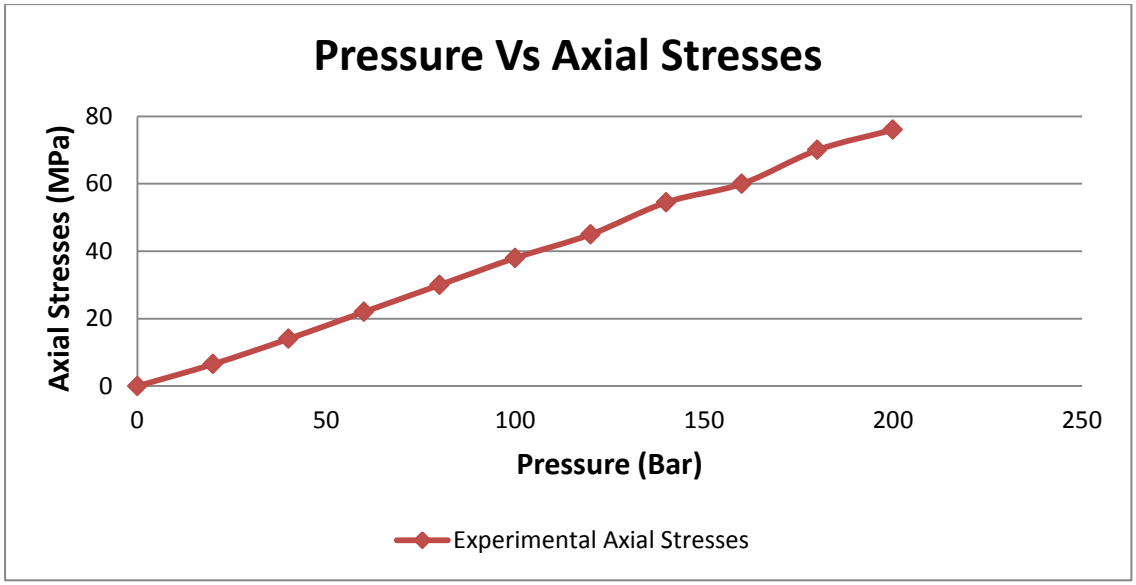

Figure 7.44 [Graph for the experimental axial stresses in case of 2.0 mm straight pipe]

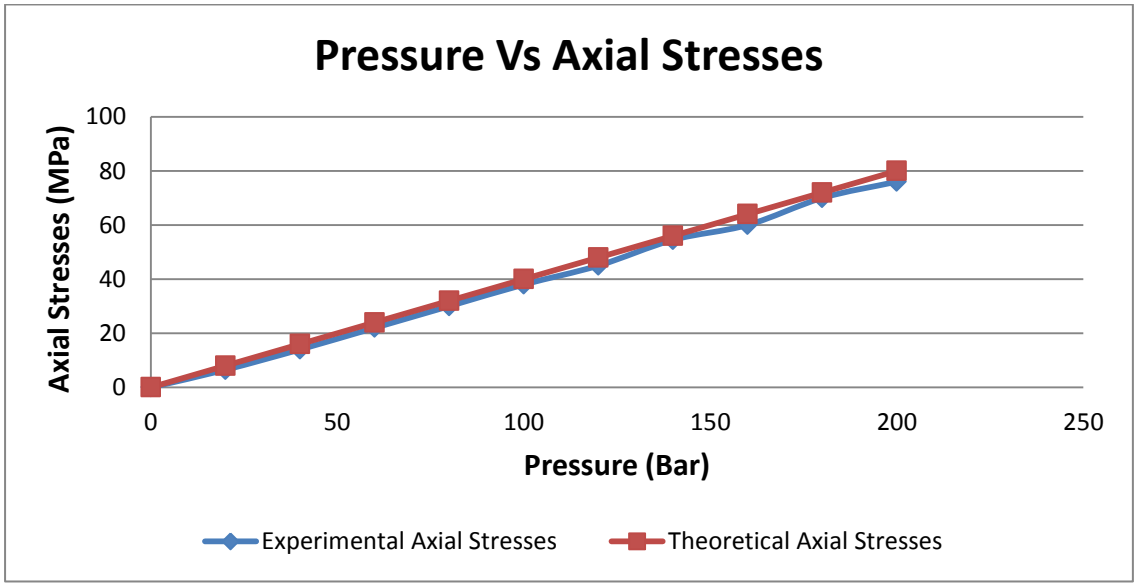

Figure 7.45 [Difference between experimental axial stresses & theoretical axial stresses]

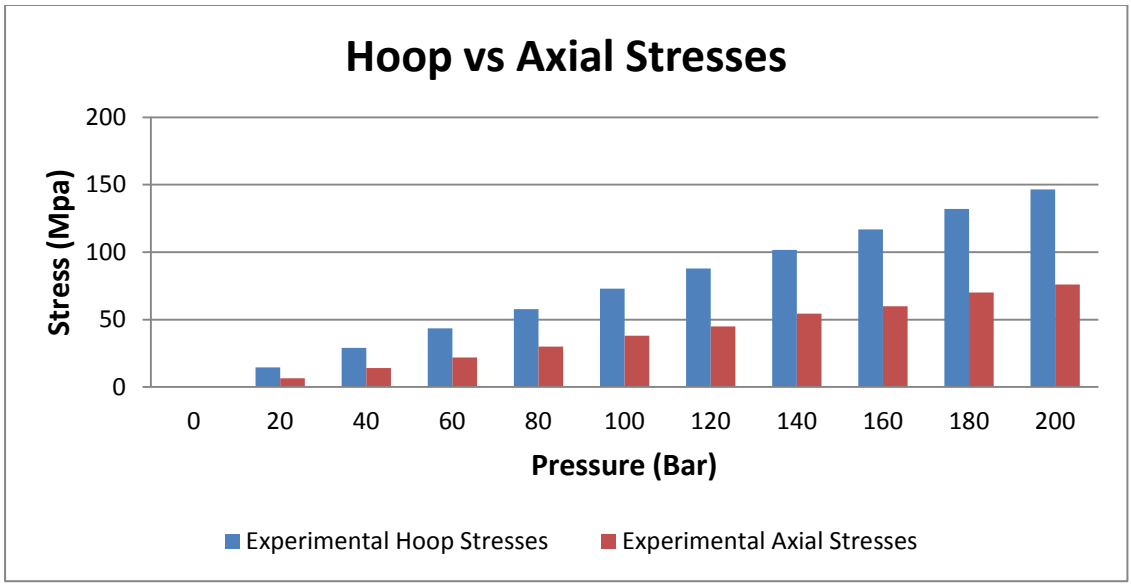

Figure 7.46 [Relation between hoop stresses & experimental axial stresses]

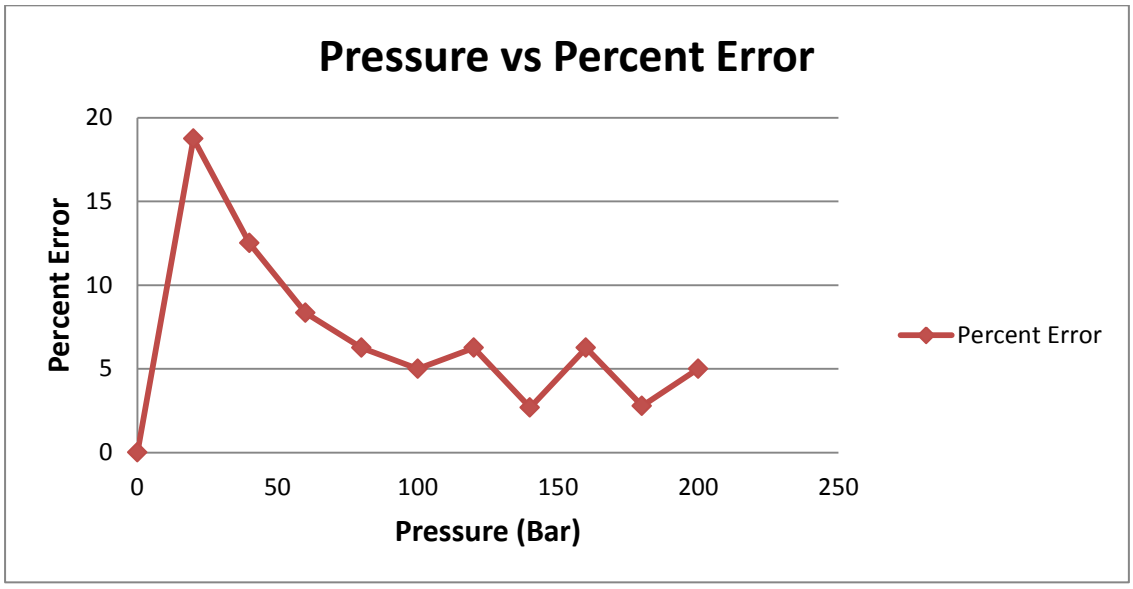

Figure 7.47 [Percent error calculated between experimental & theoretical results]

7.18 L-Shaped Pipe (2mm wall thickness)

In the next phase the pipe of wall thickness of 2mm is taken with inner diameter of 8mm. In this experimentation an L-shaped pipe is taken and the circuit is assembled as seen before. A digitalize data in case of oil hammering (Steady State Form) is obtained. The same data is tabulated in Table 7.9 with different pump pressure readings. The σ_1 hoop stresses, σ_2 longitudinal stresses achieved with respect to the different pressure readings and strain by the strain gauges while the von misses σ_{von} have been calculated by the conventional method.

A theoretical data also have been calculated by the conventional formula of the thick wall and thin wall. A percent error has also been calculated as shown in table 7.9.

As clearly from the figure 7.48 (Pressure vs Axial Stress) by increasing the pump pressure the axial stress also increased subsequently.

In Figure 7.49 (Pressure vs Axial Stress) a graph is drawn for the comparison of experimental axial and theoretical axial stresses.

In Figure 7.50 (Hoop vs Axial Stresses) a graph is drawn for the comparison of experimental Hoop stresses and experimental axial stresses. Which has shown that the axial stress is always half of the hoop stresses.

In Figure 7.51 Percent errors are plotted on a graph with respect to the pressure which shows that the percent error between the theoretical data and experimental data.

It is clear all the readings are within the range of 8% error which is acceptable in design criteria.

Table 7.9 [Experimental and Theoretical data and Percent error in case of 2.0 mm L Shaped pipe]

Stress Analysis Results										
Ref. Test Report No.: RD(029)/HPTD/09					**Inner Dia**		**Thickness**	**Test Component ID: SP-04 (L-Shaped Pipe)**		
					8.00		**2.00**			
P	Point		1	**P**	Point		2	**Percent Error**		
	Experimental Value (E)				**Theoretical Value (T)**					
	Principle Stress		Von Mises Stress		Principle Stress		Von Mises Stress	Principle Stress		Von Mises Stress
(BAR)	**σ1 (Mpa)**	**σ2 (Mpa)**	**σ (Mpa)**	**(MPa)**	***σ1 (Mpa)**	***σ2 (Mpa)**	***σ (Mpa)**	****σ1 (Mpa)**	****σ2 (Mpa)**	****σ (Mpa)**
0	0.00	0.00	0.00	0	0.00	0.00	0.00	0.00	0.00	0.00
20	14.60	7.00	12.65	2	16.00	8.00	13.86	8.75	4.50	8.72
40	29.50	13.00	25.61	4	32.00	16.00	27.71	7.81	8.75	7.60
60	44.00	23.00	38.12	6	48.00	24.00	41.57	8.33	4.17	8.30
80	58.00	28.00	50.24	8	64.00	32.00	55.43	9.38	4.50	9.36
100	74.50	35.00	64.56	10	80.00	40.00	69.28	6.88	4.50	6.82
120	87.50	45.00	75.79	12	96.00	48.00	83.14	8.85	6.25	8.84
140	102.00	54.50	88.40	14	112.00	56.00	96.99	8.93	2.68	8.86
160	118.00	60.00	102.20	16	128.00	64.00	110.85	7.81	6.25	7.81
180	131.50	70.00	113.96	18	144.00	72.00	124.71	8.68	2.78	8.62
200	145.90	76.00	126.39	20	160.00	80.00	138.56	8.81	5.00	8.79

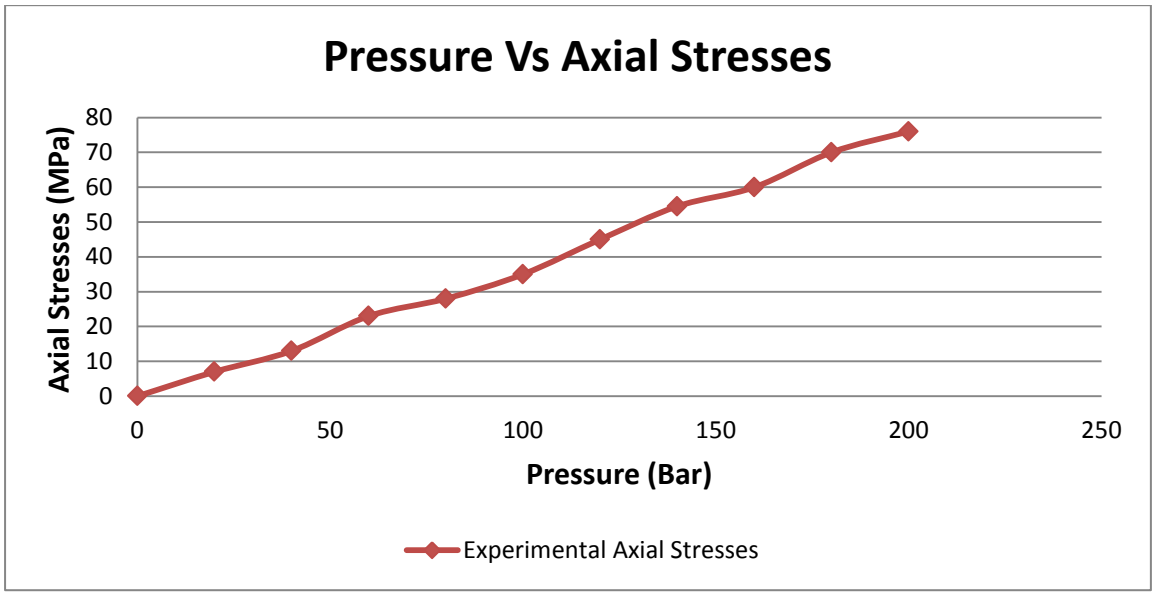

Figure 7.48 [Graph for the experimental axial stresses in case of 2.0 mm L shaped pipe]

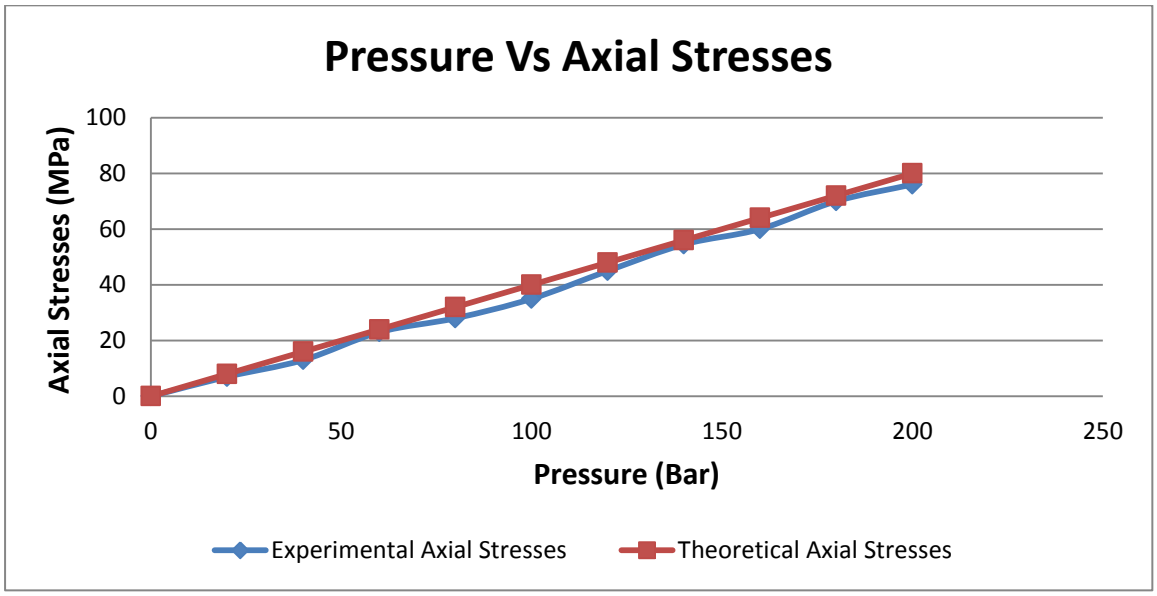

Figure 7.49 [Difference between experimental axial stresses & theoretical axial stresses]

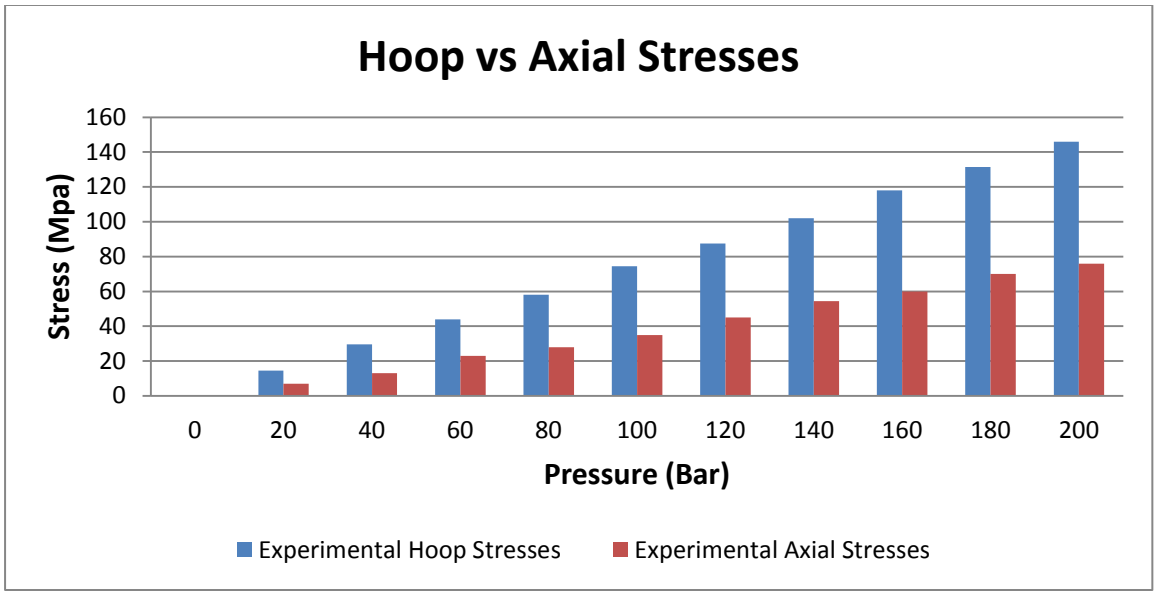

Figure 7.50 [Relation between experimental hoop stresses & experimental axial stresses]

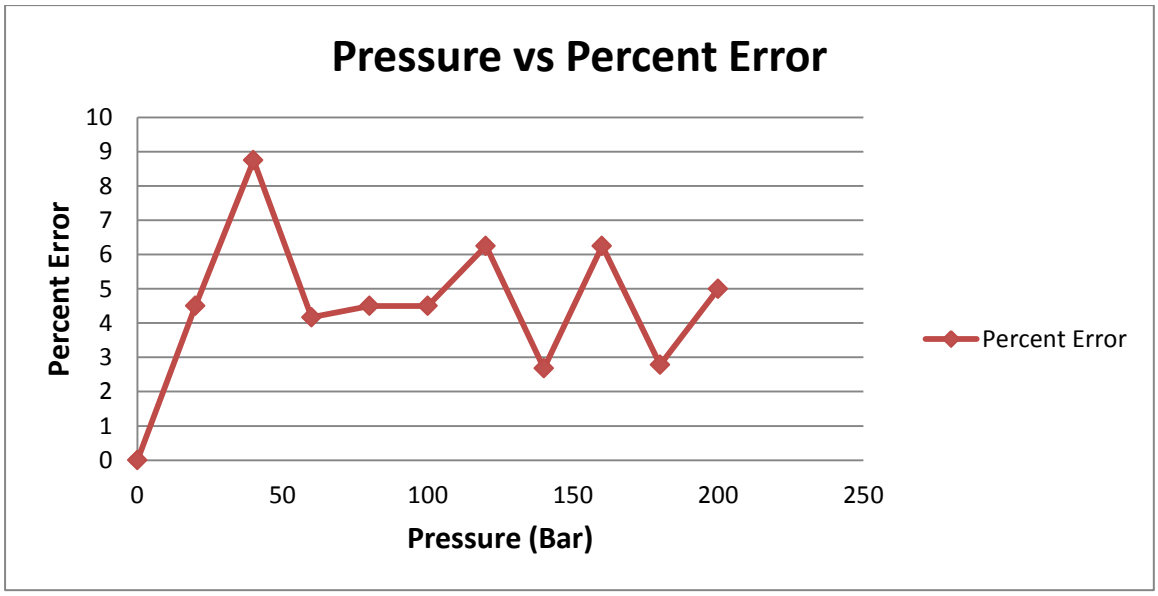

Figure 7.51 [Percent error calculated between experimental & theoretical results]

7.19 U-Shaped Pipe (2mm wall thickness)

In the next phase the pipe of wall thickness of 2mm is taken with inner diameter of 8mm. In this experimentation a U-shaped pipe is taken and the circuit is assembled as seen before. A digitalize data in case of oil hammering (Steady State Form) is obtained. The same data is tabulated in Table 7.10 with different pump pressure readings. The σ_1 hoop stresses, σ_2 longitudinal stresses achieved with respect to the different pressure readings and strain by the strain gauges while the von misses σ_{von} have been calculated by the conventional method.

A theoretical data also have been calculated by the conventional formula of the thick wall and thin wall. A percent error has also been calculated as shown in table 7.10.

As clearly from the figure 7.52 (Pressure vs Axial Stress) by increasing the pump pressure the axial stress also increased subsequently.

In Figure 7.53 (Pressure vs Axial Stress) a graph is drawn for the comparison of experimental axial and theoretical axial stresses.

In Figure 7.54 (Hoop vs Axial Stresses) a graph is drawn for the comparison of experimental Hoop stresses and experimental axial stresses. Which has shown that the axial stress is always half of the hoop stresses.

In Figure 7.55 Percent errors are plotted on a graph with respect to the pressure which shows that the percent error between the theoretical data and experimental data.

It is clear all the readings are within the range of 8% error which is acceptable in design criteria.

Table 7.10[Experimental and Theoretical data and Percent error in case of 2.0 mm U shaped pipe]

Stress Analysis Results										
Ref. Test Report No.: RD(029)/HPTD/09					**Inner Dia**		**Thickness**	**Test Component ID: SP-04 (U-Shaped Pipe)**		
					8.00		**2.00**			
P	Point		1	**P**	Point		2	**Percent Error**		
	Experimental Value (E)				**Theoretical Value (T)**					
	Principle Stress		Von Mises Stress		Principle Stress		Von Mises Stress	Principle Stress		Von Mises Stress
(BAR)	**σ1 (Mpa)**	**σ2 (Mpa)**	**σ (Mpa)**	**(MPa)**	***σ1 (Mpa)**	***σ2 (Mpa)**	***σ (Mpa)**	****σ1 (Mpa)**	****σ2 (Mpa)**	****σ (Mpa)**
0	0.00	0.00	0.00	0	0.00	0.00	0.00	0.00	0.00	0.00
20	14.60	6.50	12.67	2	16.00	8.00	13.86	8.75	8.75	8.57
40	29.50	14.00	25.56	4	32.00	16.00	27.71	7.81	6.50	7.77
60	43.80	22.00	37.93	6	48.00	24.00	41.57	8.75	8.33	8.75
80	58.00	30.00	50.24	8	64.00	32.00	55.43	9.38	6.25	9.36
100	72.50	38.00	62.81	10	80.00	40.00	69.28	9.38	5.00	9.34
120	89.50	45.00	77.51	12	96.00	48.00	83.14	6.77	6.25	6.77
140	102.50	54.50	88.83	14	112.00	56.00	96.99	8.48	2.68	8.42
160	117.00	60.00	101.34	16	128.00	64.00	110.85	8.59	6.25	8.58
180	133.00	70.00	115.23	18	144.00	72.00	124.71	7.64	2.78	7.60
200	147.00	76.00	127.33	20	160.00	80.00	138.56	8.13	5.00	8.11

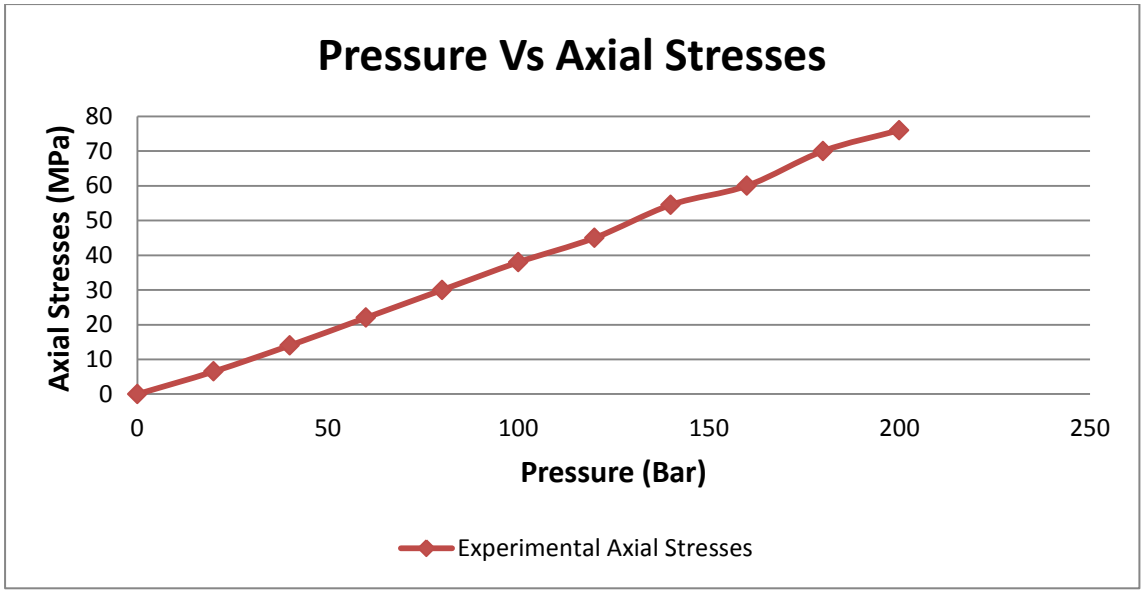

Figure 7.52 [Graph for the experimental axial stresses in case of 2.0 mm U shaped pipe]

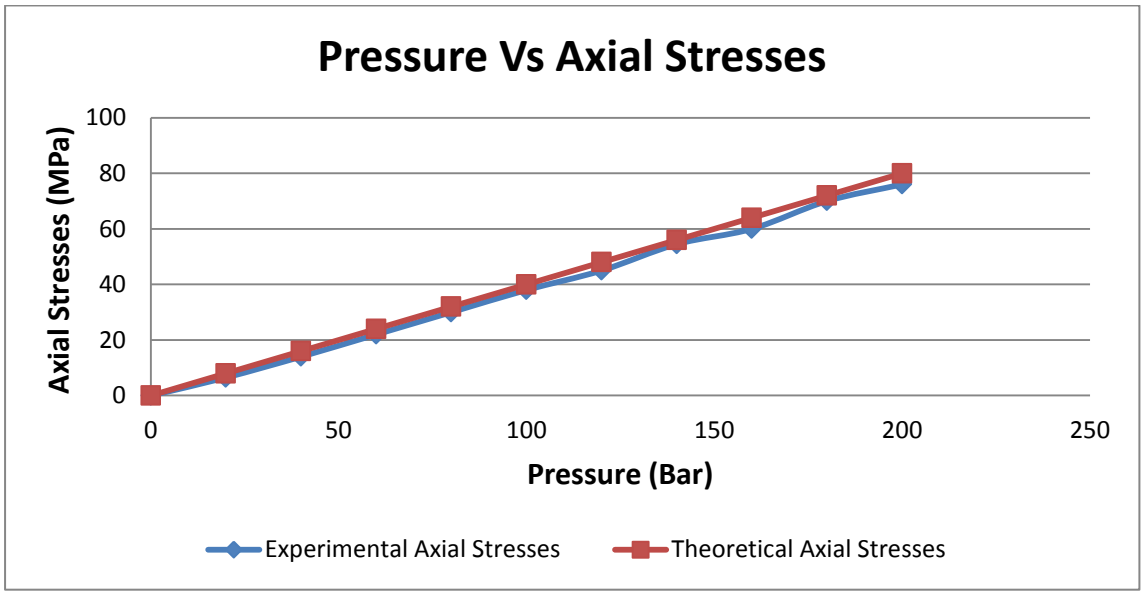

Figure 7.53 [Difference between experimental axial stresses & theoretical axial stresses]

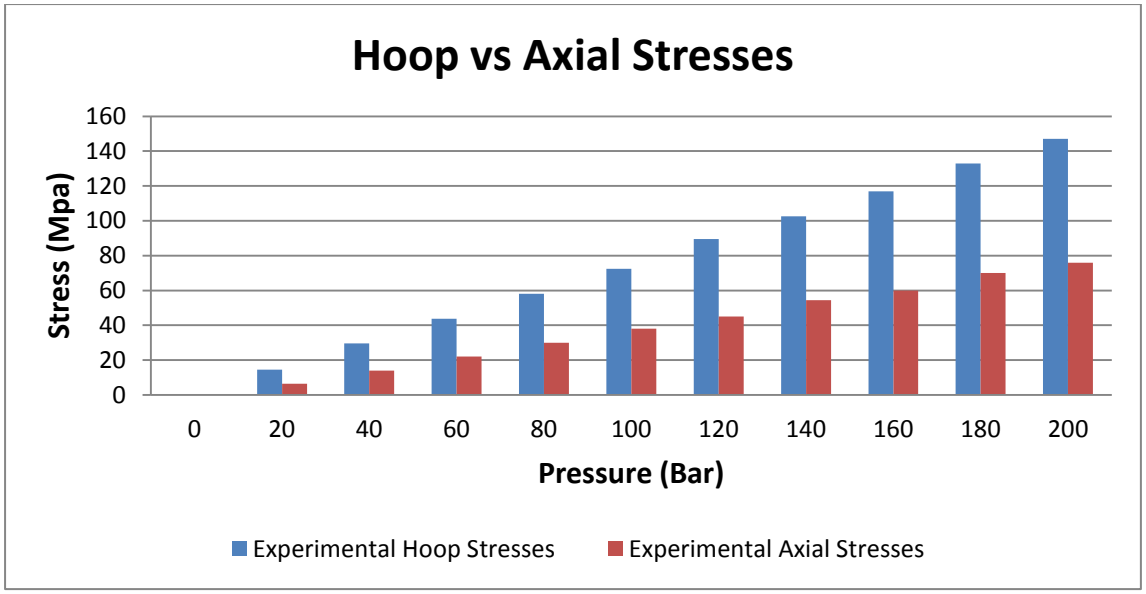

Figure 7.54 [Relation between experimental hoop stresses & experimental axial stresses]

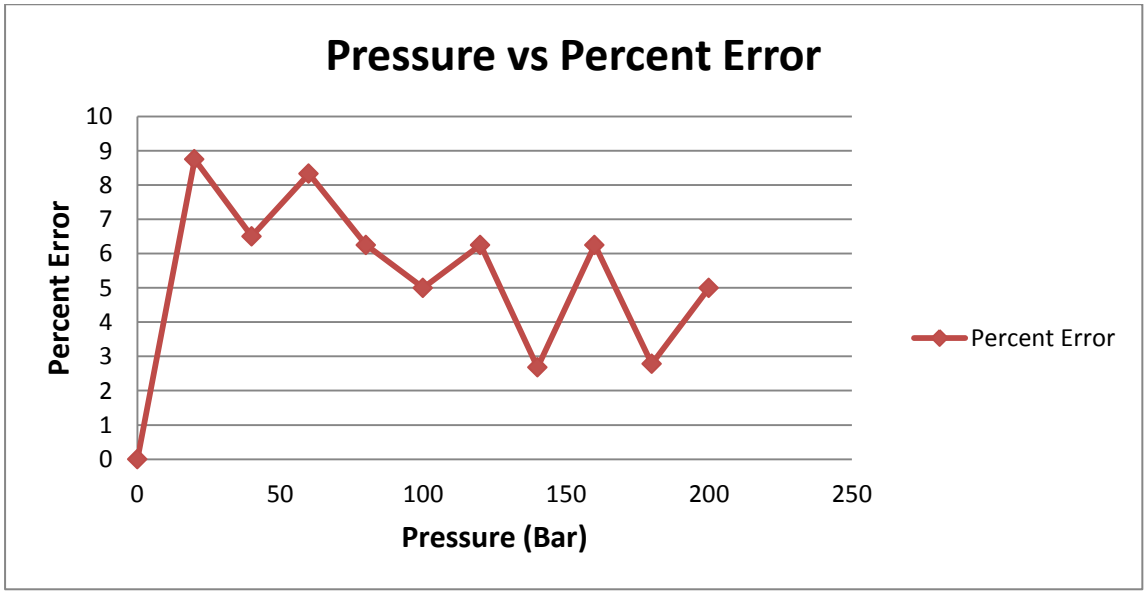

Figure 7.55 [Percent error calculated between experimental & theoretical results]

7.20 Hydraulic Jack Assembled with Straight Pipe

In this experiment the hydraulic jack is assembled with hydraulic pump unit and straight pipe. In this experiment three strain gauges in a rosette form at a three different places like near front dome, on centre of the cylinder and impact of the rear dome. A digitalize data in case of oil hammering (Steady State Form) is obtained. The same data is tabulated in Table 7.11 with different pump pressure readings. The σ_1 hoop stresses, σ_2 longitudinal stresses achieved with respect to the different pressure readings and strain by the strain gauges while the von misses σ_{von} have been calculated by the conventional method. Average principle stresses i.e. σ_1 hoop stresses, σ_2 longitudinal stresses and σ_{von} Von-misses is also calculated which is shown in Table 7.11.

A theoretical data also have been calculated by the conventional formula of the thin wall. A percent error has also been calculated as shown in table 7.11.

In Figure 7.56 (Hoop vs Axial Stresses) a graph is drawn for the comparison of experimental Hoop stresses and experimental axial stresses. Which has shown us that the axial stress is always half of the hoop stresses.

Table 7.11[Experimental and Theoretical data and Percent error in case of 15.0 mm Thick hydraulic jack]

Ref. Test Report No.: RD(034)/HPTD/09										**Inner Dia**				**Thickness**		**Test Component ID:**		
										160.00				**15.00**		**AC-04**		
P	Point		1	Point		2	Point		3	**Average (Exp.)**			Point		4	**Percent Error**		
	Near Front Dome			**On Center of Cylinder**			**Near Rear Dome**						**Theoratical (T)**					
	Principle Stress		Von Mises Stress	Principle Stress		Von Mises Stress	Principle Stress		Von Mises Stress	Principle Stress		Von Mises Stress	Principle Stress		Von Mises Stress	Principle Stress		Von Mises Stress
(BAR)	**σ1 (Mpa)**	**σ2 (Mpa)**	**σ (Mpa)**	**σ1 (Mpa)**	**σ2 (Mpa)**	**σ (Mpa)**	**σ1 (Mpa)**	**σ2 (Mpa)**	**σ (Mpa)**	**Av-σ1 (Mpa)**	**Av-σ2 (Mpa)**	**Av-σ (Mpa)**	***σ1 (Mpa)**	***σ2 (Mpa)**	***σ (Mpa)**	****σ1 (Mpa)**	****σ2 (Mpa)**	****σ (Mpa)**
0	0	0	0	0	0	0	0	0	0	0	0	0	0	0	0	0	0	0
20	10.00	6.00	8.72	10.00	5.00	8.66	9.00	5.00	7.81	9.50	5.50	8.26	10.00	5.00	8.66	5.00	-10.00	4.58
40	21.00	13.00	18.36	20.00	10.00	17.32	19.00	10.00	16.46	20.00	11.50	17.41	20.00	10.00	17.32	0.00	-15.00	0.52
60	31.00	20.00	27.22	30.00	15.00	25.98	29.00	15.00	25.12	30.00	17.50	26.17	30.00	15.00	25.98	0.00	-16.67	0.73
80	42.00	27.00	36.86	40.00	20.00	34.64	39.00	20.00	33.78	40.50	23.50	35.32	40.00	20.00	34.64	-1.25	-17.50	1.96
100	56.00	35.00	49.00	53.00	26.00	45.90	53.00	27.00	45.90	54.50	31.00	47.45	50.00	25.00	43.30	-9.00	-24.00	9.58
120	64.00	41.00	56.15	62.00	31.00	53.69	61.00	31.00	52.83	62.50	36.00	54.49	60.00	30.00	51.96	-4.17	-20.00	4.87
140	76.00	48.00	66.57	72.00	36.00	62.35	72.00	36.00	62.35	74.00	42.00	64.46	70.00	35.00	60.62	-5.71	-20.00	6.34
160	84.00	54.00	73.73	80.00	40.00	69.28	80.00	40.00	69.28	82.00	47.00	71.51	80.00	40.00	69.28	-2.50	-17.50	3.21
180	98.00	63.00	86.02	93.00	46.00	80.54	93.00	47.00	80.54	95.50	55.00	83.28	90.00	45.00	77.94	-6.11	-22.22	6.85
210	103.00	52.00	89.20	103.00	52.00	89.20	103.00	52.00	89.20	103.00	52.00	89.20	105.00	52.50	90.93	1.90	0.95	1.90
210	103.00	52.00	89.20	103.00	51.00	89.20	103.00	52.00	89.20	103.00	52.00	89.20	105.00	52.50	90.93	1.90	0.95	1.90

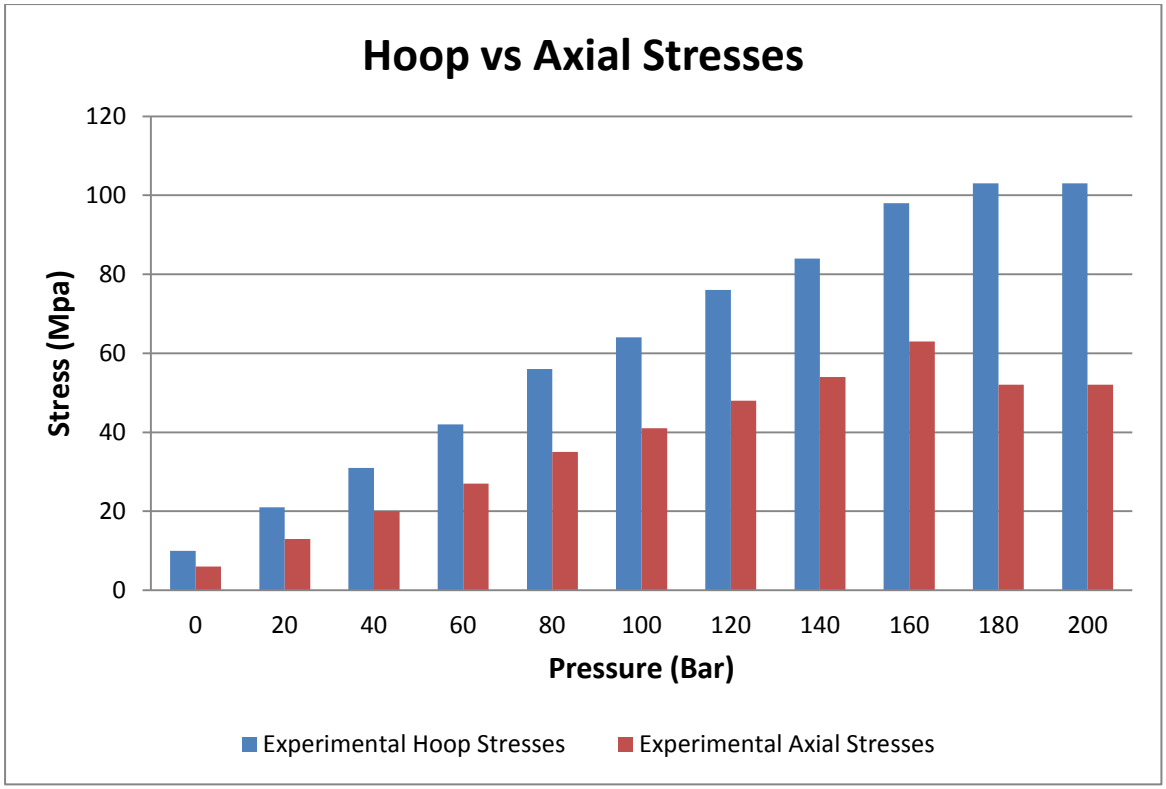

Figure 7.56 [Relation between experimental hoop stresses & experimental axial stresses]

7.21 Displacement

As in the existing system when the hydraulic system is in operation form then the hydraulic circuitry shows some movement of hydraulic pipes with the application of pump pressure for avoiding this movement a specially designed clamps are used. In this experiment the forward and reverse movement of hydraulic pipes with respect to the different rating pressure is observed. A digitalized data have been received by displacement sensors as which have already been discussed in section 7.13.

A tabulated data have shown in Table 7.12 which shows the forwarded and reverse motion of hydraulic pipes after application of different pressure.

Figure 7.57 (The graph of Pressure vs Displacement) shows the forward displacement is less than the reverse displacement at a same pressure and when the pressure is increased then the forward and reverse displacement also change vice versa. The same situation has been explained in a bar graph of Figure 7.58 in this experiment different thicknesses (1mm, 1.5mm and 2mm) of straight pipes are taken and the data obtained is tabulated in 7.12, 7.13 and 7.14.

If the result of these three tables is compared then it is concluded that the thickness has a role in the motion of forward and reverse motion. This data will be used in the optimization of clamps in next section.

7.21.1 1mm tube

Pressure (BARS)	Forward	Reverse
0	0	0
20	0.73	2.31
40	1.74	5.34
60	1.67	7.96
80	1.83	10.38
100	2.23	13.44
120	3.32	17.6
140	3.73	20.12
160	3.98	24.8
180	5.31	27.3
200	6.2	31.1

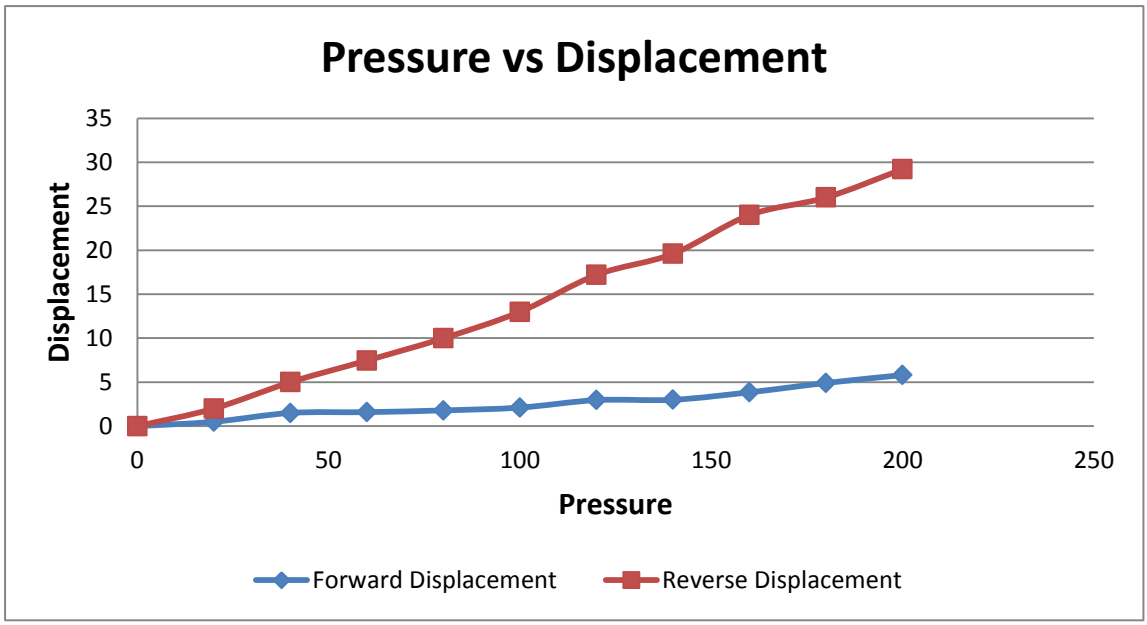

Figure 7.57 [Graph between Forward displacement & Reverse displacement]

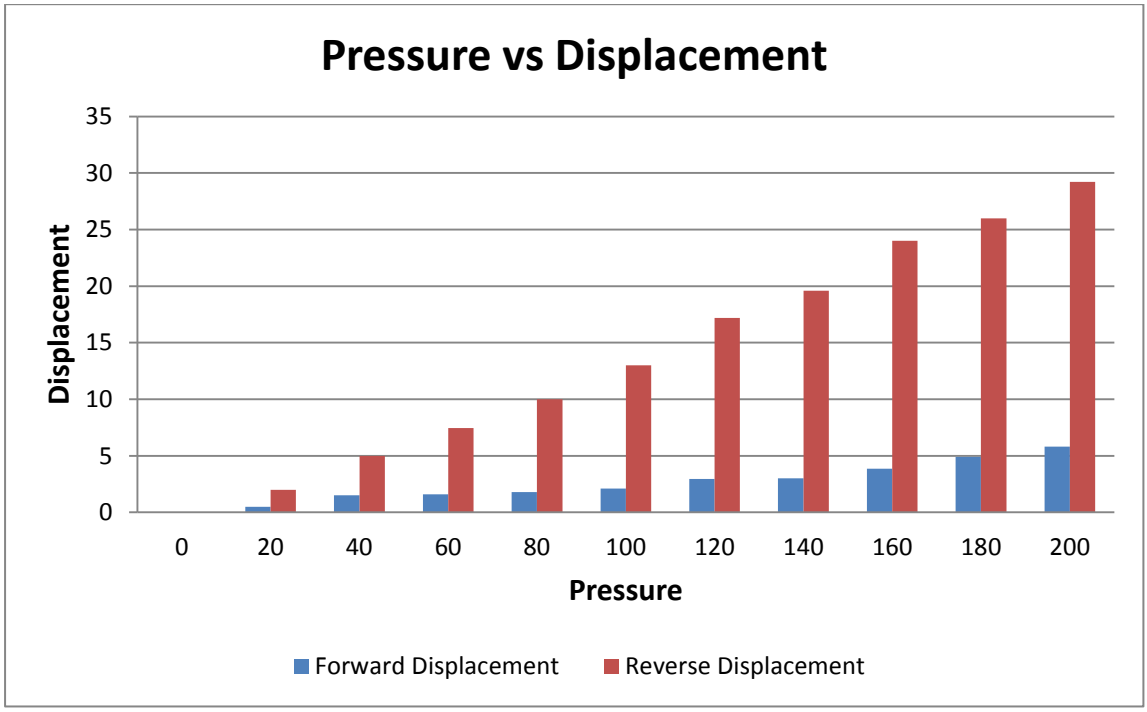

Figure 7.58 [Difference between Forward displacement & Reversed displacement]

7.21.2 1.5mm tube

Pressure (BARS)	Forward	Reverse
0	0	0
20	0.5	2
40	1.5	5
60	1.59	7.46
80	1.79	10
100	2.11	13
120	2.96	17.2
140	3	19.6
160	3.85	24
180	4.91	26
200	5.81	29.21

Table 7.13 [Pressure, Forward displacement & Reversed displacement in mm]

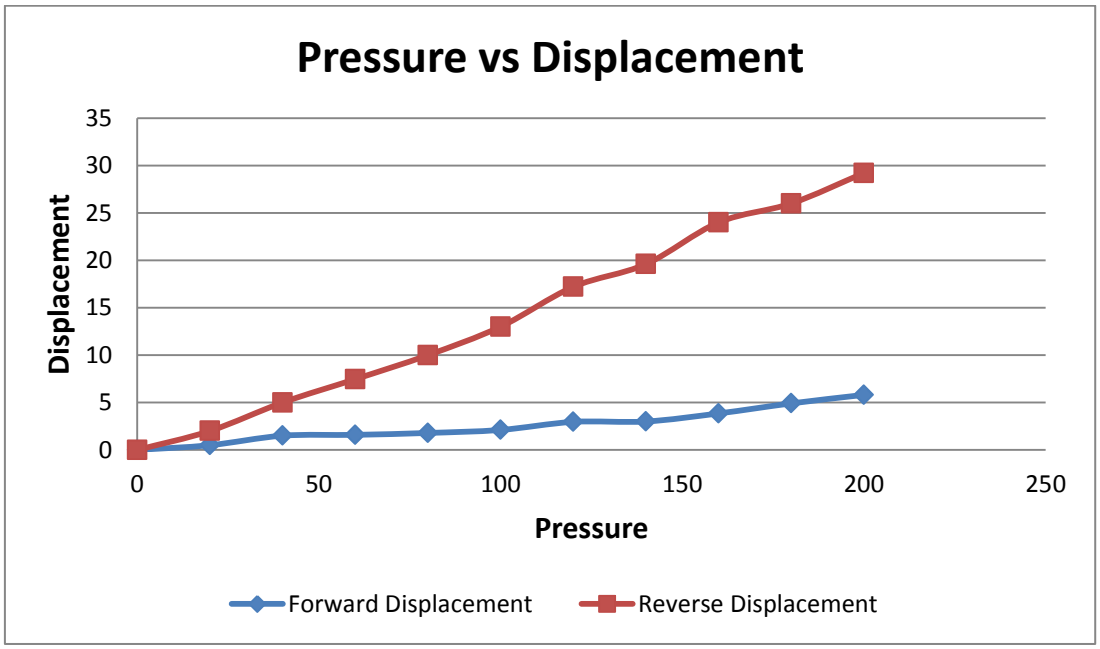

Figure 7.59 [Difference between Forward & Reversed displacement]

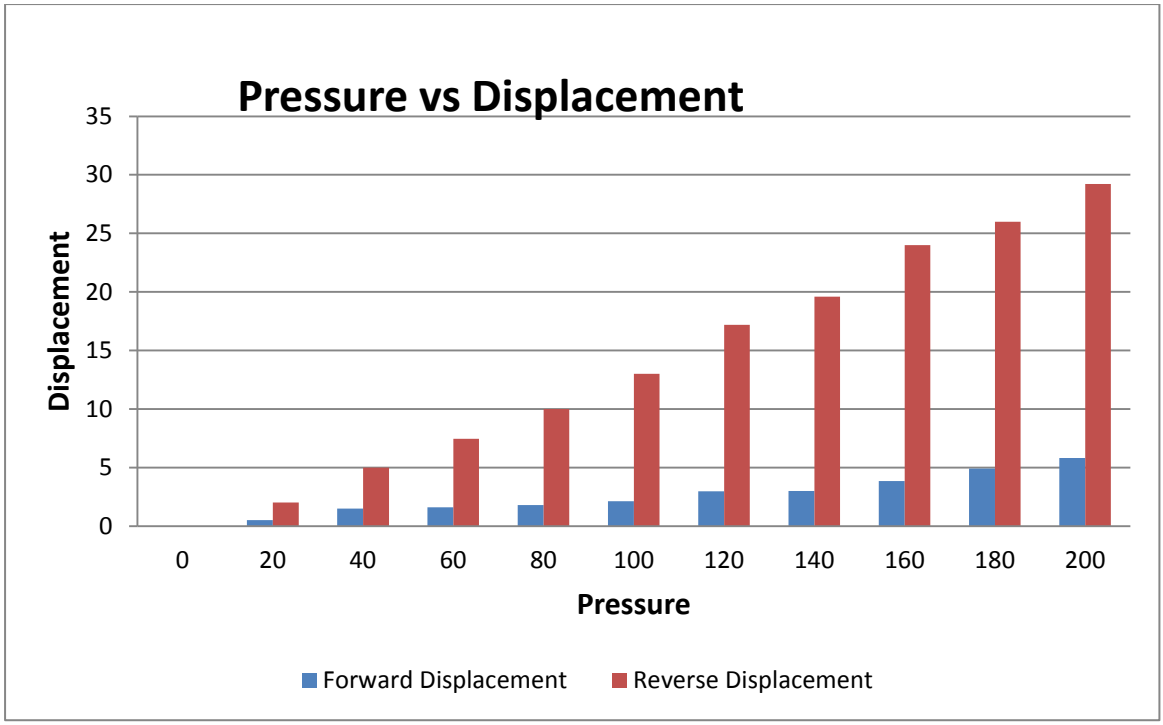

Figure 7.60 [Difference between Forward displacement & Reversed displacement]

7.21.3 2mm tube

Table 7.14 [Pressure in bars, Forward & Reversed displacement in mm]

Pressure (BARS)	Forward	Reverse
0	0	0
20	0.42	1.91
40	1.47	4.69
60	1.19	7.36
80	1.49	9.3
100	1.93	12.4
120	2.46	16.2
140	2.4	17.6
160	3.25	23.4
180	4.51	24.3
200	5.41	28.1

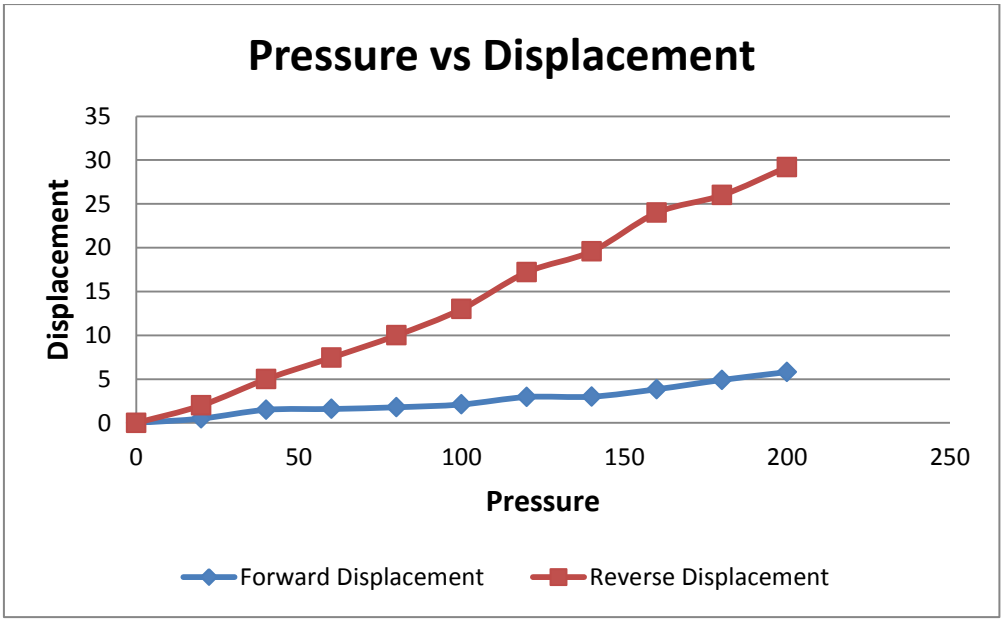

Figure 7.61 [Difference between Forward & Reversed displacement]

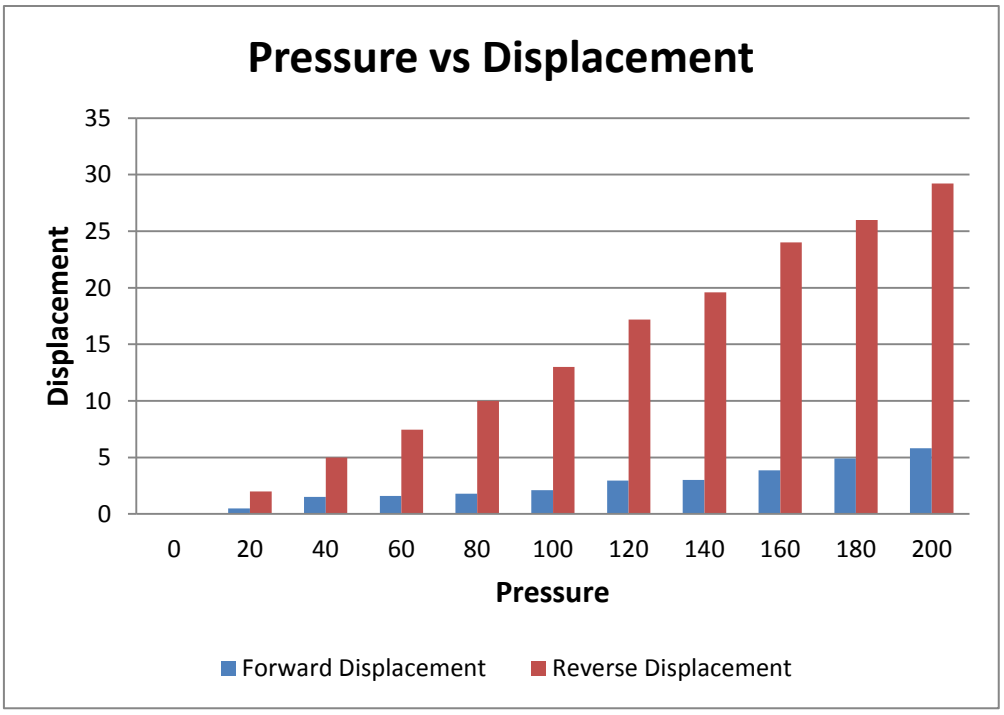

Figure 7.62 [Displacement between Forward & Reversed displacement]

7.22 Bursting of Tubes

In this section different thickness of hydraulic tubes has been burst in order to achieve the maximum bursting pressure for the optimization of wall thickness.

7.22.1 1mm Tube

A 1mm wall thickness tube has been taken with one side blocked and pump pressure has been applied with the difference of 5MPa (i.e. 50, 100, 150, 200 . . . .etc) and finally upto the bursting pressure. A digitalized data of principle stresses i.e. σ_1 hoop stresses, σ_2 longitudinal stresses has been received from strain gauges which are tabulated in Table 7.15. Von-misses Stress is also calculated by the conventional method. Theoretical Value of σ_1 hoop stresses, σ_2 longitudinal stresses with von-Misses also calculated which is shown in table 7.15. As clearly from table 7.15 we have seen that σ_2 longitudinal stresses is almost half of the σ_1 hoop stresses at their respective pressure reading. Also it is seen that by increasing the pressure the σ_1 hoop stresses, σ_2 longitudinal stresses also increase and when a certain pressure is reached there are no significant changes in σ_1 hoop stresses and σ_2 longitudinal stresses with respect to increase in pressure. The graph pressure vs stresses shown in figure 7.63 are also explained this phenomenon.

Table 7.15 [Experimental & Theoretical Principle Stresses at different pressure levels along with Von Misses and Percent Errors]

Ref. Test Report No.: RD(029)/HPTD/09				**Inner Dia**	**Thickness**	**Test Component ID: SP-02 (Straight Pipe)**					
				10.00	**1.00**						
	Point	1		Point	2	**Straight Pipe, Length 940mm**					
P	**Experimental Value (E)**			**P**	**Theoretical Value (T)**			**Percent Error**			
	Principle Stress		Von Misses Stress		Principle Stress		Von Misses Stress	Principle Stress		Von Misses Stress	
(BAR)	**σ1 (Mpa)**	**σ2 (Mpa)**	**σ (Mpa)**	**(MPa)**	***σ1 (Mpa)**	***σ2 (Mpa)**	***σ (Mpa)**	****σ1 (Mpa)**	****σ2 (Mpa)**	****σ (Mpa)**
50	23.00	11.00	19.92	5	25.00	12.50	21.65	8.00	12.00	7.97
100	46.50	22.00	40.29	10	50.00	25.00	43.30	7.00	12.00	6.96
150	70.00	35.00	60.62	15	75.00	37.50	64.95	6.67	6.67	6.67
200	95.00	48.00	82.27	20	100.00	50.00	86.60	5.00	4.00	5.00
250	115.00	60.00	99.62	25	125.00	62.50	108.25	8.00	4.00	7.97
300	136.00	72.00	117.85	30	150.00	75.00	129.90	9.33	4.00	9.28
350	163.00	86.00	141.23	35	175.00	87.50	151.55	6.86	1.71	6.81
400	182.00	97.00	157.73	40	200.00	100.00	173.21	9.00	3.00	8.93
450	210.00	110.00	181.93	45	225.00	112.50	194.86	6.67	2.22	6.63
500	230.00	122.00	199.31	50	250.00	125.00	216.51	8.00	2.40	7.94
550	249.00	134.00	215.85	55	275.00	137.50	238.16	9.45	2.55	9.37
600	279.00	146.00	241.71	60	300.00	150.00	259.81	7.00	2.67	6.97
650	302.00	160.00	261.69	65	325.00	162.50	281.46	7.08	1.54	7.02

700	315.00	172.00	273.18	70	350.00	175.00	303.11	10.00	1.71	9.87
750	341.25	184.00	295.83	75	375.00	187.50	324.76	9.00	1.87	8.91
800	362.53	196.00	314.31	80	400.00	200.00	346.41	9.37	2.00	9.27
850	386.95	208.00	335.42	85	425.00	212.50	368.06	8.95	2.12	8.87
900	406.96	221.00	352.87	90	450.00	225.00	389.71	9.56	1.78	9.45
950	433.58	234.00	375.89	95	475.00	237.50	411.36	8.72	1.47	8.62
960	439.86	237.00	381.31	96	480.00	240.00	415.69	8.36	1.25	8.27
970	436.60	239.00	378.67	97	485.00	242.50	420.02	9.98	1.44	9.84
980	463.20	243.00	401.30	98	490.00	245.00	424.35	5.47	0.82	5.43
990	479.50	246.00	415.31	99	495.00	247.50	428.68	3.13	0.61	3.12
1000	491.20	249.00	425.41	100	500.00	250.00	433.01	1.76	0.40	1.76
1010	0.00	0.00	0.00	101	505.00	252.50	437.34	100.00	100.00	100.00

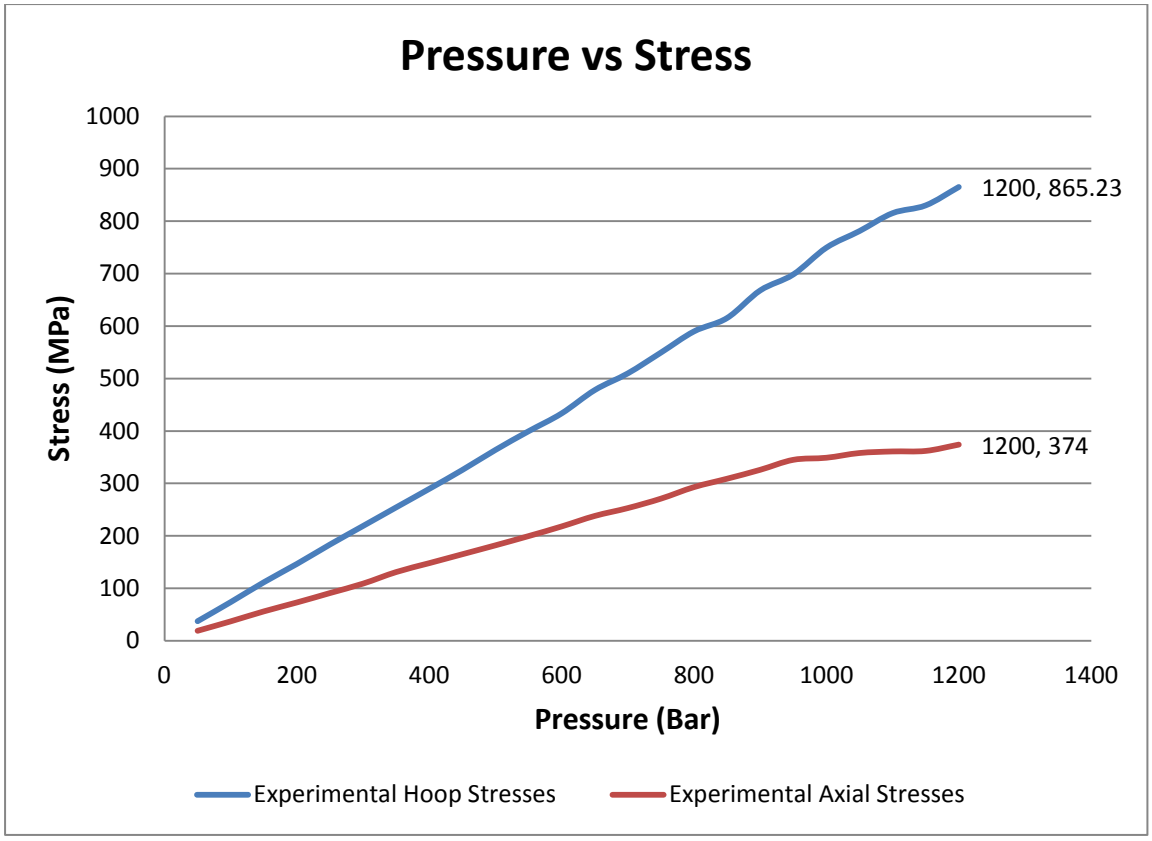

Figure 7.63 [Graph for the experimental Hoop Stresses experimental Axial Stresses]

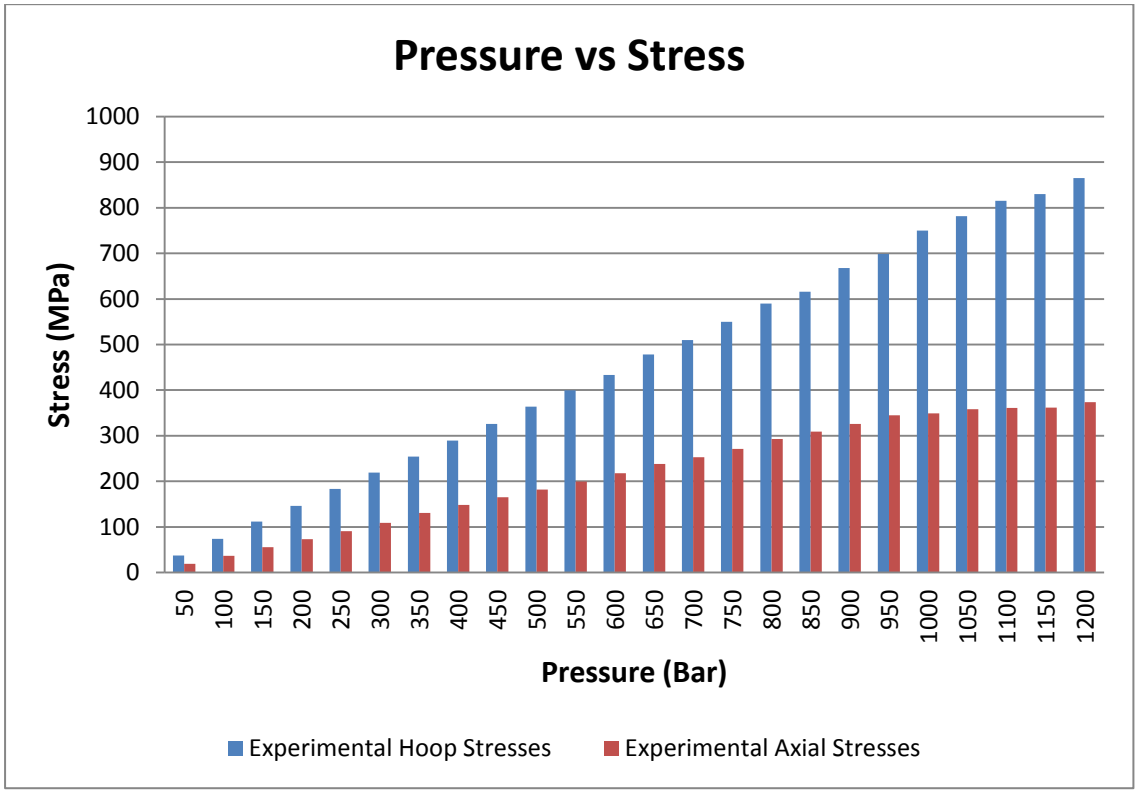

Figure 7.64 [Difference between experimental Hoop & experimental Axial stresses]

7.22.2 1.5mm Tube

In this experiment a 1.5mm wall thickness tube has been taken with one side blocked and pump pressure has been applied with the difference of 5MPa (i.e. 50, 100, 150, 200 . . . .etc) and finally up to the bursting pressure. A digitalized data of principle stresses i.e. σ_1 hoop stresses, σ_2 longitudinal stresses has been received from strain gauges which are tabulated in Table 7.16. Von-misses Stress also calculated by the conventional method. Theoretical Value of σ_1 hoop stresses, σ_2 longitudinal stresses with von-Misses also calculated which is shown in table 7.16. As clearly from table 7.16 we have seen that σ_2 longitudinal stresses is almost half of the σ_1 hoop stresses at their respective pressure reading. Also we have seen that by increasing the pressure the σ_1 hoop stresses, σ_2 longitudinal stresses also increase and when it reaches at a certain pressure when there are no significant changes in σ_1 hoop stresses and σ_2 longitudinal stresses with respect to increase in pressure. The graph pressure vs stresses shown in figure 7.65 also explained this phenomenon.

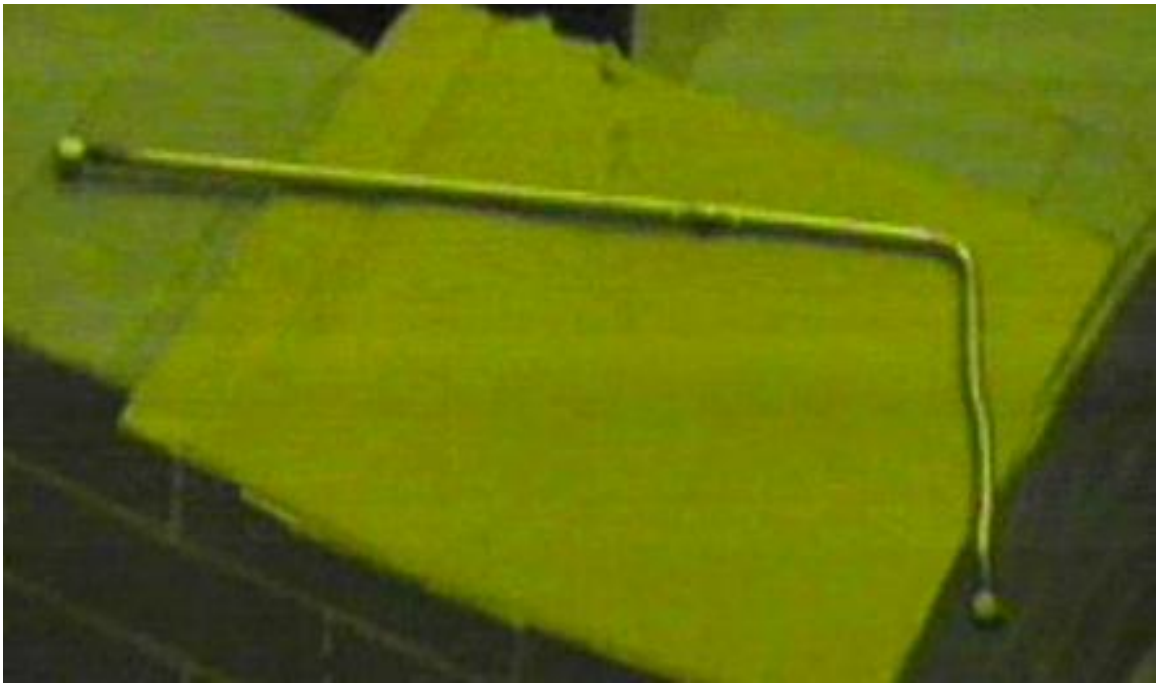

Table 7.16 [Experimental & Theoretical Principle Stresses along with Von Misses and Percent Error]

Ref. Test Report No.: RD(029)/HPTD/09			**Inner Dia**	**Thickness**			**Test Component ID: SP-02 (Straight Pipe)**			
			9.00	**1.50**						
Point	1		Point	2			**Straight Pipe, Length 940mm**			
P	**Experimental Value (E)**			**P**	**Theoretical Value (T)**			**Percent Error**		
	Principle Stress		Von Misses Stress		Principle Stress		Von Misses Stress	Principle Stress		Von Misses Stress
(BAR)	**σ1 (Mpa)**	**σ2 (Mpa)**	**σ (Mpa)**	**(MPa)**	***σ1 (Mpa)**	***σ2 (Mpa)**	***σ (Mpa)**	****σ1 (Mpa)**	****σ2 (Mpa)**	****σ (Mpa)**
50	31.25	11.00	27.46	5	33.75	16.88	29.23	7.41	34.81	6.07
100	62.85	22.00	55.24	10	67.50	33.75	58.46	6.89	34.81	5.50
150	91.85	35.00	80.29	15	101.25	50.63	87.69	9.28	30.86	8.43
200	124.20	48.00	108.48	20	135.00	67.50	116.91	8.00	28.89	7.21
250	155.34	60.00	135.68	25	168.75	84.38	146.14	7.95	28.89	7.16
300	183.60	72.00	160.23	30	202.50	101.25	175.37	9.33	28.89	8.63
350	215.39	86.00	187.79	35	236.25	118.13	204.60	8.83	27.20	8.22
400	251.20	97.00	219.42	40	270.00	135.00	233.83	6.96	28.15	6.16
450	278.30	110.00	242.77	45	303.75	151.88	263.06	8.38	27.57	7.71
500	306.30	122.00	267.09	50	337.50	168.75	292.28	9.24	27.70	8.62
550	334.25	134.00	291.36	55	371.25	185.63	321.51	9.97	27.81	9.38
600	368.90	146.00	321.78	60	405.00	202.50	350.74	8.91	27.90	8.26

650	401.25	160.00	349.86	65	438.75	219.38	379.97	8.55	27.07	7.92
700	435.23	172.00	379.67	70	472.50	236.25	409.20	7.89	27.20	7.22
750	471.25	184.00	411.37	75	506.25	253.13	438.43	6.91	27.31	6.17
800	491.50	196.00	428.55	80	540.00	270.00	467.65	8.98	27.41	8.36
850	515.50	196.00	450.69	85	573.75	286.88	496.88	10.15	31.68	9.30
900	541.90	196.00	475.25	90	607.50	303.75	526.11	10.80	35.47	9.67
950	584.50	196.00	515.26	95	641.25	320.63	555.34	8.85	38.87	7.22
1000	599.00	196.00	528.97	100	675.00	337.50	584.57	11.26	41.93	9.51
1050	625.00	196.00	553.66	105	708.75	354.38	613.80	11.82	44.69	9.80
1100	671.59	243.00	588.97	110	742.50	371.25	643.02	9.55	34.55	8.41
1140	0.00	0.00	0.00	114	769.50	384.75	666.41	100.00	100.00	100.00

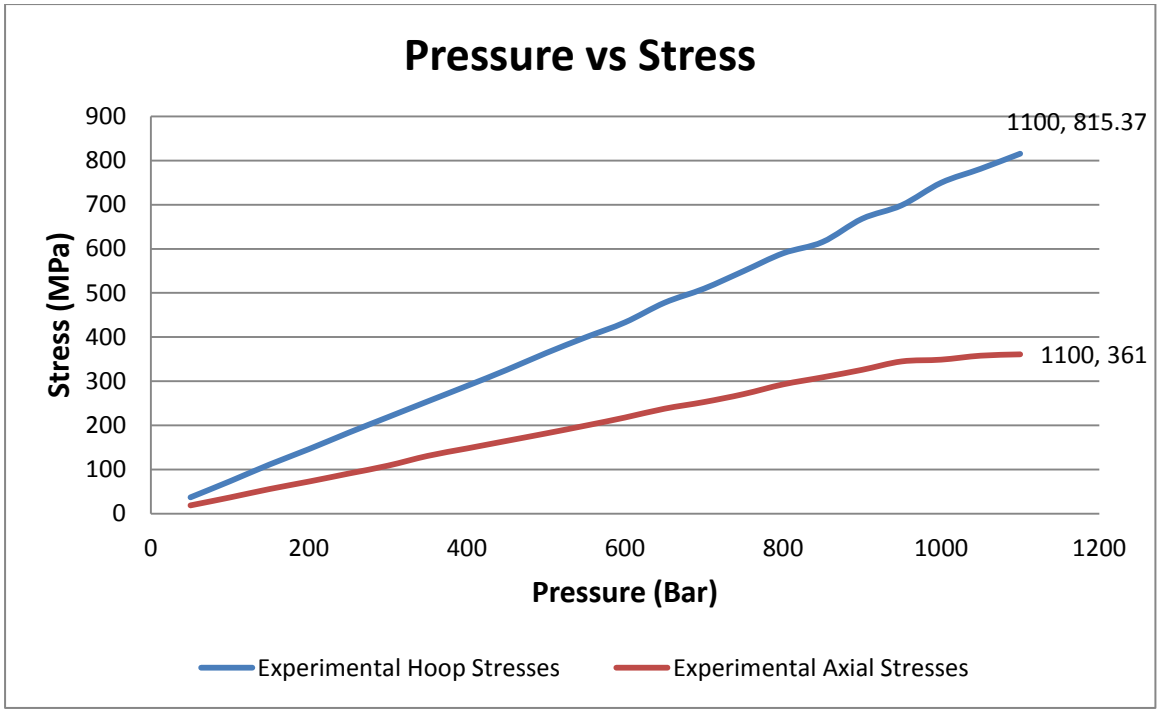

Figure 7.65 [Graph for Experimental Hoop & Axial Stresses]

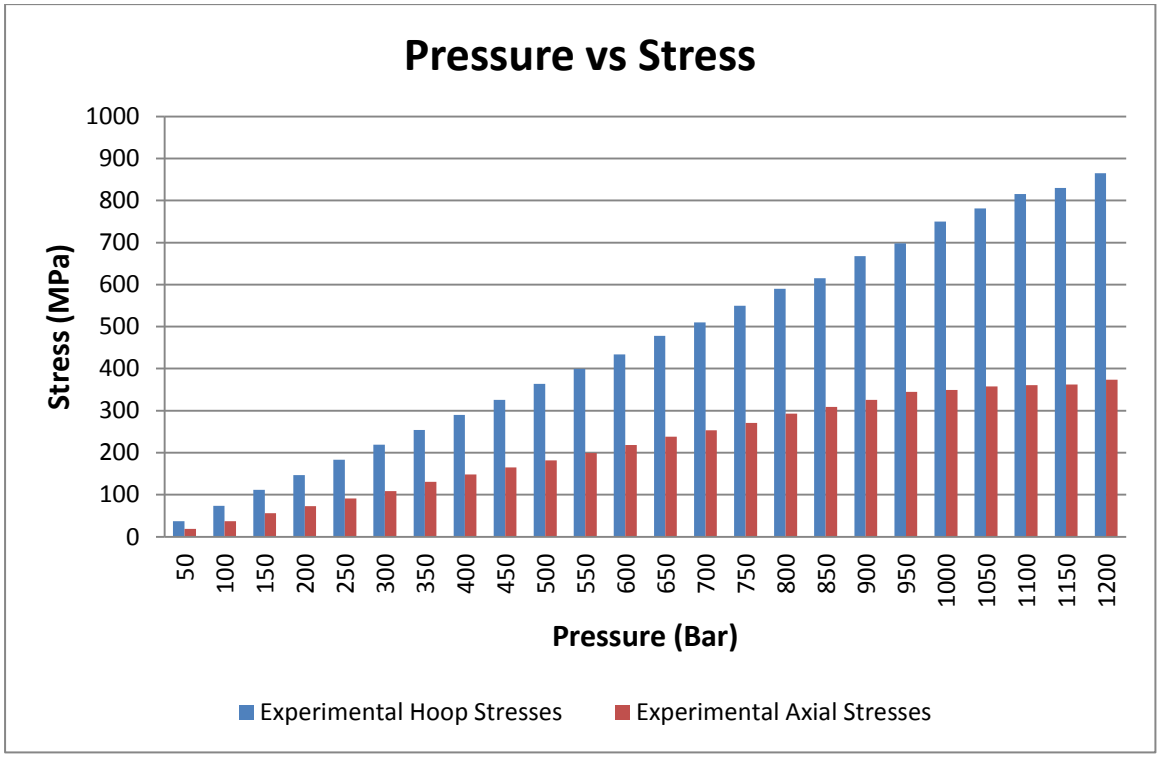

Figure 7.66 [Relation between Experimental Hoop Axial Stresses]

7.22.3 2mm Tub

In this experiment a 2mm wall thickness tube has been taken with one side blocked and pump pressure has been applied with the difference of 5MPa (i.e. 50, 100, 150, 200 . . . .etc) and finally up to the bursting pressure. A digitalized data of principle stresses i.e. σ_1 hoop stresses, σ_2 longitudinal stresses has been received from strain gauges which are tabulated in Table 7.17. Von-misses Stress also calculated by the conventional method. Theoretical Value of σ_1 hoop stresses, σ_2 longitudinal stresses with von-Misses also calculated which is shown in table 7.17. As clearly from table 7.17 it is seen that σ_2 longitudinal stresses is almost half of the σ_1 hoop stresses at their respective pressure reading. Also it is seen that by increasing the pressure the σ_1 hoop stresses, σ_2 longitudinal stresses also increase and when it reaches at a certain pressure when there are no significant changes in σ_1 hoop stresses and σ_2 longitudinal stresses with respect to increase in pressure. The graph pressure vs stresses shown in figure 7.67 also explained this.

Table 7.17 [Experimental Theoretical Principle Stresses Along with Von Misses and Percent Errors]

Ref. Test Report No.: RD(029)/HPTD/09			**Inner Dia**	**Thickness**	**Test Component ID: SP-02 (Straight Pipe)**
			8.00	**2.00**	
Point	1	Point	2		**Straight Pipe, Length 940mm**

P	**Experimental Value (E)**			**P**	**Theoretical Value (T)**			**Percent Error**		
	Principle Stress		Von Misses Stress		Principle Stress		Von Misses Stress	Principle Stress		Von Misses Stress
(BAR)	**σ1 (Mpa)**	**σ2 (Mpa)**	**σ (Mpa)**	**(MPa)**	***σ1 (Mpa)**	***σ2 (Mpa)**	***σ (Mpa)**	****σ1 (Mpa)**	****σ2 (Mpa)**	****σ (Mpa)**
50	37.25	19.00	32.26	5	40.00	20.00	34.64	6.88	5.00	6.87
100	73.69	37.00	63.82	10	80.00	40.00	69.28	7.89	7.50	7.89
150	111.50	56.00	96.56	15	120.00	60.00	103.92	7.08	6.67	7.08
200	146.50	73.00	126.87	20	160.00	80.00	138.56	8.44	8.75	8.44
250	183.50	91.00	158.92	25	200.00	100.00	173.21	8.25	9.00	8.25
300	218.90	109.00	189.57	30	240.00	120.00	207.85	8.79	9.17	8.79
350	254.36	131.00	220.32	35	280.00	140.00	242.49	9.16	6.43	9.14
400	289.60	148.00	250.82	40	320.00	160.00	277.13	9.50	7.50	9.49
450	325.69	165.00	282.06	45	360.00	180.00	311.77	9.53	8.33	9.53
500	363.90	182.00	315.15	50	400.00	200.00	346.41	9.03	9.00	9.02

550	399.50	199.60	345.98	55	440.00	220.00	381.05	9.20	9.27	9.20
600	433.50	218.00	375.42	60	480.00	240.00	415.69	9.69	9.17	9.69
650	478.00	238.00	413.96	65	520.00	260.00	450.33	8.08	8.46	8.08
700	509.90	253.00	441.59	70	560.00	280.00	484.97	8.95	9.64	8.95
750	549.50	271.00	475.90	75	600.00	300.00	519.62	8.42	9.67	8.41
800	589.90	293.00	510.87	80	640.00	320.00	554.26	7.83	8.44	7.83
850	615.50	309.00	533.04	85	680.00	340.00	588.90	9.49	9.12	9.49
900	668.00	326.00	578.56	90	720.00	360.00	623.54	7.22	9.44	7.21
950	698.50	345.00	604.93	95	760.00	380.00	658.18	8.09	9.21	8.09
1000	749.56	349.00	649.65	100	800.00	400.00	692.82	6.31	12.75	6.23
1050	781.20	358.00	677.32	105	840.00	420.00	727.46	7.00	14.76	6.89
1100	815.37	361.00	707.67	110	880.00	440.00	762.10	7.34	17.95	7.14
1150	830.20	362.00	720.93	115	920.00	460.00	796.74	9.76	21.30	9.52
1200	865.23	374.00	751.60	120	960.00	480.00	831.38	9.87	22.08	9.60
1250	899.50	374.00	782.66	125	1000.00	500.00	866.03	10.05	25.20	9.63
1300	934.27	374.00	814.44	130	1040.00	520.00	900.67	10.17	28.08	9.57
1350	965.50	374.00	843.19	135	1080.00	540.00	935.31	10.60	30.74	9.85
1400	999.00	374.00	874.21	140	1120.00	560.00	969.95	10.80	33.21	9.87
1450	1036.52	374.00	909.17	145	1160.00	580.00	1004.59	10.64	35.52	9.50
1500	1069.83	374.00	940.37	150	1200.00	600.00	1039.23	10.85	37.67	9.51
1550	1102.35	374.00	970.96	155	1240.00	620.00	1073.87	11.10	39.68	9.58

1600	1135.36	374.00	1002.14	160	1280.00	640.00	1108.51	11.30	41.56	9.60
1650	1172.35	374.00	1037.22	165	1320.00	660.00	1143.15	11.19	43.33	9.27
1700	1198.36	374.00	1061.96	170	1360.00	680.00	1177.79	11.89	45.00	9.83
1750	1242.35	374.00	1103.93	175	1400.00	700.00	1212.44	11.26	46.57	8.95
1800	1282.30	374.00	1142.19	180	1440.00	720.00	1247.08	10.95	48.06	8.41
1850	1324.35	374.00	1182.57	185	1480.00	740.00	1281.72	10.52	49.46	7.74
1900	1362.35	374.00	1219.16	190	1520.00	760.00	1316.36	10.37	50.79	7.38
1950	1389.63	374.00	1245.48	195	1560.00	780.00	1351.00	10.92	52.05	7.81
2000	1405.60	374.00	1260.91	200	1600.00	800.00	1385.64	12.15	53.25	9.00
2050	1459.60	374.00	1313.17	205	1640.00	820.00	1420.28	11.00	54.39	7.54
2100	1486.90	374.00	1339.64	210	1680.00	840.00	1454.92	11.49	55.48	7.92
2150	1517.36	374.00	1369.22	215	1720.00	860.00	1489.56	11.78	56.51	8.08
2200	1652.36	374.00	1500.73	220	1760.00	880.00	1524.20	6.12	57.50	1.54
2250	1702.92	374.00	1550.14	225	1800.00	900.00	1558.85	5.39	58.44	0.56
2300	0.00	0.00	0.00	230	1840.00	920.00	1593.49	100.00	100.00	100.00

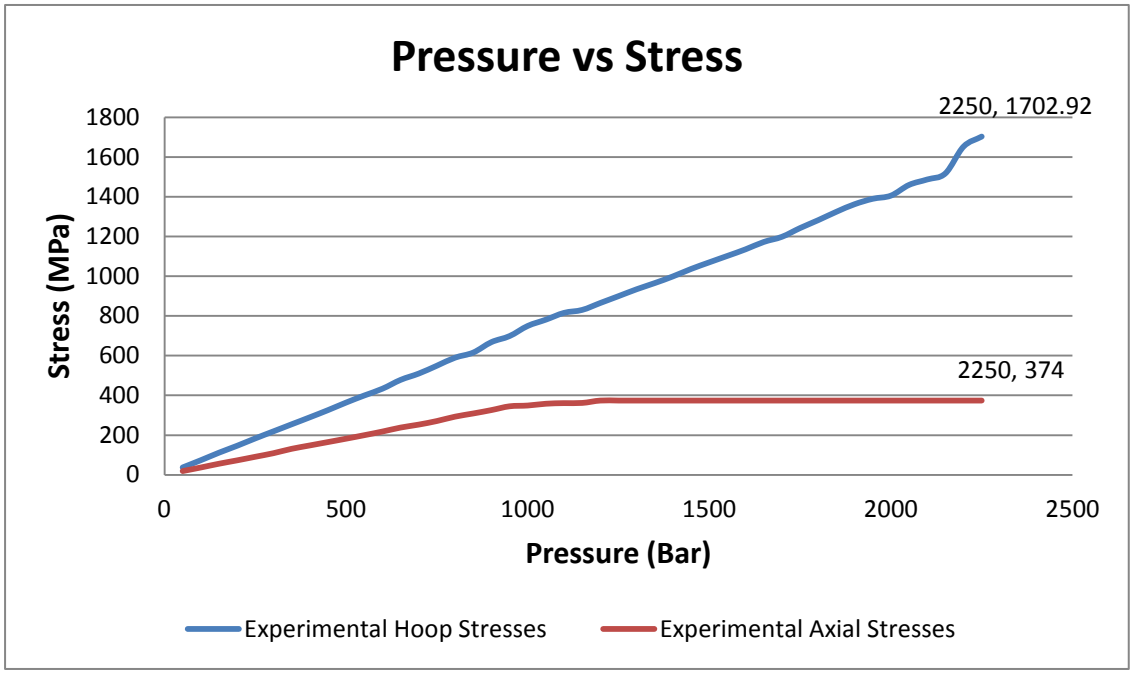

Figure 7.67 [Graph for the experimental Hoop & Axial stresses]

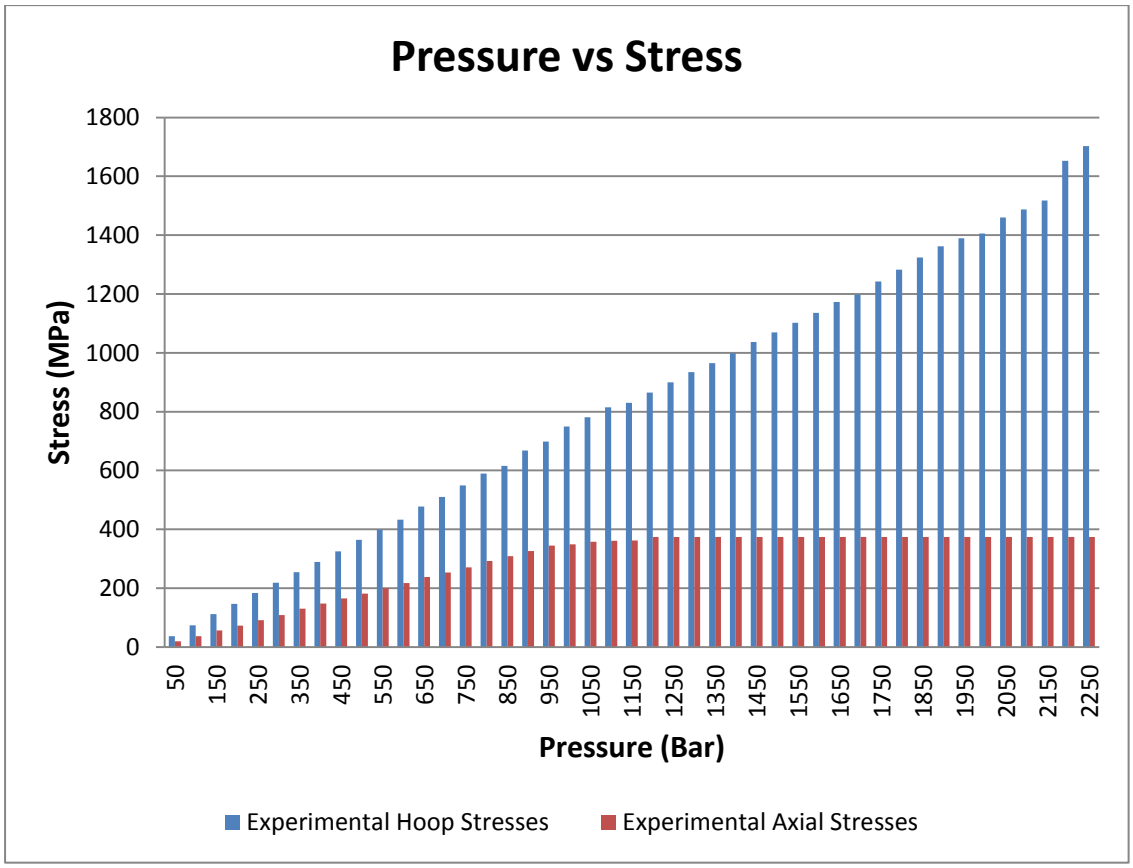

Figure 7.68 [Relation between Experimental Hoop and Axial Stresses]

7.23 Summarizing the Bursting of tubes

Table 7.18

S no	Thickness	Bursting pressure					
		Straight		L shaped		U shaped	
		Theoretical Yield strength	Exper.	Theoretical	Exper.	Theoretical	Exper.
1	1 mm						
2	1.5 mm						
3	2 mm						

Note: All pipes outer diameter = 12 mm

7.24 Optimization of clamps

The commonly used tube in the hydraulic system under study is the Thickness (t) =1.5mm straight tube. Although other thicknesses (1mm and 2mm) and shapes (L and U Shapes) of tubes are also used but this experiment only optimizes the number of clamps for the most commonly used tubes. Currently the system has clamps placed at 0.25 m distance recommended on the basis of experience. In this study the distance would optimized for which the displacement is minimum and the number of clamps are also minimized.

Displacement data for t=1.5 mm, straight tube with equally spaced clamps along a 4 m tube is as follows:

7.24.1 No clamp

7.24.1.1 Effective distance between clamps = 4m

Table 7.20 [Pressure in bars, Forward & Reversed displacement in mm]

Pressure (BARS)	Forward	Reverse
0	0	0
20	0.5	2
40	1.5	5
60	1.59	7.46
80	1.79	10
100	2.11	13
120	2.96	17.2
140	3	19.6
160	3.85	24
180	4.91	26
200	5.81	29.21

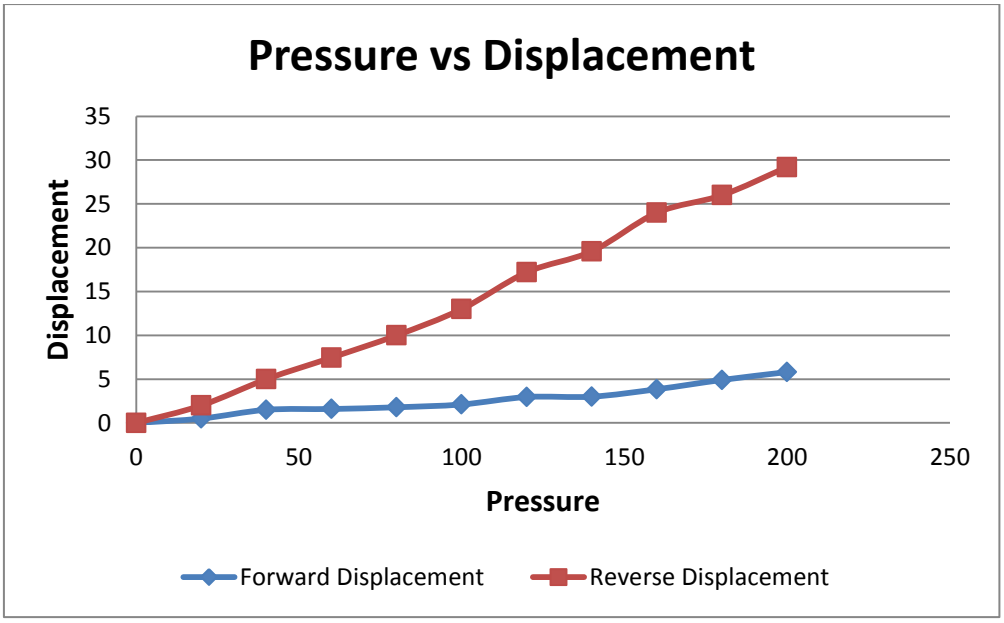

Figure 7.69 [Graph for the Forward & Reversed displacement]

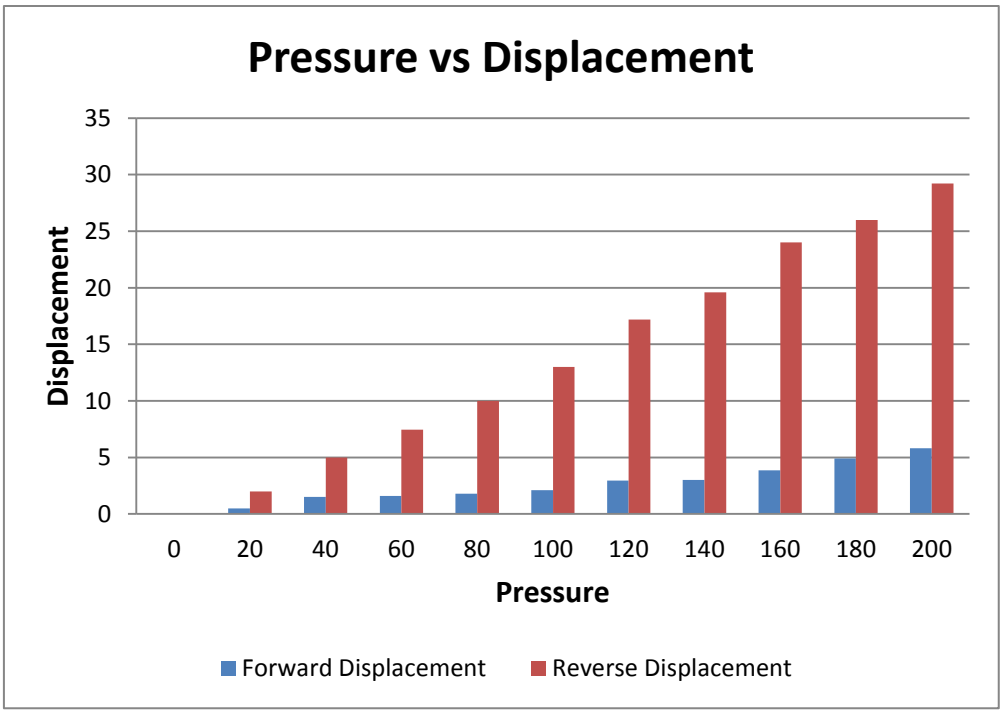

Figure 7.70 [Relation between Forward & Reversed displacement]

7.24.2 02 Clamps

7.24.2.1 Effective distance between clamps = 1.3m

The axial displacement suggests the use of a clamp over a length of 1.3m. However, we need to investigate if the inter clamp distance is small enough to keep the flexural deflection in control. If the flexural deflection is not controlled over this inter clamp distance we may need to use further clamps to control the flexural deflection.

The flexural deflection under 2 clamps is given below:

Table 7.21 [Pressure in bars, Forward & Reversed displacement in mm]

Pressure (BARS)	Forward (mm)	Reverse (mm)
0	0	0
20	0.1	0.95
40	0.16	1.19
60	0.21	1.64
80	0.39	1.97
100	0.48	2.21
120	0.75	2.78
140	0.97	3.11
160	1.06	3.65
180	1.24	4.02
200	1.5	4.5

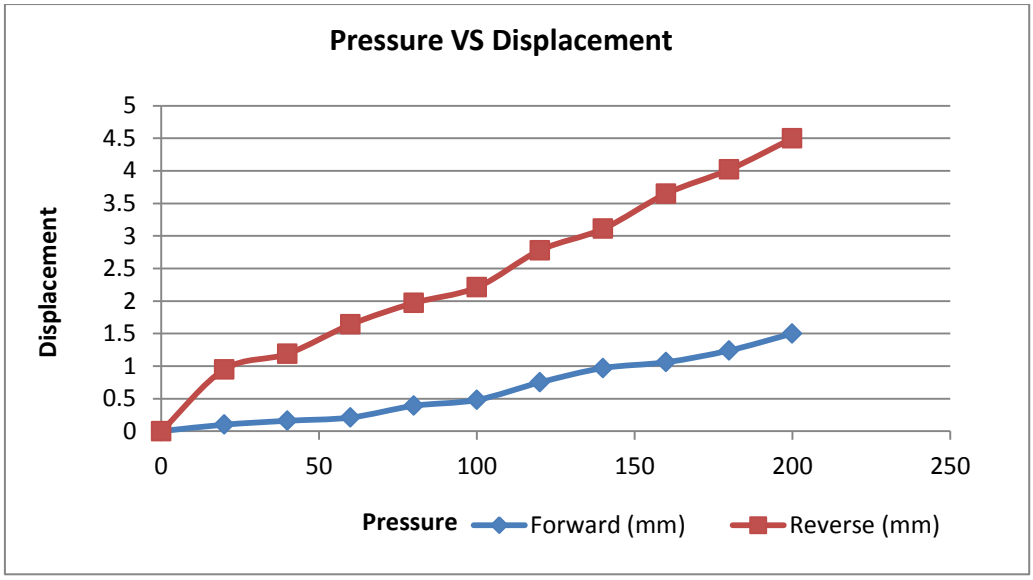

Figure 7.71 [Graph for the Forward & Reversed displacement]

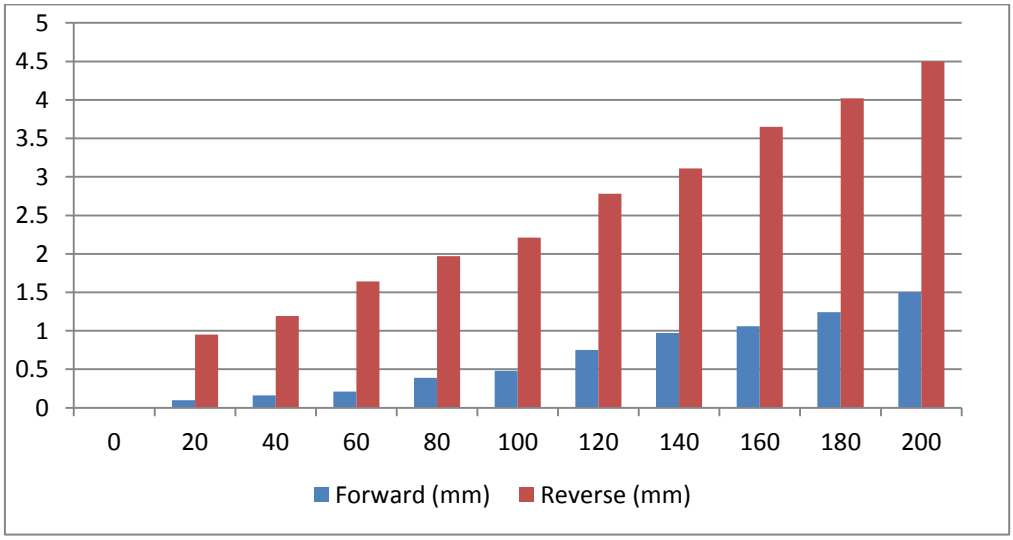

Figure 7.72 [Relation between Forward & Reversed displacement]

7.24.3 04 clamp

7.24.3.1 Effective distance between clamps = 0.8m

The axial displacement suggests the use of a clamp over a length of 0.8m. However, we need to investigate if the inter clamp distance is small enough to keep the flexural deflection in control. If the flexural deflection is not controlled over this inter clamp distance we may need to use further clamps to control the flexural deflection.

The flexural deflection under 4 clamps is given below:

Table 7.22 [Pressure in bars, Forward Reversed displacement in mm]

Pressure (BARS)	Forward (mm)	Reverse (mm)
0	0	0
20	0.07	0.43
40	0.12	0.94
60	0.18	1.15
80	0.27	1.27
100	0.32	1.34
120	0.48	1.42
140	0.54	1.59
160	0.68	1.72
180	0.81	1.87
200	0.94	2

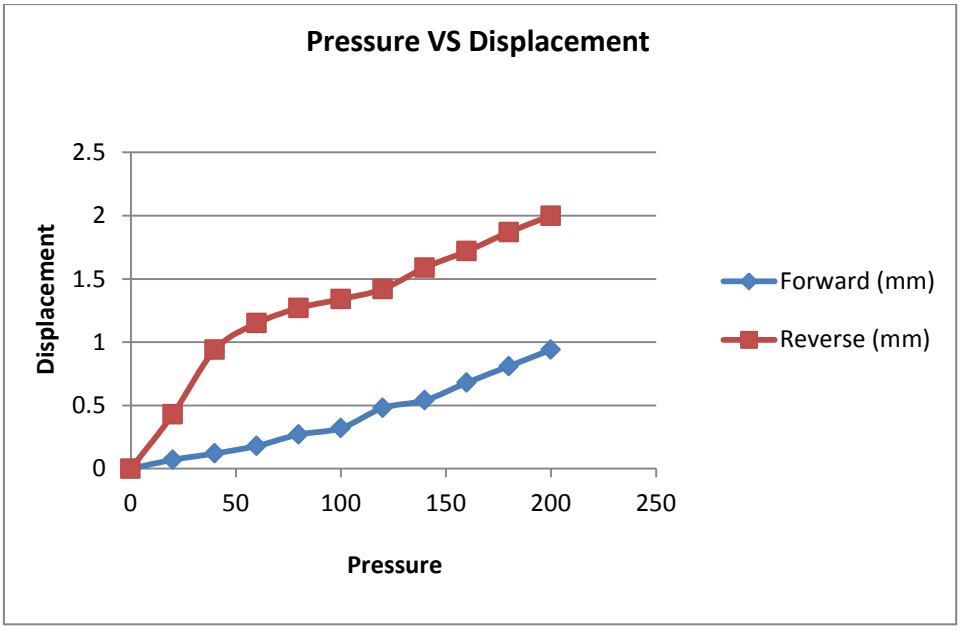

Figure 7.73 [Graph for the Forward & Reversed displacement]

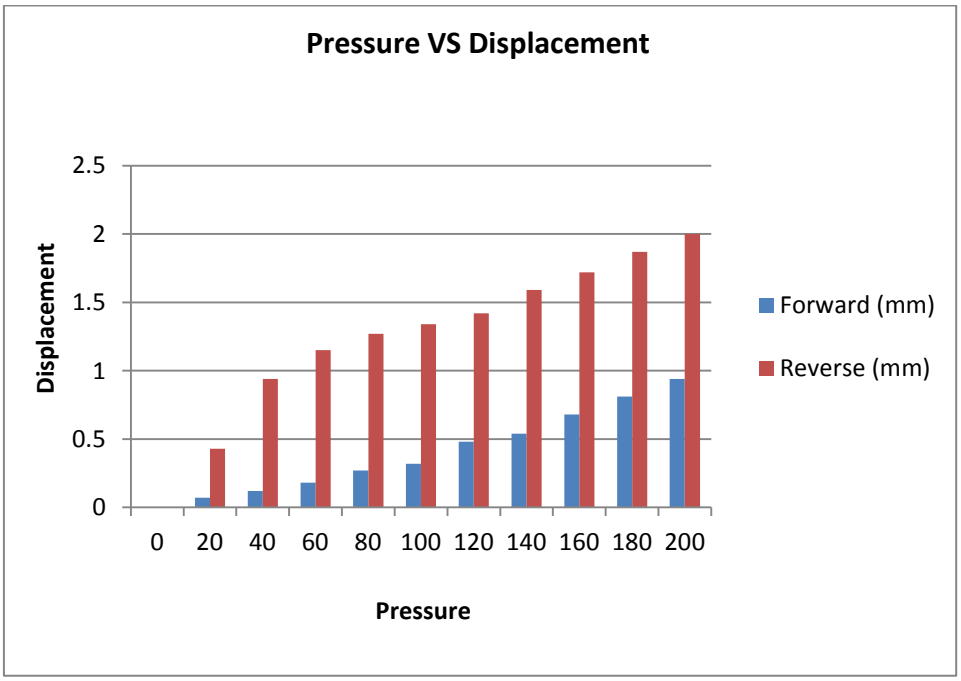

Figure 7.74 [Relation between Forward & Reversed displacement]

7.24.4 05 clamp

7.24.4.1 Effective distance between clamps = 0.67m

The axial displacement suggests the use of a clamp over a length of 0.67m. However it, is needed to investigate if the inter clamp distance is small enough to keep the flexural deflection in control. If the flexural deflection is not controlled over this inter clamp distance it may be needed to use further clamps to control the flexural deflection.

The flexural deflection under 5 clamps is given below:

Table 7.23 [Pressure in bars, Forward & Reversed displacement in mm]

Pressure (BARS)	Forward (mm)	Reverse (mm)
0	0	0
20	0.025	0.05
40	0.045	0.18
60	0.05	0.24
80	0.065	0.32
100	0.071	0.39
120	0.075	0.46
140	0.08	0.61
160	0.09	0.73
180	0.11	0.86
200	0.12	0.92

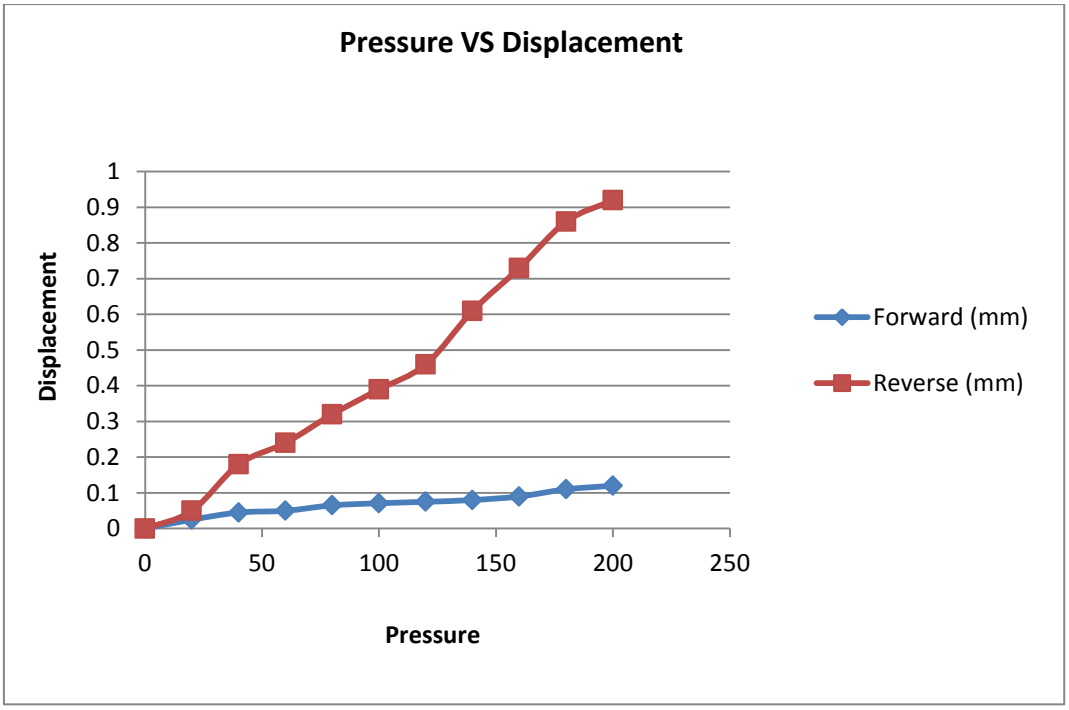

Figure 7.75 [Graph for the Forward & Reversed displacement]

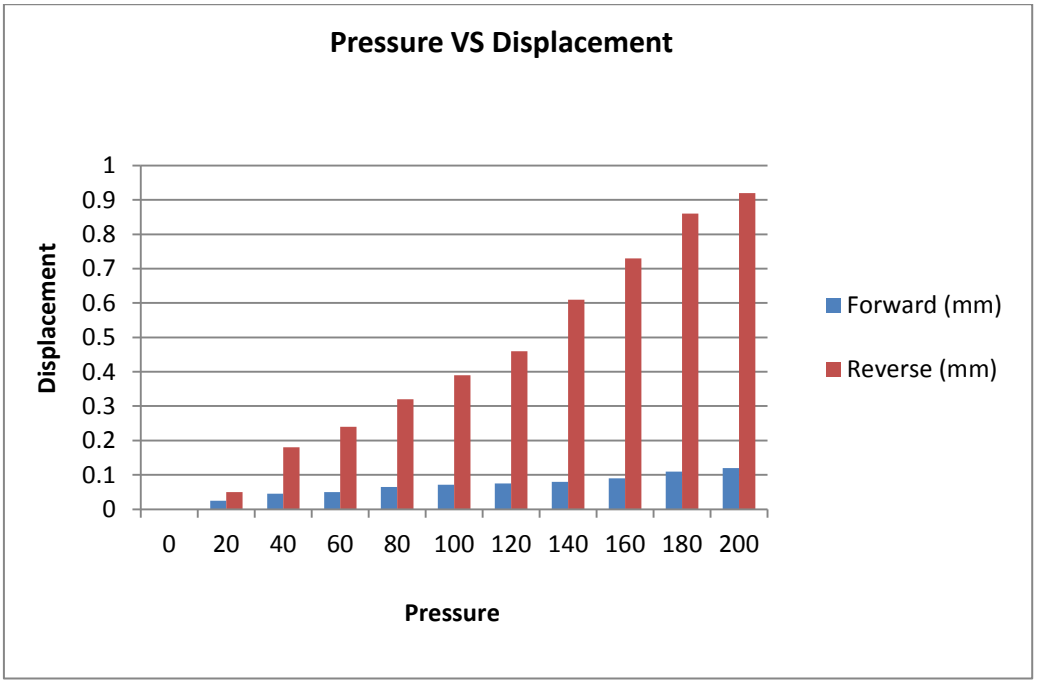

Figure 7.76 [Relation between Forward & Reversed displacement]

7.25 Comparison

The comparison between 4 clamps and 5 clamps is shown in figure 7.77 and figure 7.78.

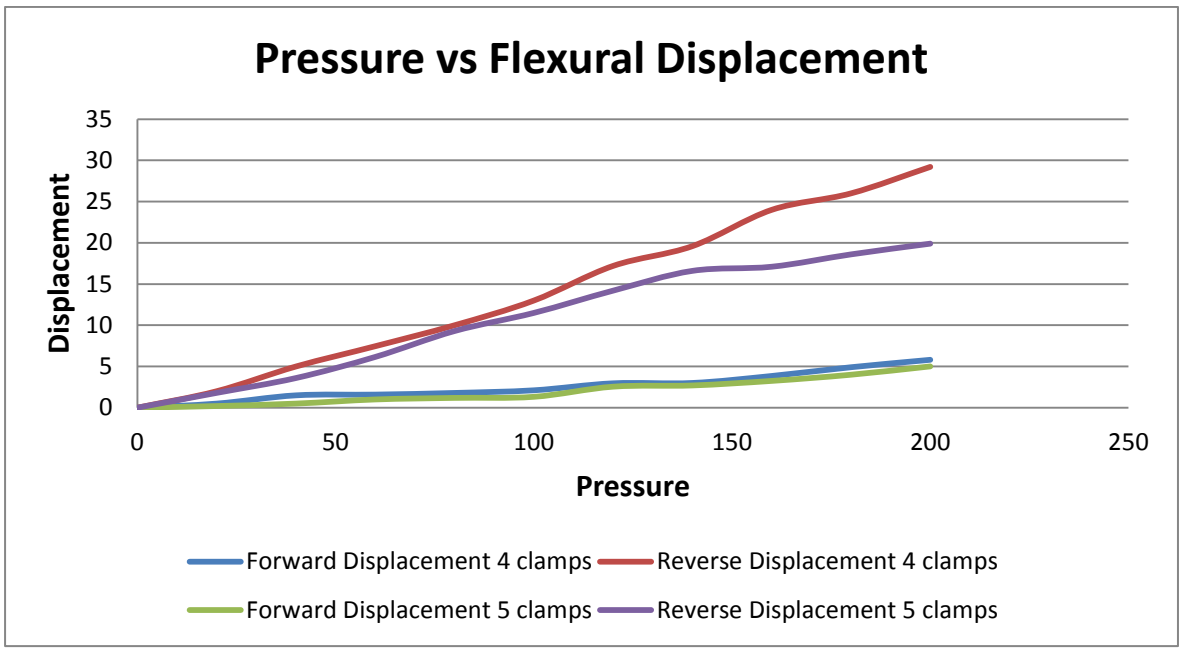

Figure 7.77 [Comparison graph for Forward & Reversed displacement in case of 4 and 5 Clamps]

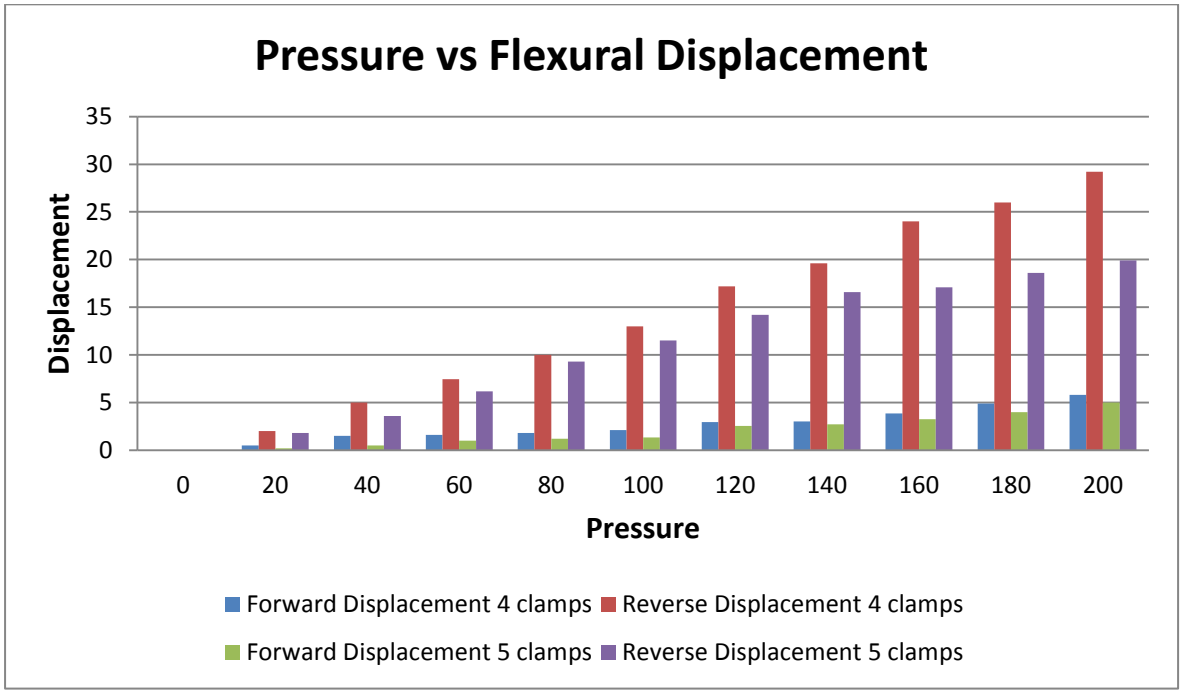

Figure 7.78 [Relation between the Forward 7 Reversed displacement in case of 4 & 5 clamps]

7.26 Discussion

Currently the clamps are used at 0.25m distance in the existing system. Whereas the results show that the clamps could be placed slightly farther away at a distance of 0.67m. The distance between the clamps could be more than doubled thus the number of clamps mounted on the hydraulic system could be halved. This would reduce the number of clamps used on the system and thus reduced the weight and cost of the hydraulic system as well.

Chapter # 8

8 CONCLUSIONS

8.1 Conclusions

In this research project Fluid Power System and Fluid Structure Interaction (FSI) with oil hammering phenomena have been studied.

A brief study regarding the fluid power system has been presented. The fluid structure terminology has been explained broadly with respect to the water and oil hammering phenomenon. A brief literature review has also been studied with the context regarding the oil hammering, water hammering, structural dynamics, fluid excitation and Fluid Structure Interaction.

A problem is formulated in the light of literature review with different shapes of pipes.

A mathematical model is presented to explain the FSI phenomena in a piping network of a mobile crane based on Oil Hydraulic System.

The mathematical behavior of Partial differential equation is explained on the bases of Eigen Value Method. Discretization and Discretization procedure has been studied Mac Cormack's techniques is applied in order to solve the partial differential equation and finally the stability analysis on the bases of Von Neumann criterion is presented.

Experimentation is carried out with the most available equipments and the digitalize data has been tabulated and compared the data with the result obtained from the mathematical model and percent difference calculated.

Experimentation for the bursting of pipes has been carried out in order to achieve the optimistic thickness of the pipe for the existing system.

The axial To and Fro movement of hydraulic pipes after the application of different amplitude pressure has been studied. A number of clamps putted in order to minimize the to and fro motion of hydraulic pipes.

An optimistic number of clamps achieved after applying the clamps in a specific length of pipe.

Chapter # 9

9 RECOMMENDATIONS

9.1 Introduction

This section presents the recommendation based upon the conclusions drawn from the experimentation conducted earlier.

9.2 Recommendations

As a humble student I present my recommendation as follows:

- The whole circuitry of the said system should be analyzed by the oil hammering phenomenon.
- A bond graph can be drawn for the whole circuitry of hydraulic control system.
- Verification of FSI due to oil hammering for the said system through Ansys CFX.
- Jerk control of opening of Multi stage jack through servo based valve.

Chapter # 10

10 REFERENCES

Aga J, Karterud T.J**.** & Nielsen T.K. 1980 *Testing of transient flow and column separation in crude oil pipelines,* Proc. of the 3rd Int. Conf. on Pressure Surges, BHRA, Canterbury, UK, March 1980, pp. 113-126. [2.2]

Allievi L. 1903 *General theory of perturbed flow of water in pressure conduits*. (French translation by Allievi himself, in Revue de M&anique, Paris, 1904; German translation by R. Dubs andV. Bataillard, Berlin: Springer, 1909) [2.1]

Allievi L. 1913. *The theory of water hammer*. (in Italian). (French translation by D. Gad en, 1921, Paris: Dunod; English translation by E.E. Halmos, New York: ASME, 1925, Rome: Riccardo Garoni) [2.1]

Anderson J.D. 1995 *Computational fluid dynamics the basics with applicstion*

Anderson A., Sandoval-Pena R. & Arfaie M. 199 la *Column separation behaviour modes in a simple test rig*. Proc. of the Int. Meeting on Hydraulic Transients with Water Column Separation, 9th Round Table of the IAHR Group, Valencia, Spain, September 1991, pp. 33-50. [2.2,6.1]

Anderson A. & Arfaie M. 1991b *Variable water hammer wavespeed in column separation.*Proc. of the Int. Meeting on Hydraulic Transients with Water Column Separation, 9th Round Table of the IAHR Group, Valencia, Spain, September 1991, pp. 183-199. [2.2]

Anderson J.D, Dale A,John C.et.al 1984, *Computational fluid mechanics & Heat transfer.* Mac Graw Hill, New York.

Anes, W.F: 1965 *Nonlinear partial differential equation in engineering* . New York

Angus R.W. 1935 *Simple graphical solution for pressure rise in pipes and discharge lines.* Journal of the Engineering Institute of Canada, Vol. 18, No. 2, pp. 72-81, 264-273. [2.2]

Angus R.W. 1937a *Water hammer in pipes, including those supplied by centrifugal pumps:graphical treatment.* Proc. of the Institution of Mechanical Engineers, Vol. 136, pp. 245-331. Also: Bulletin No. 152, University of Toronto, Canada, 1938. [2.2]

Angus R.W. 1937b Air chambers and valves in relation to water hammer. Trans, of the ASME, Vol. 59, pp. 661-668. [2.2]

A.S. Tijsseling., **A.E.Vardy** 2005 *Fluid- structure interaction and transient cavitation tests in a T-piece pipe*, Journal of Fluids and Structures 20 (2005) 753-762]

A.S.Tijsseling, Martin F.Lambert, Angus R. Simpso 26 November 2007

A.S Tijsseling,2 January 2007 *Water hammer with fluid –structure in interaction in thick-walled Pipes* Computers and Structures 85 (2007) 844-851]

A.S Tijsseling 2 January 2007 *Water hammer with fluid –structure in interaction in Thick-walled pipes.*

Arris S. Tijsseling Alan E. Vardy *Twenty years of FSI experiments in Dundee University of Dundee,* Civil Engineering Division, *Dundee* DDI 4HN, UK

Anthony Esposit. 2003, *Fluid Power with application*: 6th edition. (2003, Sec 1.1, P 1-2)

Aberrant, A.R. Simpson, A.S. Tijsseling 4 August 2005 *water hammer with column separation*: A historical review .journal of Fluid and Structures 22 (2006) 135-171

A.S Tijsseling 24 November 1995 *Fluid –Structure interaction in liquid-filled Pipe Systems:* A review Journal of Fluid and Structure (1996) 10,109-146

Arati Nanda Pati 1 March 2007 *Fluid-structure interaction for a pressure driven flow* [Mathematical and Computer Modeling 47 (2008) 1-26]

Baltzer R.A. 1967 *Column separation accompanying liquid transients in pipes.* ASME Journal of Basic Engineering, Series D, Vol. 89, No. 4, pp. 837-846. [2.2]

Barbero G. & Ciaponi C. 1991 *Experimental validation of a discrete free gas model for 85numerical simulation of hydraulic transients with cavitation*. Proc. of the Int. Meeting on Hydraulic Transients with Water Column Separation, 9th Round Table of the IAHR

Bergeron L, 1935 (*Study on the steady-state variations in water-filled conduits. General graphical solution.*) Revue generale de 1'Hydraulique, Vol. 1, No. 1, pp. 12-25 (in French).

Bergeron L. 1939 Discussion of "*Experiments and calculations on the resurge phase of water hammer"* by J.N. LeConte and discussion of "*Air chambers for discharge lines' by L. Allievi.* Trans, of the ASME, Vol. 61, pp. 441-445. [2.2]p, Valencia, Spain, September 1991, pp. 51-69.

Billings A.W.K., Dodkin O.K., Knapp F. & Santos A. 1933 *High head penstock design*. ASME Water Hammer Symposium, Chicago, USA, pp. 29-61. [2,2]

Blade R.J., Lewis W. & Goodykoontz J.H. 1962 *Study of a sinusoidal perturbed flow in a line including a 90 degrees elbow with flexible supports. National* Aeronautics & Space Administradon, Technical Note D-1216. [23.4, 2.3.5, 3.3.2]

Budny D.D. 1988 *The influence of structural damping on the internal fluid pressure during a fluid transient pipe flow*. Dissertation, Michigan State University, Dep. of Civil Engineering, East Lansing, USA. [2.3.5, 3.1.1, 3.1.2, 4.11]

Budny D.D., Wiggert D.C. & Hatfield F.J. 1989 *Energy dissipation in the axialty-coupled model for transient flow*. Proc. of the 6th Int. Conf. on Pressure Surges, BHRA, Cambridge, UK, October 1989, pp. 15-26. [2.3.5]

Budny D.D., Hatfield F.J. & Wiggert D.C. 1990 *An experimental study on the influence of structural damping on internal fluid pressure during a transient flow*. ASME Journal of Pressure Vessel Technology, Vol. 112, No. 3, pp. 284-290. (2.3.5]

Budny D.D., Wiggert D.C. & Hatfield F.J. 1991 *The influence of structural damping on internal pressure during a transient flow*. ASME Journal of Fluids Engineering, Vol. 113, No. 3, pp. 424-429. [2.3.5]

Biirmann W. 1974a DruckstGfie in koaxialen Rohrsystemen. (*Water hammer in coaxial pipe systems.)* Dissertation, Universitat Karlsruhe, Karlsruhe, Germany: O. Berenz (in German).

Biirmann W, 1974b DruckstOfte in koaxialen Rohrsystemen. (*Water hammer in coaxial pipe systems.*) 3R international, Vol. 13, No. 3, pp. 155-163 (in German).

Biirmann W. 1975 *Water hammer in coaxial pipe systems*. ASCE Journal of the Hydraulics Division, Vol. 101, No. HY6, pp. 699-715. [2.3.5, 3.1.2]

Biirmann W., Janson H. & Thielen H. 1979 (*Water hammer theory for non-axisymmetrically deformed pipes.*) Universitat Karlsruhe, Institut fur Hydromechanik, Bericht Nr. 614, May 1979, Karlsruhe, Germany (in German). [2.3.5]

Burmann W. 1979 (*Water hammer measurements in coaxial pipes.*) 3R international, Vol. 18, No. 10, pp. 624-628 (in German). [2.3.5]

Burmann W. 1980a *(Longitudinal motion of pipelines laid in the open due to water hammer.)* 3R international, Vol. 19, No. 1/2, pp. 84-91 (in German). [2,3.5, 3.1.2]

Burmann W. 1980b (*Longitudinal motion of coaxial pipes due to water hammer,)* 3R international, Vol. 19, No. 7/8, pp.398-404 (in German). [2.3,5]

Burmann W., Janson H. & Thielen H. 1980 (*Pipeline motion due to water hammer*.) Universitat Karlsruhe, Institut fur Hydromechanik, Bericht Nr. 618, JDecember 1980, Karlsruhe, Germany (in German). [2.3.5]

Bird R.B., Stewart W.E & Lightfoot E.N. 1960 *Transport phenomena*. New York: John Wiley & Sons. [3.1.2].

Budny D.D., 1988 *The influence of structural damping on the internal fluid pressure during a fluid transient pipe flow*. Dissertation, Michigan State University, Dep. Of civil Engineering, East Lansing, USA. [2.3.5, 3.1.1, 3.1.2, 4.11]

Budny D.D., Wiggert D.C & Hatfield F.J. 1989 *Energy dissipation in the axially-coupled model for transient flow*. Proc. of the 6th Int. Conf. on Pressure Surges, BHRA, Cambridge, UK, October 1989, pp. 15-26. [2.3.5]

Budny D.D., Hatfield F.J. & Wiggert D.C 1990 *An experimental study on the influence of structural damping on internal fluid pressure during a transient flow*. ASME Journal of Pressure Vessel Technology, Vol. 112, No. 3, pp. 284-290. [2.3.5]

Budny D.D., Wiggert D.C. & Hatfield F.J. 1991 *The influence of structural damping on internal pressure during a transient flow*. AMSE Journal of Fluid Engineering, Vol. 113, No. 3, pp. 424-429. [2.3.5]

Carmona R., Sanchez A. & Sanchez J.L. 1987 *Experimental relation between the highest transient pressure and the severity of water column separation*, Proc. of the 8th Int. Round Table on Hydraulic Transients in Power Stations, IAHR, Madeira, Portugal, PaperD2. [2.2,6.1]

C.W. Park S.J. Lee 27 November 2003 *Effect of free-end corner shape on flow structure around a finite cylinder* Journal of Fluid and Structures 19 (2004) 141-158]

Davidson L.C. & Smith J.E. 1969 *Liquid-structure coupling in curved pipes.* The Shock and Vibration Bulletin, No. 40, Part 4, pp. 197-207. [2.3.4, 2.3.5, 2.3.6]

Davidson L.C. & Samsury D.R. 1972 *Liquid-structure coupling in curved pipes* - II. The Shock and Vibration Bulletin, No. 42, Part 1, pp. 123-136. [2.3.4, 2.3.5]

Davies R.M., Trevena D.H., Rees N.J.M. & Lewis G.M. 1956 *The tensile strength of liquids under dynamic stressing.* Proc. of the 1955 NPL (National Physical Laboratory) Symp. on Cavitation in Hydrodynamics, Paper 5, 20 pp. [6.3.1]

DeArmond R.P. & Rouleau W.T. 1972 *Wave propagation in viscous, compressible liquids confined in elastic tubes*. ASME Journal of Basic Engineering, Vol. 94, December, pp.811-817. [2.3.2]

D'Souza A.F. & Oldenburger R. 1964 *Dynamic response of fluid lines*. ASME Journal of Basic Engineering, Vol. 86, No. 3, pp. 589-598. [2.3.4, 2.3.5, 3.1.2, 3.3.2} D'Souza A.F. & Oldenburger R. 1964 Dynamic response of fluid lines. ASME Journal of Basic Engineering, Vol. 86, No. 3, pp. 589-598. [2.3.4, 2.3.5, 3.1.2, 3.3.2]

David C Wiggert Arris S Tijsseling 5 September 2001*Fluid Transints and fluid structure interaction in flexible liquid filled piping*

D. Adechy, R.I Issa 03 April *2003Modeling of annular flow through pipes and T-junctions* Computers & Fluid 33 (2004) 289-313

Damodar Maity Sriman Kumar Bhattacharyya 17 July 2002 *A parametic study on fluid-structure interaction problems*] [Journal of Sound and Vibration 263 (2003) 917-935]

Ellis J. 1980 *A study of pipe-liquid interaction following pump-trip and check-valve closure in a pumping station*. Proc. of the 3rd Int. Conf. on Pressure Surges, BHRA, Canterbury, UK, March 1980, pp. 203-220. [2.3.4, 2.3.5]

Evans E.P. & Sage P.V. 1983 *Surge analysis of a large gravity pipeline*. Proc. of the

4th Int. Conf. on Pressure Surges, BHRA, Bath, UK, September 1983, pp. 447-460 [2.2]

Fletcher, C.A 1988 *Computational Technique for Fluid Dynamics Vol I: Funamental & General Technique;* spring veriag , Berlin 1988

Frizell J.P. 1898 *Pressures resulting from changes of velocity of water in pipes*. Trans, of the ASCE, Vol. 39, Paper No. 819, June 1898, pp. M8. [2.1]

Golia U.M. & Greco M. 1990 *Cavitation during water-hammer: quick closure of a downstream valve.* Proc.of the 3rd Int. Conf. on Hydraulic Engineering Software, Hydrosoft '90, Boston, USA, April 1990, pp. 121-129. [2.2]

Gottlieb L., Lamses G. & Vasehus J. 1981 T*ransient cavitation in pipelines - Laboratory tests and numerical calculations*. Proc. of the 5th Int. Symp. on Water Column Separation, IAHR, Obernach, September 1981, pp. 487-508. [2.2]

Graze H.R. & Horlacher H.B. 1983 *Pressure transients following the collapse of vapour cavities.* Proc. of the 6th Int. Symp. on Hydraulic Transients in Power Stations, IAHR, Gloucester, UK,September 1983. [2.2, 5.3.1]

Gromeka I.S. 1883 (*On the velocity of propagation of wave-like motion of fluids in elastic tubes.*) Mathematical Section of the Scientific Society of the Imperial University of Kazan, Kazan, Russia, May 1883, pp. 1-19 (in Russian). [2.3.1,4.2.3]

Halliwell A.R. 1963 *Velocity of a water-hammer wave in an elastic pipe*. ASCE Journal of the Hydraulics Division, Vol. 89, No. HY4, pp. 1-21. (Discussed by V.L. Streeter in No. HY6, pp. 295-296.) [2.3.3]

Herrmann G. & Mirsky I. 1956 *Three-dimensional and shell-theory analysis of axialfy symmetric motions of cilinders*. ASME Journal of Applied Mechanics, Vol. 23, No. 4, pp. 563-568. [2.3.2,2.3.5]

Hirsch,Charles, 1988 *Numerical Computational of internal & external flows*, Vol: I Fundamental of numerical discretization. Willey, New York

Hogg T.H. & Traill J.J. 1926 *Discussion of "Speed changes of hydraulic turbines for sudden changes of load"* by E.B.Stronger & S.L. Kerr. Trans, of the ASME, Vol. 48, pp. 252-257. [2.2]

Herrmann G. & Mirsky I. 1956 *Three-dimensional and shell-theory analysis of axially symmetric motions of cilinders*. ASME Journal of Applied Mechanics, Vol. 23, No. 4, pp. 563-568. [2.3.2, 2.3.5]

Jones S.E. & Wood D.J. 1972 *The effect of axial boundary motion on pressure surge generation.* ASME Journal of Basic Engineering, Vol. 94, No. 2, pp. 441-446. [2.3.4]

Joukowsky N. 189. (*On the hydraulic hammer in water supply pipes.)* the American Water Works Association, Vol. 24, pp. 341-424, 1904) [p. ii, 2.1, 2.3.1]

J. Izquierdo and P.L. Iglessias June 2001 *Mathematical Modeling of Hydraulic Transients in Simple*

Systems] [Mathematical and Computer Modeling 35 (2002) 801-812]

King W.W. & Frederick D. 1968 *Transient elastic waves in a fluid-filled cylinder*. ASCE Journal of the Sanitary Engineering Mechanics Division, Vol. 94, No. EMS, pp. 1215-1230. [2.3.2]

Knapp F. 1937a Discussion of "*Water hammer in pipes, including those supplied by centrifugal pumps:* graphical treatment" by R.W. Angus. Proc. of the Institution of Mechanical Engineers, Vol. 136, pp. 304-309. [2.2]

Knapp F. 1937b *Operation of emergency shutoff valves in pipelines*. Trans, of the ASME,Vol. 59, pp. 679-682. [2.2]

Knapp F. 1939 Discussion of "*Experiments and calculations on the resurge phase of water hammer"* by J.N. Le Conte. Trans, of the ASME, Vol. 61, pp. 440-441. [2.2]

Knapp R.T., Daily J.W. & Hammitt F.G. 1970 Captation, New York: McGraw-Hill. [2.2]

Korteweg D.J. 1878 (*On the velocity of propagation of sound in elastic pipes*.) New Series, Vol. 5,No. 12, pp. 525-542 (in German). [2.1, 2.3.1, 2.3.3]

Kot C.A. & Youngdahl C.K. 1978a *Transient captation effects in fluid piping systems*. Nuclear Engineering and Design, Vol. 45, January, pp. 93-100. [2.2, 6.3.1]

Kot C.A. & Youngdahl C.K. 1978b *The analysis of fluid transients in piping systems, including the effects of captation*. Fluid Transients and Acoustics in the Power Industry, Winter Annual Meeting of the ASME, San Francisco, USA, December 1978, pp. 45-52. [2.2,6.3.1]

Krause N., Goldsmith W. & Sackman J.L. 1977 *Transients in tubes containing liquids.* Int. Journal of Mechanical Sciences, Vol. 19, No. 1, pp. 53-68. [2.3.5, 6.2.1]

Kuiken G.D.C. 1984a *Wave propagation in initially stressed orthotropic compliant tubescontaining a compressible, viscous and heat-conducting fluid*. Dissertation, Delft University of Technology, Dep. of Mechanical Engineering, WTHD 165, September 1984, Delft, The Netherlands. [1.2.3, 2.3.2]

Kuiken G.D.C. 1986 *Amplifications of pressure fluctuations due to fluid-structure interaction.* Proc. of Seminar on Fluid-Structure Interaction, Delft Hydraulics, Delft, The Netherlands, October 1986, Report J0113. [1.2.3, 3.1.2]

Kuiken G.D.C. 1988 *Amplification of pressure fluctuations due to fluid-structure interaction*.Journal of Fluids and Structures, Vol. 2, pp. 425-435. [1.2.3, 2.3.5, 4.2.3]

Kulak R.F. 1985 *Three-dimensional fluid-structure coupling in transient analysis.* Computers & Structures, Vol. 21, No. 3, pp. 529-542. [2.3.6]

Kolsky H. 1953 *Stress waves in solids. Oxford*: Clarendon Press. (Reprint in 1963, New York: Dover Publications.) [3.1.2, 4.3, 4.3.3, 4.4]

Kuiken G.D.C. 1984a *Wave propagation in initially stressed orthotropic complaint tubes containing a compressible, viscous and heat-conducting fluid*. Dissertation, Delft University of Technology, Dep. Of Mechanical Engineering, WTHD 165, September 1984, Delft, The Netherlands. [1.2.3, 2.3.2]

Kuiken G.D.C. 1984b *Approximate dispersion equations for thin walled liquid-filled tubes*.Applied Scientific Research, Vol. 41, pp. 37-53 [1.2.3, 2.3.2]

Kuiken G.D.C. 1984c *Propagation in fluid lines.* Applied Scientific Research, Vol. 41, pp. 69-91. [1.2.3, 2.3.2]

Kuiken G.D.C. 1984d *Wave propagation in a thin-walled liquid-filled initially stressed tube.* Journal of Fluid Mechanics, Vol. 141, pp. 289-308. [1.2.3, 2.3.2]

Kuiken G.D.C. 1986 *Amplifications of Pressure fluctuations due to fluid-structure interaction*. Proc. Of seminar on Fluid-Structure Interaction, Delft Hydraulics, Delft, The Netherlands, October 1986, Report J0113. [1.2.3, 3.1.2]

Kuiken G.D.C. 1988 *Amplification of pressure fluctuations due to fluid-structure interaction.* Journal of Fluids and Structures, Vol. 2, pp. 425-435. [1.2.3, 2.3.5, 4.2.3]

Lamb H. 1898 *On the velocity of sound in a tube, as affected by the elasticity of the walls.* Memoirs of the Manchester Literary and Philosophical Society, Manchester, UK, Vol. 42,No. 9, pp. 1-16. [2.3.1, 2.3.2, 4.2.3]

Langevin A. 1928 In (Reference in [Bergeron 1939, 1950]) (in French). [2.2]

LeConte J.N. 1937 *Experiments and calculations on the resurge phase of water hammer*. Trans, of the ASME, Vol. 59, Paper HYD-59-12, pp. 691-694, [2.2]

Lesmez M.W., Wiggert D.C. & Hatfield F.J. 1990 *Modal analysis of vibrations in liquid-filled piping-systems.* ASME Journal of Fluids Engineering, Vol. 112, No. 3, pp.311-318. [2.3.5]

Lin T.C. & Morgan G.W. 1956a *A study of axisymmetric vibrations of cylindrical shells as affected by rotatory inertia and transverse shear*. ASME Journal of Applied Mechanics,Vol. 23, June, pp. 255-261. [2.3.2, 3.1.2]

Lin T.C. & Morgan G.W. 1956b *Wave propagation through fluid contained in a cylindrical,elastic shell.* Journal of the Acoustical Society of America, Vol. 28, No. 6, pp. 1165-1176. [2.3.2,3.1.2,4.2.3]

Lin T.C. & Morgan G.W. 1956a *A study of axisymmetric vibrations of cylindrical shells as affected by rotatory inertia and transverse shear*. ASME Journal of Applied Mechanics, Vol. 23, June, pp. 255-261. [2.3.2, 3.1.2]

Lin T.C. & Morgan G.W. 1956b *Wave propagation through fluid contained in a cylindrical, elastic shell.* Journal of the Acoustical Society of America, Vol. 28, No. 6, pp. 1165-1176. [2.3.2, 3.1.2, 4.2.3]

L. Zhang, A.S Tijesling and A.E. Vardy 04 January 1999 *FSI Analysis of Liquid –Filled Pipes* Journal of sound vibration (1999) 224(1), 69-99

Martin C.S. 1973 *Status of fluid transients in Western Europe and the United Kingdom*. Report on laboratory visits by Freeman scholar. ASME Journal of Fluids Engineering,Vol. 95, No. 2, pp. 301-318. [2.1]

Martin C.S. 1983 *Experimental investigation of column separation with rapid closure of downstream valve.* Proc. of the 4th Int. Conf. on Pressure Surges, BHRA, Bath, UK, September 1983, pp. 77-88. [2.2,4.10.4,6.1]

Menabrea L.-F, 1858. (*Note on effects of water shock in conduits*. Vol. 47,July-December, pp. 221-224[2.1] Menabrea L.-F. 1862 (Note on effects of water shock in conduits.) Vol. 1, pp. 269-275 [2.1]

Mac Cormack R.W 1969 *The impact of viscosity in Hypervelocity Impact cratering*, AIAA paper 69-354

Mirsky I. & Herrmann G. 1958 *Axialty symmetric motions of thick cylindrical shells*. ASME Journal of Applied Mechanics, Vol. 25, March, pp. 97-102. [2.3.2]

Moens A.I. 1878 Die Pulscurve. (*The pulsation*.) [2.3.1]

Mase G.E. 1970 *Continuum mechanics*. New York: McGraw-Hill. [3.1.2]

M.P. Paidoussis 4 March 2005 *Some unresolved issues in fluid structure interactions* Journal of Fluids and Structure 20 (2005) 871-890

Marco Anghileri, Luigi-M.L.,Castelletti13 December *2003Fluid-structure interaction of water filled tanks during the impact with the ground*] [International journal of Impact Engineering 31 (2005) 235-254]

Maichael P. Paidoussis 1998 *Fluid-structure Interactions: Slender Structure and Axial flow.*Vol.1[Journal of fluid and structure (2004 14, 753- 754]

Otwell R.S. 1982 *the effect of elbow translations on pressure transient analysis of piping systems.* ASME - PVP, Vol. 64, Fluid transients and fluid-structure interaction, pp 127-136. [2.3.5]

Otwell R.S. 1984 *The effect of elbow restraint on pressure transients*. Dissertation, Michigan State University, Dep. of Civil and Sanitary Engineering, East Lansing, USA. [2.3,5,4.7.3,4.11]

O.O Bendiksen,G. Seber 19 March 2008 *Fluid- structure interactions with both structural and fluid nonlinearities* Journal of Sound and Vibration 315 (2008) 664-684

Paynter H.M. 1961 *Fluid transients in engineering systems.* Section 20 in Handbook of Fluid Dynamics by V.L. Streeter (Editor), New York: McGraw-Hill. [2.1]

Provoost G.A. 1975 (*Waterhammer measurements on the Biesbosch-Berenplaat pipeline.)* Delft Hydraulics Laboratory, ReportR 1014, November 1975, Delft, The Netherlands [1.2.2]

Provoost G.A. 1976 *Investigation into cavitation in a prototype pipeline caused by water hammer*, Proc. of the 2nd Int. Conf. on Pressure Surges, BHRA, London, UK, September 1976, Paper D2, pp. 13-29. Also: Delft Hydraulics Laboratory, Publication No. 170,November 1976. [1.2,2,2.2,4.5.3]

Provoost G.A. 1978 *Waterslag in PVC-transportleidingen. (Waterhammer in PVC transmission lines*.) Delft Hydraulics Laboratory, Publication No. 196N, April - May 1978, pp. 91-111, Delft, The Netherlands (in Dutch), [1.2.1]

Provoost G.A. & Wylie E.B. 1981 *Discrete gas model to represent distributed free gas in liquids.* Proc, of the 5th Int. Symp. on Water Column Separation, IAHR, Obemach,Germany, September 1981, 8 pp. Also: Delft Hydraulics Laboratory, Publication No. 263, April 1982. [1.2.2, 2.2, 4.5.3]

Rankine WJ.M. 1870 *On the thermodynamic theory of waves of finite longitudinal disturbance,* Trans, of the Royal Society, London, Vol. 160, Paper 15, pp. 277-288.[2.1]

Regetz J.D., Jr. 1960 *An experimental determination of the dynamic response of a long hydraulic line.* National Aeronautics & Space Administration, Technical Note D-576,December 1960. [2.3,4]

Resal H. 1876 (*Note on the small motions of incompressible fluids in an elastic tube*.) Journal Of Pure Mathematics, 3rd series, Vol. 2, pp. 342-344 (in French). [2.3.1]

Rubinow S,I. & Keller J.B. 1978 *Wave propagation in a viscoelastic tube containing a viscous fluid.* Journal of Fluid Mechanics, Vol. 88, Part 1, pp. 181-203. [2,3.2]

Schnyder O. 1929 (*Waterhammer in pump risers.)* Vol. 94, No. 22, pp. 271-273, No. 23, pp. 283-286 [2.1]

Schwarz W. 1978 (*Waterhammer calculations taking into account the radial and longitudinal displacement of the pipe wall*.) Dissertation,, ISSN 0343-1150 (in German). [2.3.3,2.3.5, 3.1.2, 4.2.1]

Sharp B.B. 1977 *A simple model for water column rupture*. Proc. of the 17th 1AHR Congress, Baden-Baden, Germany, Vol. D, pp. 155-160. [2.2]

S**iemens J. 1967** *The phenomenon of Cavitation in a horizontal pipe-line due to a sudden pump-failure*. IAHR Journal of Hydraulic Research, Vol. 5, No. 2, pp. 135-152. Also: Delft Hydraulics Laboratory, Publication No. 53, February 1967. [1.2.2, 2.2]

Simpson A.R. & Wylie E.B. 1985 *Problems encountered in modeling vapor column separation.* Proc. Symp. on Fluid Transients in Fluid-Structure Interaction, ASME Winter Annual Meeting, Miami Beach, Florida, USA, November 1985, pp. 103-107. [2.2,4.5.3]

Simpson A.R. 1986 *Large water hammer pressures due to column separation in sloping pipes.* Dissertation, The University of Michigan, Dep. of Civil Engineering, Ann Arbor,USA. [p. iii, 2.2, 3.1.5, 4.5.3, 4.10.4, 5, 5.1, 5.4, 6.1, 6.4, 7]

Simpson A.R. & Wylie E.B. 1989 *Towards an improved understanding of waterhammer column separation in pipelines.* Civil Engineering Transactions 1989, The Institution of Engineers, Australia, CE31 (3), pp. 113-120. [2.2]

Simpson A.R. & Wylie E.B. 1991 *Large water-hammer pressures for column separation in pipelines.* ASCE Journal of Hydraulic Engineering, Vol. 117, No. 10, pp. 1310-1316. (Discussed by M. Greco, B. Brunone and U.M. Golia in Vol. 119, No. 1, pp. 142-145.)[2.2]

Simpson A.R. & Bergant A. 1991a *Column separation research at the University of Adelaide, South Australia.* Proc. of the Int. Meeting on Hydraulic Transients with Water Column Separation, 9th Round Table of the IAHR Group, Valencia, Spain, September 1991, pp. 253-269. [5.3.1,6.3.1]

Simpson A.R. & Bergant A. 1991b *The accuracy of a pipe column separation numerical model.* Submitted for publication to ASCE Journal of Hydraulic Engineering. [4.5.3]

Skalak R. 1956 An *extension of the theory ofwaierhammer*. Trans, of the ASME, Vol. 78, No. 1, pp. 105-116. [2.3.2, 2.3.5, 3.1.2]

Spillers W.R. 1965 *Wave propagation in a thin cylindrical shell*. ASME Journal of Applied Mechanics, Series E, Vol. 32, No. 2, pp. 346-350. [2.3.2]

Streeter V.L. & Wylie E.B. 1967 *Hydraulic transients*. New York: McGraw-Hill. [2.1, 2.2,3.3.7]

Slreeter V.L. 1983 *Transient cavitating pipe flow*. ASCE Journal of Hydraulic Engineering,Vol. 109, No. HY11, pp. 1408-1423. [2.2, 3.1.5]

Tang S.-C. 1965 *Dynamic response of a tube under moving pressure*. ASCE Journal of the Engineering Mechanics Division, Vol. 91, No. EMS, pp. 97-122. [2.3.2]

Thorley A.R.D. 1969 *Pressure transients in hydraulic pipelines*. ASME Journal of Basic Engineering, Vol. 91, September, pp. 453-461. [2.3.2]

Thorley A.R.D. 1976 *A survey of investigations into pressure surge phenomena*. Research Memorandum ML83, The City University, Dep. of Mechanical Engineering, London,UK, April 1976. [2.1,2.2]

Tijsseling A.S. & Lavooij C.S.W. 1989 *Fluid-structure interaction and column separation in a straight elastic pipe,* Proc. of the 6th Int. Conf. on Pressure Surges, BHRA,Cambridge, UK, October 1989, pp. 27-41. [1.2.4, 4.2.6, 4.10.1, 4.10.4]

Tijsseling A.S. & Lavooij C.S.W. 1990 *Waterhammer with fluid-structure interaction.*Applied Scientific Research, Vol. 47, No. 3, pp. 273-285. [1.1.4, 1.2,3, 4.10.1]

Tijsseling A.S, & Fan D. 1991a *The response of liquid-fined pipes to vapour cavity collapse*.Trans, of SMiRTll, Tokyo, Japan, August 1991, Paper J10/2, pp. 183-188. [1.2.4]

Tijsseling A.S. & Fan D. 1991b *The concentrated cavity model validated by experiments in a closed tube.* Proc. of the Int. Meeting on Hydraulic Transients with Water Column Separation, 9th Round Table of the IAHR Group, Valencia, Spain, September 1991, pp. 145-155, [1.2.4]

Tijsseling A.S. & Fan D. 1992 *Fluid-structure interaction and column separation in a closed pipe.* Proc. of the Second National Mechanics Congress, Kerkrade, The Netherlands,November 1992; Dordrecht, The Netherlands: Kluwer Academic Publishers, [1.2.4,6.3.1]

Timoshenko S.P. 1921 *On the correction for shear of'the differential equation fortransverse vibrations of prismatic bars*. Philosophical Magazine, Vol. 41, Paper 66, pp. 744-746.[3.1,3,4.3]

Timoshenko S.P. 1922 On *the transverse vibrations of bars of uniform cross-section.* Philosophical Magazine, Vol. 43, Paper 10, pp. 125-131. [3.1.3, 4.3]

Valentin R.A., Phillips J.W. & Walker J.S. 1979 *Reflection and transmission of fluid transients at an elbow.* Trans, of SMiRTS, Berlin, Germany, August 1979, Paper B 2/6. [2.3.5] Vardy A.E. 1976 On the use of the method of characteristics for the solution of unsteady flows in networks. Proc. of the 2nd Int. Conf. on Pressure Surges, BHRA, London, UK,September 1976, Paper H2, pp. 15-30, X65-X71. [4.2.6}

Vardy A.E. & Chan L.I. 1983 *Rapidly attenuated water hammer and steel hammer*. Proc.of the 4th Int. Conf. on Pressure Surges, BHRA, Bath, UK, September 1983. pp. 1-12.[4.6.2]

Vardy A.E. & Fan D. 1986 *Water hammer in a closed tube*. Proc. of the 5th Int. Conf.on Pressure Surges, BHRA, Hanover, Germany, September 1986, pp. 123-137. {2.3.5,4.10.1,5.2,5.2.1]

Vardy A.E. & Fan D. 1987 *Constitutive factors in transient internal flows*. Proc. of the NUMETA'87 Conf., Swansea, UK, Vol. 2, Paper T37. [2.3.5]

Vardy A.E. & Alsarraj A.T. 1989 *Method of characteristics analysis of one-dimensional members.* Journal of Sound and Vibration, Vol. 129, No. 3, pp. 477-487. [4,3, 4.7.3]

Vardy A.E. & Fan D. 1989 *Flexural waves in a closed tube*. Proc. of the 6th Int. Conf. on Pressure Surges, BHRA, Cambridge, UK, October 1989, pp. 43-57. [p. iii, 2.3.5, 3.1.3,4.3, 4.10.1, 5, 5.2, 5.4, 6.2, 6.2.1, 6.3.1, 6.4, 7]

Vardy A.E. & Hwang K.-L. 1991 *A characteristics model of transient friction in pipes*.IAHR Journal of Hydraulic Research, Vol. 29, No. 5, pp. 669-684. [3.1.2]

Vardy A.E. & Fan D. 1993 *Measurements of fluid/structure interactions in pipes*, (to be offered for publication) [p. Hi, 2.3.5, 5, 5.2, 5.4, 6.2, 6.2.2, 7]

Walker J.S. & Phillips J.W. 1977 *Pulse propagation in fluid-filled tubes*. ASME Journal of Applied Mechanics, Vol. 44, March, pp. 31-35. [2.3.5]

Wallis G.B. 1969 *One-dimensional two-phase flow*. New York: McGraw-Hill. [2.2, 4.5.3]

Wang J.S. & Locher F.A. 1991 *Verification of modeling water column separation*. Proc. of the Int. Meeting on Hydraulic Transients with Water Column Separation, 9th Round Table of the 1AHR Group, Valencia, Spain, September 1991, pp. 343-354. [2.2]

Weber W. 1866. (*Theory of waves propagating in water or other incompressible liquids contained in elastic pipes*.) Mathematical-Physical Section, Vol. 18, pp. 353-357 (in German). [2.3.1]

Wiggert D.C. & Hatfield F.J. 1983 *Time domain analysis of fluid-structure interaction in multi-degree-of-freedom piping systems*. Proc. of the 4th Im. Conf. on Pressure Surges,BHRA, Bath, UK, September 1983, pp. 175-188. [2.3.5, 3.3.2]

Wiggert D.C., Hatfield F.J. & Otwell R.S. 1983 *Fluid-structure interaction in piping systems.* Proc. DruckstoBberechnung von Rohrleitungssystemen, Hausder Technik, Essen,Germany, December 1983. [2.3.5]

Wiggert D.C., Otwell R.S. & Hatfield F.J. 1985a *The effect of elbow restraint on pressure transients.* ASME Journal of Fluids Engineering, Vol. 107, No. 3, pp. 402-406.(Discussed by R.E. Schwirian and J.S. Walker in Vol. 108, No. l,pp. 121-122.) [2.3.5]

Wiggert D.C., Hatfield F.J. & Stuckenbruck S. 1985b *Analysis of liquid and structuraltransients in piping by the method of characteristics.* ASME-FED, Vol. 30, pp. 97-102.[2.3.5]

Wiggert D.C. 1986 *Coupled transient flow and structural motion in liquid-filled piping systems: a survey.* Proc. of the ASME Pressure Vessels and Piping Conf., Chicago, USA, July 1986, Paper 86-PVP-4. [2.3.5]

Wiggert D.C., Hatfield F.J. & Lesmez M.W. 1986 *Coupled transient flow and structural motion in liquid-filled piping systems.* Proc. of the 5th Int. Conf. on Pressure Surges, BHRA, Hanover, Germany, September 1986, pp. 1-9. [2.3.5, 3.1.3, 4.2.6]

Wiggert D.C., Hatfield FJ. & Stuckenbruck S. 1987a *Analysis of liquid and structural transients by the method of characteristics.* ASME Journal of Fluids Engineering, Vol. 109, No. 2, pp. 161-165. [2.3.5, 3.1.3, 4.1, 4.11, 7]

Wiggert D.C., Lesmez M.L. & Hatfield FJ. 19875 *Modal analysis of vibration in liquid-fllled piping systems.* ASME - FED, Vol. 56, Fluid transients in fluid-structur interaction, pp. 107-113. [2.3,5,3.1.3]

Williams D.J. 1977 *Waterhammer in non-rigid pipes: precursor waves and mechanical damping.* Journal of Mechanical Engineering Science, Institution of Mechanical Engineers,Vol. 19, No. 6, pp. 237-242. [2.3,5]

Wood D.J. 1968 *A study of the response of coupled liquid flow-structural systems subjected to periodic disturbances*. ASME Journal of Basic Engineering, Vol. 90, December, pp.532-540. [2.3.4]

Wood D.J. 1969 *Influence of line motion on waterhammer pressures*, ASCE Journal of the Hydraulics Division, Vol. 95, May, pp. 941-959. [2.3.4]

www.tpub.com

www.truckcranedirectory.com

www.howstuwork.com

www.tml.jp.com

www.phy.isk.edu

www.parker.com

www.resrothbosch .com

Wood F.M. 1970 *History of waterhammer*. Report No. 65, Dep. of Civil Engineering Queen's University at Kingston, Ontario, Canada, April 1970. [2.1]

Wylie E.B. & Streeter V.L. 1978a *Fluid transients*. New York: McGraw-Hill. (Republished with minor corrections by FEB Press, Ann Arbor, Michigan, USA, 1983) [2.1, 2.3.3,3.1.2,4.1]

Wylie E.B. & Streeter V.L. 1978b *Column separation in horizontal pipelines*. Proc. of the Joint Symp. on Design and Operation of Fluid Machinery, IAHR/ASME/ASCE, Colorado State University, Fort Collins, USA, June 1978, Vol. 1, pp. 3-13. [2.2, 3.1.5]

Wen-Bin Shangguan Zhen –Hua Lu] [12 May 20041][*Experimental study and simulation of a hydraulic engine mount with fully coupled fluid-structure interaction finite element analysis model*][Computers and Structures 82 (2004) 1751-1771]

Walker J.S. & Philips J.W. 1977 *Plus propagation in fluid-filled tubes*. ASME Journal of Applie Mechanics, Vol. 44, March, pp. 31-35. [2.3.5]

Young F.R. 1989 Captation. London: McGraw-Hill. [2.2]

Young T, 1808 *Hydraulic investigations, subservient to an intended Cwonian lecture on the motion of the blood*. Philosophical Trans, of the Royal Society, London, Vol. 98, Part 2,Paper 13, pp. 164-186. [2,3.1]

Zhong-Min Wang,[Soon-Keat Tan 02 March 1997 *Vibration and Pressure Fluctuation a Flexible Hydraulic power system on an aircraft]* [NIL]

Chapter # 11

11 APPENDIX

Appendix –A

11.1 Compressibility & Bulk Modulus:

The property by virtue of which fluid undergoes a change in volume under the action of external pressure is known as compressibility.

The compressibility is decrease with the increase in pressure of fluid as the volume modulus increase with the increase of pressure.

The variation in volume of oil or H_2O with variation of pressure, is so small (i.e. at a atmospheric pressure and a temperature of 60^{o}F "*l*" require a pressure of 3120 PSI to compress a unit volume of water (1%) this result is representative of the compressibility of liquid since such a large pressure are required to effect a change in volume, so we conclude that liquid cab be consider as incompressible for practical engineering applications,

However in case of water/oil flowing through pipes when sudden or large change in pressure (e.g. water hammer) tales place, the compressibility cannot be neglected.

"The compressibility in fluid mechanics is considered mainly when the velocity of the flow is high enough reaching % of speed of sound in the medium" [By: R.K. Jain]

Elasticity of the fluid is measured in term of Bulk modulus of elasticity "β" which is defined as "The ratio of compressive stress to volumetric strain."

While the compressibility is the reciprocal of bulk modulus of elasticity

i.e. Compressibility $= \frac{1}{\beta}$

Figure 1

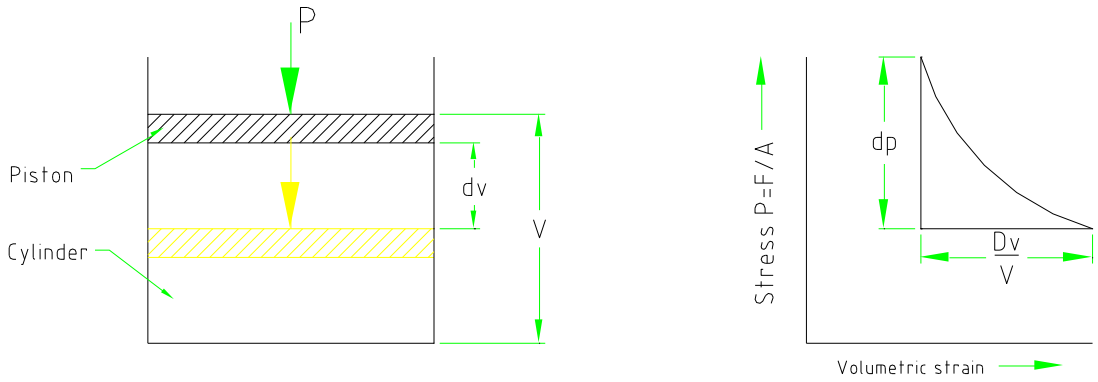

Consider a cylinder filled with a piston as shown in Figure1 (above)

Let

V = volume of the gas enclosed in the cylinder

P = Pressure of gas where volume is V

~ $P = \frac{P}{A}$, where "A" is the area of cross-section of cylinder

Let the pressure is increased to $P + d_p$, the volume of gas decrease from V to $V - d_v$

Thus increase in pressure is $d_p$and decrease in volume is d_v

Volumetric strain = - $\frac{d_v}{V}$

Negative (-) sign shows that decrease in volume with increase of pressure.

Bulk Modulus, $\beta = \frac{Increase\ of\ Pressure}{Volumatirc\ strain}$

$$\beta = \frac{d_p}{-\frac{d_v}{V}}$$

And compressibility $= \frac{1}{\beta}$

Steeping the curve in Figure1 shows us that with increasing pressure the fluids are compressed, it becomes increasingly difficult to compress than further.

In other words we can say that the bulk modulus increase with increasing of pressure.

The following points we have concluded:

1. The Bulk Modulus of elasticity of fluid is not constant, but it increase with increase in pressure. This is so because when a mass of fluid is compressed its molecules become close together and it's resistance to further compression increases i.e. β increases (i.e. the value of β roughly do unable as the pressure is raised from 1 atmospheric to 3500 atmospheric.
2. The Bulk modulus of elasticity β of the fluid is affected by the temperature of the fluid. In this case of liquid with increases of temperature β is decrease. However for gases since pressure and temperature are interrelated i.e. when temperature increases pressure also increases and an increase in temperature result in an increase in the valve of β

As we know that by definition Bulk modulus of elasticity β

$$\beta = \frac{d_p}{-\frac{d_V}{V}} = -V\frac{d_p}{d_V}$$

Where V is the volume of the fluid, while in case of specific volume:

$$\beta = -\vartheta\frac{d_p}{d_v}$$

Where ϑ is specific volume of fluid.

$$\vartheta = \frac{Volume}{mass} = \frac{V}{m} = \frac{1}{\frac{m}{V}} = \frac{1}{\rho}$$

Or $P\vartheta = 1$ or $\frac{d\vartheta}{\vartheta} = -\frac{d_\rho}{d_\rho}$

$$\beta = \rho\frac{d\rho}{dp}$$

Or $$\frac{d\rho_{oil}}{d_p} = \frac{\rho_{oil}}{\beta} \ldots\ldots\ldots\ldots\ldots\ldots\ldots 4$$

As we know that Bulk modulus β is a function of pressure and temperature and as we know that our fluid are incompressible fluid for which $\rho_{oil}$is constant and temperature is assume to be constant so, we can say that if ρ_{oil}, k are constant than

Eq. 4 => $\frac{d\rho_{oil}}{d_p} = Constant$

Or $d\rho_{oil} = d_p$

Eq. 4 $d\rho_{oil} = d\rho_{oil}\frac{dp}{\beta}$ 5

Determining Tube Size for Hydraulic Systems

Proper tube material, type and size for a given application and type of fitting is critical for efficient and trouble free operation of the fluid system. Selection of proper tubing involves choosing the right tube material, and determining the optimum tube size (O.D. and wall thickness).

Proper sizing of the tube for various parts of a hydraulic system results in an optimum combination of efficient and cost effective performance.

A tube that is too small causes high fluid velocity, which has many detrimental effects. In suction lines, it causes cavitation which starves and damages pumps. In pressure lines, it causes high friction losses and turbulence, both resulting in high pressure drops and heat generation. High heat accelerates wear in moving parts and rapid aging of seals and hoses, all resulting in reduced component life. High heat generation also means wasted energy, and hence, low efficiency.

Too large of a tube increases system cost. Thus, optimum tube sizing is very critical. The following is a simple procedure for sizing the tubes.

Step 1: Determine Required Flow Diameter

Use Table A29 to determine recommended flow diameter for the required flow rate and type of line.

The table is based on the following recommended flow velocities:

Pressure lines — 25 ft./sec. or 7.62 meters/sec.
Return lines — 10 ft./sec. or 3.05 meters/sec.
Suction lines — 4 ft./sec. or 1.22 meters/sec.

If you desire to use different velocities than the above, use one of the following formulae to determine the required flow diameter.

$$\text{Tube I.D. (in.)} = 0.64 \sqrt{\frac{\text{Flow in GPM}}{\text{Velocity in ft./sec.}}}$$

OR

$$\text{Tube I.D. (mm)} = 4.61 \sqrt{\frac{\text{Flow in liters per minute}}{\text{Velocity in meters/sec.}}}$$

Step 2: Determine Tube O.D. and Wall Thickness

Using Table A30, determine the tube O.D. and wall thickness combination that satisfies the following two conditions:

A. Has recommended design pressure equal to or higher than maximum operating pressure.
B. Provides tube I.D. equal to or greater than required flow diameter determined earlier.

Design pressure values in Table A30 are based on the severity of service rating "A" (design factor of 4) in Table A26, and temperature derating factor of 1 in Table A27.

If more severe operating conditions are involved, the values in Table A30 should be multiplied by appropriate derating factors from Tables A26 and A27 before determining the tube O.D. and wall thickness combination. Contact the Tube Fittings Division when in doubt.

Allowable design stress levels and formula used to arrive at the design pressure values are given in the following chart.

Material and Type	Allowable Design Stress for Design Factor of 4 at 72 Degrees F
Steel C-1010	12,500 PSI
Stainless Steel 304 & 316	18,800 PSI
Alloy Steel C-4130	18,800 PSI
Copper, K or Y	6,000 PSI
Aluminum 6061-T6	10,500 PSI
Monel, 400	17,500 PSI

Table A24 — Design Stress Values

Design Pressure Formula (LAME'S)

$$P = S\left(\frac{D^2 - d^2}{D^2 + d^2}\right) \text{ where:}$$

D = Outside diameter of tube, in
d = Inside diameter of tube (D-2T), in
P = Recommended design pressure, psi
S = Allowable stress for design factor of 4, psi
T = Tube wall thickness, in

Table A25 — Design Pressure Formula

For thin wall tubes ($D/T \geq 10$) the following formula may be Used: **$P = 2ST/D$**

Severity of Service	Description	Design Factor	Derating Factor
A (Normal)	Moderate mechanical and hydraulic shocks.	4.00	1.00
B (Severe)	Severe hydraulic shocks and mechanical strain.	6.00	0.67
C (Hazardous)	Hazardous application with severe service conditions.	8.00	0.50

Table A26 — Severity of Service Design and Derating Factors

The design factor is generally applied to ultimate strength of material (or burst pressure of tubing) to provide a measure of safety against the unknowns in material and operating conditions. The derating factors listed here should be applied directly to the design pressure values in Table A30 to arrive at maximum recommended working pressures (i.e., multiply values in Table A30 by these derating factors).

Besides severity of service, high operating temperature also reduces allowable working pressure of the tubing. Temperature derating factors for various tube materials are given in Table A27. Where applicable, derating factors for severity of service and temperature should be applied to the design pressure values in Table A30 to arrive at the maximum recommended working pressure.

Example:
Combined derating factor for 316SS tubing for B (severe) service and 500° F. operation is .67 X .9 = .603

Tube Selection Example:

Maximum Operating Temperature (degrees F)	Steel C-1010 and C-4130	Stainless Steel 304	Stainless Steel 316	Copper	Aluminum 6061-T6	Monel Type 400
100	1.00	1.00	1.00	1.00	1.00	1.00
150	1.00	0.91	1.00	0.85	1.00	0.97
200	1.00	0.84	1.00	0.80	1.00	0.94
250	1.00	0.79	1.00	0.80	0.94	0.91
300	1.00	0.75	1.00	0.78	0.80	0.88
350	0.99	0.72	0.99	0.67	0.60	0.86
400	0.98	0.69	0.97	0.50	0.43	0.85
500	0.96	0.65	0.90			0.84
600		0.61	0.85			0.84
700		0.59	0.82			0.84
800		0.57	0.80			0.83
900		0.54	0.78			
1000		0.52	0.77			
1100		0.47	0.62			
1200		0.32	0.37			

Table A27 — Temperature Derating Factors* for Tubes

* The derating factors are based on allowable design stress values at various temperatures per ASME B31.1 code for pressure piping (1986).

To select tube material and tube sizes for pressure, return and suction lines for a hydraulic power unit with the following operating parameters known:

Type of fluid: Petroleum base hydraulic fluid

Operating temperature range: -20° to +140°F.

Maximum operating pressure: 3500 psi

Maximum flow rate through each line: 10 GPM

Severity of service: A (normal)

1. **Selecting Tube Material:** Table A21 indicates that carbon steel, C-1010, tubing would meet the media, operating temperature range, and maximum operating pressure (high) requirements.
2. **Sizing the Tube:** From Table A29, the recommended flow diameters for various lines for 10 GPM flow rate are: 0.405 for pressure line, 0.639 for return line, and 1.012 for suction line.

   Now, using Table A30, we need to find tubes with inside diameters (I.D.) equal to or larger than the above flow diameters, and wall thicknesses appropriate for design pressures of 3500 psi minimum for the pressure line and about 500 psi for return and suction lines. Since derating factors for Severity of Service (Table A26) and Max. Operating Temperature (Table A27) are both 1, design pressure values in Table A30 do not need to be reduced.

   Matching tube I.D.s and design pressures in Table A30 for above conditions, we find:

   A) For the pressure line, we would choose 5/8" O.D. X .083" wall tubing. The .095" and .109" wall tubes would also be satisfactory if .083" wall is not readily available.

   B) For the return line, either 3/4" X .035" or 3/4" X .049" would meet the requirements. If Ferulok fittings are being used, we will need to go to 3/4" X .065" because .065" is the smallest wall thickness recommended for 3/4" O.D. tubing used with Ferulok fittings in Table A14. This reduces the flow diameter about 3% below the recommended value, but is still in the acceptable range. The alternative is to go to 7/8" O.D. X .072" wall tubing, which is way too large.

Tube Material / Size		Steel St. Steel Copper Aluminum	Steel St. Steel Monel	Steel Alloy Steel St. Steel Copper Monel	Copper Aluminum Plastics
O.D. Inches	Dash Number	SAE 37° Flare Triple-Lok	SAE Flareless Ferulok	SAE O-ring Face Seal Seal-Lok 1)	Intru-Lok
1/8	-2	.010 - .035	.010 - .035	—	.012 - .028
3/16	-3	.010- .035	.020 - .049	—	.012 - .035
1/4	-4	.020 - .065	.028 - .065	.020 - .083	.020 - .049
5/16	-5	.020 - .065	.028 - .065	.020 - .095	.020 - .065
3/8	-6	.020 - .065	.035 - .095	.020 - .109	.028 - .065
1/2	-8	.028 - .083	.049 - .120	.028 - .148	.035 - .083
5/8	-10	.035 - .095	.058 - .120	.035 - .134	.035 - .083
3/4	-12	.035 - .109	.065 - .120	.035 - .148	.035 - .095
7/8	-14	.035 - .109	.072 - .120	—	.049 - .095
1	-16	.035 - .120	.083 - .148	.035 - .188	.049 - .120
1 1/4	-20	.049 - .120	.095 - .188	.049 - .220	
1 1/2	-24	.049 - .120	.095 - .220	.049 - .250	
2	-32	.058 - .134	.095 - .220	.065 - .220	

1) Brazing to attach sleeve can be used for all wall thicknesses. For flanging tool availability, see page N23.

Table A28 — Recommended "Min./Max" Tube Wall Thickness for Common Fittings

C) For the suction line, we can use any one of the following tubes: 1-1/4" O.D. X .049" to .083" wall tube for Triple-Lok or Seal-Lok fittings and 1-1/4" O.D. X .095" wall tube for Ferulok fittings.

One final consideration in choosing the right wall thickness for tubing is bending. If bending without the use of a mandrel is desired, then wall thickness of less than 7% of tube O.D. should not be used.